

TECTONICS OF THE SHILLONG PLATEAU AND ADJOINING REGIONS IN NORTHEAST INDIA USING FIELD AND REMOTELY SENSED DATA

A THESIS

*submitted in fulfilment of the
requirements for the award of the degree*

of

DOCTOR OF PHILOSOPHY

in

EARTH SCIENCES

By

JOSODHIR DAS



DEPARTMENT OF EARTH SCIENCES
UNIVERSITY OF ROORKEE
ROORKEE - 247 667 (INDIA)

DECEMBER, 1995

Gratis

CANDIDATE'S DECLARATION

I hereby certify that the work which is being presented in the thesis entitled "TECTONICS OF THE SHILLONG PLATEAU AND ADJOINING REGIONS IN NORTHEAST INDIA USING FIELD AND REMOTELY SENSED DATA" in fulfilment of the requirement for the award of the Degree of DOCTOR OF PHILOSOPHY and submitted in the Department of Earth Sciences of the University is an authentic record of my own work carried out during a period from December, 1987 to November, 1995 under the supervision of Prof. A. K. Jain, Prof. A. R. Chandrasekaran and Dr. A. K. Saraf.

The matter presented in this thesis has not been submitted by me for the award of any other degree of this or any other University.

Josodhir Das

This is to certify that the above statement made by the candidate is correct to the best of our knowledge.

Dr. A. K. Saraf
Lecturer,
Dept. of Earth Sciences
University of Roorkee
Date: 30/11/95

Dr. A. R. Chandrasekaran
Professor,
Dept. of Earthquake Engg.
University of Roorkee

Dr. A. K. Jain
Professor,
Dept. of Earth Sciences
University of Roorkee

The Ph. D. viva voce examination of Mr. Josodhir Das, Research Scholar, has been held on 04/10/96.

Signature of Supervisors

Signature of H.O.D.

Signature of External Examiner

(Dr. S. K. UPADHYAY)
Professor & Head
Department of Earth Sciences
University of Roorkee
ROORKEE-247667

A B S T R A C T

Northeast India is one of the most tectonically active regions in the world and frequently affected by minor to moderate earthquakes. In this region, the Shillong Plateau was the locale of one of the largest known earthquakes of the world of 1897. The Archean gneissic basement of the Shillong Plateau has been experiencing earth movements since Early Proterozoic. It is bounded by relatively young Himalayan and Indo-Burman fold belts and documents prolonged tectonic activity. This part of India has been subjected to the collision tectonics from the north and east since the subduction of the Indian Plate under the Tibetan and Burmese Plates respectively. The southern margin of the Shillong Plateau is demarcated by the well known E-W trending Dauki Fault, that has played an important role in its geotectonic history. Initially, eastward lateral movements of the order of 200 km or more along the Dauki Fault were postulated. However, later investigations have indicated vertical fault movements along this fault.

Satellite images of this region provide a synoptic view of numerous geological structures. Remote sensing data have been integrated with geological, geomorphological, structural and seismological studies for a better understanding of various tectonic structures of the Northeast India, mainly the Shillong Plateau. The plateau is bounded by the prominent N-S trending Jamuna Fault along its western margin, E-W trending Dauki Fault and Brahmaputra lineament along the northern and southern edge of the plateau respectively and Kopili graben to the east.

On satellite images, the Shillong Plateau can be seen criss-crossed by innumerable fractures with predominant trends in N-S and NE-SW. Frequency plotting of lineaments indicate that NW-SE trending lineaments become scarce gradually from west to east of the plateau. Further, joint data from the Precambrian rocks also show dominant trend in N-S and NE-SW directions.

Numerous horst and graben structures could be seen on satellite images along southern margin of the plateau which have formed due to the extensional tectonics across the pre-existing N-S and NE-SW trending fractures.

The N-S trending dextral Um Ngot Fault dissects the Shillong Massif at longitude 90°E , and was active only before the Eocene. The N-S trending Dudhnai Fault, located in the western Shillong Massif, runs across the whole width of the massif and displaces the Dauki Fault. These faults are deep-seated, as indicated by the intrusion of carbonatite along these faults. A set of N-S trending Kopili fracture lineament has been identified in the area between the Shillong and Mikir Hills Massifs showing lateral movements. The Mikir Hills Massif has shifted northward along these fractures.

The Dapsi Reverse Fault and the Haflong Thrust Zone in the western part and southeastern part of the Shillong Massif are the result of NE-SW and NW-SE trending compressional stresses respectively.

On satellite images, the most spectacular folds can be seen in region south of the Haflong Thrust. The limbs of these folds are curved and hinges compressed. The morphological features of the folds indicate that these could have formed due to the NW-SE trending compressive stress.

In the Himalayan Foothills, the Siwalik rocks are missing at longitude $90^{\circ}30'\text{E}$. The faulted river fans adjacent to the foothills indicate recent active character of the Main Frontal Thrust (MFT). In Arunachal Himalaya, the Dafla Hills tectonic block shows southward migration due to N-S compressional stress. In the Naga Foothills, an interlocking structure has formed due to translational fault movement. Under the intense compressional tectonism, the foothill rocks exhibit migration tendency towards the Brahmaputra valley. This effect is very conspicuous in a region where the Brahmaputra Basin is bordered by the Dafla Hills tectonic block in the north and the Mikir Hills block in the south respectively. The deformation pattern and nature of migration of the Brahmaputra River suggests that the Brahmaputra Basin is getting compressed gradually.

The Brahmaputra River in the Northeast India flows through tectonically very active narrow valley, bounded by the hills and plateau. This river has conspicuously migrated northward for considerable length between Shillong and Mikir Hills Massifs. Northward shift of the Brahmaputra River is attributed to the probable southward thrusting of the Brahmaputra Basin against the Shillong Plateau.

On satellite images, the E-W trending Dauki Fault Zone is, at places, represented by very high landforms, and very steep escarpment between longitudes 91° and 92° E with huge blocks of sandstones with the E-W trending vertical slip surfaces. Further, western and eastern segments of the Dauki Fault Zone show uplift and thrusting effects respectively. Two troughs could be recognized in the Bangladesh area adjacent to this zone. The various folds in sedimentary rocks just south of the DFZ are convex indicating variation in stress orientation between NW-SE to NE-SW.

The satellite images also clearly depict a prominent NE-SW trending Barapani Shear Zone. Landform, developed along this shear zone, reveal structural characteristics of the shear zone and nature of shearing. This shear zone is located within the Precambrian phyllites belonging to the Shillong Group. The elongated lens-shaped ridges and dragged narrow long ridges clearly indicate left-lateral slip along the shear zone. The Barapani Shear Zone had undergone reactivation due to horizontal shearing probably in Miocene as a result of intense N-S compression.

Drainage system in the Shillong region is strongly influenced by structural grains and mostly fracture-controlled. Along the Barapani Shear Zone, the northeastward flow of the Wah Umiam River has been obstructed by a ridge and the river takes a U-turn.

Careful examinations of fracture lineaments and various joints indicate that the region has suffered multi-directional tectonic stresses, most prominent being in NW-SE and N-S directions. Neotectonic activities are expressed through deformation of soft sediments. Present-day deformations are actively taking place in foothill zone of the Himalaya and Naga Hills and the younger sediments south of the Shillong Massif.

The region is seismically very active and some of the earthquake potential zones have been identified viz., Tura Block, Shillong Block, Dafla Hills Block and the area between DFZ and HTZ.

It is likely that the Brahmaputra Basin is thrust against the northern margin of the massif, while the rigid massif, in turn, appears to override the Bangladesh Plains at depth. This study also postulates presence of thrusts beneath the Brahmaputra Basin and the Shillong Massif. These structures are thrust southward against the northern margin of the Shillong Massif and the Bangladesh Plains respectively.

ACKNOWLEDGEMENTS

I am highly indebted to Professor A.K. Jain, Dr. A.K. Saraf, Department of Earth Sciences and Professor A.R. Chandrasekaran, Department of Earthquake Engineering, University of Roorkee, for providing me valuable guidance and suggestions in completing this thesis. I am specially grateful to Prof. A.R. Chandrasekaran for his full support to me in this endeavor. I must acknowledge the Department of Science and Technology, Government of India for providing Satellite data under the Project Strong Motion Arrays in India which were essential to carry out the research work.

Professor and Head, Department of Earthquake Engineering and Department of Earth Sciences, University of Roorkee have provided all kind of facilities to carry out my thesis work. Also, I wish to express my sincere gratitude to Prof. L.S. Srivastava for his valuable scientific suggestions.

Mr. Anand Agrawal, Scientist, Central Ground Water Board, Shillong and Mr. B. Venkateshwaran, Atomic Mineral Division, Shillong have provided logistic support during my stay in the field. Geological Survey of India, Shillong has kindly permitted me to consult their geological reports.

Remote Sensing and Photogrammetric Engineering Laboratory, Civil Engineering Department, University of Roorkee had been kind enough to permit me to use Rectifier for making enlarged paper prints of the satellite images. I am thankful to Sri R.M. Sundaram and Miss Anupma for technical help during the initial stage of digital image processing. Dr. S. Balakrishna was kind enough to allow me to use his colour printer.

Thanks are also due to my colleagues R.N. Dubey, S.C. Gupta, A.K. Jindal and M.L. Sharma who helped me sincerely from time to time and made my stay in the department very pleasant and meaningful.

Generous support of my colleagues Sri A.P. Sharma, Dinesh Chandra, Mukesh Kumar, Dharmvir Sharma, Veer Pal, Deepak and Satyender is greatly acknowledged. Sri Veer Pal and Deepak have helped me during compilation work.

My Mother, elder Brother and Sisters have always been the source of encouragement and inspiration for completion of this Ph.D. work.

My wife, Mrs. Shyamali has provided encouragement and given me full support and company at home and work.

Sri S.C. Sharma and Lakshman Singh have drafted most of the drawings. I am also thankful to Sri Puran Sharma for regenerating the prints of photographs.

My sincere thanks are also due to all who directly or indirectly helped me to carry out this work.

I dedicate the thesis to my Ma and Dada whom I owe my career.

JOSODHIR DAS

CONTENTS

ABSTRACT	i
ACKNOWLEDGEMENTS	v
CHAPTER 1 - INTRODUCTION	
1.1 PREAMBLE	1
1.2 AREA OF STUDY	3
1.2.1 Physiography of the Area	4
1.2.2 Drainage System of the Area	4
1.3 SCOPE AND OBJECTIVE	5
1.3.1 Objectives	5
1.4 DATA USED	6
1.4.1 Remote Sensing Data	6
1.4.2 Topographic Maps	7
1.4.3 Field Data	7
CHAPTER 2 GEOTECTONIC HISTORY OF NORTHEAST INDIA: A REVIEW	
2.1 INTRODUCTION	10
2.2 SHILLONG PLATEAU AND DAUKI FAULT	11
2.3 EASTERN HIMALAYAN BELT	13
2.4 INDO-BURMAN FOLD BELT	14
2.5 BASINS OF NORTHEAST INDIA	16
2.5.1 Brahmaputra Basin	16
2.5.2 Barak Basin	17
2.5.3 Bengal Basin	17
2.6 SEISMIC ACTIVITY OF THE REGION	18
2.6.1 Shillong Plateau Region and Dauki Fault Zone	18
2.6.2 Eastern Himalayan Belt	20
2.6.3 Indo-Burman Fold Belt	20
2.6.4 Brahmaputra Basin	21
2.6.5 Barak Basin	22
2.6.6 Bengal Basin	22
2.7 GRAVITY TECTONICS	22
2.8 DISCUSSIONS	23

CHAPTER 3 FRACTURE LINEAMENTS, JOINTS AND FAULTS

3.1 INTRODUCTION	34
3.2 PROMINENT FRACTURE LINEAMENTS	35
3.2.1 Brahmaputra Lineament	35
3.2.2 Sylhet Lineament	35
3.2.3 Tista Lineament	36
3.2.4 Kopili Mega-Fractures	36
3.2.5 Kalyani Lineament	36
3.2.6 Indo-Burman Fold Belt Lineaments	36
3.3 LINEAMENTS AND JOINT TRENDS	37
3.3.1 Lineament Trends	37
3.3.2 Joint Trends	38
3.4 GEOLOGIC AND TECTONIC DESCRIPTION OF LINEAMENT	39
3.5 PROMINENT FAULTS	39
3.5.1 Um Ngot Fault	40
3.5.2 Dudhnai Fault	40
3.5.3 Jamuna Fault	41
3.5.4 Kopili Fault	41
3.5.5 Guwahati Fault	41
3.5.6 Haflong Thrust Zone	42
3.5.7 Dapsi Reverse Fault	42
3.5.8 Tyap Fault	43
3.5.9 Mohanganj and Chandghat Fault	43
3.6 HORST AND GRABEN STRUCTURE	43
3.7 OTHER IMPORTANT STRUCTURAL FEATURES	44
3.7.1 Himalayan Foothills	44
3.7.2 Dafla Hills block	45
3.7.3 Naga-Patkai Hills Region	45
3.7.4 Interlocking Structure	45
3.7.5 Folds in Haflong Thrust Zone	45
3.8 RIVER MORPHOLOGY AND TECTONICS	46
3.8.1 Brahmaputra River	46
3.8.2 Barak River	47
3.8.3 Tista River System	48
3.9 DISCUSSIONS	49

CHAPTER 4 DAUKI FAULT AND BARAPANI SHEAR ZONE

4.1 INTRODUCTION	86
4.2 DAUKI FAULT ZONE	87
4.2.1 Geological Background	87
4.2.2 Morphotectonics	88
4.2.3 Drainage Pattern and Tectonics	89
4.2.4 Structural Features	89
4.3 FRACTURE PATTERN ALONG THE DAUKI FAULT ZONE	90
4.3.1 Borhir-Dauki-Muktapur Sector	91
4.3.2 Shella-Balat Sector	92
4.3.3 Ratacherra Sector	92
4.4 SHILLONG REGION AND BARAPANI SHEAR ZONE	93
4.4.1 Geological Background	93
4.4.2 Morphological Features	94
4.4.3 Landforms in the BSZ	95
4.4.4 Drainage Systems	95
4.5 DEFORMATION AND FRACTURE PATTERN ALONG THE BSZ	97
4.5.1 Shillong-Barapani Sector and Barapani Area	97
4.5.2 Mawphlang-Tyrsad Road Section	97
4.5.3 Mawangap-Sohiong Sector	98
4.6 DISCUSSIONS	98

CHAPTER 5 IMAGE PROCESSING OF IMPORTANT STRUCTURES

5.1 INTRODUCTION	134
5.2 DATA USED	135
5.2.1 Types of Data	135
5.3 IMAGE PROCESSING SYSTEM	136
5.3.1 Integrated Land and Water Information System (ILWIS)	137
5.3.2 Aldus Photostyler	137
5.4 ENHANCEMENT TECHNIQUE	137
5.4.1 Contrast Stretching	138
5.4.2 Linear Stretching	138
5.4.3 Non-Linear Stretching	139
5.4.4 Enhancement by Using Colours	139
5.5 IMAGE PROCESSING METHODOLOGY ADOPTED IN THIS STUDY	140

5.6 CONCEPT OF INVERSE IMAGE	140
5.7 INTERPRETATION OF VARIOUS GEOLOGICAL FEATURES	141
5.7.1 Shillong Region	141
5.7.2 Fold Structures	142
5.7.3 Alluvium Fault	144
5.7.4 River Morphology	145
5.8 OBSERVATIONS	146

CHAPTER 6- SUMMARY AND CONCLUSIONS

6.1 INTRODUCTION	179
6.2 FRACTURE LINEAMENTS, JOINTS AND FAULTS	179
6.2.1 River Channel Migration	181
6.3 DAUKI FAULT ZONE AND MORPHOTECTONICS	181
6.4 BARAPANI SHEAR ZONE AND MORPHOTECTONICS	181
6.5 SEISMICITY AND ACTIVE TECTONICS	182
6.6 QUALITATIVE ASSESSMENT OF EARTHQUAKE-PRONE FAULT ZONES	183
6.6.1 Shillong Block	184
6.6.2 Dafla Hills Block	184
6.6.3 Tura Block	184
6.6.4 Other Structures	184
6.7 TECTONIC MODEL	185
6.8 CONCLUSIONS	186
REFERENCES	192

APPENDIX-I

INTRODUCTION

1.1 PREAMBLE

Geological structures are the manifestation of the earth's internal geodynamic processes arising mainly from regional plate movements. The deformational processes should be very intense in the region, which has undergone convergent plate tectonism from two different directions. And, the present-day high seismicity of a region should be the testimony of active earth movements.

Such a region in the northeastern parts of India is characterized by the Archean landmass which is surrounded by the Tertiary Himalayan mountain belt in the north and Indo-Burman fold belt in the east and southeast. These mountain belts are the result of continent-continent collisions due to convergent plate tectonism. The Northeast India is a unique example where collisional tectonics have been affected from two different directions. As a result, the whole region has suffered multiple phases of deformational processes which have resulted into numerous geological structures. It is interesting to observe that the Shillong Plateau has witnessed prolonged crustal deformation since Archean. The adjoining Brahmaputra and Bengal Basins had been sensitive to the recent tectonic activities.

Occurrences of many geotectonic units in relatively small space and associated structural features in a region demands a regional understanding of the tectonic history.

Further, the region is seismically very active and locale of some of the most severe earthquakes of magnitude greater than 8 on Richter scale, e.g., June 12, 1897 and August 15, 1950 earthquakes.

Satellite-based remote sensing data provide a synoptic view of a region with multispectral approach and reveal various geological structures on the earth's surface, which, otherwise, are very difficult to recognize in the field. The Shillong Plateau depicts the geological structures clearly as most part of the plateau is barren or has scanty vegetation. Deformational patterns in young sediments along the foothills of the Himalaya, Naga Hills and in the adjoining region south of Shillong Plateau are displayed remarkably well on satellite images. At some places, neotectonic activities could be identified with the help of satellite images. In fact, remote sensing technique is a very successful tool, especially when the area receives heavy rains and has thick vegetation.

The Northeast India is represented by complex tectonic regime. Numerous structural features could be seen in a very small area e.g., the thrusts in the Himalaya, Mishmi Thrust (MT) and Naga Thrust (NT) in the north, northeast and east respectively and Haflong Thrust (HT) in the southeastern margin of the Shillong Plateau. The E-W trending Dauki Fault (DF) forming steep scarps, is a very prominent linear feature and marks the southern edge of the Shillong Massif. The basement rocks of the Shillong Plateau had faulted downward along the DF for around 13 km. In Bangladesh, the basement rocks is overlain by thick sediments. This neighbouring part of Bangladesh also has suffered intense earth movements.

The oldest landmass in the area is the Shillong Plateau which was the only landmass before break up of the Gondwanaland in Jurassic time (Powell et al., 1988). It seems that the extreme eastern part of Indian Plate was gliding over the hot spot,

located at the longitude 70⁰E, north of Antarctica, and during its north-northeastward drift the eruption of magmatic rocks took place in the region. Prior to break up of the Gondwanaland, the Shillong Plateau has suffered protracted thermal event during late Proterozoic-early Paleozoic (Kumar, 1990 and Ghosh et al., 1991), possibly related to mantle upwelling which could have triggered the generation of the igneous plutons. This activity in turn affected Shillong Plateau structurally.

The whole northeastern region especially the Shillong Plateau is riddled by numerous fractures and faults. The tectonic model of Northeast India has always remained a challenging quest to the geoscientific community due to lack of sufficient geological and geophysical data. There is no unanimity about the origin and tectonic history of the Shillong Plateau. Evans (1964) postulated lateral movement of the Shillong Plateau towards east along the Dauki Fault for more than 200 km. However, Murthy (1970), Auden (1972), Desikachar (1974) and G.S.I. (1974) have suggested vertical fault movements along the Dauki Fault. Further, Mukhopadhyay (1990) and Khattri et al. (1992) have indicated southward thrusting of the Shillong Plateau along the Dauki Fault, based on geophysical data. Of course, it is evident that intense crustal shortening have taken place in the Himalayan and Indo-Burman fold belt. Different geotectonic features in the Northeast India have played an important role in framing up of the present tectonic setup. These tectonic features are discussed in detail in this thesis.

1.2 AREA OF STUDY

In the present study, fault tectonics of the Shillong Plateau and adjoining regions have been investigated in details. The area includes the Shillong Plateau, the Brahmaputra and Barak Basins, the Himalayan Foothills, the Naga Foothills, the Bangladesh Plains and the Frontal Fold Belt (Fig. 1.1). In this study, the whole Northeast India and adjoining countries also have been referred for better understanding of regional tectonics.

1.2.1 Physiography of the Area

Physiographically, the Shillong Plateau represents a remnant of an ancient plateau of Precambrian Indian Peninsular Shield, block uplifted to its present height. The ancient peneplaned surface of the plateau is still preserved, with marks of different cycles of denudation. The Shillong peak (1964 mts) is the highest spot over the plateau. The southern part of the Shillong Plateau is marked by very steep scarp at many places and forms Bangladesh Plains to the south.

The Brahmaputra Basin occupy areas to the north of the Shillong Plateau and separates the plateau from the Eastern Himalaya. The highest place in the Arunachal Himalaya is the Kongtu peak which is over 7000 mts. The E-W configuration of the Brahmaputra Basin in the western side is controlled by the Himalaya and the Shillong Plateau. In the east, the NE-SW configuration of the basin is controlled by the Himalaya in the NW and the Naga Hills in the SE.

1.2.2 Drainage System of the Area

The whole Assam is drained by the mighty Brahmaputra River. The course of the Brahmaputra River is tectonically controlled, and numerous migratory channels have developed as the river floods vast area frequently. This river shows migration at some places. The second major river in the study area is the Barak River, which is prominent in the Barak Basin. In the Barak Basin, the river flows zig-zag and shows changes and abandoning of the river course.

The drainage pattern in the Shillong Plateau represents most spectacular feature revealing extraordinary straight courses of the rivers and streams, evidently along faults and joints. Most of the rivers flow southward and enters the Bangladesh Plains after scooping out gorges along the southern margin of the Shillong Plateau.

1.3 SCOPE AND OBJECTIVE

It is established that the Northeast India is seismically very active and frequently affected by minor to moderate earthquakes. Also, the area is traversed by numerous faults, joints, fractures and shear zone. Some of these had been tectonically active and requires identification and special attention. Moreover, in Northeast India, some hydroelectrical projects are located and quite a few are coming up in near future. For safe engineering design of the dams and other structures, it is essential to know the earthquake hazard of the region.

The river systems in the Northeast India show migration and change of river courses under active tectonism. Studies of river morphological activities would provide a data platform to organize the future land planning.

Considering the tectonic significance of the area, this study would provide useful scientific results.

1.3.1 Objectives

The basic objectives of the present studies are as follows:

1. Regional tectonic framework of Northeast India.
2. Identification and studies of characteristic structural features mainly from Shillong Plateau and adjoining areas.
3. Tectonics of the Shillong Plateau and adjoining areas.
4. Identification of faults and their morphological characteristics.
5. Identification of earthquake-potential fault zones.
6. Neotectonic studies and effect of active tectonics on river morphology.
7. Digital image processing of IRS LISS-II data of Shillong Plateau for structural feature enhancement and better interpretation.

8. Seismicity and active tectonics.
9. Tectonic model.

1.4 DATA USED

Remote sensing data have been used extensively in this study. The present study involves large area and complicated tectonic structures for which detailed investigations were required. Therefore, a thorough scanning of both geological and geophysical literatures have been carried out. Figure 1.2 shows satellite data coverage of the study area.

1.4.1 Remote Sensing Data

Well controlled black and white mosaic was prepared from Landsat Thematic Mapper scenes in infrared range of 0.76-0.90 microns (band 4). Satellite based remote sensing data in this spectral range has been selected owing to its high reflectance and absorption by vegetation and water body respectively, providing clear picture of the geological structures. The scale of the individual images is 1:1,000,000 and mosaic has been prepared directly from these scenes keeping the scale unchanged. This mosaic covers the whole Northeastern India and adjoining countries of Bangladesh, parts of Myanmar (Burma), Tibet and Bhutan. A few scenes were also enlarged to 2 to 4 times for a particular area in order to improve interpretation, which is otherwise difficult in small scale images. It is observed that extent and nature of the regional structural features are better understood from mosaic of satellite images on the scale 1:1,000,000 as this provides a synoptic view.

Indian Remote Sensing LISS-II FCC's (scale 1:250,000) and digital data covering Shillong Plateau have also been used. Details of Satellite data used in the present study are given in Appendix I.

1.4.2 Topographic Maps

The study area is restricted, hence the topographic maps were not easily available from Survey of India. With great difficulty, some topographic maps could be collected and were used extensively during the field work. Topographic maps were also used to study and compare the drainage patterns and morphology of the area.

1.4.3 Field Data

Field work had been carried out extensively mainly in the Shillong Plateau during the winter seasons. Data on joints, fractures, deformation pattern in rocks of Barapani Shear Zone and also the fracture pattern of rocks from some locations of the Shillong Plateau have been collected. Considerable length of the Dauki Fault was covered during the field work and collected valuable data on structural patterns.

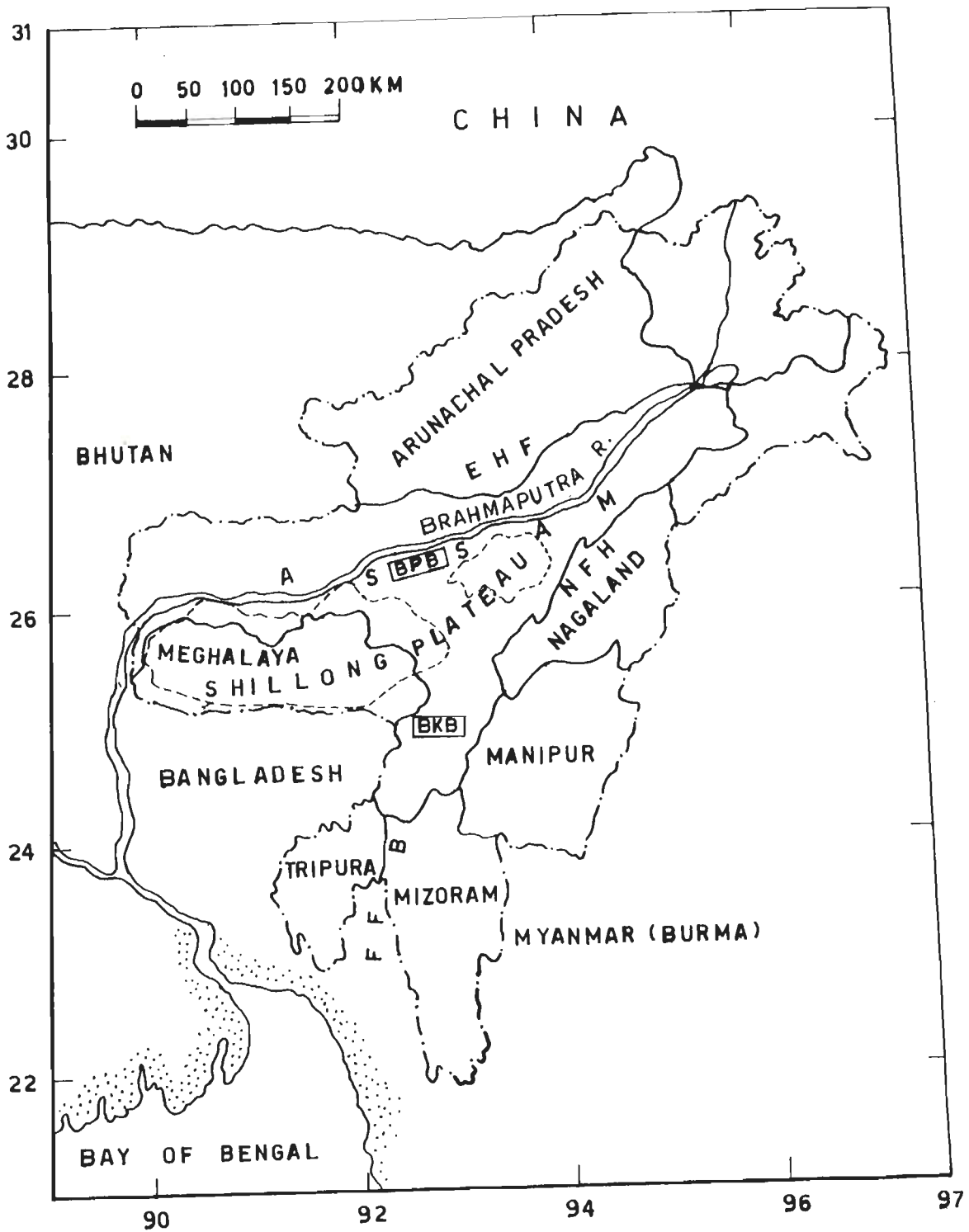


Figure 1.1 Map showing the study area in Northeast India which includes the Shillong Plateau and adjoining regions, viz. the Brahmaputra basin (BPB) and Barak basin (BKB) in Assam, Eastern Himalayan foothills (EHF) in Bhutan and Arunachal Pradesh, Naga foothills (NFH) in Nagaland, Frontal Fold Belt (FFB) and Bangladesh plains. Seven states along with boundaries are also shown.

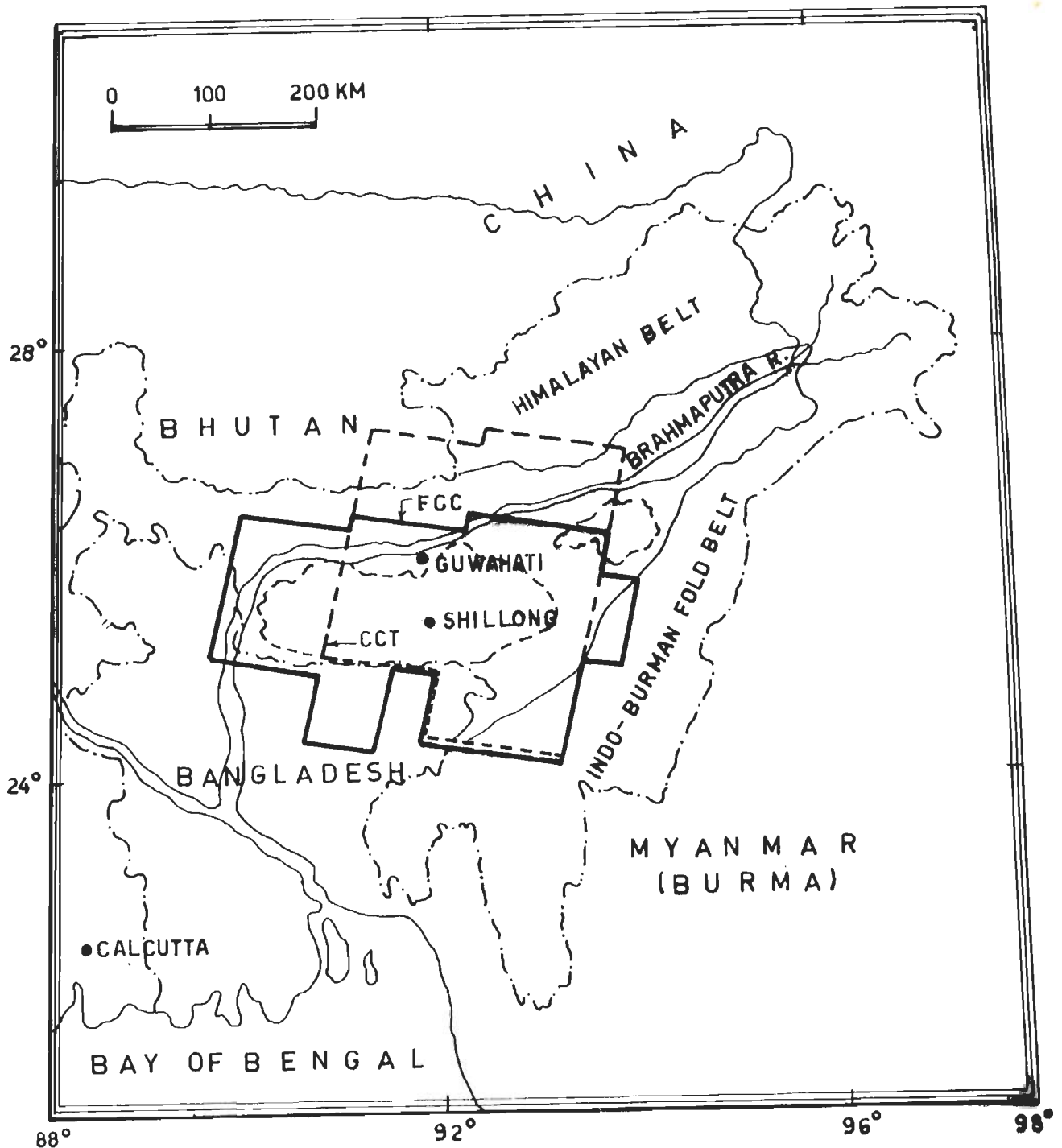


Figure 1.2 Map showing the satellite based remote sensing data coverage of the study area. Landsat TM (Band-4) data for the whole area is shown by the double lines coinciding with the map boundary. IRS LISS-II data: FCC of the area is shown by the thick line; Digital data (CCT) of the area is shown by the broken line.

**GEOTECTONIC HISTORY OF NORTHEAST INDIA :
A REVIEW**

2.1 INTRODUCTION

Geological history of Northeast India is quite interesting due to the fact that the different geotectonic provinces have undergone different episodes of tectonic movements through geological time. The region could be categorized into different distinct geological units, based on geomorphological characteristics.

The major geotectonic provinces, on the basis of geological data and Landsat image mosaic prepared for this study, are shown in Figure 2.1. Geological information of the area is widely available in the works of Evans (1964), Murthy (1970), Desikachar (1974), G.S.I. (1974), Murthy et al. (1976), Nandy (1976), Sarkar and Nandy (1976), Acharyya et al. (1986) and Mazumdar (1986). Therefore, a relatively strong geological background of the area could be developed.

Geological map of the Northeast India is shown in Figure 2.2, while Figure 2.3 shows basement configuration of northeastern part of India. Our interest lies mainly on the geotectonic aspects of the Shillong Plateau and adjoining regions. However, in order to have proper understanding of the regional tectonics, whole of Northeast India and part of adjacent countries have been discussed below.

2.2 SHILLONG PLATEAU AND DAUKI FAULT

The shield area is comprised of the Shillong Massif (SM) and Mikir Hills Massif (MHM), and they, together, form the Shillong Plateau (Fig. 2.1). The MHM is separated from the SM by an alluvial tract, which is located in the central part of Northeast India. A large part of the shield area of Northeast India exposes Archean folds. These zones show schistose tracts grading into vast stretches of granitic gneisses incorporating metasedimentary and metavolcanic rocks within the gneissic complex. A major part of this complex has apparently been formed by metasomatism of these sediments and volcanics. Intrusive augen gneisses occur within the Archean and these could possibly mark late-tectonic magmatic episodes of older orogenies (Mazumdar, 1978).

The Archean rocks have been subjected to polycyclic folding and metamorphism. The plateau has suffered thermal events in the Proterozoic-Early Paleozoic (Kumar, 1990; Ghosh et al., 1991). The Shillong Group was deposited in central parts of the plateau (Fig. 2.2), as this area developed into a trough. The post-Precambrian landmass experienced peneplanation till Jurassic, resulting into the formation of a flat-levelled surface, which is preserved over the plateau till today (G.S.I., 1974). The MHM, with an average elevation of 1,000 m, represents a peneplaned surface of predominantly gneissic rocks. The sedimentary rocks are exposed along the southern and eastern flanks.

By the end of Jurassic, the southern margin of the Shillong Plateau experienced eruption of Sylhet Traps through E-W trending fissures (Murthy, 1970; G.S.I., 1974). Around 150 m.y., carbonatite complex was emplaced along a N-S trending fault at longitude $92^{\circ}05'E$ in the eastern part of the Shillong massif (Sarkar et al., 1992). The Cretaceous sediments were deposited along the subsiding southern block. Towards the Paleocene-Eocene, the plateau attained a stable shelf condition due to lower subsidence rate. The eastern and western parts of the Shillong massif remained landmass till mid-Eocene and experienced progressive down-sinking which initiated the deposition of coal-bearing sandstone (G.S.I., 1974). Shillong Plateau represents

a unique structural unit in the area, as it is block- uplifted to its present height (Murthy, 1970; G.S.I., 1974).

The southern margin of Shillong Plateau is marked by the remarkably linear E-W trending Dauki Fault (Figs. 2.1, 2.3, 2.4, 2.8 and 2.9). Evans (1964) gave detailed geological and tectonic set up along the Dauki Fault Zone and suggested that this zone is essentially a tear-fault with a lateral movement of over 200 km. Even though presence of slickensides on a fault surface shows horizontal E-W movement, extent of movement was not possible to be estimated. Similarly, due to lack of evidences on the extension of this zone below the alluvial gap between Shillong Plateau and Rajmahal Hills, its westward continuation can not be ascertained. Evans's (1964) arguments were based on the following.

(i) Towards east, the Dauki Fault has brought the rocks of geosynclinal facies within 7 km of the calcareous shelf facies of the Eocene.

(ii) Further west, the Surma Group (Miocene age) overlie the Eocene to the north of the Dauki Fault, whereas to the south thick early Miocene rocks overlie the Oligocene Barails. The Early Miocene rocks and Barails are missing on the northern side.

These two important differences in the stratigraphy of two sides of the Dauki Fault indicate that the beds, deposited far apart, are now brought close together.

Later, Murthy (1970), Desikachar (1974) and G.S.I. (1974) have suggested vertical movements along the Dauki Fault, as it is evidenced by the extrusion of lava through the deep-seated vertical fracture system. Also, Murthy (1970) has reported evidences to indicate activity along a number of E-W, N-S and NW-SE basement faults throughout the Tertiary period. It seems that the fault zone is characterized by uplift and down-sinking of adjacent basement blocks along the fractures.

In the western part of the Shillong Massif, NW-SE trending high-angle Dapsi Reverse Fault upthrust the Tura range southward. This fault forms the boundary between the Precambrians in the north and Tertiary rocks in the south. The depositional sequence was affected by this reverse fault, which probably demarcated

the northern boundary of the sedimentary basin from Mid-Eocene through Miocene (Murthy, 1970).

The Shillong Plateau and Mikir Hills show a criss-cross fracture pattern which affects the ancient basement. Towards west, the Shillong Plateau is bordered by the N-S trending Jamuna/ Dhubri Fault, which is indicated by the difference in basement levels (Fig. 2.3) and linear north-south Brahmaputra River course for about 150 km to 200 km. The eastern part of the Shillong Massif is marked by the NW-SE trending Kopili Fault (Figs. 2.4; 2.9). This fault separates the SM from MHM, which may be connected with each other at depth. A graben-type of structure is responsible for the down-sinking of this region.

2.3 EASTERN HIMALAYAN BELT

Physiographically, the Eastern Himalaya forms the highest mountain belt in the northeastern part of India. Wide varieties of rock types have been reported from this belt (Krishnan, 1956; Wadia, 1957; Le Fort, 1975; Sinha-Roy, 1976). The Eastern Himalayan mountain ranges, which formed during major mountain building orogenies in the Miocene, include thrusts, faults and overfolding as major structural elements.

The prominent tectonic feature is the Indus-Tsangpo Suture Zone (ITSZ) along which the river Tsangpo (Brahmaputra) River flows remarkably in a E-W rectilinear valley, as also can be seen on satellite image mosaic. The ITSZ marks the collision boundary of the Indian and Tibetan plates. The rock units south of ITSZ, the highest grade metamorphites and gneisses of the axial belt, are separated from Precambrian sedimentary sequence and its equivalents by the Main Central Thrust (MCT). The Main Boundary Thrust (MBT) separates the Siwalik rocks from the pre-Tertiary rocks. Beyond MBT, different stratigraphic units are disposed in intricate thrust slices.

In the foothills of the Arunachal Himalaya, the Siwaliks are represented by a thick pile of molassic sub-greywacke. This belt is continuous all along the Himalaya foot hills from Kashmir to Arunachal Pradesh. The Siwalik sequence was deposited during the Mio-Pliocene in an unstable sinking basin, developed along E-W fractures north of

the Shillong Plateau and south of rising Himalaya. The Siwaliks, are folded and thrust over by the older rocks from the north along the MBT. The lithological assemblages of the Siwaliks were also controlled by the vigor of tectonism in the source area of the rising Himalaya. The southern fringe of the Siwalik belt, bordering the Brahmaputra basin, is marked by the Main Frontal Thrust (MFT).

The regional structural trend of the Eastern Himalaya is mostly E-W to ENE-WSW from Bhutan to the northeastern Arunachal Pradesh (Siang valley). This trend gradually changes to NE-SW near the Siang valley and terminates against the Siang fracture (Nandy, 1976). In this part of the Himalaya, the MCT can not be recognized and this might have taken a north-eastward swing and passed beyond the Indian territory (Nandy, 1976). Regarding the MBT, Sinha-Roy (1976) indicated that this feature flattens at depth, as indicated by the absence of Gondwana rocks in southern Bhutan and in the west-central Arunachal Pradesh. This is possibly due to the fact that the MBT merges at depth with some dislocation zones in the inner belt.

Further northeast, the Himalayan belt abuts against the Mishmi massif. This massif is comprised of diorite-granodiorite crystalline complex (Murthy et al., 1976). The southwestern boundary of the massif is marked by high angle NW-SE trending Mishmi Thrust (MT) along which this block is thrust on the adjoining rocks. In Mishmi Hills, the NW-SE trending metamorphic belt is in direct contact with the Brahmaputra alluvium. This massif was already a land area, surrounded by basinal area (Murthy et al., 1976). This massif acts as a linkage between the Himalayan and Indo-Burman structural and stratigraphical trends in north and east respectively.

2.4 INDO-BURMAN FOLD BELT

This mountain range forms a N-S trending arc (Burmese arc) of 1100 km length and appears to be continuous with the Andaman-Nicobar ridge and non-volcanic fore-arc along the Sunda trench. The northern part of this fold belt forms border zone between Northeast India and Burma. This fold belt exhibits a typical structural trends. In the Naga hills, it is northeast-southwest and swings to NNW-SSE along the Arakan Yoma. The maximum width of the range is about 230 km, and the average elevation

increases from 1000 m to about 3000 m from south to north.

Geologically, the hill ranges of this fold belt are mainly formed of thick turbiditic Cretaceous to upper Eocene shales and sandstones (Brunnschweiler, 1966; G.S.I., 1974 and Mitchell, 1981). This belt has been folded more intricately in Nagaland. NE-SW trending Naga Thrust traverses the whole of Nagaland and then verges with the Dauki Fault after taking a swing towards southwest to west near Haflong (Figs. 2.3, 2.4, 2.8 and 2.9). This thrust divides the Patkai synclinorium and the 'Belt of Schuppen' (G.S.I., 1974).

The anticlines, close to the Naga Thrust, show reversal in topography with anticlines forming sites of valleys and synclinal hills Ganju et al. (1986). These anticlines appear like upwarps on the edge of the moving Naga slice with gently eastern limbs and a steep, much sheared western limbs. Remarkably, most of the thrusts in the region of Belt of Schuppen diverge from northwest and then unite with the Naga Thrust. Thrust shows successive increase in magnitude of overriding movement towards north (Ganju et al., 1986). This zone has undergone large dislocation, as is indicated by enormous variation in lithotectonic associations and attributes on either side of the Naga Thrust.

Towards south in the state of Mizoram and Tripura, the folded belt continues uninterruptedly with some variation in structures. Structurally, the area lies on high anticlinal ridges and synclinal valleys of Surmas and Tipams (Miocene) having major N-S trending strike faults. The Oligocene rocks (Barail) consist of a series of N-S trending marginal to basin faults and mark the eastern contact with the Tipam and Surma rocks. The general strike of the folded layers is $N15^{\circ}W-S15^{\circ}E$ to $N15^{\circ}E-S15^{\circ}W$. Axial planes of upright slightly asymmetrical, low-plunging folds are sub-vertical to vertical and are similar in geometry throughout the area rectilinear fault planes (Sarkar and Nandy, 1976).

The intensity of fold movements and amplitudes of folded layers are higher in the eastern part than in the western part of the basin. The axes of the folds in southern Mizoram converge towards south at latitude $21^{\circ}30' N$ with plunge towards south. In

the Tripura and adjacent Bangladesh area, the folds are characterized by compressed anticlines alternating with broad, very gently depressed synclines, which becomes more compressed towards east. Both anticlines and synclines are traversed by sub-parallel and sub-vertical regional strike faults adjacent to the crestal region of the folds. Stratigraphic sequences reveal vertical throw of the order of 700 m to 1,100 m in south central part of Tripura, while and in Mizoram it is 800 m and 1,700 m (Sarkar and Nandy, 1976).

The north-south trending folds all along the arc are significant features, developed due to shortening of the crust. And this fold belt was formed in early Tertiary due to subduction of the Indian Plate under the Burmese Plate. In the Naga hills, orientation of shortening axis changes to northwest-southeast. The Plio-Pleistocene beds in Bangladesh plains just west of Tripura folded belt are affected due to folding.

2.5 BASINS OF NORTHEAST INDIA

2.5.1 Brahmaputra Basin

The shape of relatively narrow Brahmaputra basin is governed by mountain ranges in the north, northeast, southeast and Shillong Plateau in the south (Figs. 2.1 and 2.8). This basin was formed due to the underthrusting of basement rocks below the Himalaya and the E-W trending down to basin faults along the northern margin of the Shillong Plateau. According to Murthy et al. (1976), the basin area between the Himalayan foothills and north of Shillong Plateau was a sinking basin during Mio-Pliocene time. The basin is filled up by sediments brought down by the Brahmaputra River system and forms a huge alluvial tract. Presently, the Brahmaputra River flows southwesterly in Upper Assam before taking westerly turn in the area north of the Shillong Plateau. The alluvial deposits of the Brahmaputra basin is underlain by the basement rocks, which are exposed in the western part of the basin. The slope of basement increases eastward and the sediments are found to be 6 km thick in the region northeast of Mikir hills at longitude 94°E (Mukhopadhyay, 1984).

Earthquakes of large magnitude, occurring in the region, might have changed the morphology of the basin. Oldham (1899) documented many changes in the river valley and other areas, affected by the great 1897 Shillong earthquake. From numerous observations, Oldham (1899) inferred upheaval of river channels and suggested that the whole alluvial plain of Lower Assam is raised due to the earthquake. Goswami (1986) has recognized Quaternary landforms bounded by scarps in the alluvial tract of Upper Assam. These scarps have been affected or reactivated by 1897 and 1950 earthquakes. Garg (1953) reported raising and heavy silting of the river beds. Changes in the Brahmaputra River course is a usual feature and the river is gradually becoming wider and causing frequent floods. In the report of survey on effects of 1950 earthquake Garg (1953), Gee (1953) and Ramesh and Gadagkar (1990) mentioned changes in the river courses in Upper Assam region. Goswami (1986) reported changes in the river courses and surface relief, widening of the river from 2.5 km to 10 km and general increase in water level. A detailed study of this basin, based on satellite images, is discussed later in Chapter 3.

2.5.2 Barak Basin

The Barak Basin is very narrow and occupies the area south of the Haflong Thrust (Fig. 2.1). This basin was formed during the uplift of the Barail range (Oligocene rocks) towards the north and northeast. The Miocene Tipam Group was deposited in the area south of this basin and was folded later. These folds are N-S trending gentle doubly-plunging overlapping anticlines and synclines. This basin extends westward bordering the Shillong Plateau. The river Barak flows in this basin westerly in a zig-zag manner. The river shows intense migration and abandoning of the course. This basin is seismically active and tectonically controlled.

2.5.3 Bengal Basin

To the south of the Dauki Fault, the plains of Bangladesh are covered by enormously thick alluvium (Fig. 2.1). The Bangladesh plains are a part of the Bengal Basin and located at the head of the Bay of Bengal. The Bengal Basin is bordered on its

west by the Precambrian basement complex of crystalline metamorphics of the Indian Shield. To the east, the frontal folds of Tripura are seen. The basement below the basin is marked by the Hinge zone, a high and a trough (Fig. 2.3). Thickness of these sediments increases rapidly across the hinge zone towards deeper part (Mukhopadhyay and Dasgupta, 1988). This hinge zone trends NNE-SSW to NE-SW and is an extensive regional curvilinear tectonic feature. From Bengal basin, the hinge zone continues into the Bay of Bengal, and further south, it appears to be related to the continental crust along the east coast of India (Talukdar, 1982). Nandy (1980) has reported NE-oriented lineaments, correlatable to the Eocene hinge zone at depth. However, it could not be established whether any tectonic movement took place along this hinge zone, even though gravity signature indicates continent-ocean transition across this zone (Mukhopadhyay and Dasgupta, 1988).

The western shelf of the Bengal basin is characterized by NE to NNE-trending down-to-basin normal faults with minor displacement, whereas northern foreland shelf, facing the Shillong Massif is narrow and tectonically disturbed (Desikachar, 1974). From the western margin of the basin, the basement surface dips gently southeastward with increasing thickness of sedimentary cover. The Bengal basin has attained its land status as early as late Oligocene (Evans, 1964; Nandy, 1982).

2.6 SEISMIC ACTIVITY OF THE REGION

From time immemorable, the northeastern part of India had been experiencing earthquakes ranging from micro tremor to very large ones. This region is seismically one of the most active regions in the world, as it has witnessed two most severe earthquakes of 1897 and 1950. The 1897 event had occurred in the vicinity of Shillong and caused large-scale devastation. To date, this earthquake is the most widely felt earthquake (Richter, 1958). Seismicity of the different tectonic units are discussed below. Seismotectonic map of Northeast India is shown in Figure 2.4.

2.6.1 Shillong Plateau Region and Dauki Fault Zone

From local earthquake recording, as reported by Khattri et al. (1983) and Kayal

(1987), it seems that the Shillong massif exhibits very high seismicity at micro level. Molnar (1987) has suggested tectonic movement beneath the Shillong Plateau on the basis of the information given by Oldham (1899). He has suggested underthrusting of the Indian subcontinent beneath the Shillong Plateau, which caused the 1897 earthquake. Recently, Mukhopadhyay (1990) has predicted, on the basis of microearthquake studies, a gently-dipping heterogeneous zone at the depth of 11.5-26 km along which Shillong Plateau is overthrusting southward and producing a horst-type of vertical movement.

Chen and Molnar (1990) have studied six earthquakes, which occurred beneath or near the Shillong Plateau. However, the style of deformation or sense of slip could not be resolved on the Dauki Fault. The focal depths indicated deformation deep in the crust or in the uppermost mantle and not at shallow depths beneath the surface near Shillong Plateau. Also, Chen and Molnar (1990) opined that the earthquake of Feb. 6, 1988, which occurred on the southern edge of the Shillong Plateau had no association with the Dauki Fault. Instead, the fault plane solution indicates compression in a north-south direction, normal to the fault. Further, from focal mechanism of an earthquake occurred along the southern edge of Shillong Plateau, Rastogi et al. (1973) had suggested underthrusting towards the north along the north-dipping plane. According to Dasgupta and Nandy (1982), the Dauki Fault remained inactive during the historical past.

Kayal (1987) has suggested NW-SE compressional stress in the Shillong area and ENE-WSW compressional stress in the Tura area on the basis of fault plane solution. However, high microearthquake activities along the WNW-ESE trending Dapsi Reverse Fault (Tura area) indicates concentration of high stress in that area.

Earthquake activities of Mikir Hills Massif is also considerably high. A few moderate earthquakes have been reported from this massif (Verma, 1991). It seems that the Kopili gap has been undergoing deep and high magnitude seismic activities. Two earthquake events are prominent. These are in 1943 (depth less than 50 km and magnitude 7 to 8) and an event with a depth of more than 100 km and magnitude 6 to

7 (Verma 1991).

2.6.2 Eastern Himalayan Belt

Appreciable seismicity has been noticed along the MBT and MCT between longitudes 88°E and 96°E (Fig. 2.4), which appear to be related to the MBT (Verma and Krishna Kumar, 1987). In the Eastern Himalaya, many earthquakes are also located close to the MCT (Fig. 2.4). Some of the lineaments trending in a northeasterly direction also appear to be active. In the Mishmi Massif area, several thrusts (including the Lohit and Mishmi Thrusts) trending NW-SE, appear to be quite active upto 100 km depth (Fig. 2.4). The main shock of 1950 earthquake was located in this orographic bend nearly 100 km east of Mishmi thrust (Verma and Krishna Kumar, 1987). In the region between the MBT and Tsangpo region, a large number of aftershocks of 1950 event were located. These aftershocks suggest that tectonic activities rejuvenated in the area far away from the region of main shock and seismic energy released by several faults and thrusts. Occurrence of this big earthquake event tends to suggest that the Himalayan thrust front may extend eastward into the Mishmi region (Verma and Krishna Kumar, 1987).

The focal mechanism solution, obtained from earthquakes of the Eastern Himalayan region, indicate predominantly thrust mechanism with a few strike-slip mechanism along some transverse tectonic features (Verma and Krishna Kumar, 1987). However, on the basis of data of earthquake in 1950, Seeber and Armbruster (1981) have concluded that this earthquake was caused by the detachment along the Himalaya and can be considered as the locus of all great Himalayan earthquakes, whereas Chen and Molnar (1990) suggested that a shallow-dipping thrust plane was responsible for this earthquake.

2.6.3 Indo-Burman Fold Belt

Innumerable earthquakes have occurred along this 1100 km long arc. Utilizing seismic data for different periods and from various agencies, several authors have tried to draw correlation of seismicity to tectonics of this N-S trending arcuate belt (Santo,

1969; Fitch, 1970, 1972; Chandra, 1975, 1978; Verma et al., 1976; Khattri et al., 1984; Le Dain et al., 1984 and Mukhopadhyay and Dasgupta, 1988). Shallow and intermediate earthquakes are very frequent in this region, but deep earthquakes more than 180 km deep are also reported (Fig. 2.5). Mukhopadhyay (1984), Biswas and Dasgupta (1986) and Mukhopadhyay and Dasgupta (1988) have suggested subduction of the Indian plate below Burmese arc, which extends up to 180 km deep below the central lowlands east of the Arakan-Yomas. Figure 2.5 shows earthquake activities and plate tectonics along the Indo-Burman Fold Belt.

In this fold belt, a different rate of subduction of the Indian Plate may be occurring, depending on the tectonic settings (Mukhopadhyay and Dasgupta, 1988). Chen and Molnar (1990) documents a NNE-SSW regional compression within the subducted Indian Plate and most of the earthquakes are occurring only within the Indian Plate. Strike-slip fault mechanism probably indicate that the northward movement of Indian plate still continues to drag its east-dipping slab beneath the Indo-Burman ranges northward through the asthenosphere. Moreover, northward translation of Indian Plate is largely accommodated by strike-slip movement along the Sagaing Fault (Le Dain et al., 1984), since transform faulting and sea floor spreading (Curry et al., 1982), occurring in the Andaman sea drifts the Indian Plate towards the north (Fig. 2.8).

According to Biswas and Dasgupta (1986), extensional stress was in NW-SE direction in Manipur-Burma region with shallow focus earthquakes revealing normal faulting as a major element in this region. But, Ichikawa et al. (1972), Molnar et al. (1973), Chandra (1975) and Verma et al. (1980) have suggested earthquakes with normal as well as thrust-type faulting in this region. From fault mechanism solutions for earthquakes below the Tripura Fold Belt, Mukhopadhyay and Dasgupta (1988) have observed E-W compression along the N-S faulting.

2.6.4 Brahmaputra Basin

In this basin, high concentration of earthquakes may be seen in the area between the longitudes 92° and 93°E (Fig. 2.4). The seismically-active Kopili fracture

zone, according to Khattri et al. (1983), extends across the Brahmaputra basin into the Himalaya. The seismicity of upper basin seems to be very low and, on the basis of seismic quiescence, Khattri and Wyss (1978) have postulated a 240 km long seismic gap in the region east of Mikir Hills.

2.6.5 Barak Basin

Quite a few moderate earthquakes have occurred in this basin. In 1943, an earthquake event occurred near Silchar, which had a magnitude between 6 and 7 (Fig. 2.4). Singh (1991) has studied the earthquake of December 30, 1984 (magnitude = 5.6) and suggested a combination of thrust and strike-slip faulting along the N12°E trending fault.

2.6.6 Bengal Basin

Although the Bengal basin is occupied by very thick sediments, the high seismic activity of the region indicate tectonic movement occurring probably within the basement. Some high intensity earthquakes have been reported from this basin. It may be seen in Figure 2.4 that the northeastern part of the basin has shown quite high seismic activity (Verma, 1991).

2.7 GRAVITY TECTONICS

The gravity map of the region reveals the nature of underlying geology in the crust and the upper mantle Mukhopadhyay and Dasgupta (1974). The Bouguer anomaly in the region varies from +44 mgals over Shillong Plateau to -225 mgals near North Lakhimpur (latitude 27°15'N and longitude 94°07'E) in the Brahmaputra basin (Verma et al., 1976). In this entire northeastern part of India, two major trends in the anomaly contours are prevalent. One is an east-west trend, almost parallel to the structural trend of the eastern Himalaya, and the other north-south, parallel to the structural trend of Indo-Burman ranges on the east. Figure 2.6 shows the gravity anomaly map of Northeast India.

Very high gravity value over the Shillong Plateau indicates presence of relatively

higher density rocks beneath the plateau. The large positive isostatic anomaly is due to excess mass per unit area and this could be due to intrusion of high density material from the mantle into the crust through deep seated faults like Dauki Fault (Verma et al., 1976). Maximum gravity value is observed towards south of the plateau bordering the Dauki Fault. Across the Dauki Fault system, the area is associated with a very steep gravity gradients (Mukhopadhyay and Dasgupta, 1988). Towards east, a conspicuous increase in gravity of about 20 mgal is observed near Haflong around the complex junction of the Haflong Thrust and Dauki Fault possibly due to buried intrusive body at 4 to 23 km depth (Verma and Gupta, 1973).

In Bengal basin, the Bouguer anomalies range between 0 to -25 mgal in comparison to very high anomaly over Shillong Plateau (Fig. 2.6). Bengal basin shows alternating gravity highs and lows (Mukhopadhyay and Dasgupta, 1988) indicating existence of structural high and depressions underlying this basin. In general, gravity values decrease towards north in the Rajmahal gap area between longitudes 86°E to 90°E . From west of Bengal basin, gravity increases gradually and is high over Barisal high. In the east, gravity decreases to -175 mgal over the Burmese central plain land and again increases further east (Fig. 2.6).

Towards east, lithosphere is descending below the Burmese Fold Belt. An oceanic crust is required for this type of plate movement and subduction zone. Burke and Dewey (1973) and Verma and Mukhopadhyay (1977) believe that the Bengal basin is underlain by oceanic crust in its deeper part. However, Brune and Singh (1986) have suggested a continental crust below the sediments in the alluvial cone on the basis of dispersion study of surface waves. Mukhopadhyay and Dasgupta (1988) and Brune et al. (1990) recently suggested that the crust underlying the basin may be semioceanic type.

2.8 DISCUSSIONS

From geotectonic history of the northeastern part of India, it is evident that the region has suffered prolonged and complex tectonism. The Indian plate, with the Shillong Plateau as its minimum eastern extension has suffered collisional tectonics

from both the north and east directions during the Cenozoic (Powell et al., 1988). However, prior to beginning of the compressional tectonism, the India Plate should have subjected to extensional tectonics, which was responsible for the formation of the Rajmahal and Kopili grabens in Northeast India (Fig. 2.7).

The Shillong Plateau documents intense tectonism in the Archean rocks which show polycyclic folding and metamorphism. The plateau has suffered extensive thermal events. Numerous fracture lineaments and faults within the plateau are the testimony of intense tectonism.

The strikingly linear Dauki Fault along the southern margin of the Shillong Plateau must have played an important role in the tectonic history of the plateau. However, fault mechanism along the prominent Dauki Fault remained unclear till today, as three types of mechanism have already been put forward. Convergence in the Himalaya has shifted southward across the thrusting sequence (Le Fort, 1975; Mattauer, 1975). Hence, it is a matter of discussion whether the Dauki Fault may be considered as the southernmost tectonic feature of the thrusting sequence.

The northern Indo-Burman Fold Belt has been subjected to different type of deformation from the north to south. This belt shows intense thrusting in the Naga Hills, but is characterized by fold belt in Tripura, Mizoram and Bangladesh region.

The present tectonic set-up in whole of Northeast India is that of compressional with stresses oriented in NW-SE, N-S, E-W and NE-SW directions (Fig. 2.8). Active sea floor spreading in the Andaman sea prospects for further compressional tectonism in Northeast India. This type of tectonism has resulted various type of structural features in Northeast India, as can be seen in Figure 2.9, which also shows cross sections across the Himalaya and Naga hills.

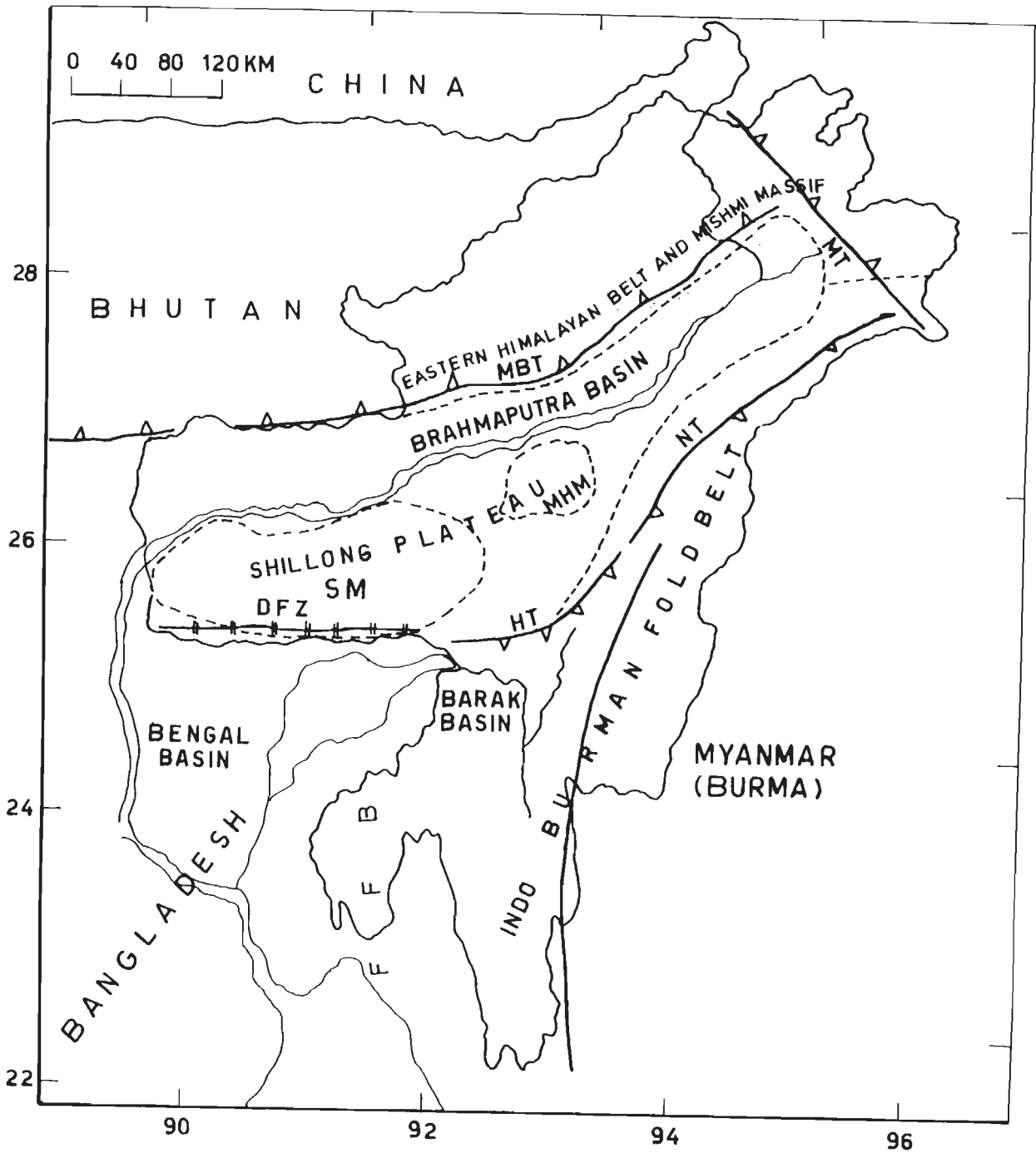


Figure 2.1. Major geotectonic provinces of Northeast India. SM-Shillong Massif, MHM-Mikir Hills Massif, MBT-Main Boundary Thrust, MT-Mishmi Thrust, NT-Naga Thrust, HT-Haflong Thrust, DFZ-Dauki Fault Zone, FFB-Frontal Fold Belt.

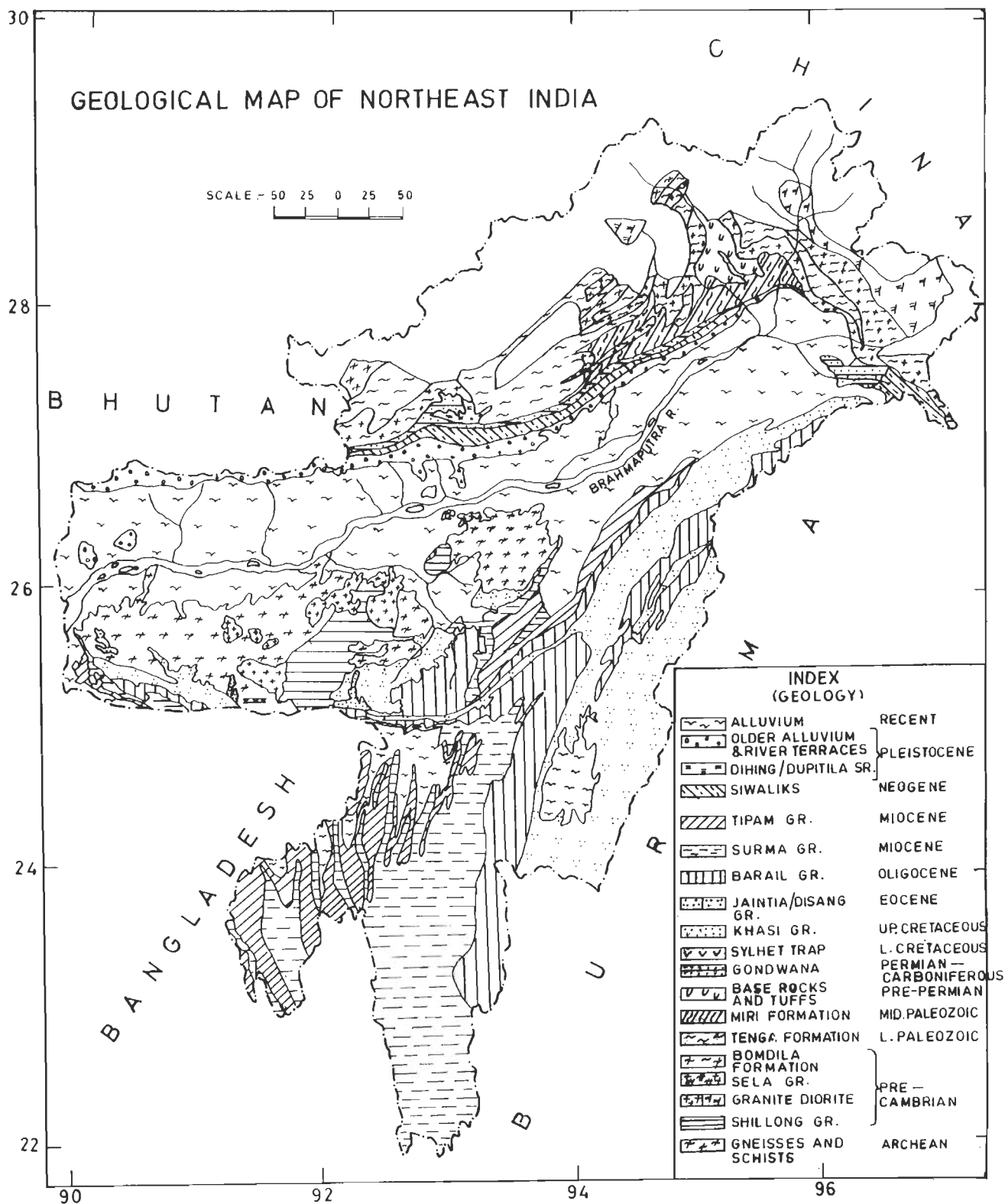


Figure 2.2. Generalized geological map of Northeast India. The complete geological information of Arunachal Pradesh is not available which is shown by the blank area. (After Geological Survey of India, 1974)

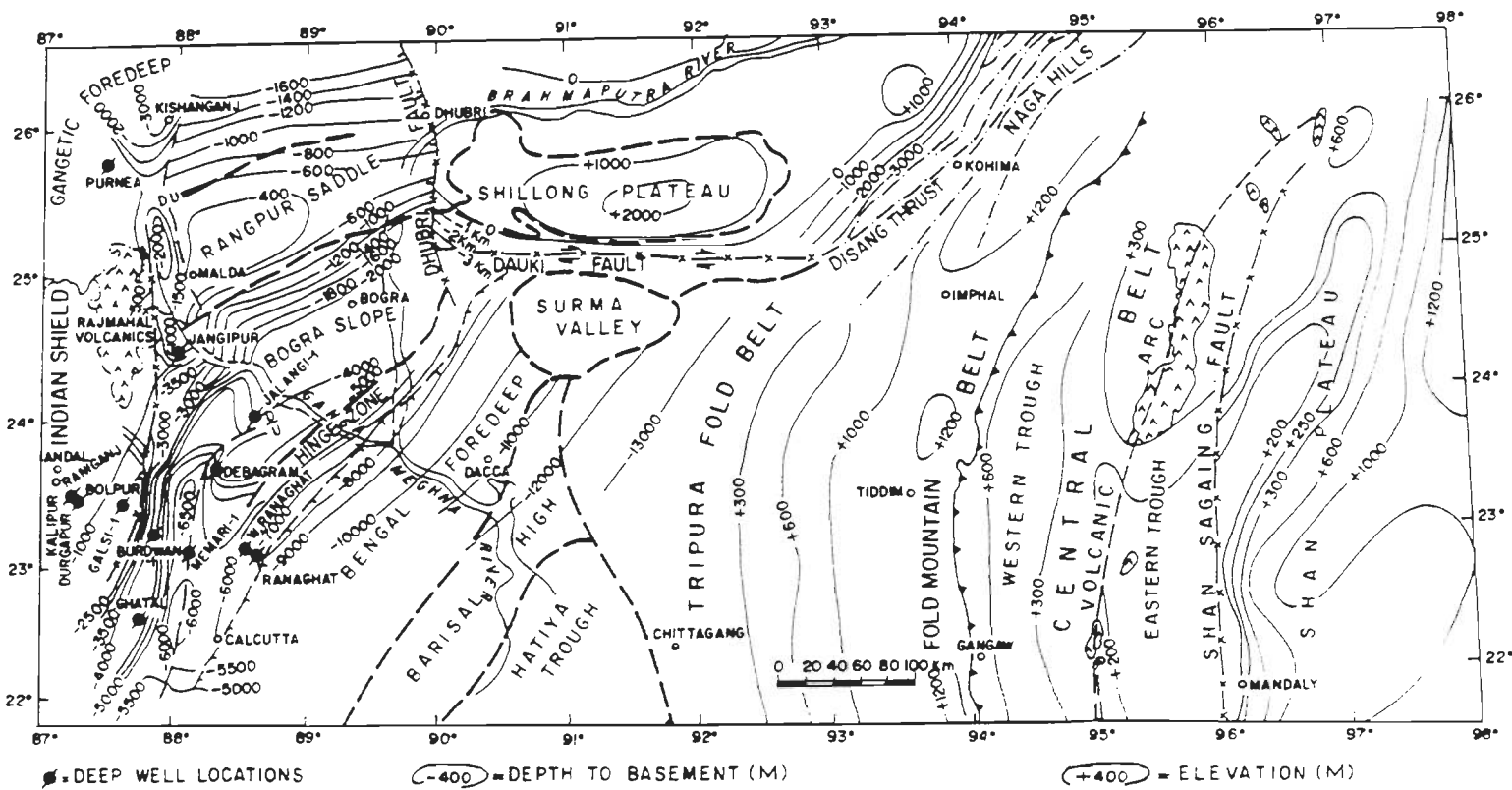


Figure 2.3. Basement configuration map for the Shillong Plateau and adjoining regions in Northeast India. Contours are in meters. (After Mukhopadhyay and Dasgupta, 1988).

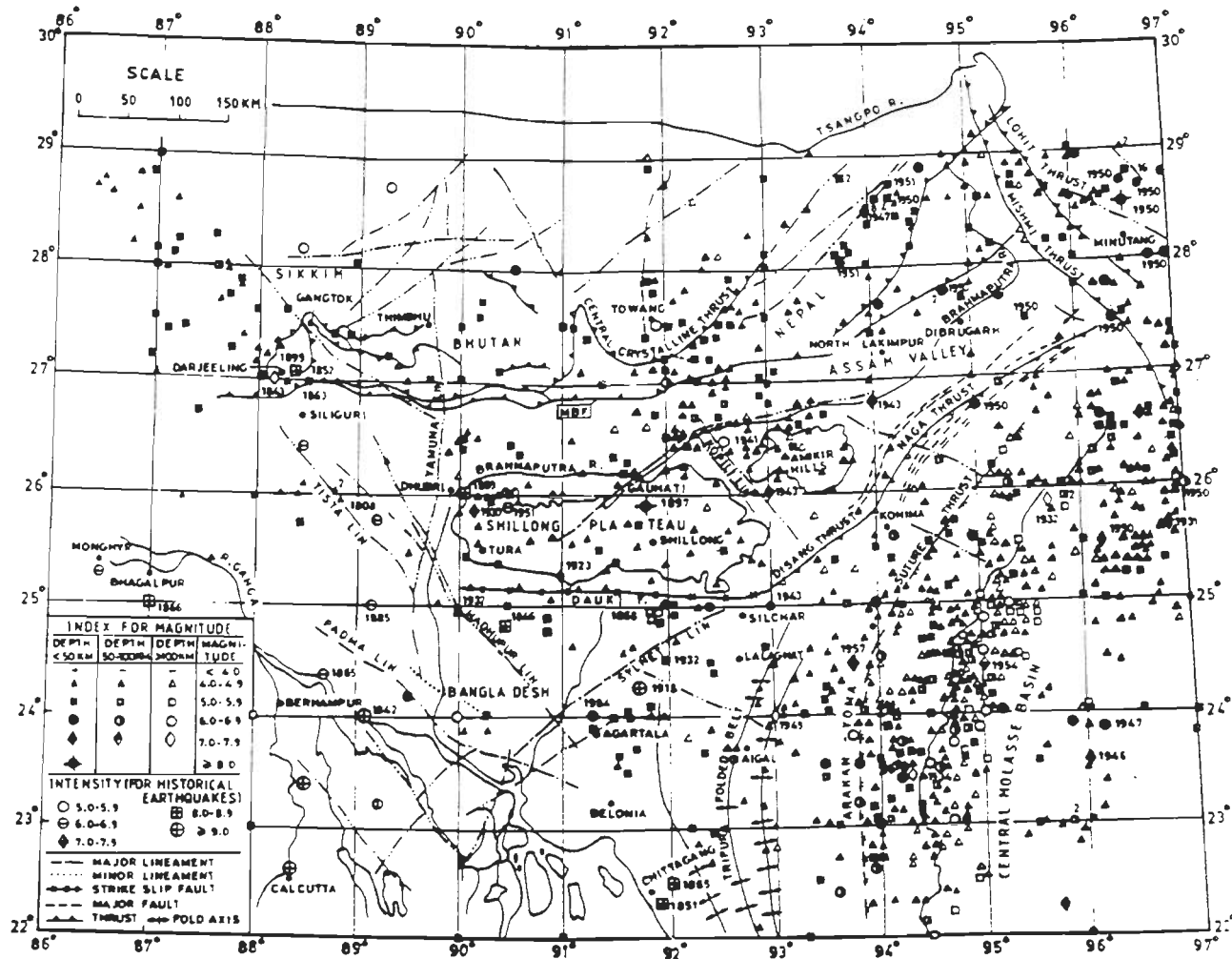


Figure 2.4. Map shows the earthquake occurrences and tectonic features in Northeast India and adjoining regions. Earthquake distribution are shown with respect to depth and magnitude. (After Verma, 1991).

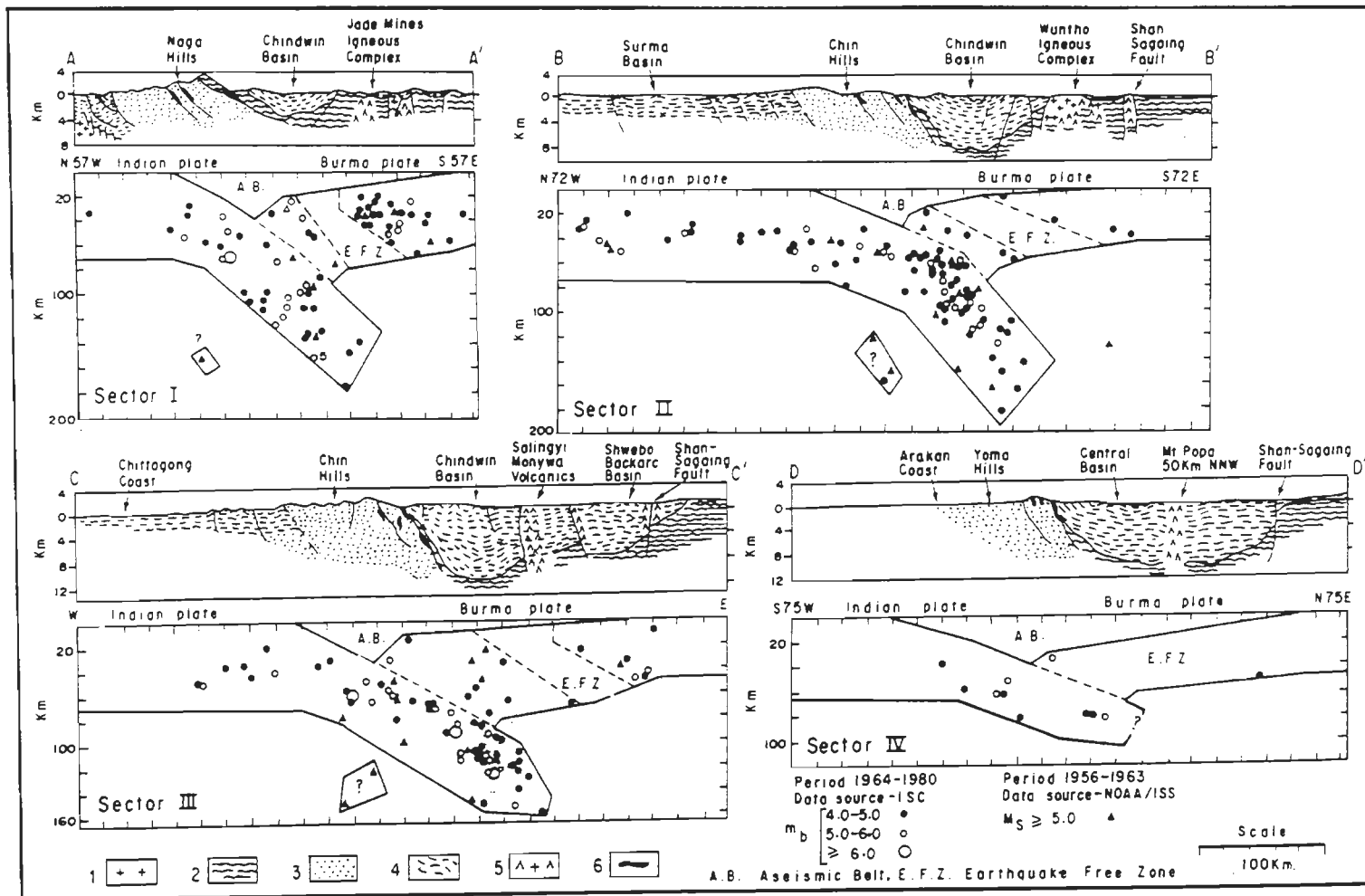


Figure 2.5. Surface geology and the underlying seismic zones along the Indo-Burman fold belt. Geologic index: 1=crystalline basement; 2=metamorphics; 3=flysch; 4=molasse; 5=volcanics; 6=ophiolites. Sections AA', BB', CC' and DD' are along the latitudes 26.5°, 25°, 22° and 19.5° N respectively from north to south (After Mukhopadhyay and Dasgupta, 1988).

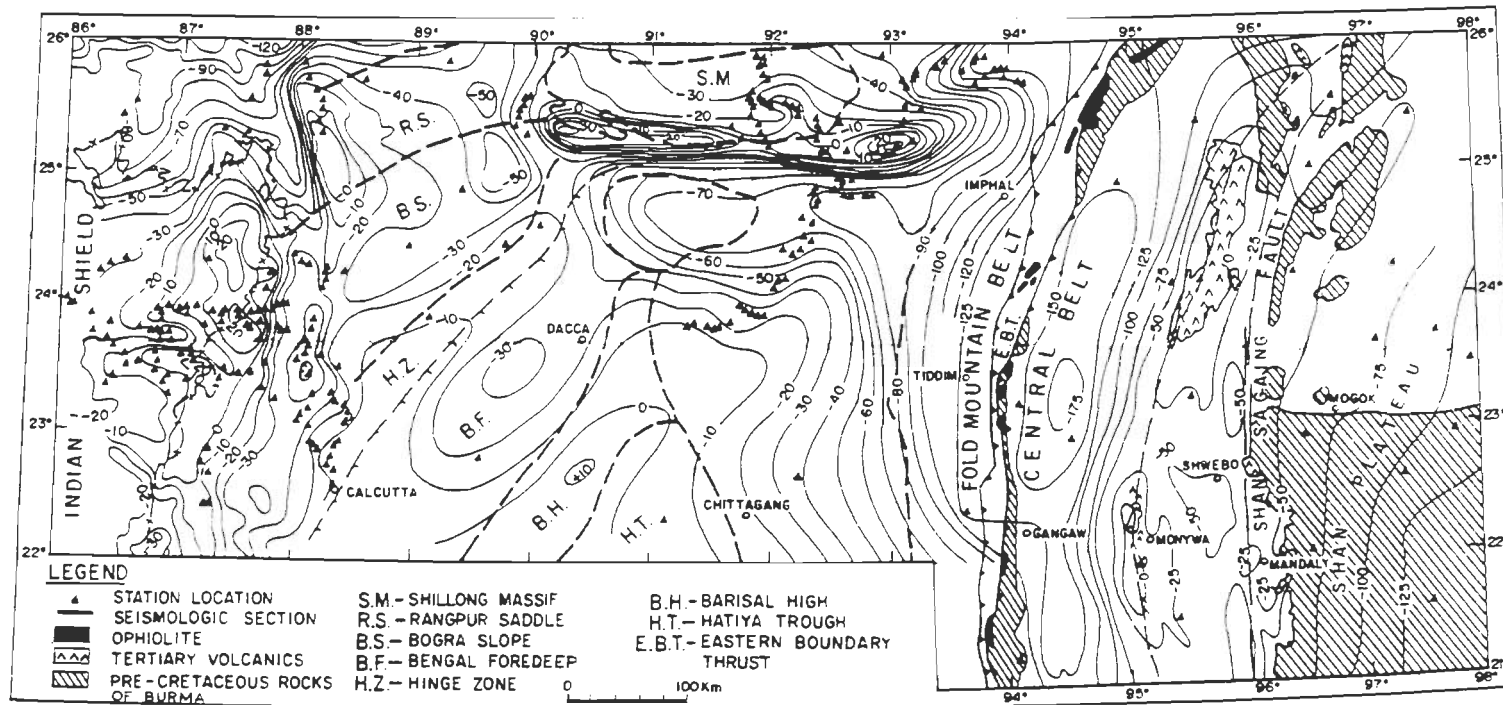


Figure 2.6. Bouguer gravity map of Shillong Plateau and adjoining areas. (After Mukhopadhyay and Dasgupta, 1988).

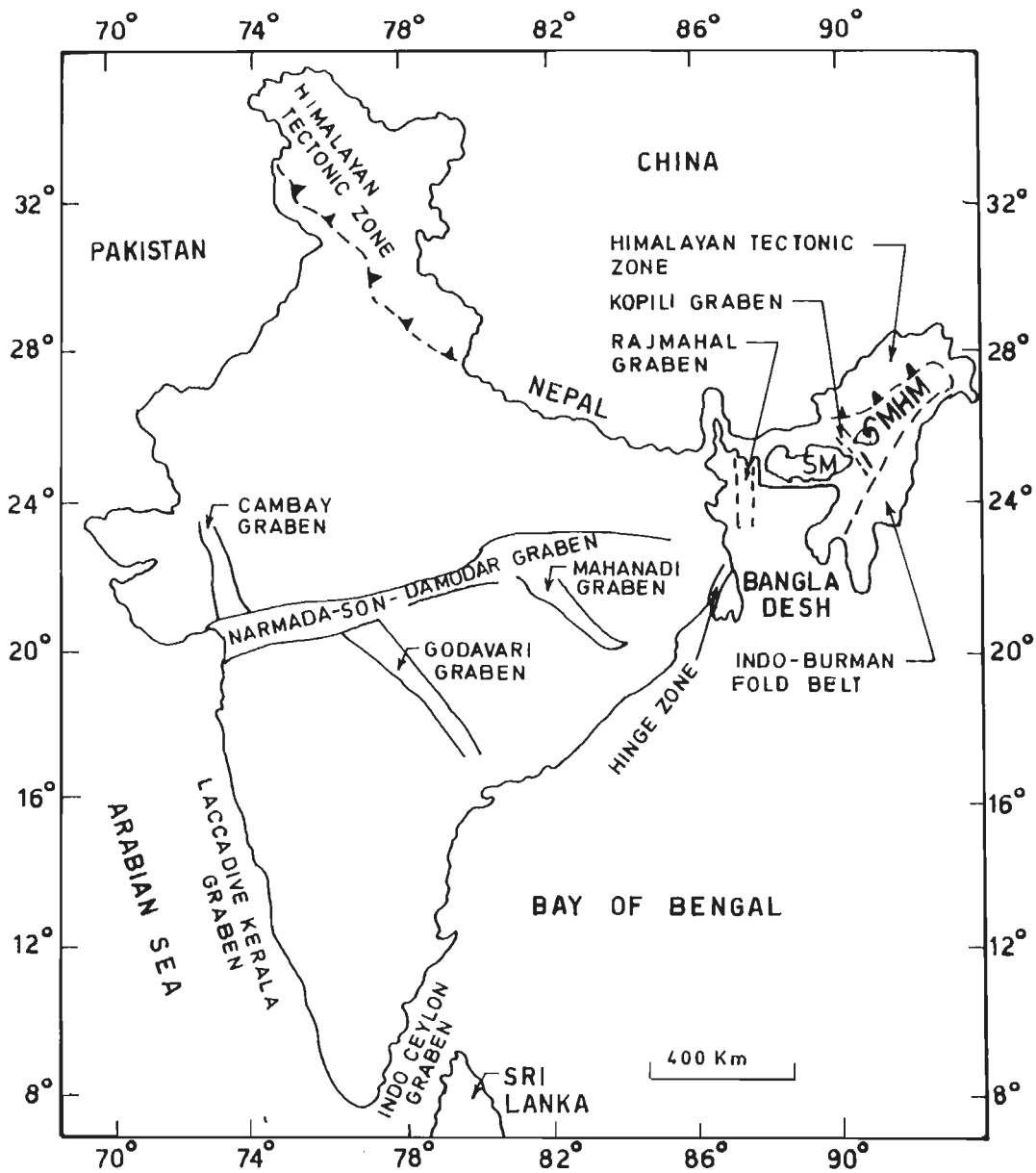


Figure 2.7. Map of India shows Kopili and Rajmahal grabens in Northeast India and other major graben structures formed in the main land mass. SM-Shillong Massif, MHM-Mikir Hills Massif.

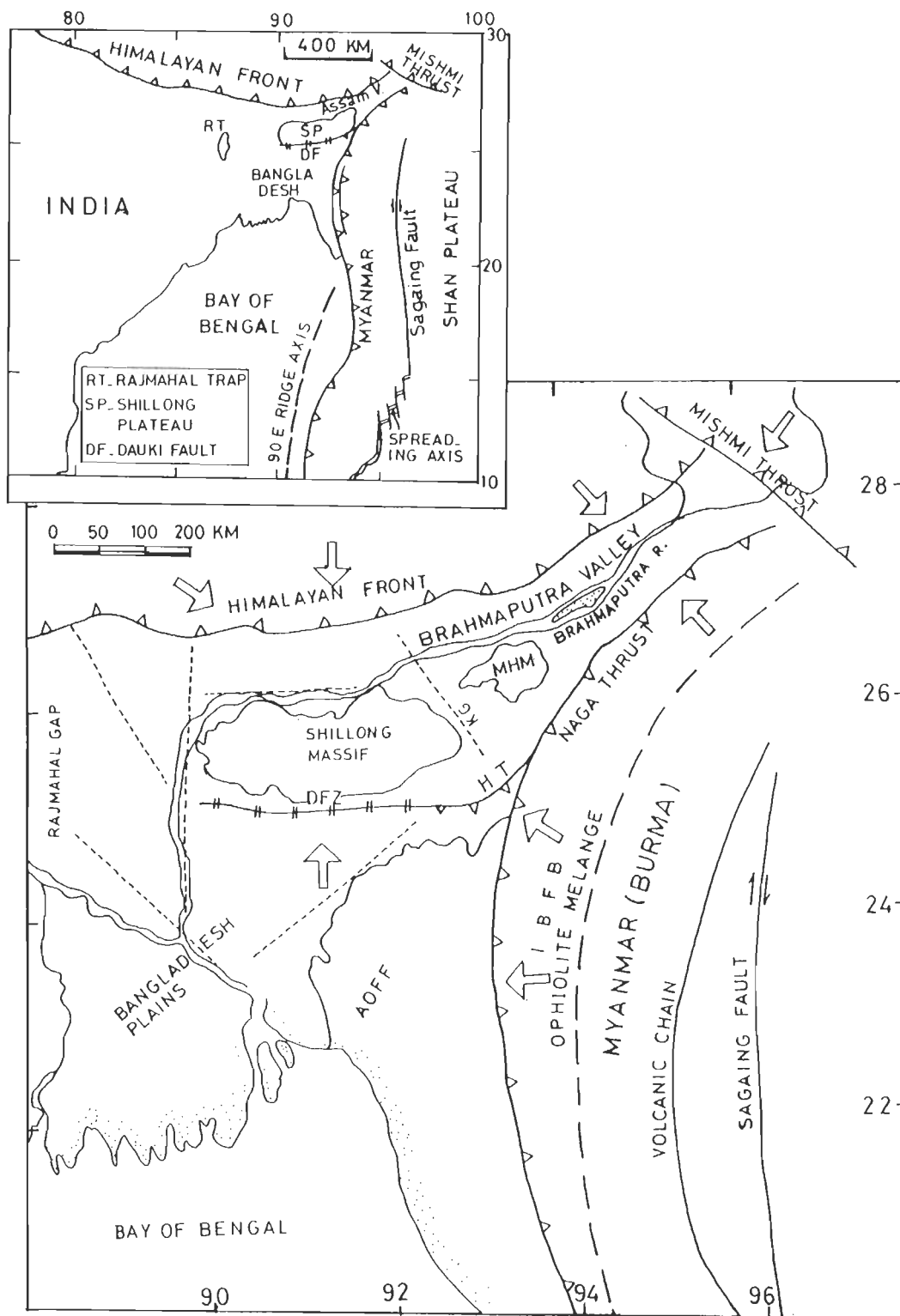


Figure 2.8. Regional tectonic features of Northeast India and orientation of tectonic forces and regional tectonic set up showing nature of spreading of sea floor in Andaman sea.

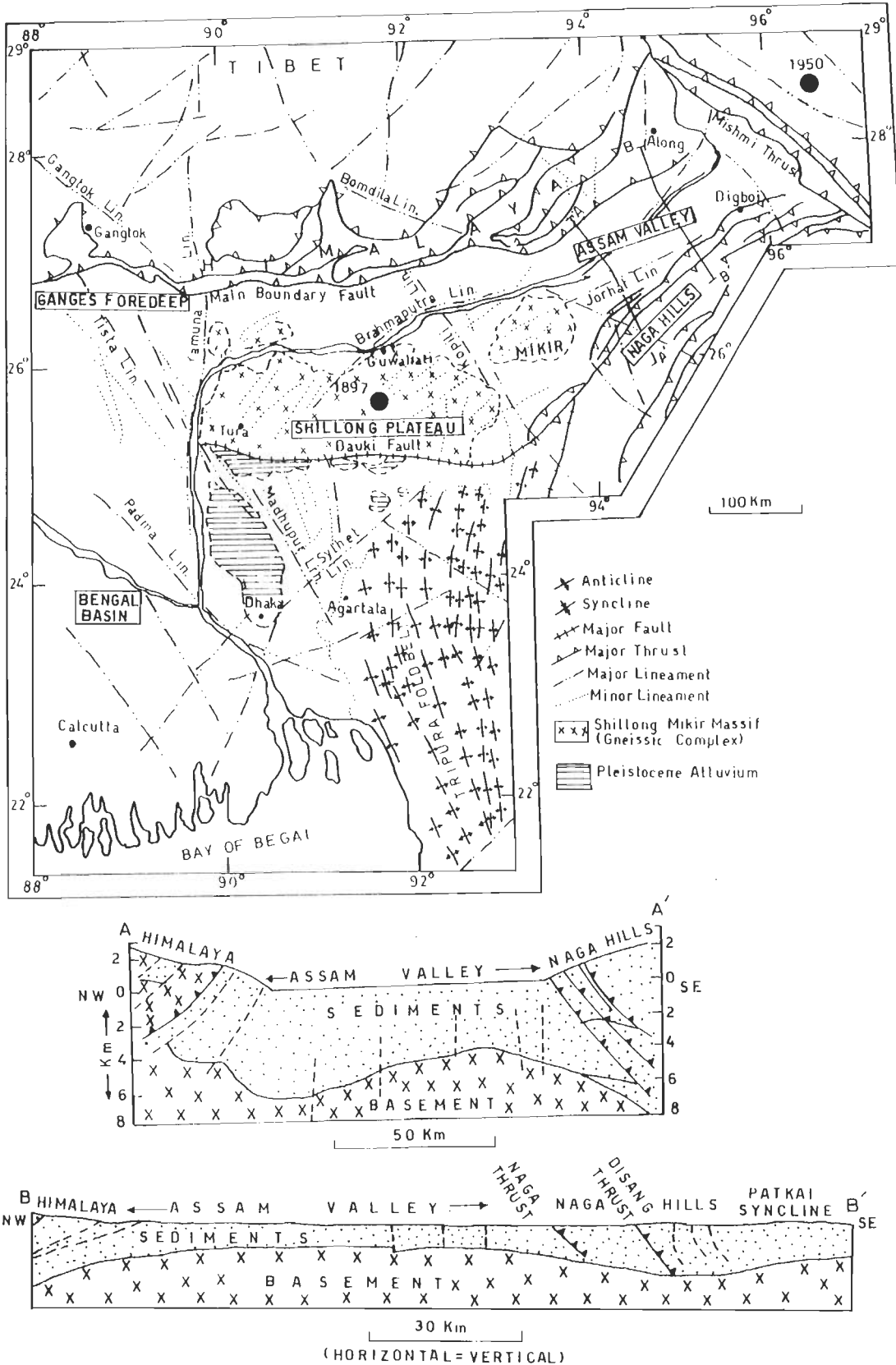


Figure 2.9. Regional tectonic map of the Northeastern India showing thrusts, folds and lineaments. Tectonic features are adopted from Nandy (1980) and Mukhopadhyay (1984). Schematic cross sections along AA' and BB' are adopted from Mukhopadhyay (1984).

FRACTURE LINEAMENTS, JOINTS AND FAULTS

3.1 INTRODUCTION

Presence of numerous tectonically-significant fractures, lineaments and major/minor faults, which could be identified on the satellite images, indicate that northeastern part of India and adjoining regions have undergone intense tectonic activity. These features are described systematically to work out a comprehensive overall tectonic picture of the region with a special emphasis on the Shillong Plateau. The Dauki Fault and Barapani Shear Zone are very prominent tectonic feature which are studied in detail and presented in Chapter 4. A satellite mosaic (Fig. 3.1) provides a bird's eye view of major geotectonic and structural features of the Northeast India and adjoining regions.

In this study, lineaments are well marked, because these appear as a sharp linear cracks and are identifiable very distinctly on satellite images on the basis of tone, texture, pattern and shape variations across the features and context and scale of the feature. Any linear feature, which may be marked merely by linear arrangement of tonal variations only, are not considered in this study. Fracture lineaments should have formed due to some internal geological processes. O'Leary et al. (1976) have reviewed the concept of lineaments and proposed the following definition:

"A lineament is a mappable single or composite linear feature of a surface, whose parts are aligned in a rectilinear or slightly curvilinear relationship and which differs distinctly from the pattern of adjacent features and presumably reflects a subsurface phenomenon".

Data on joints from the rock exposures at different road sections of Shillong

Plateau have been collected and are analyzed. The Schmidt equal area projection chart has been used in plotting of joints.

The alluvial deposits of the Brahmaputra and Barak River Basins have been greatly affected tectonically, as the region had undergone collisional tectonism from the north and east. These two major rivers show migration of their channels.

In this chapter, different lineaments, joints, faults, structural features and river morphology have been studied and correlated with the tectonics.

3.2 PROMINENT FRACTURE LINEAMENTS

In a tectonically-active area, the lineaments of regional scale may play an important role. A few tectonically significant lineaments from the area have been identified and are discussed in this chapter (Fig. 3.2).

3.2.1 Brahmaputra Lineament (BL)

Remarkably linear course of the mighty Brahmaputra River seems to be controlled by some tectonic features. The river course is specially linear between longitudes 90°E and $94^{\circ}30'\text{E}$ (Fig. 3.1). In this sector, the river flows along the northern margin of the Shillong and Mikir Hills Massifs, except the river shows northward migration in the area between these two massifs. The river flows linearly in a WSW direction for 280 km between the longitudes $91^{\circ}45'\text{E}$ and $94^{\circ}30'\text{E}$. Further, the river course is remarkably E-W along the northern fringe of the Shillong Massif.

3.2.2 Sylhet Lineament (SL)

The prominent Sylhet lineament has long been recognized in this region. This lineament trends NE and truncates the N-S trending frontal fold belt. These fold ridges exhibit eastward dragging affect along this lineament, as these fold takes eastward swing (Figs. 3.1, 3.13). This lineament extends for about 140 km. The Kusiya River flows along this lineament for 35 km. The area is occupied by alluvial deposits and numerous water bodies and hence, the characteristics of the lineament on surface are masked.

Study of a 1968 earthquake indicate thrust faulting along this feature (Tandon and Srivastava, 1975). However, Dasgupta and Nandy (1982) suggested deep-seated high angle reverse fault, having a dip of about 70° towards southeast along this lineament.

3.2.3 Tista Lineament (TL)

This lineament controls the almost linear course of the Tista River and has a length of about 200 km (Fig. 3.2). This lineament may continue southeastward until the Madhupur highland in Bangladesh (Fig. 3.13). The eastern margin of this highland has very sharp contact with the alluvium and is marked by a lineament, which trends NNW-SSE. Moreover, the Brahmaputra River takes a south southeastward turn for a short distance and follow this lineament in the area of the highland.

3.2.4 Kopili Mega-Fracture (KFR)

The prominent N-S trending fracture systems could be recognized between the Shillong and Mikir Hills Massifs (Figs. 3.2; 3.13). These faults have dissected the plateau in such a manner that the area show different N-S trending blocks. The satellite images reveal translational movement along these fractures. These blocks show systematic northward shift, indicating drifting of the Mikir Hills Massif farther north in comparison to the Shillong Massif.

3.2.5 Kalyani Lineament (KYL)

This is a E-W trending fracture system dissecting almost whole length of the Mikir Hills (Figs. 3.2, 3.13). The Kalyani River flows along this fracture linearly before taking a northward turn at longitude $93^{\circ}45'E$. The occurrences of hot springs are also reported from this fracture zone, indicating deep nature of the fault. This fault is marked by distinct fractures, as can be seen on the satellite image. A number of minor earthquake epicenters are also located along this fracture zone (Fig. 3.13).

3.2.6 Indo-Burman Fold Belt Lineaments (IBL)

Four major transverse lineaments could be recognized in the northern Indo-

Burman Fold Belt. These are IBL1, IBL2, IBL3 and IBL4 (Fig. 3.2). These lineaments dissect the N-S trending fold ridges of the frontal fold belt. The IBL2 traverses through the central Manipur and Barak Basin. Another lineament intersects with IBL2 at longitude $93^{\circ}15'E$, and at the intersection the rocks show intense deformation and lateral slip too.

The IBL3 trends WNW-ESE and coincides with the southern margin of the Mikir Hills and northern edge of the Shillong Massif (Fig. 3.2). This is highly linear and disturbs the Naga Foothill sediments.

It may be observed that parts of northern Indo-Burman Fold Belt had suffered different degree of deformation (Fig. 3.1). The southernmost block between IBL1 and IBL2 has migrated westward into the Bangladesh Plains, whereas the block north of IBL2 has suffered intense deformation.

3.3 LINEAMENTS AND JOINT TRENDS

3.3.1 Lineament Trends

Lineament map of whole northeastern India and adjacent area have been prepared from satellite image mosaic (Landsat TM band 4). The region has been classified into different zones on the basis of geotectonic set up, and the general lineament trends are shown in Figure 3.3. In the northern Indo-Burman fold belt and Himalaya, the predominant lineament trend follow the regional structure (Figs. 3.3, 3.4, 3.5). However, the lineament trend shows a variation in the Shillong Plateau.

Azimuth distribution of lineament in the Shillong Plateau shows that the northeastern quadrant has the maximum occurrences of lineaments (Fig. 3.3). However, it appears that distribution of lineament in northwestern quadrant has a reduced tendency in the eastern part in comparison to the western part of the plateau. This indicates that the NE-SW trending lineaments are the predominant ones. Therefore, this variation in lineament trends within the Shillong Plateau is attributed to the tectonic activities. Figures 3.6 and 3.7 show the fracture lineament pattern of the western and central part of the Shillong Massif.

3.3.2 Joint Trends

Joints are probably the most common structures exposed at the present day surface. Joints may be defined as fractures of geological origin along which no appreciable displacement has occurred (Ramsay and Huber, 1987). Joints are generally confined within the uppermost crust. Joints may be of extensional and shear origin.

During the field visits, data on joints have been collected from the Precambrian quartzite, phyllite, dolerite and Tertiary sedimentary rocks. Since the Shillong Plateau had been subjected to multiple phases of extensional and compressional tectonism in different directions, it became difficult to recognize particular stress orientation belonging to a episode from data analysis.

Joint data collected from different sectors and their rose diagrams are shown in Figure 3.8. Figure 3.9 shows stereonet plotting of joints from different sectors.

(i) Pynursla Sector: In this sector, the Precambrian quartzite show systematic development of two to three set of joints, whereas many set of joints have developed in dolerite rocks. In Figure 3.10A, a systematic joint set in quartzite can be seen. The rocks dip $28^{\circ}/N110^{\circ}$ and are affected by joints dipping $75^{\circ}/NE$, $65^{\circ}/N$ and $77^{\circ}/S$. The joints are closely-spaced with surfaces showing widening effect. An antiformal fold in quartzite with fractures along axial plane can be seen in Figure 3.10B. Stereo plotting of joints show that J3 and J4 may form conjugate pattern (Fig. 3.9).

(ii) Mawphlang-Tyrsad Sector: The Precambrian phyllite are predominantly exposed in this sector. Since this sector falls in a shear zone, the rocks show multiple set of fractures and joints. Joints plotting reveal that the prominent trend is NE-SW (Fig. 3.9).

(iii) Mawngap-Sohiong Sector: In this sector, the Precambrian quartzites are intercalated with phyllites. This sector also falls in a shear zone, where these rocks show multiple joint sets and trends. Joints J4 and J5 may form conjugate pattern (Fig. 3.9).

Fracture/joint trends from the Precambrian rocks reveal that N-S oriented fractures are predominant. The NW-SE and NE-SW oriented fractures are also

common. This pattern corroborates with the general lineament pattern.

(iv) Dauki Fault Zone: Data from four sectors-Balat-Shella, Borhir-Dauki-Muktapur, Umkiang-Ratacherra and Umkiang-Sonapur have been analyzed. The rocks in these sectors are predominantly sandstones. Rose diagrams show that the E-W oriented fractures are prominent in Balat-Shella and Borhir-Dauki-Muktapur sectors (Fig. 3.8). Towards east, the fracture trend shows swing to the NE in Umkiang sector (Fig. 3.8).

3.4 GEOLOGIC AND TECTONIC DESCRIPTION OF LINEAMENT

The domain of NE-SW trending strong lineament pattern affects the Shillong Massif throughout. These lineaments are parallel to the NE-SW trending Barapani Shear Zone. Similar trending lineaments may have shear origin. Joints from the Precambrian quartzite and phyllites show extensional and shearing fractures. Therefore, it may be inferred that the shear fractures had formed due to the compressional forces. Mostly, the granite bodies of the Shillong Plateau show prominent N-S and E-W oriented fractures. But, the granite pluton adjacent to the BSZ show also the NE-SW oriented fractures.

In the Dauki Fault Zone, the E-W trending fractures are parallel to the Dauki Fault and probably formed under extensional environment. Whereas, the N-S trending fractures cutting the Dauki Fault may have different origin. Field studies of fracture and joints on rocks show the NE-SW and NW-SE trending shear conjugate fractures. There are also a few N-S and E-W trending fractures. Figure 3.11 shows the stress model for fracture lineaments.

3.5 PROMINENT FAULTS

The Shillong Plateau and adjoining areas had been dissected by many faults, as can be seen on satellite images (Fig. 3.12). Different faults, major and minor, as identified on images are shown in Figure 3.13 along with epicenters of important earthquakes.

3.5.1 Um Ngot Fault (UGF)

The Um Ngot Fault is strikingly linear N-S trending feature and located just east of longitude 90°E (Figs. 3.7, 3.12, 3.13). A river flows along this fracture for a distance of more than 30 km before taking westward turn at latitude $25^{\circ}18'\text{N}$ (Fig. 3.7). Actually, this river again shows a huge westward curvature before entering into Bangladesh. The course of this river follows the lithological contact between Eocene and Precambrian rocks.

In this region, the general strike of the Precambrian rocks is NE-SW. These rocks have been cut cross by the UGF east of Shillong (in fact, minor linear ridges are truncated by this fault). The rocks show northward dragging effect due to dextral movement (Fig. 3.7). This fault can not be traced in the Eocene rocks, south of latitude $25^{\circ}15'\text{N}$ indicating that this fault was active only before the Eocene time.

A huge intrusive body, expressed as a circular feature on satellite images, is also fractured by this fault. Chattopadhyay and Hashimi (1984) and Krishnamurthy (1985) reported that there is an alkaline-ultramafic-carbonatite complex exposed along this fault. Recently, Gupta and Sen (1988) speculated that the N-S trending Um Ngot fracture and their associated carbonatite rocks are genetically-related to Ninety-East Ridge.

This fault must be very deep-seated, so that magmatic intrusions could take place along this fault. The Um Ngot Fault and BSZ intersect at latitude $25^{\circ}50'\text{N}$ to form a triangle-shape zone where the Um Ngot Fault shifts the BSZ northward (Figs. 3.7, 3.12, 3.13, also see Fig. 5.7). The intersection of these two faults is tectonically significant, as it may likely be the site for future earthquake occurrences. Intersection forms the locked area of a fault and controls stress build-up. Moreover, movement on one fault is inhibited by intersecting fault and results into high stress build-up, sufficient to generate the major earthquake (Talwani, 1989).

3.5.2 Dudhnai Fault (DNF)

The N-S oriented Dudhnai Fault controls the course of a river for around 40 km,

and to the south, displaces the Dauki Fault dextrally (Figs. 3.6, 3.12, 3.13). The initial 35 km long course of the Dudhnai River is controlled by this fault. Towards north, this fault forms erosional valley and quite a few NE-SW trending fracture traces terminate against this fault (Fig. 3.12).

This fault coincides with the Nongchram Fault, as described by Golani (1991). Along this fault, a zone of fault breccia, gouge, silicification and rare mylonitization has been observed. The alkaline magmatic rocks, e.g., carbonatite was emplaced along this fault, which indicate deep-seated nature of the dislocation. This fault traverses rocks of Precambrian to Tertiary age. From the disposition of the porphyroblastic biotite granitoid, displacement for 1.5 km in a right lateral-sense could be estimated. Golani (1991) suggested the development of fault in a tensional regime with a very insignificant strike-slip component. He also observed change in the course of a minor river. Quite a few micro earthquakes epicenters are found to be located along this fault (Kayal, 1987). These features indicate activity of the fault in recent past.

3.5.3 Jamuna Fault (JF)

The Jamuna Fault represents a regionally important fault. The straight N-S course of the Brahmaputra River, running along the western margin of the Shillong Plateau is mainly controlled by this fault. Also, this river takes amazingly 90° southward turn and follows this fault for about 200 km (Figs. 3.12, 3.13). The Jamuna Fault extends toward north until the Bhutan Himalaya (Nandy, 1980).

3.5.4 Kopili Fault (KF)

The Kopili Fault zone trends NW-SE and separates Shillong Massif from Mikir Hills Massif. The Kopili River flows along this fault zone and coincides with the well-known Kopili graben. Now, the area is covered under alluvial deposits (Fig. 3.12).

3.5.5 Guwahati Fault (GF)

A prominent sinistral fault (Guwahati Fault) traverses Shillong Plateau and the Brahmaputra River valley (Figs. 3.2, 3.6, 3.13). Beyond Guwahati, the Brahmaputra

River follows the trend of this fault.

3.5.6 Haflong Thrust Zone (HTZ)

The effects of thrusting on sedimentary rocks can be seen in the eastern parts of the Shillong Plateau between longitudes $92^{\circ}15'$ and $93^{\circ}30'E$. This is known as the Haflong Thrust, which trends in the E-W direction in the western parts. Sediments in the adjacent area south of the thrust show intense folding (Figs. 3.14 A, B). This thrust gradually changes to northeast and merges with the **Disang** Thrust. Towards east, beyond longitude $92^{\circ}E$, the DFZ has been overlapped by the thrust zone (Figs. 3.14 A, 3.15). This area is tectonically significant, as quite a few important structural features have developed (Das et al., in press). Initially, E-W trending HTZ should have formed due to the N-S oriented compression, whereas the NE-SW trending part had formed due to NW-SE oriented compressive forces.

Earthquake activity in the HTZ is reported to be extremely low. It is quite strange phenomena that the HTZ is relatively seismically less active, whereas many earthquake events had occurred in the surrounding areas. It is probably due to creep phenomena, which is taking place along the HTZ.

3.5.7 Dapsi Reverse Fault (DRF)

In the western part of the Shillong Plateau, a minor WNW-ESE trending high angle reverse fault (Dapsi Reverse Fault) could be recognized on satellite images (Fig. 3.16). As discussed earlier, the Precambrian rocks are thrust southward on the Tertiary rocks. This fault forms the boundary between these two group of rocks.

This reverse fault can be traced for 55 km on satellite images (LISS II, FCC). This fault is sigmoidal in shape and forms a highland with a steep scarp to the south. This area acts as a watershed with the Simsang River flowing eastward north of this fault and taking a 90° southward turn only at the eastern end of this highland (Fig. 3.6, 3.16). Incidentally, this reverse fault is parallel to the MBT in the Himalaya. Along this fault, intense microearthquake activity indicate concentration of high stress. The fault plane solution indicate ENE-WSW compressional stress in the area (Kayal, 1987).

3.5.8 Tyap Fault (TF)

The most significant longitudinal fault in Mizoram area is the Tyap Fault, which is located along its eastern border. This fault is marked by well-defined fractures in geological formations. Towards the north, development of characteristic array of shear fractures could be seen (Figs. 3.17 A, B). These shear fractures are antithetic Riedel shears (R_2) and additional shear fractures are P and X type (Fig. 3.17B). Moreover, the course of Tyap River is controlled by this fault. This river has been shifted southward by the fault at two places at latitudes 23°N and 22°N . Incidentally, the N-S trending folded Tertiary sediments in the area west of this fault are truncated against a NNW-SSE trending feature, marked as thrust indicating E-W compression (Fig. 3.17 A).

3.5.9 Mohanganj and Chandghat Fault (MF & CF)

The N-S trending Mohanganj Fault is tectonically significant. This fault seems to be southern extension of the Dudhnai Fault in the Shillong Plateau (Figs. 3.2, 3.13). The area east of Mohanganj Fault has been subsiding and producing huge marshy land. Remarkably, the Surma River takes a sharp turn towards south along this fault after flowing westward. Farther south, the Mohanganj Fault controls part of the Old Brahmaputra River and Padma River. Another important N-S trending fault is the Chandghat Fault, located east of Sylhet Trough (Fig. 3.13). This fault is probably the southward extension of the Um Ngot Fault. E-W trending folds in the area south of the Dauki Fault Zone has been truncated sharply along this fault. The Surma River has shifted southward in Chandghat area, probably due to southward movement of eastern side of the fault.

3.6 HORST AND GRABEN STRUCTURE

These geological features are easily identified on the images in the southern parts of the Shillong Plateau. These are mostly concentrated in the region south and southeast of Shillong (Figs. 3.12, 3.18). Mostly, the grabens have formed in the Precambrian Group rocks, but some are also found in the Tertiary sediments, exposed to the southeast of Shillong.

Horst and graben structures were formed due to vertical faulting of horizontally-stratified quartzitic sandstones along well-defined fractures. The main fracture trends, responsible for formation of these structures, are the N-S, NE-SW and E-W (Fig. 3.19). Maximum number of fracture trends fall in the $N11^{\circ}$ to $N30^{\circ}$ range. The length of the large number of fractures lie in the range 400 to 1000 meters. The statistical azimuth-length distribution can be seen in Figure 3.20.

Further, length, azimuth and width of a graben have been measured by drawing a middle line dividing the particular graben into two halves (Fig. 3.21). It has been observed that azimuths have a preferred NE-SW trend. The maximum length is found out to be 27 km and maximum width 6.5 km. The relation between azimuth-length-width is shown in Figure 3.22 A & B. The width of grabens indicate that the region, where grabens have formed, had opened up considerably.

The horst and graben structures could have initiated by development of fractures with above-mentioned trends and subsequently formation of gorge (Fig. 3.23 A). Type of faulting, that has affected the rocks, may be seen in Figure 3.23 B.

3.7 OTHER IMPORTANT STRUCTURAL FEATURES

3.7.1 Himalayan Foot Hills

The Siwalik outcrops along the foothills with a gap at some places. Most remarkable and significant gap is located in the Hatisar region at longitude $90^{\circ}30'$ E i.e., west of Manas River, where northernmost crystalline spur of the Shillong Plateau coincides with this gap (Fig. 3.24). At this place, the Siwaliks are missing, while conspicuous Quaternary terraces are displaced along the MFT (Gansser, 1983). Beyond this gap towards east, the Siwaliks are more or less continuously exposed.

The Siwaliks in Arunachal Himalaya show intense deformation (Figs. 3.1, 3.5). The river courses reveal neotectonic activity in this region. The Kameng River flows initially westward in the higher reaches and after taking a sharp turn, it flows southeastward (Fig. 3.5). The area south of the Kameng River in the foothills has been elevated considerably due to thrusting, which possibly prevented its flow southward.

In the Himalayan Foothills between longitudes $90^{\circ}30'E$ and $91^{\circ}30'E$, the recent water-saturated river fans show faulting, as marked by sharp tonal break (Fig. 3.25, also see Fig. 5.18). This feature and occurrences of marshy land in this area indicate continuous activity of the MFT in this region.

3.7.2 Dafla Hills Block

A tectonic block could be recognized in the Arunachal Himalaya around Dafla and is demarcated by lineaments trending NE-SW and NW-SE (Figs. 3.26 A, B). Movement along these faults had been responsible for southward displacement of Dafla Hills block. Incidentally, this structural feature is located north of Mikir Hills across the Brahmaputra River, where the valley appears to be narrow. The Dafla Hills block is located only 35 km north of the Mikir hills.

3.7.3 Naga-Patkai Hills Region

Intense swerving of the sedimentary rocks in extreme northeastern parts can be observed in the area around latitude $27^{\circ}N$ in Patkai hills (Fig. 3.1). It seems that the Tertiary sedimentary belt wrapped around a point forming a wide arc and is subsequently truncated by the overriding Mishmi metamorphics. This swing could be attributed to the resistance offered by the Mishmi massif to the northward extension of the Indo-Burman Fold Belt and the rotational movement along the arc.

3.7.4 Interlocking Structure

This structure occurs in the Naga foothills at longitude $94^{\circ}E$ and latitude $26^{\circ} N$ (Figs. 3.27 A, B). At this place, two different fold ridges overlap and wrap around each other. This structure could have developed due to left-lateral strike slip movement along a fault, as shown in the Figure 3.27 B.

3.7.5 Folds in Haflong Thrust Zone

The spectacular display of folds in the Tertiary sedimentary rocks, located in the adjacent area south of the Haflong Thrust Zone, can be seen on images (Figs 3.28, 3.15, also see Fig. 5.12). The morphological features of these folds are very

prominently displayed. The limbs of these folds are curved and the hinges are compressed. The folds axes trend NE-SW and parallel to the major trend of the Haflong Thrust.

A few translational faults could be identified between the adjacent folds (Fig. 3.15). The morphological features of the folds indicate that these could have formed due to the NW-SE trending compressive stress.

3.8 RIVER MORPHOLOGY AND TECTONICS

The Brahmaputra and Barak are the two major rivers in northeast India beside other rivers, which drains the landmass. The nature of river course and the probable cause of migration have been studied here.

3.8.1 Brahmaputra River

Changes in the course of Brahmaputra River is a usual feature with its gradually becoming wider and causing frequent floods. On satellite images, the present Brahmaputra can be clearly seen as a migrated river course. The morphological changes of the Brahmaputra River has been studied at different sectors.

(i) Pasighat to Jorhat: In the area between longitudes $94^{\circ}30'$ and $95^{\circ}30'E$, the Brahmaputra River shows recent migration towards north, which is indicated by channel abandoning and dried-up channel (Fig. 3.29). At this place, the river migrated towards north recently for about 12 km. Moreover, innumerable paleochannels were abandoned by the river and can be seen in large area around longitude $95^{\circ}E$ (Fig. 3.29). At longitude $95^{\circ}E$, many new channels have formed along both banks of the river at Dibrugarh indicating continued northward migration.

At Neamati, the Brahmaputra takes a sharp westward turn, which is probably caused by the Jorhat Fault. This fault zone is located along the southern bank of the river and extends up to Naga foothills (Murthy and Sastry, 1981).

(ii) Jorhat-Tezpur-Guwahati: In Figures 3.30 A and B, the Brahmaputra River shows northward migration for small distance in front of the Mikir hills (Fig. 3.30 A) and for

large distance along a almost 110 km length from the longitude 93⁰E till Guwahati (Fig. 3.30 B). In latter region, the Brahmaputra River shows northward migration making a huge northward curvature (Fig. 3.30 B). The area, north of Kopili gap in Nagaon region, shows a lot of paleochannels and highly water-saturated zones. A FCC shows abandoned channels in the area north of Kopili gap (Fig. 3.31, also see Fig. 5.27). The area, north of Kopili gap, might have uplifted forcing the Brahmaputra River to migrate northward.

(iii) Guwahati to Goalpara: In this sector, the Brahmaputra River is not extensively braided and flows through granitic hills. Near Goalpara, the river flows through the massif rocks; and lot of water-saturated zones can be seen (Fig. 3.32). In this sector, the Brahmaputra flows linearly in E-W direction. It is likely that the river course is controlled by the fault running along the northern edge of the Shillong Massif.

(iv) Brahmaputra in Bangladesh: The Brahmaputra River takes a sharp southward turn at the northwestern end of the Shillong Massif. The river morphology is shown in Figure 3.33. The river flows straight southward for about 85 km. The initial 45 km part of the river flows along the western edge of the Shillong Massif.

The southward flowing Brahmaputra River course is controlled by well-known Jamuna Fault, which runs N-S along the western edge of the Shillong Plateau. There is a branch of the Brahmaputra, which flows encircling the Madhupur high to the east of present river (Fig. 3.33). Earlier, the Brahmaputra is supposed to follow this course, now known as Old Brahmaputra, only 200 years ago (Coleman, 1969).

3.8.2 Barak River

The Barak valley in southern Assam is very narrow and relatively very small. The Barail (Oligocene) hill ranges rise to the north and are located very close to the Barak River. To the south of this river, series of N-S trending anticlines and synclines are exposed.

The Barak River, after it rises from the Naga Hills, flows through the regional strike of the geological formation. The Barak River flows zig-zag in the valley (Figs.

3.28, 3.34). Then the river meanders very strongly for around 30 km. The Barak River branches out into two separate rivers at longitude $92^{\circ}30'E$, as Surma and Kusiara and enters in Bangladesh. The Surma flows close to the southern fringe of the Shillong Plateau and then takes southwest turn. Later, it follows the southern margin of the Sylhet anticline.

The Barak valley is marked by numerous lowlands filled in by water and a few ox-bow lakes (Figs. 3.28, 3.34). The river shows a tendency to straighten up the course. At longitude $93^{\circ}53'E$, the river flows southwestward and forms a semi-closed meandering loop, which is going to be abandoned in near future (see Fig. 5.29). Between longitudes $92^{\circ}50'$ and $92^{\circ}55'E$, the river shows change in its course, as can be seen on topographic map surveyed in 1971-72 and the IRS LISS II image of 1991 (Fig. 3.34, also see Fig. 5.29). Also, drying up of some water bodies have been observed in this valley. This nature of river morphology is probably due to overall upliftment of the area due to tectonic compression.

After branching of the Barak River at longitude $92^{\circ}30'E$, the Surma River flows northward as Yazoo river (shown in bottom inset Fig. 3.34). It can be seen that the Kusiara River carries most of the water following a normal course. This indicate that the Surma River formed later due to development of a depression close to southern fringe of the Shillong Plateau. This depression, is indicated by numerous ponds which are seen as blue patches on FCC (see Fig. 4.6, bottom right).

3.8.3 Tista River System

The Tista River forms a mega-fan along the Bhutan Himalayan foothills and shows eastward migration. (Fig. 3.35). In the region south of the Bhutan Himalaya between longitudes $88^{\circ}30'$ and $90^{\circ}E$, the Sankosh, Amo and other Rivers, which join with the Brahmaputra River, flow southeastward (Fig. 3.35). Eastward migration of the Tista River, as evidenced by abandoned channels, may reveal upliftment of the Rajmahal gap area.

3.9 DISCUSSIONS

The satellite image of Northeast India depicts several tectonically significant structural features. The plateau has been dissected by many faults, with its northern margin also appears to be faulted and controlling the flow of the Brahmaputra River. Morphological features, associated with the structures, have revealed nature of tectonic stresses.

Study of lineaments, faults, joints and other structural features reveals that the Shillong Plateau has suffered deformation in multiple directions and phases. Field data on joints and fractures are scanty. Nevertheless, observations have been made on the pattern of joints and fractures in order to have a correlation with the data obtained from the study of remote sensing data.

It may be observed that the Mikir Hills Massif has shifted northward more than the Shillong Massif along the N-S trending Kopili fractures (these faults are identified in the area between the Shillong and Mikir Hills Massifs at longitude 93°E as shown in Figure 3.13). Interestingly, many earthquake events are also located in this region (most of them located in the northern part of the Mikir Hills) indicating recent activity along the fault. An earthquake having depth >100 km is also located in the Kopili gap south of the Brahmaputra River indicating deep-seated character of the Kopili Fault.

The whole Assam basin has been compressed due to northward movement of the Shillong Plateau, especially in the region of the Mikir Hills. Nature of drift in the Brahmaputra River and the development of structural features in the Himalayan foothills, Naga foothills and the Shillong Plateau suggests that the Brahmaputra basin is getting compressed gradually. Das (1992) has suggested that the basin may become more narrow gradually. The Brahmaputra River shows strong northward migration, especially in the area between longitudes 92° and $92^{\circ}45'\text{E}$ indicating active tectonism. Further, deformation pattern of the Himalayan foothills also reveal recent compressional tectonics.



Figure 3.1. Satellite image (TM Band 4) mosaic giving synoptic view of Northeast India and adjacent countries. AH-Arunachal Himalaya, SM-Shillong Massif, MHM-Mikir Hills Massif, FFB-Frontal Fold Belt, IBFB-Indo-Burman Fold Belt, BR-Brahmaputra River, DFZ- Dauki Fault Zone, HTZ-Haflong Thrust Zone, NT-Naga Thrust, SF-Sagaing Fault.



247387

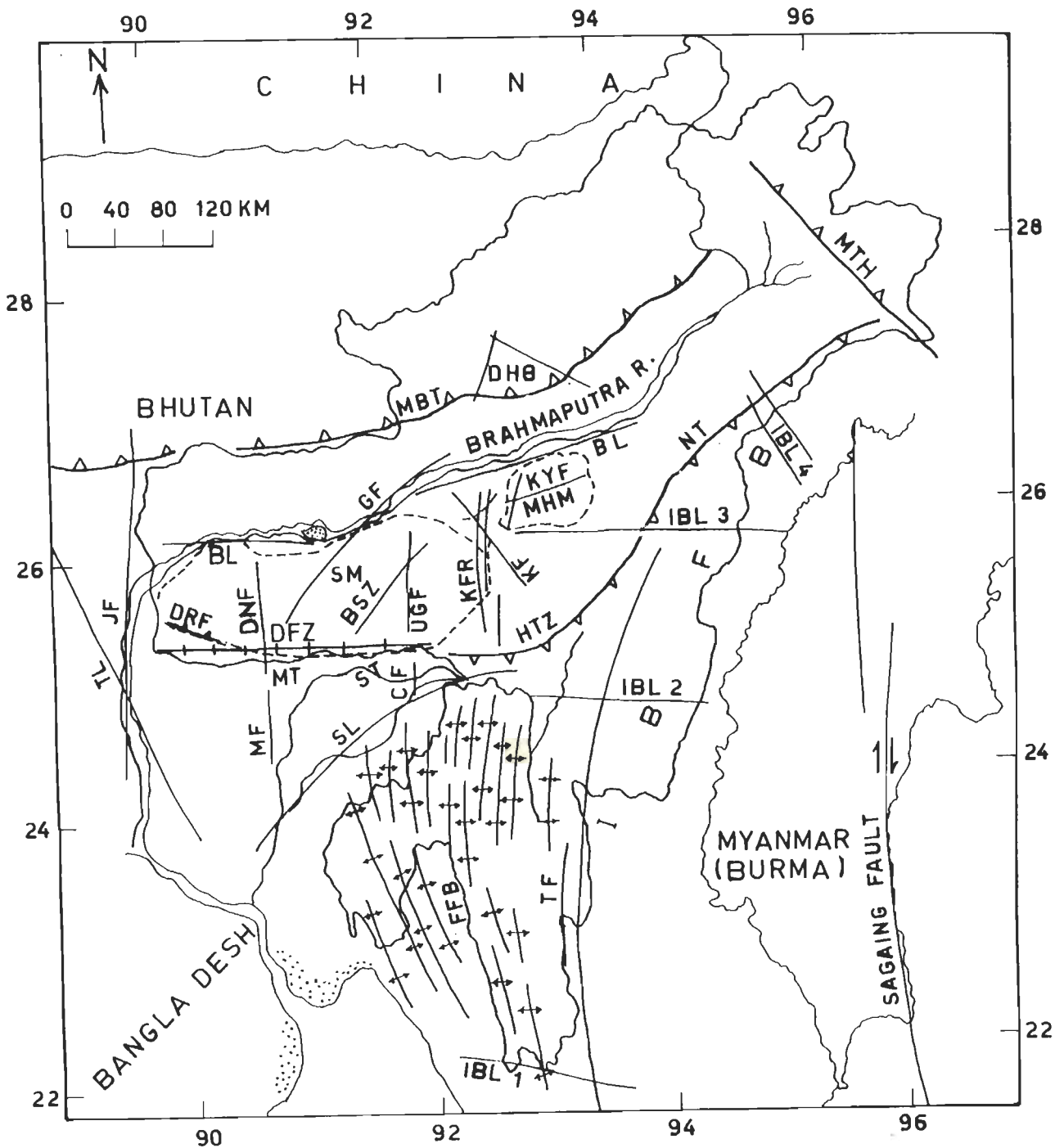


Figure 3.2. Tectonic features of Northeast India. SM-Shillong Massif, MHM-Mikir Hills Massif, FFB-Frontal Fold Belt, IBFB-Indo-Burman Fold Belt, MBT-Main Boundary Thrust, DFZ-Dauki Fault Zone, HTZ-Haflong Thrust Zone, NT-Naga Thrust, MTH-Mishmi Thrust, DHB-Dafla Hills Block, JF-Jamuna Fault, TL-Tista Lineament, SL-Sylhet Lineament, BL-Brahmaputra Lineament, IBL1, IBL2, IBL3, IBL4-Indo-Burman Lineaments 1, 2, 3 and 4, DRF-Dapsi Rverse Fault, DNF-Dudhnai Fault, GF-Guwahati Fault, BSZ-Barapani Shear Zone, UGF-Um Ngot Fault, KFR-Kopili Fracture, KF-Kopili Fault, KYF-Kalyani Fault, TF-Tyap Fault, MF-Mohanganj Fault, CF-Chandghat Fault, MT-Mohanganj Trough, ST-Sylhet Trough.

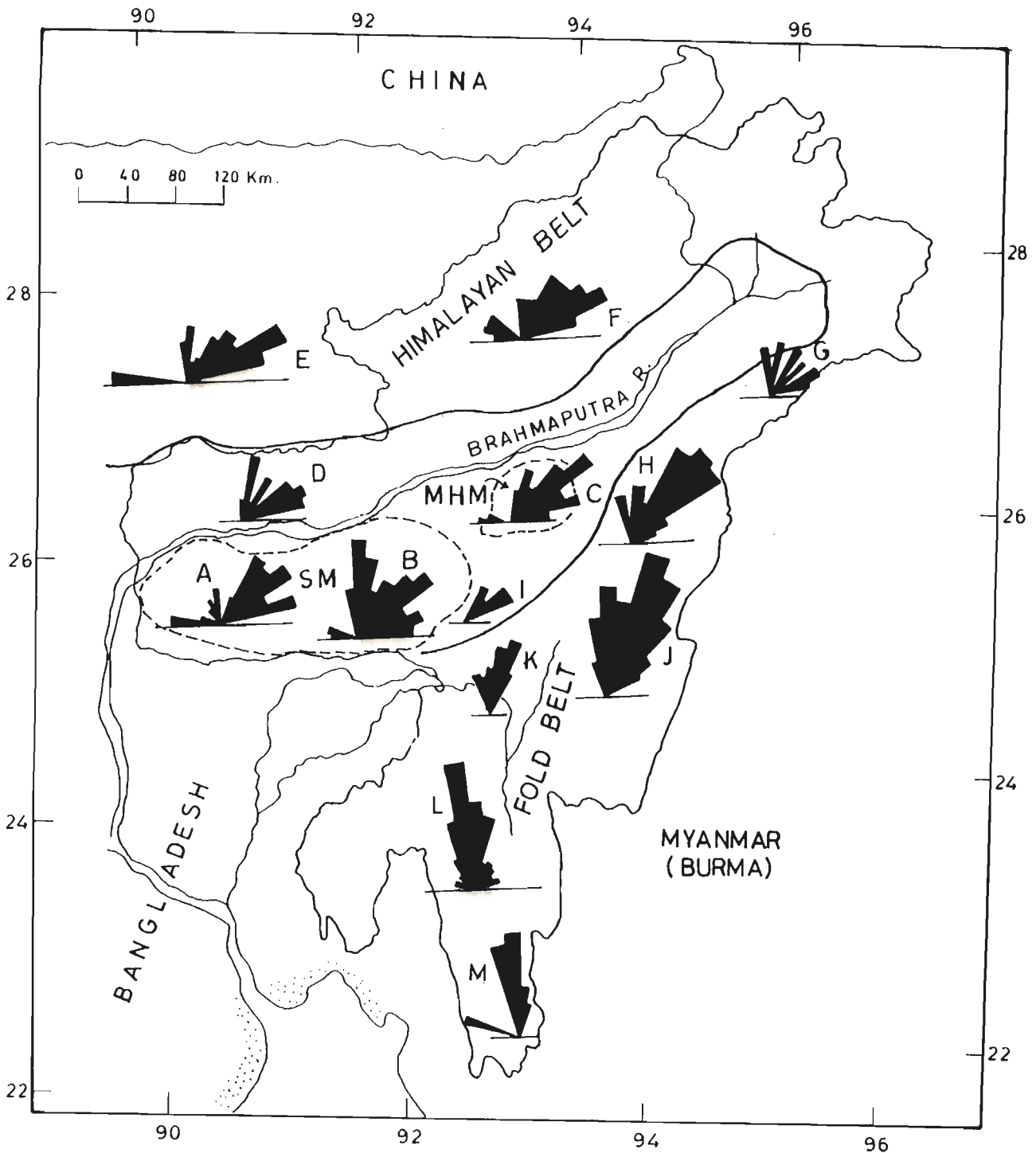


Figure 3.3. Lineament pattern of different geotectonic unit, Northeast India. A- Western Shillong Massif, B-Eastern Shillong Massif, C-Mikir Hills Massif, D-Western Brahmaputra basin, E-Bhutan Himalaya, F-Arunachal Himalaya, G-Patkai hills, H-Naga hills, I-Barail hills, J-Fold belt in Manipur, K-Barak basin, L-Frontal fold belt in Tripura-Mizoram, M-Frontal fold belt in southern Mizoram.

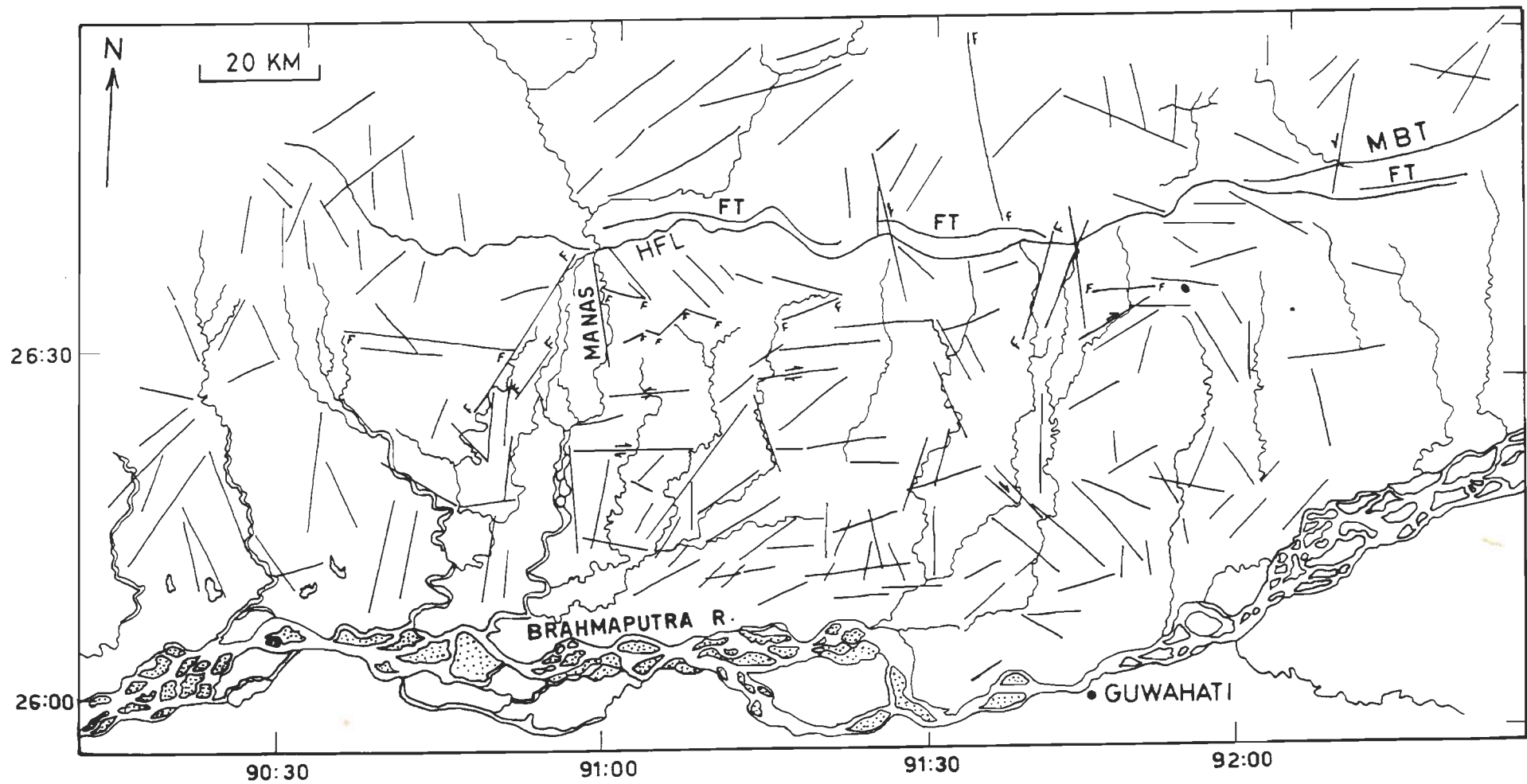


Figure 3.4. Fracture lineament pattern in Bhutan Himalayan foothills and Brahmaputra basin. Prepared from enlarged (4x) TM images. MBT-Main Boundary Thrust, FT-Frontal Thrust, HFL-Himalayan Foothills Limit.

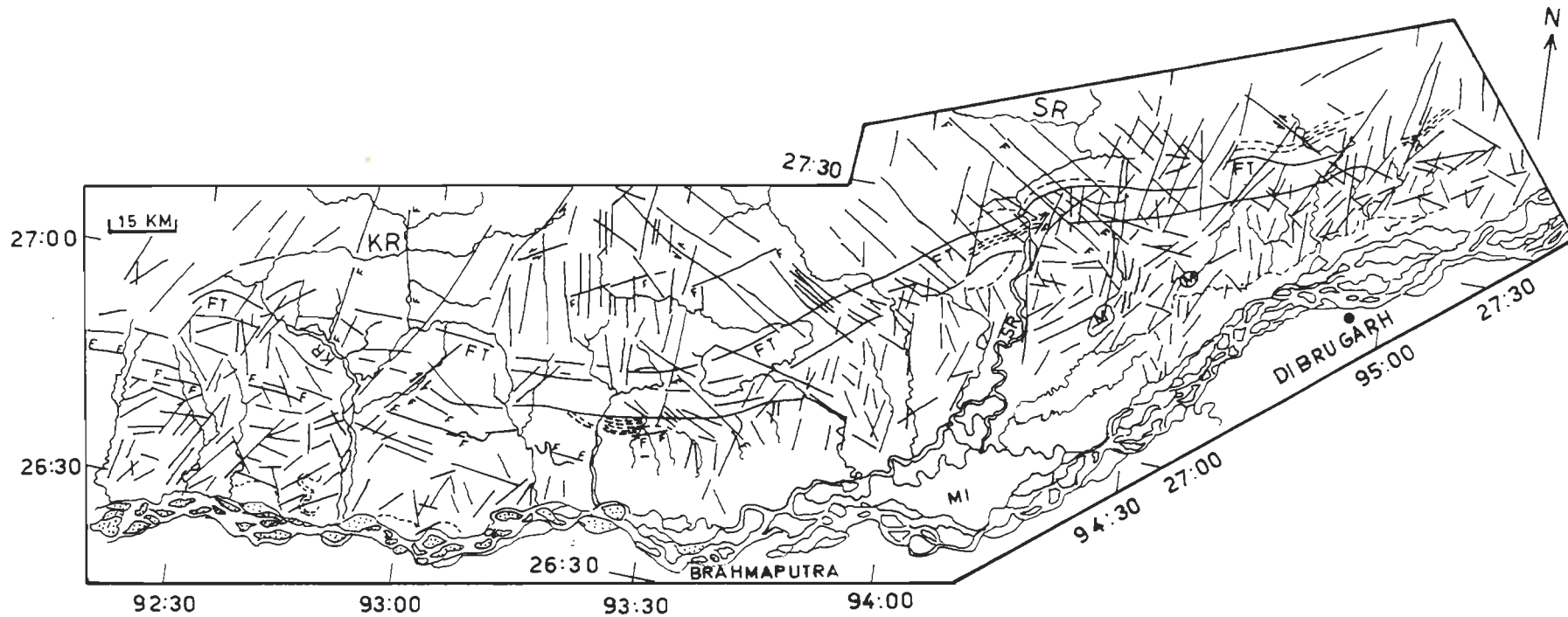


Figure 3.5. Fracture lineament pattern of Arunachal Himalaya and Brahmaputra Basin. Prepared from enlarged (4x) TM images. FT-Frontal Thrust, M-Marsh, KR-Kameng River, SR-Subansiri River, MI-Majuli Island.

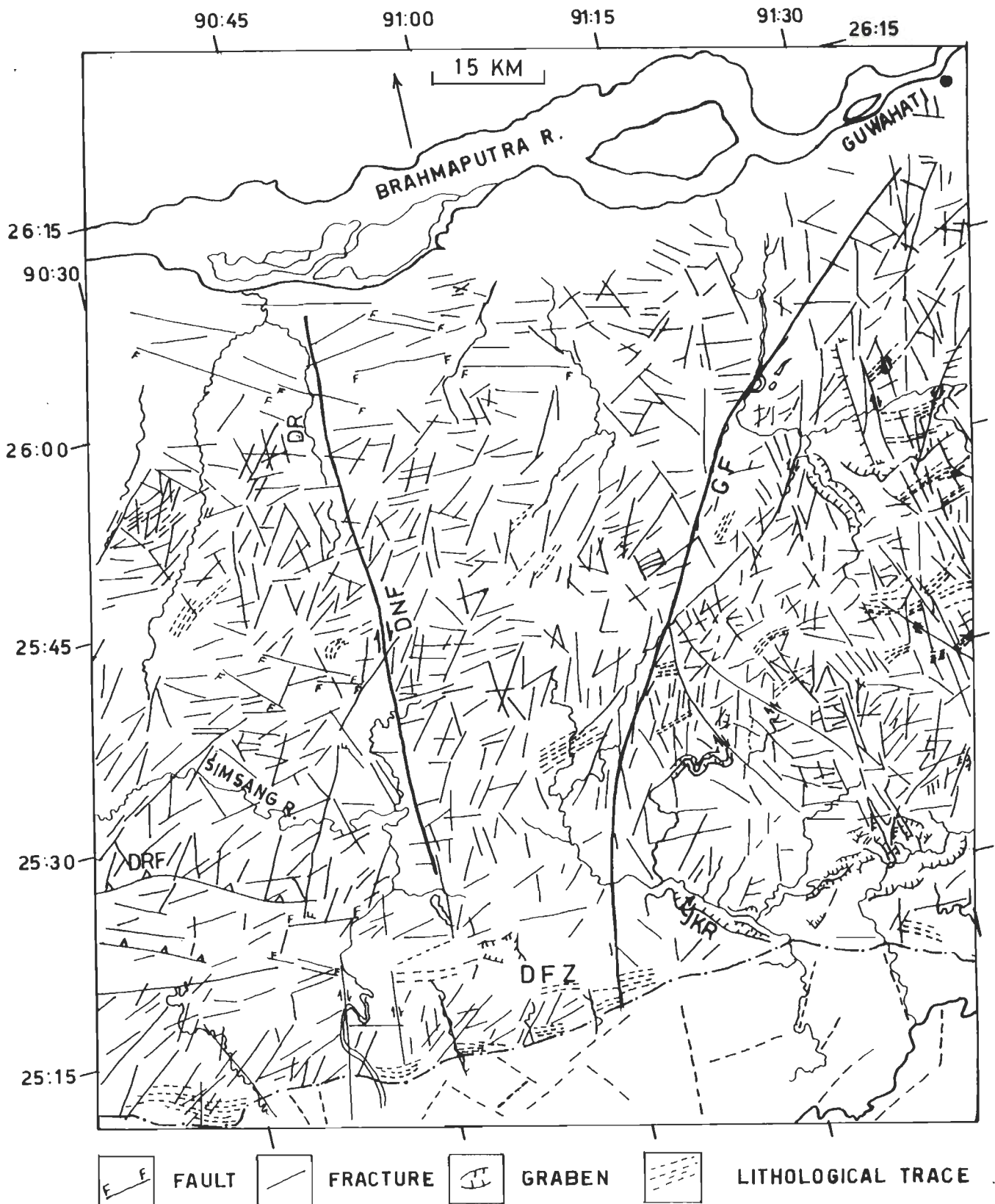


Figure 3.6. Fracture lineament pattern of western Shillong massif. Prepared from IRS LISS II FCC (scale 1:250,000). DNF-Dudhnai Fault, GF-Guwahati Fault, DRF-Dapsi Reverse Fault, DR-Dudhnai River, JKR-Jadukata River, DFZ-Dauki Fault Zone.

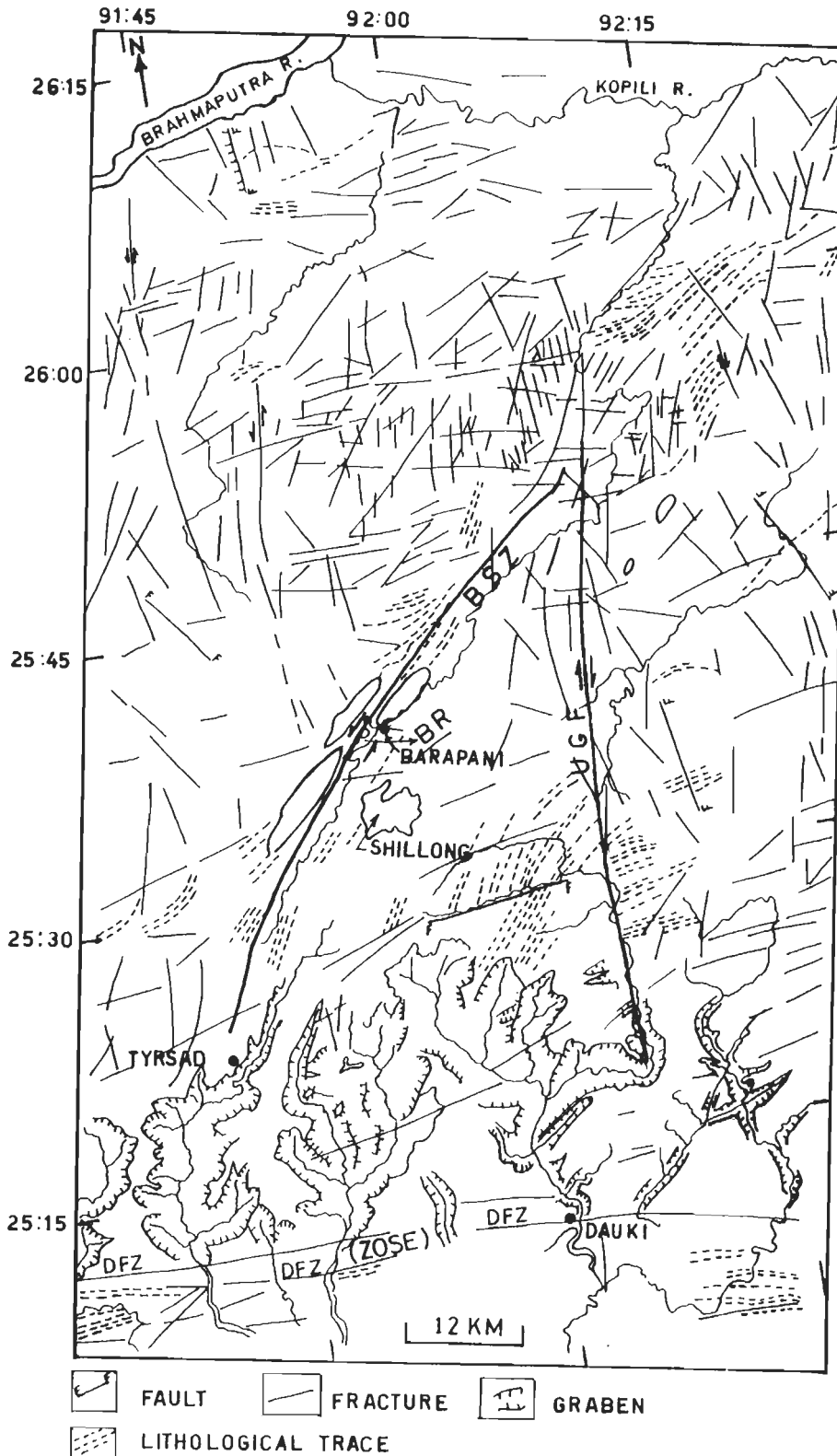


Figure 3.7. Fracture lineament pattern of Barapani Shear Zone and Shillong region. Prepared from IRS LISS-II FCC (scale 1:250,000). BSZ-Barapani Shear Zone, BR-Barapani Reservoir, UGF-Um Ngot Fault, DFZ-Dauki Fault Zone, ZOSE-Zone of Steep Escarpment.

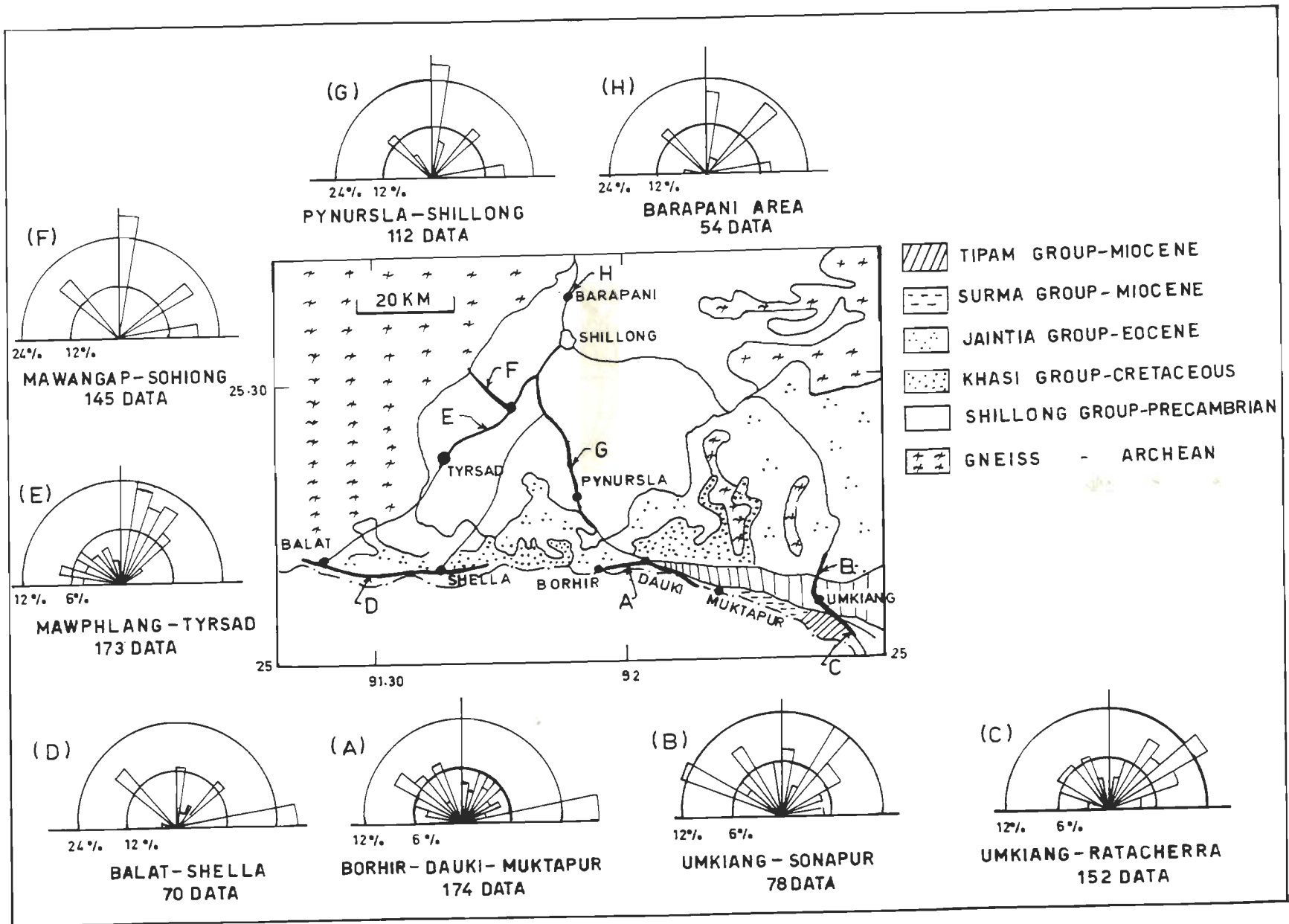
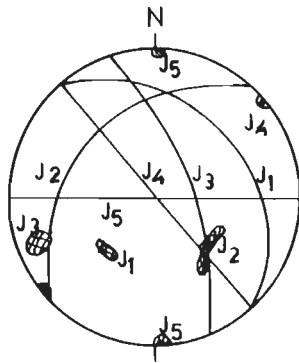
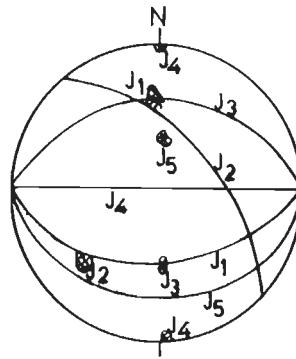


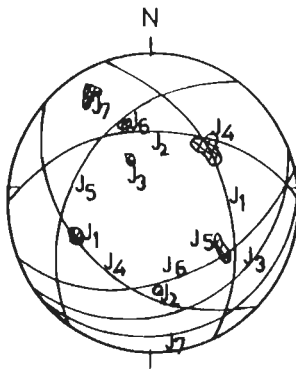
Figure 3.8. Joint trends for the various sectors from the area south of Shillong. Different sectors are shown as A, B, C, D, E, F, G and H.



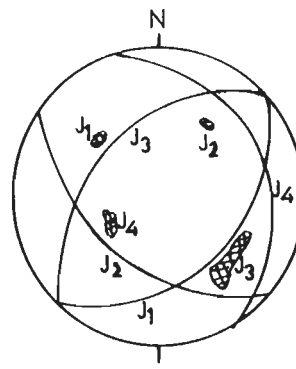
DAUKI-MUKTAPUR



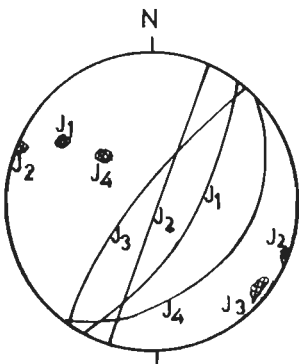
BALAT-SHELLA



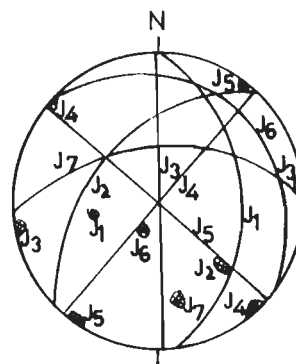
UMKIANG-RATACHERRA



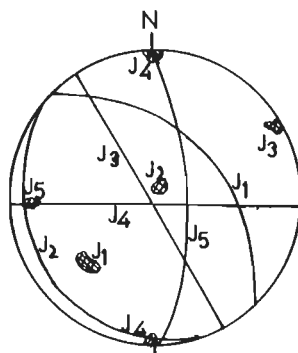
UMKIANG-SONAPUR



MAWPHLANG-TYRSAD



SOHIONG-MAWANGAP



PYNURSLA-SHILLONG

Figure 3.9. Stereonet plot of joints from different sectors as shown in Figure 3.8.



Figure 3.10 (A). Field photograph showing closely spaced fractures in Precambrian quartzite. Bedding- 28° due N 110° . Fracture trends are 75° due NE, 65° due N and 77° due S. Loc.-28 km south of Shillong towards Pynursla.



Figure 3.10 (B). Field photograph showing closely spaced fractures in Precambrian folded quartzite. The axis of the fold has been faulted and show numerous fractures. Loc.-29 km south of Shillong towards Pynursla.

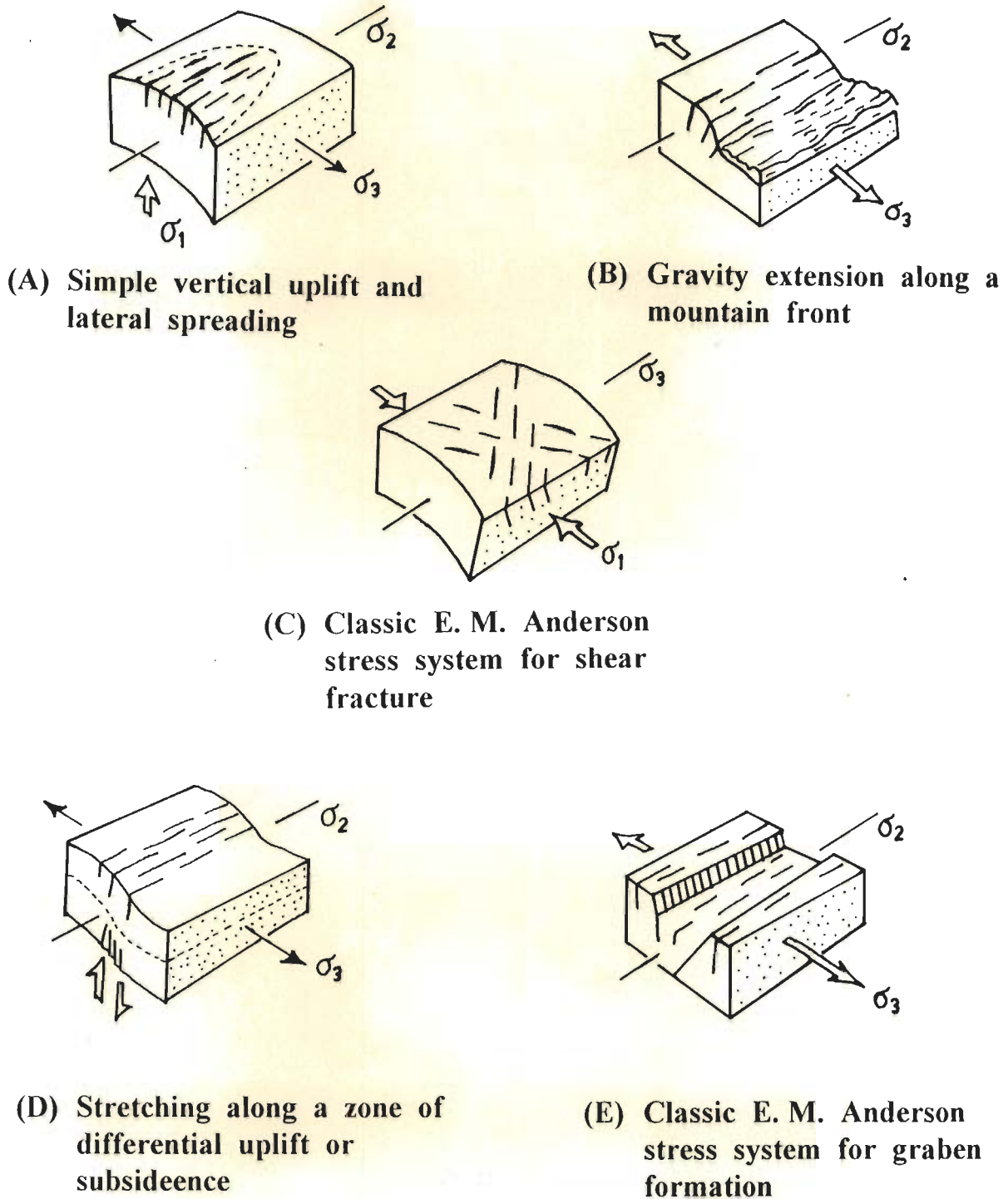


Figure 3.11. Possible tectonic settings and stress fields from Northeast India lineament swarms.



Figure 3.12. Satellite image (TM Band 4) of Shillong plateau and adjoining regions showing various structures. SM-Shillong Massif; MHM-Mikir Hills Massif; DFZ-Dauki Fault Zone; HTZ-Haflong Thrust Zone; JF-Jamuna Fault; KF-Kopili Fault; DRF-Dapsi Reverse Fault; DNF-Dudhinai Fault; BSZ-Barapani Shear Zone; UGF-Um Ngot Fault

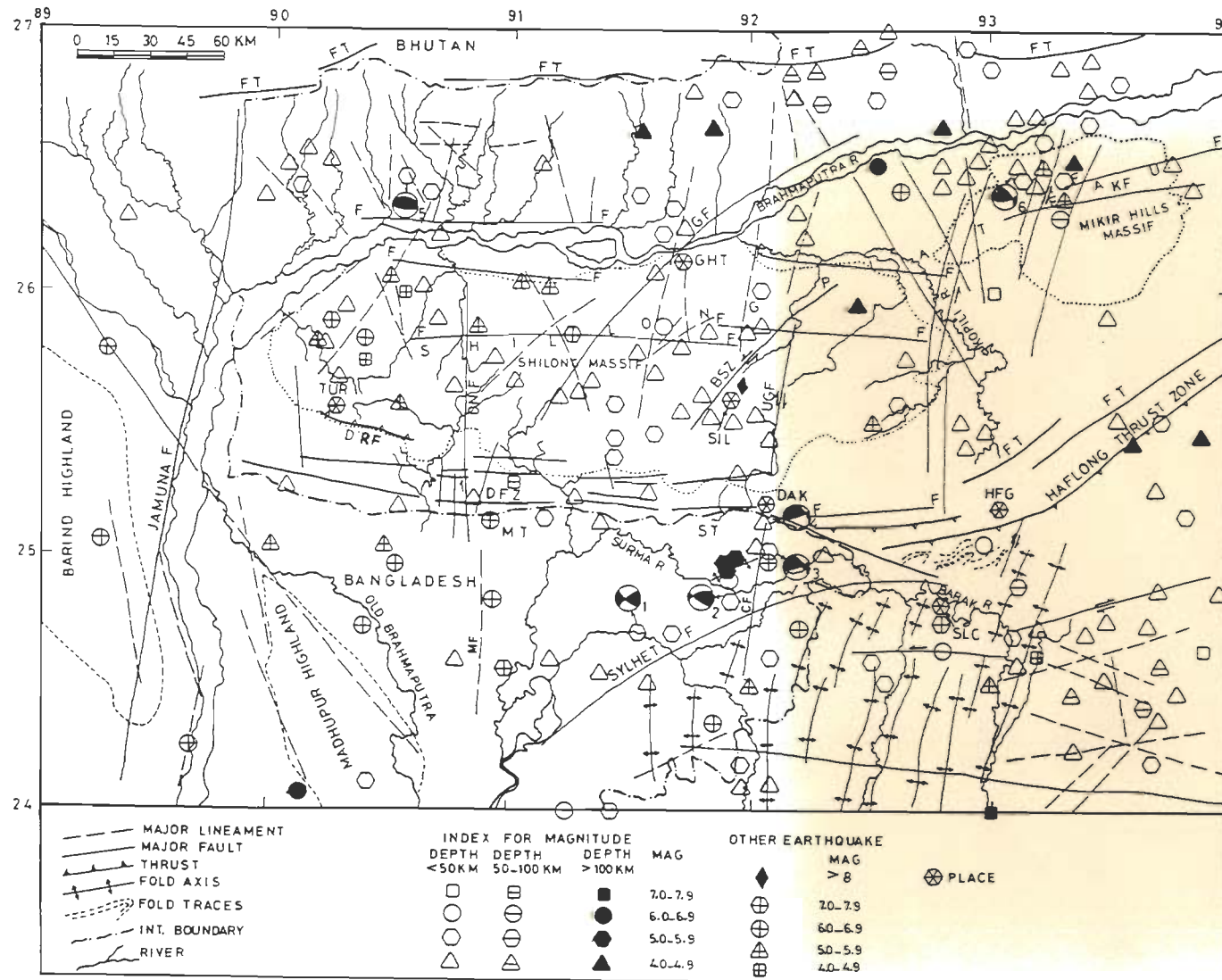


Figure 3.13. Different structural features as identified on satellite images along with seismicity of Shillong Plateau and adjoining regions. GHT-Guwahati, SIL-Shillong, TUR-Tura, DAK-Dauki, HFG-Haflong, SLC-Silchar. FT-Frontal Thrust, GF-Guwahati Fault, DFZ-Dauki Fault Zone, BSZ-Barapani Shear Zone, DRF-Dapsi Reverse Fault, UGF-Um Ngot Fault, MF-Mohanganj Fault, CF-Chandghat Fault, KF-Kopili Fracture, MT-Mohanganj Trough, ST-Sylhet Trough. Fault plane solutions 1-February 6, 1988, 2-June 12, 1968, 3-June 19, 1963, 4-June 21, 1963, 5-August 18, 1968, 6-July 17, 1971.

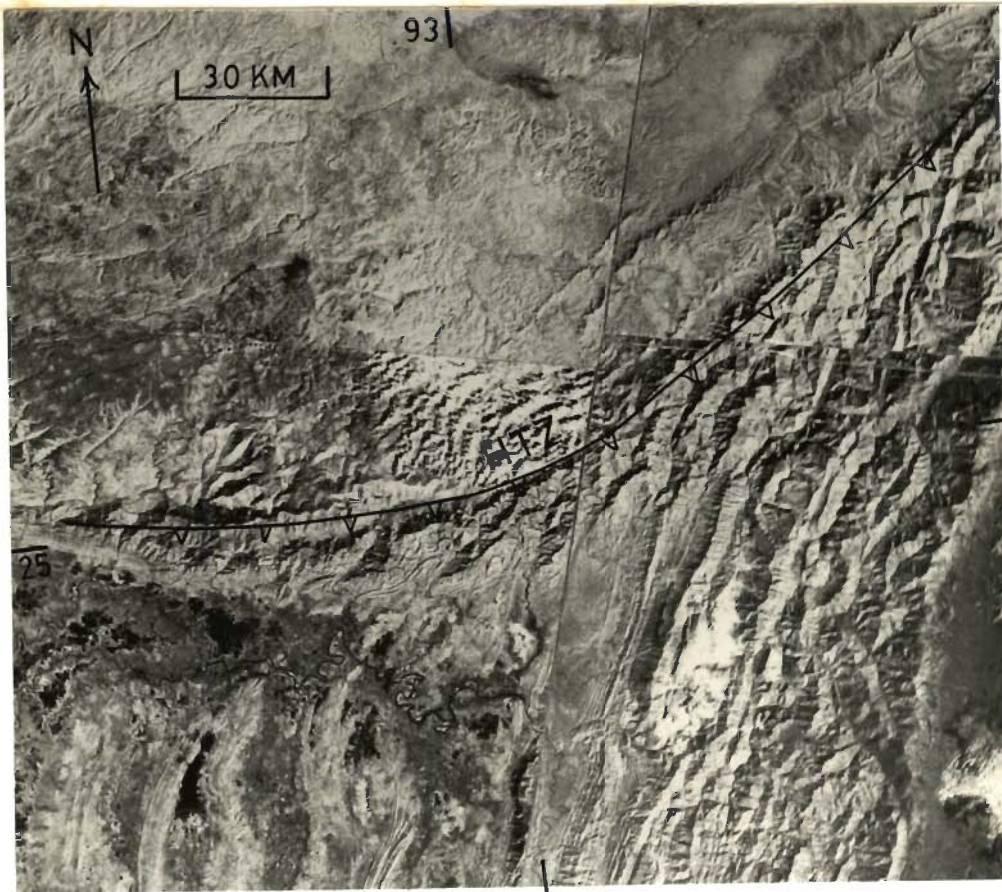


Figure 3.14 (A). Satellite image (TM-Band-4) showing Haflong Thrust Zone (HTZ) and associated structural features.

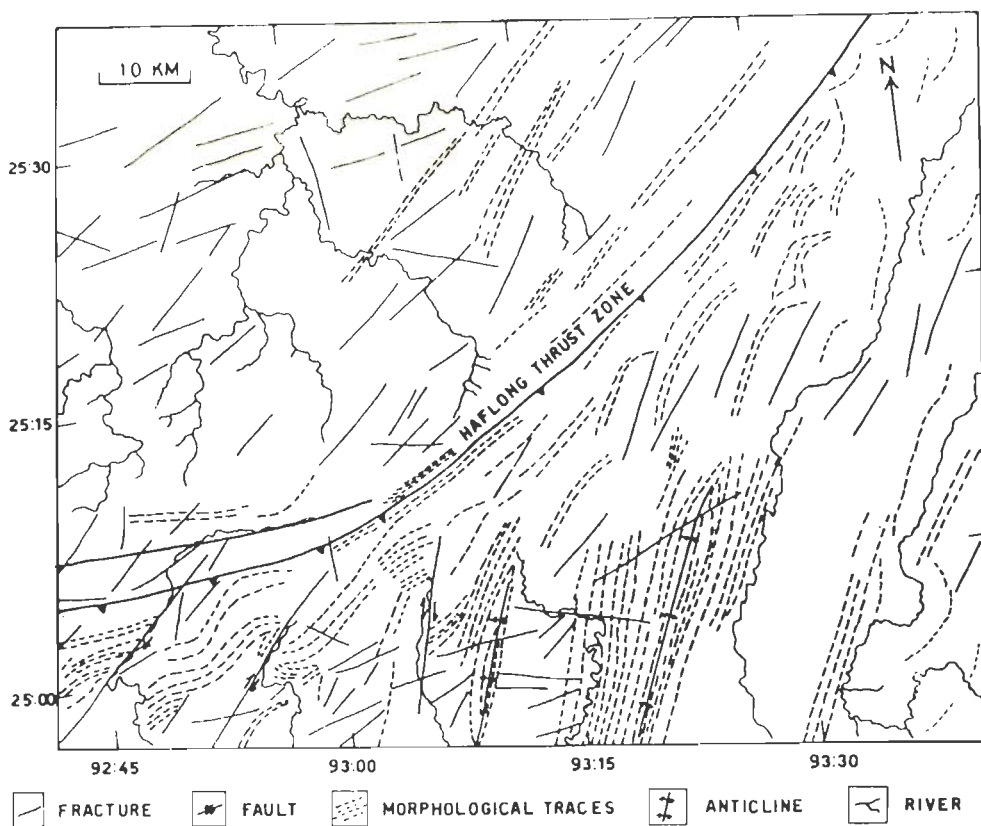


Figure 3.14 (B). Interpretation map of Haflong Thrust Zone and associated structural features. Prepared from IRS IISS-II FCC (scale. 1:250,000).

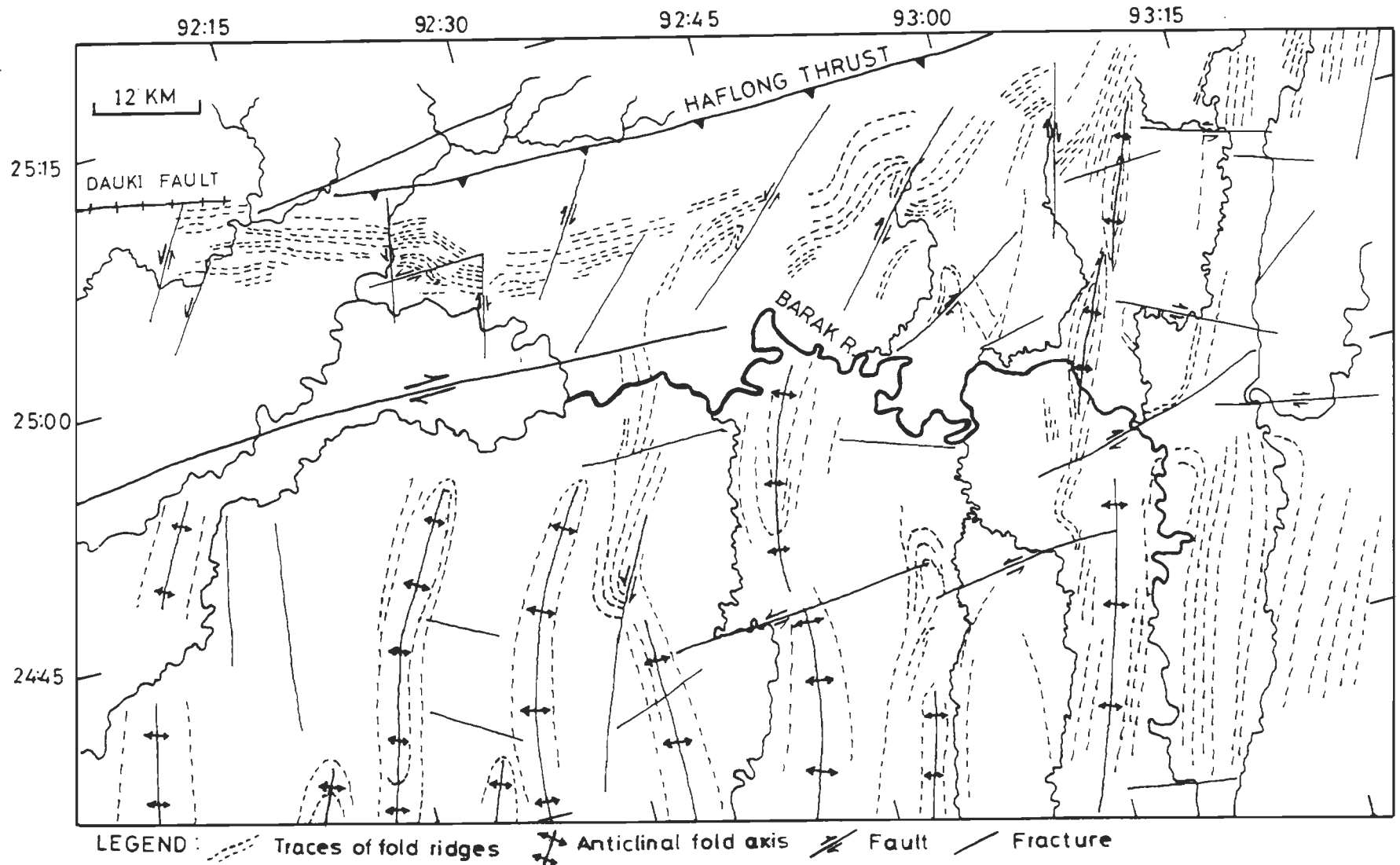


Figure 3.15. Structural features of frontal fold belt and southern part of Haflong Thrust Zone. Prepared from IRS IISS-II FCC (scale 1:250,000).

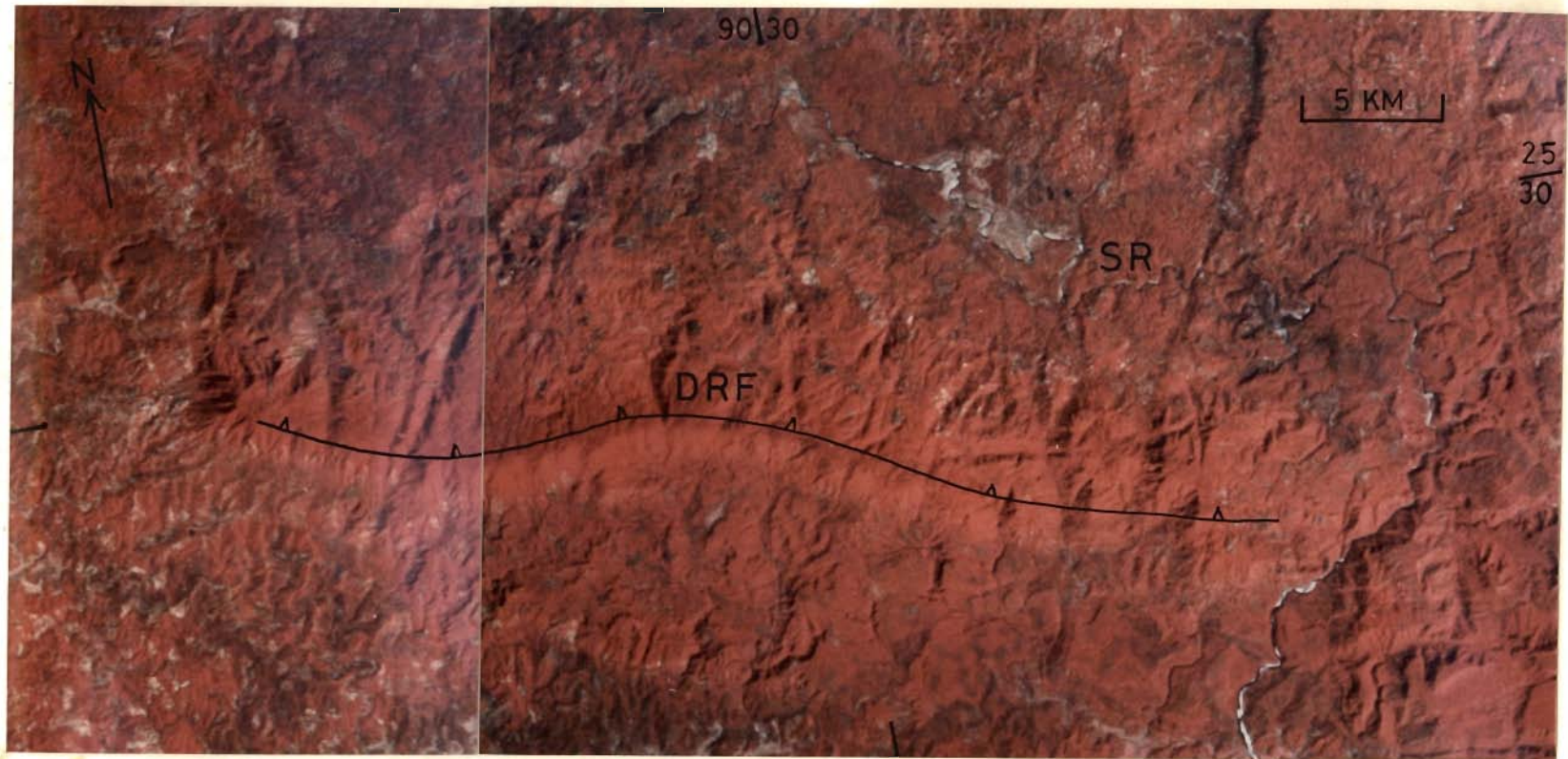


Figure 3.16. FCC (ISS LISS II) shows Dapsi Reverse Fault (DRF) and associated structures. SR- Simsang River.

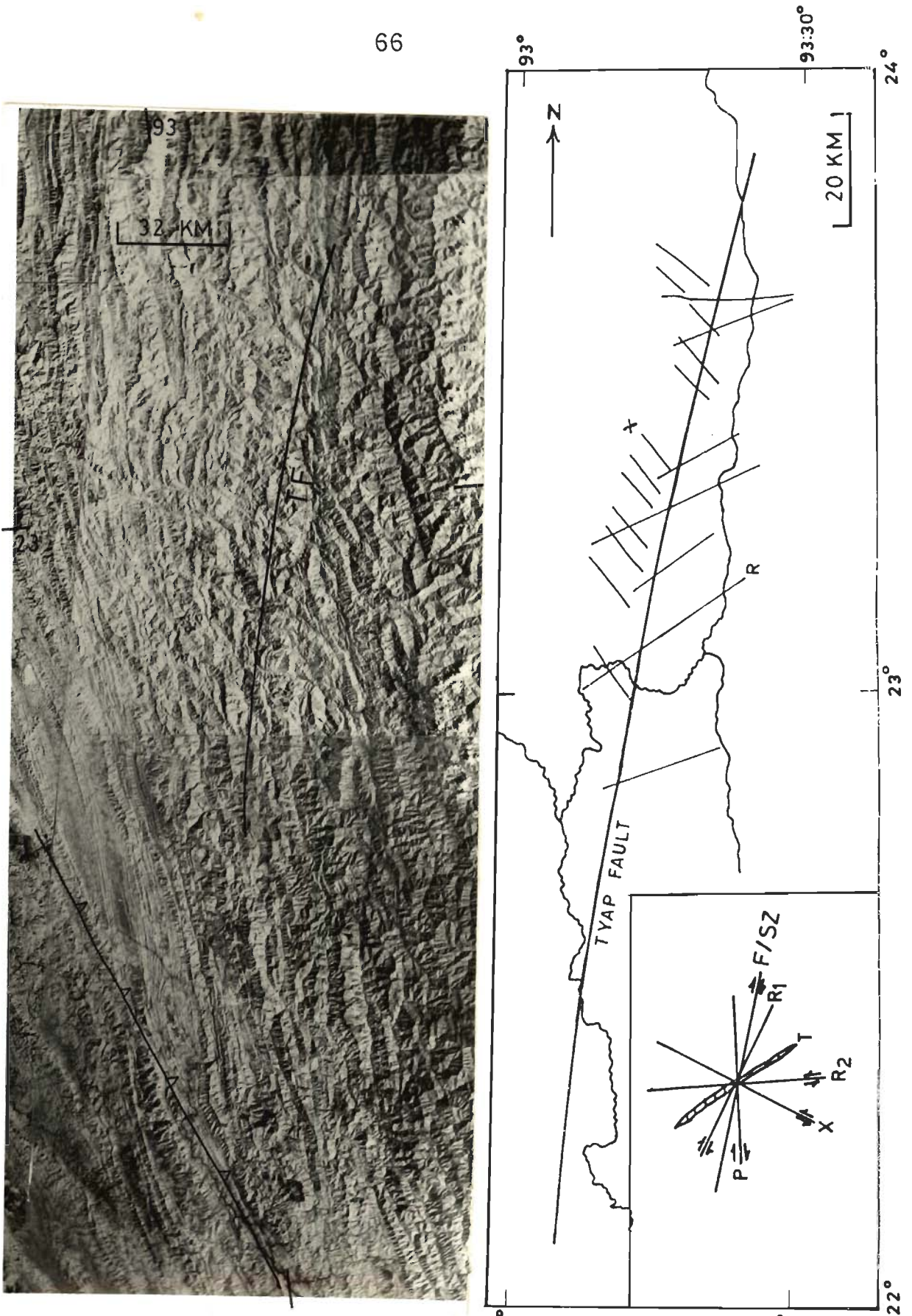


Figure 3.17 (A) & (B). Satellite image (TM-Band-4) shows Tyap Fault (TF) and associated shearing fractures and a thrust (A). Interpretation map of Tyap Fault and associated shear fractures (B).

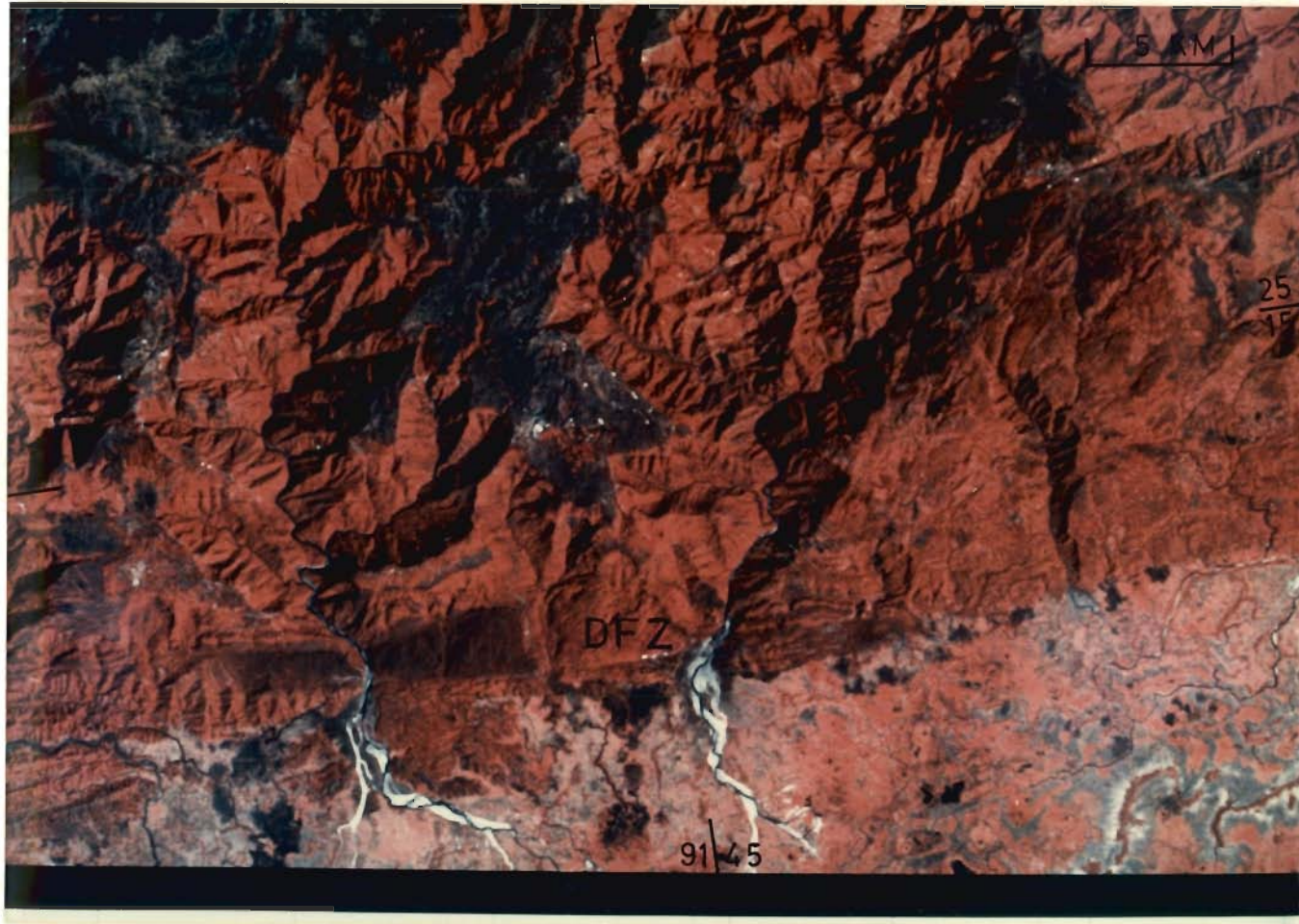


Figure 3.18. FCC shows horst and graben structures in a area south of Shillong. This area shows intense formation of this structure. DFZ-Dauki Fault Zone.

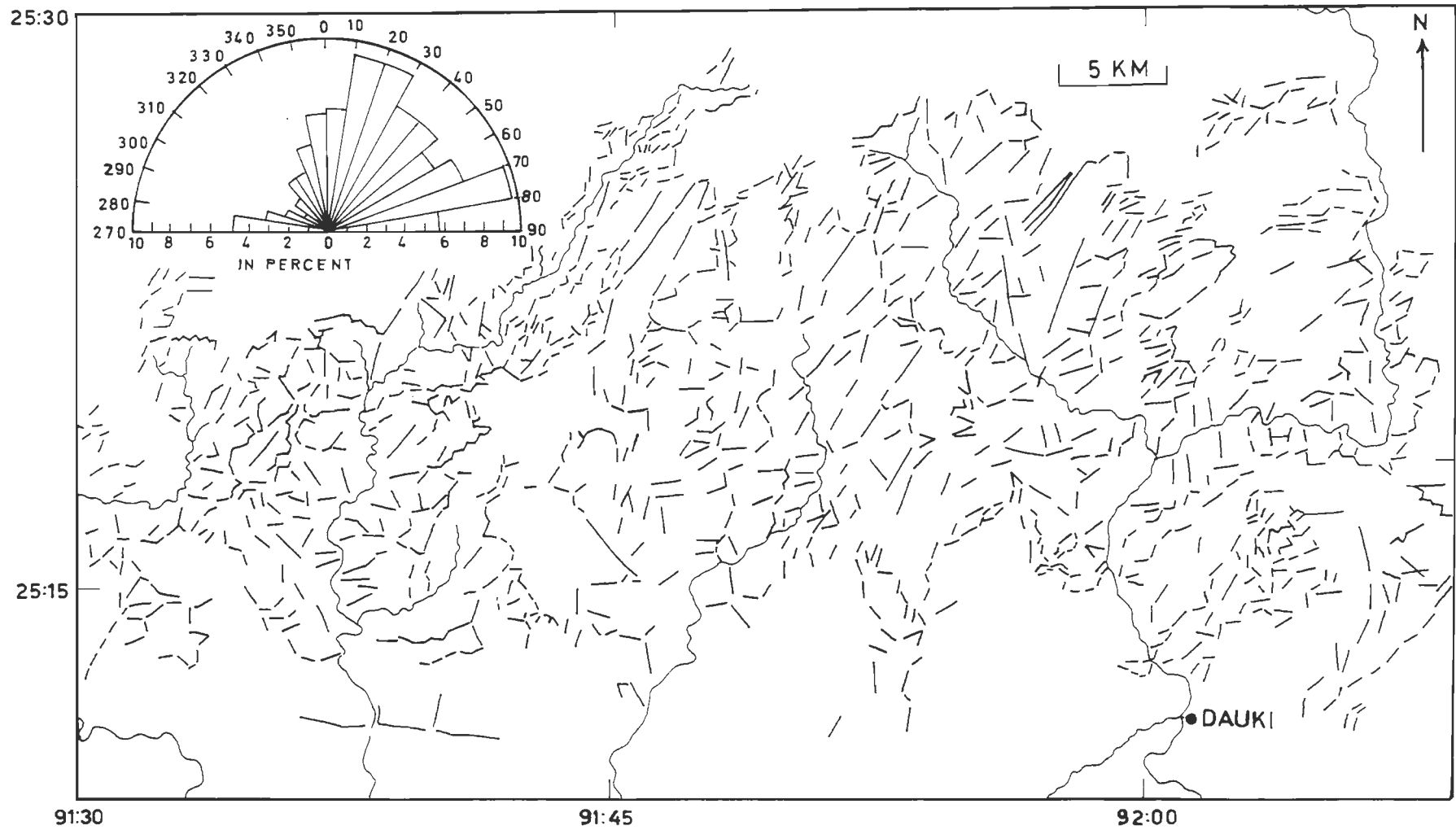


Figure 3.19. Fracture traces of block faulting which formed graben. Prepared from IRS LISS-II FCC (scale 1:250,000)

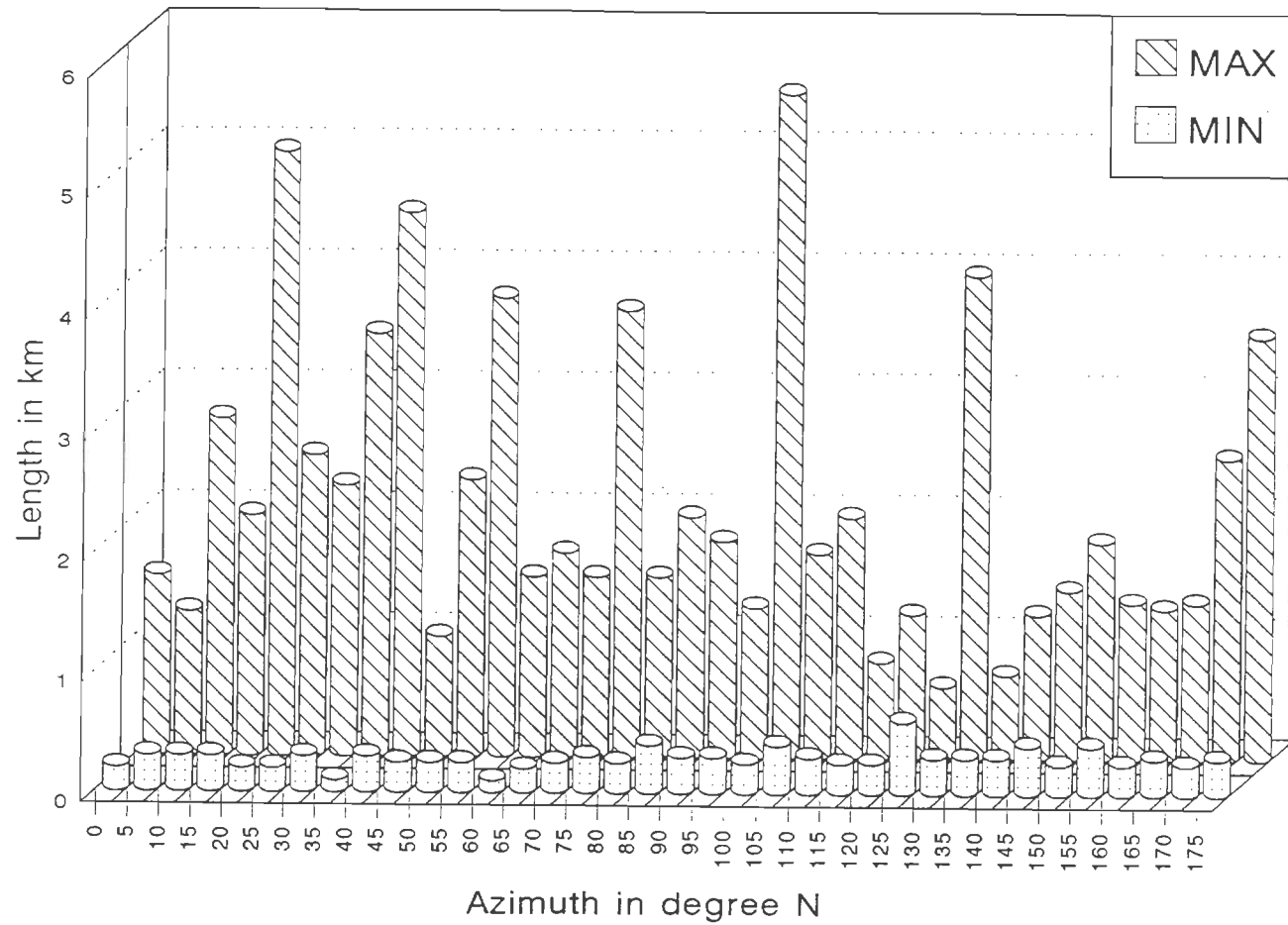


Figure 3.20. Bar diagram showing distribution of minimum and maximum length of fracture traces of graben boundaries of various azimuth.

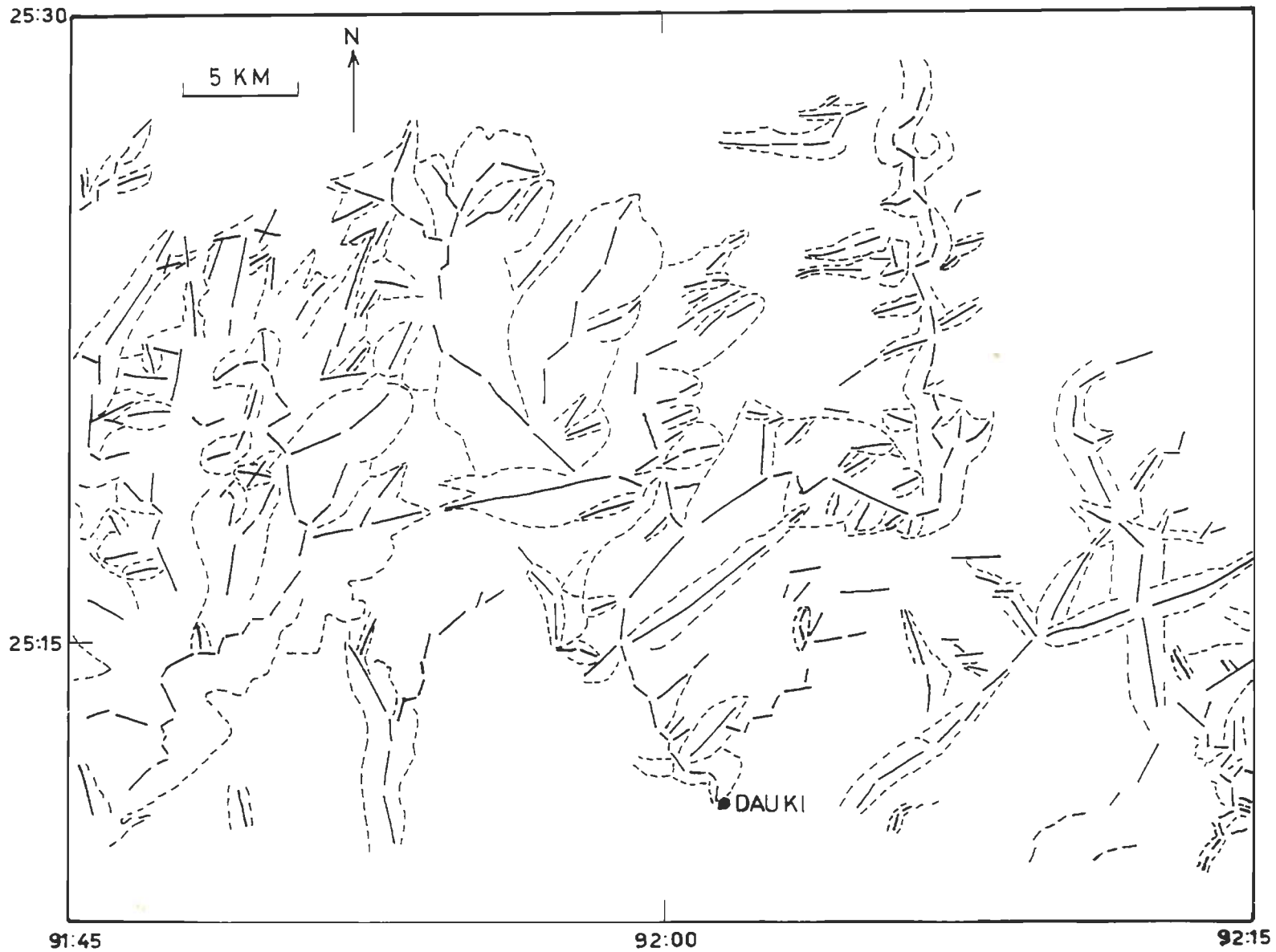


Figure 3.21. Map shows general graben morphology. Solid lines are the central line of graben. Dashed line show boundary of graben. Prepared from IRS LISS-II FCC (scale 1:250,000)

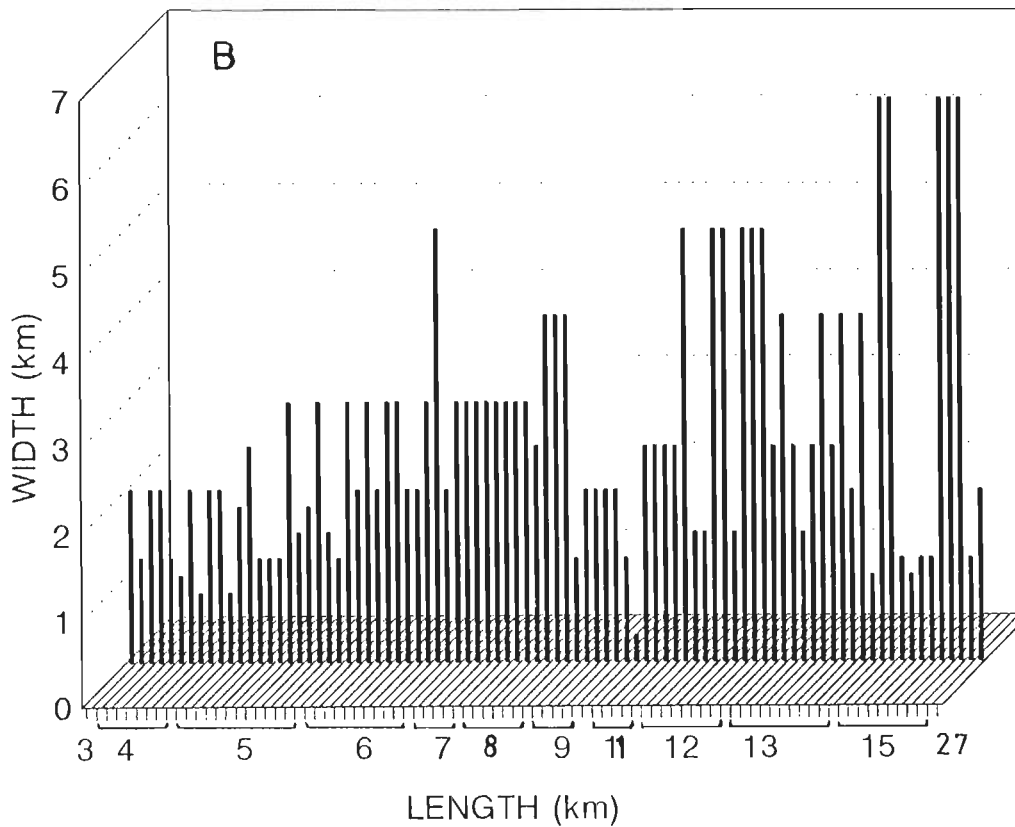
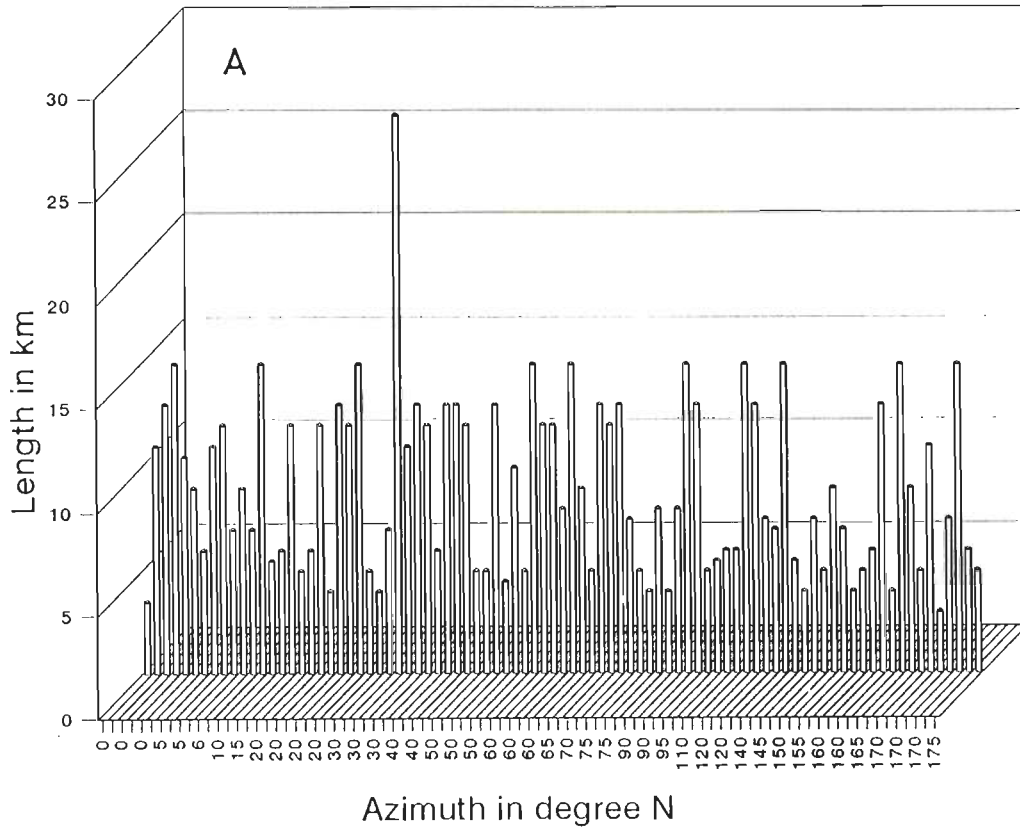


Figure 3.22 (A) & (B). Bar diagrams showing relationship between azimuth and length (A) and length and width (B) of the grabens. Length of the grabens computed by drawing a central line within a graben.

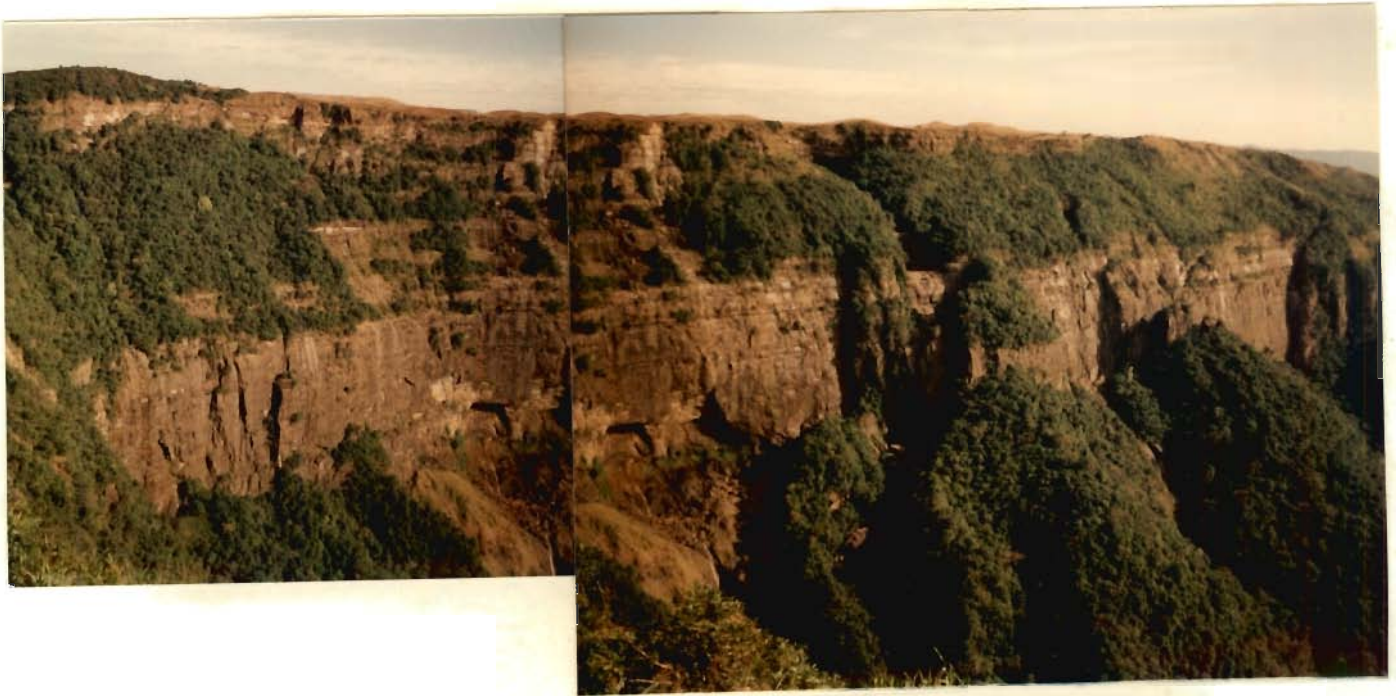


Figure 3.23 (A). Field photograph showing steep surface of the graben. The slip surfaces are oriented in a N-S, NE-SW and E-W directions. Loc.- 75 km south of Shillong at Cherrapunji.



Figure 3.23 (B). Field photograph showing block faulting on a graben wall. The faults have dips 70° due SE and 50° due NW. Loc.-3 km south of Mawsynram.

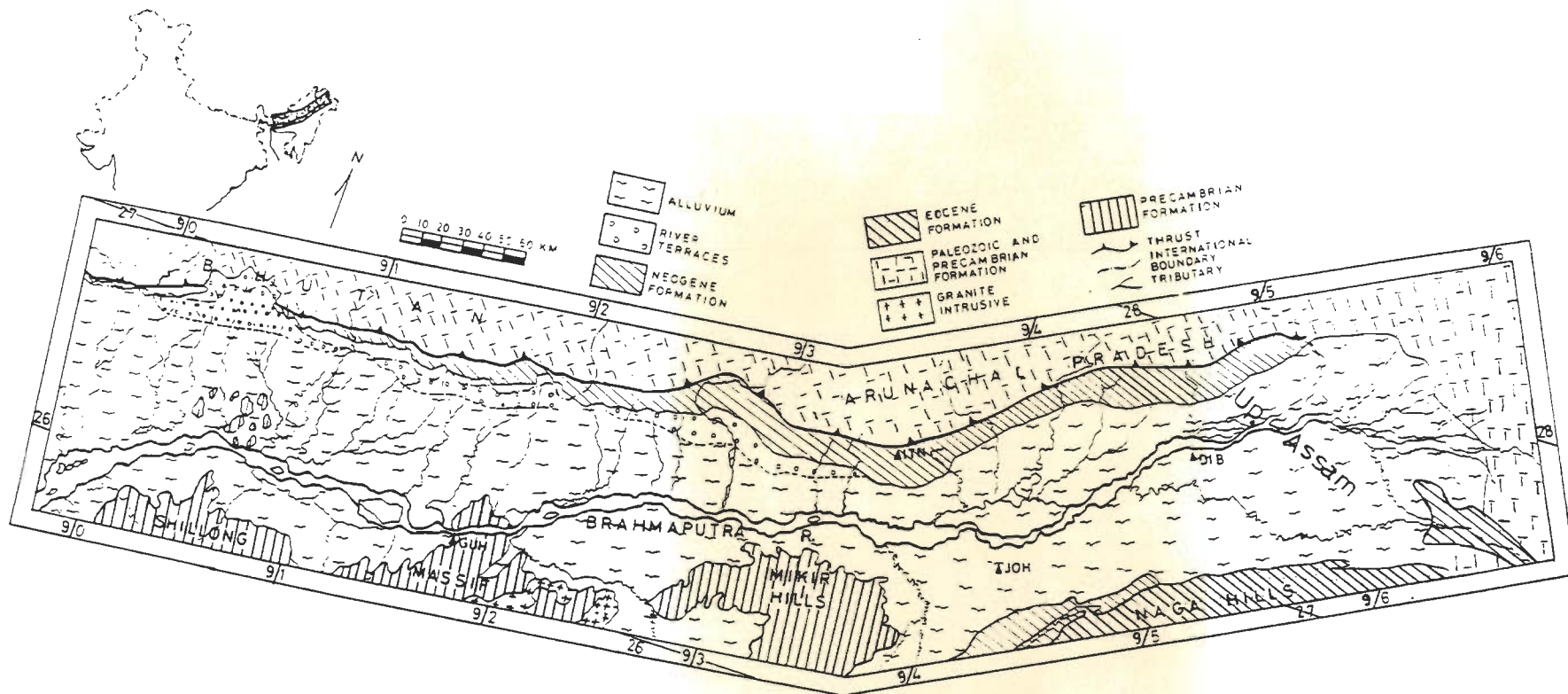


Figure 3.24. Map shows geological features of the Brahmaputra basin and adjoining areas. ITN-Itanagar, DIB-Dibrugarh, JOH-Jorhat, GUH-Guwahati.



Figure 3.25. Satellite image (TM:Band-4) shows Manas River Fans in the Bhutan Himalayan foothills. AF-Alluvial Fan.



Figure 3.26 (A). Satellite image (TM:Band-4) of Dafla Hills tectonic block in Arunachal Himalaya. DHB-Dafla Hills Block.

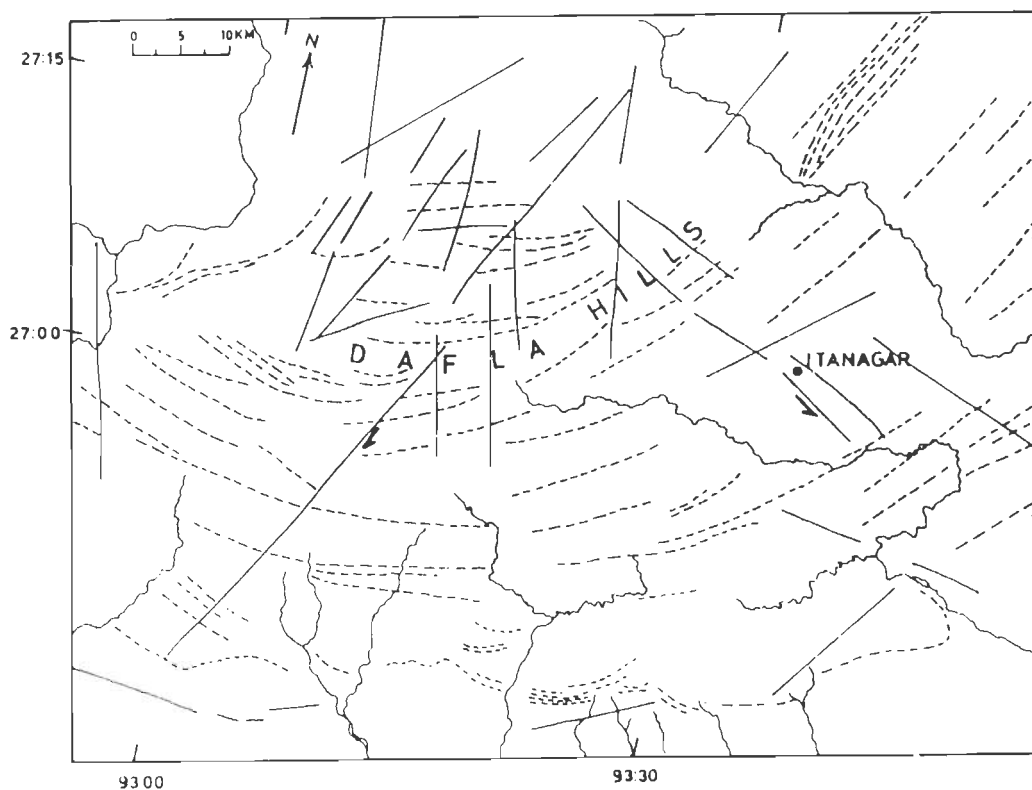


Figure 3.26 (B). Interpretation map showing structural features of Dafla hills tectonic block in Arunachal Himalaya as identified on image.

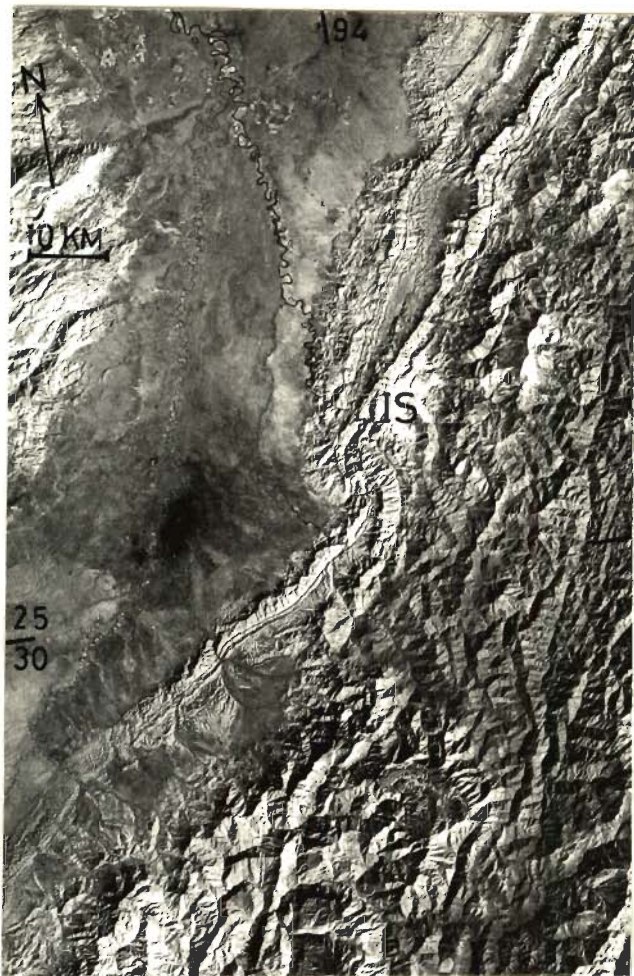


Figure 3.27 (A). Satellite image (TM Band-4) shows Interlocking Structures (IS) in the Naga Foothills.

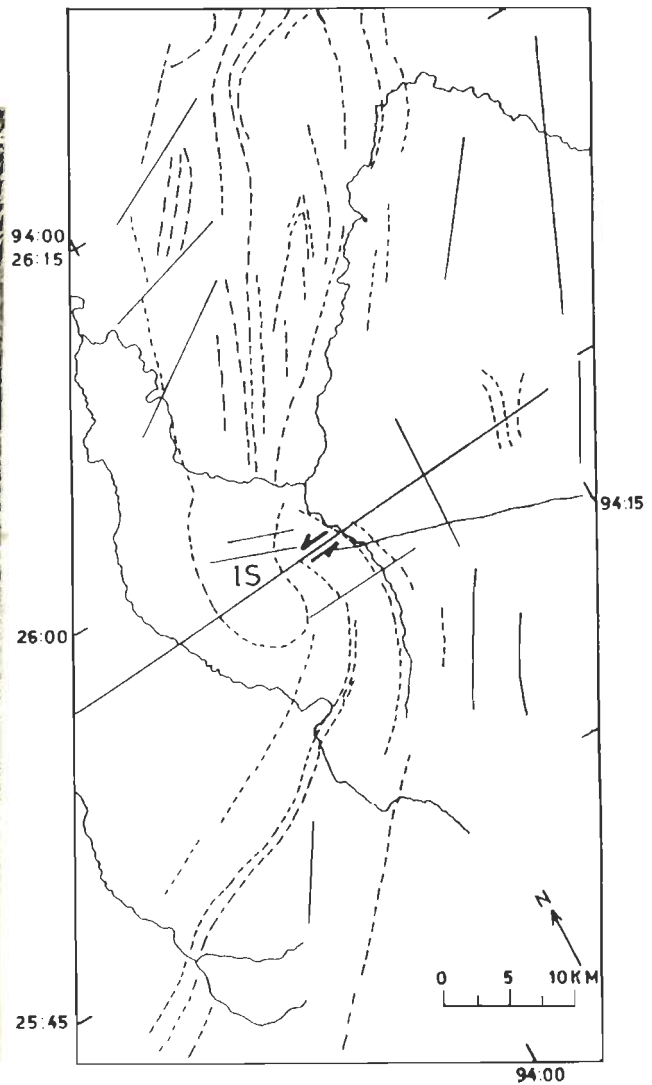


Figure 3.27 (B). Interpretation map shows structural features of Interlocking Structures (IS) in the Naga Foothills as identified on image.

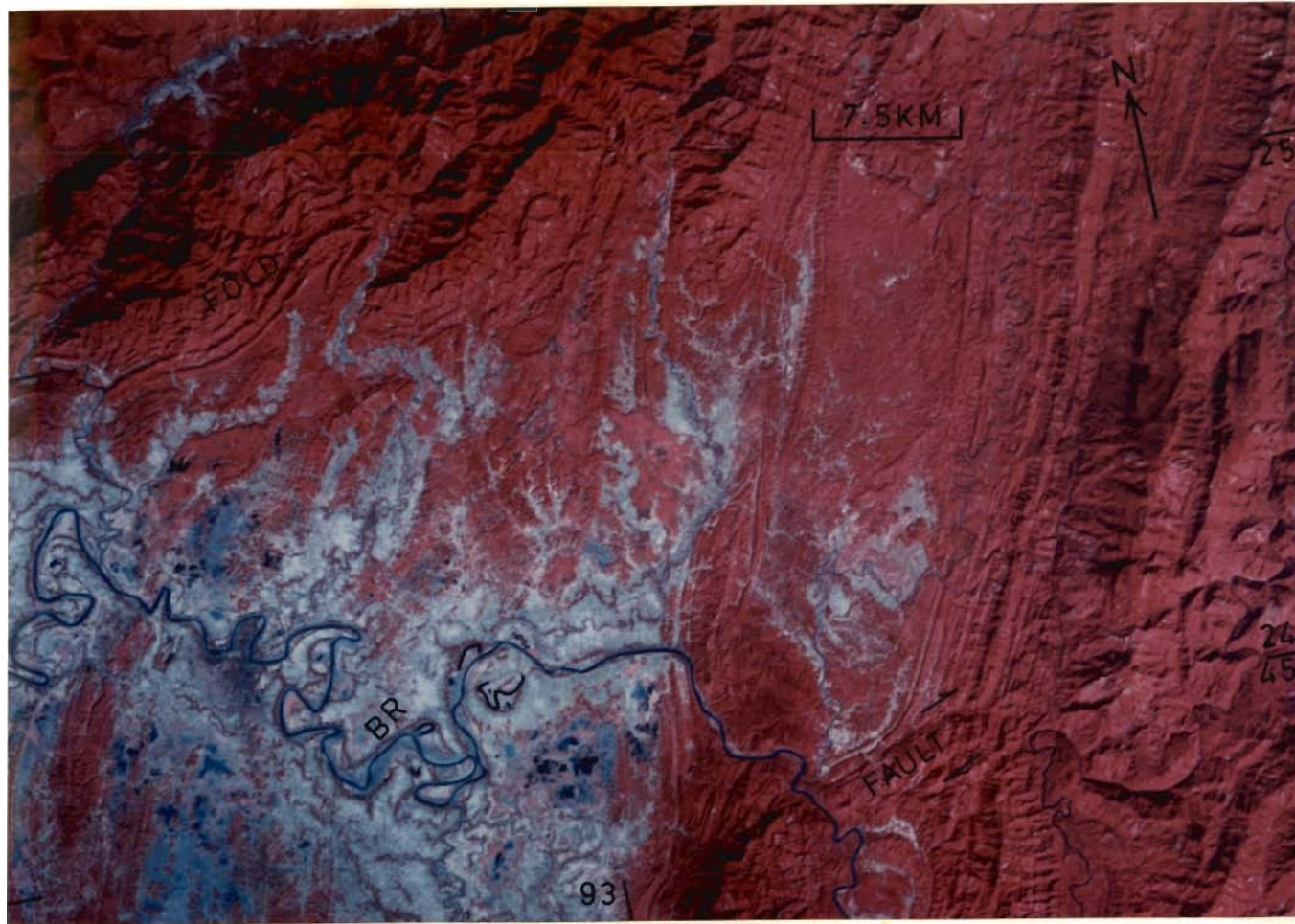


Figure 3.28. FCC (IRS LISS-II) shows folds in sedimentary rocks in the area south of Haflong Thrust Zone. BR-Barak River.

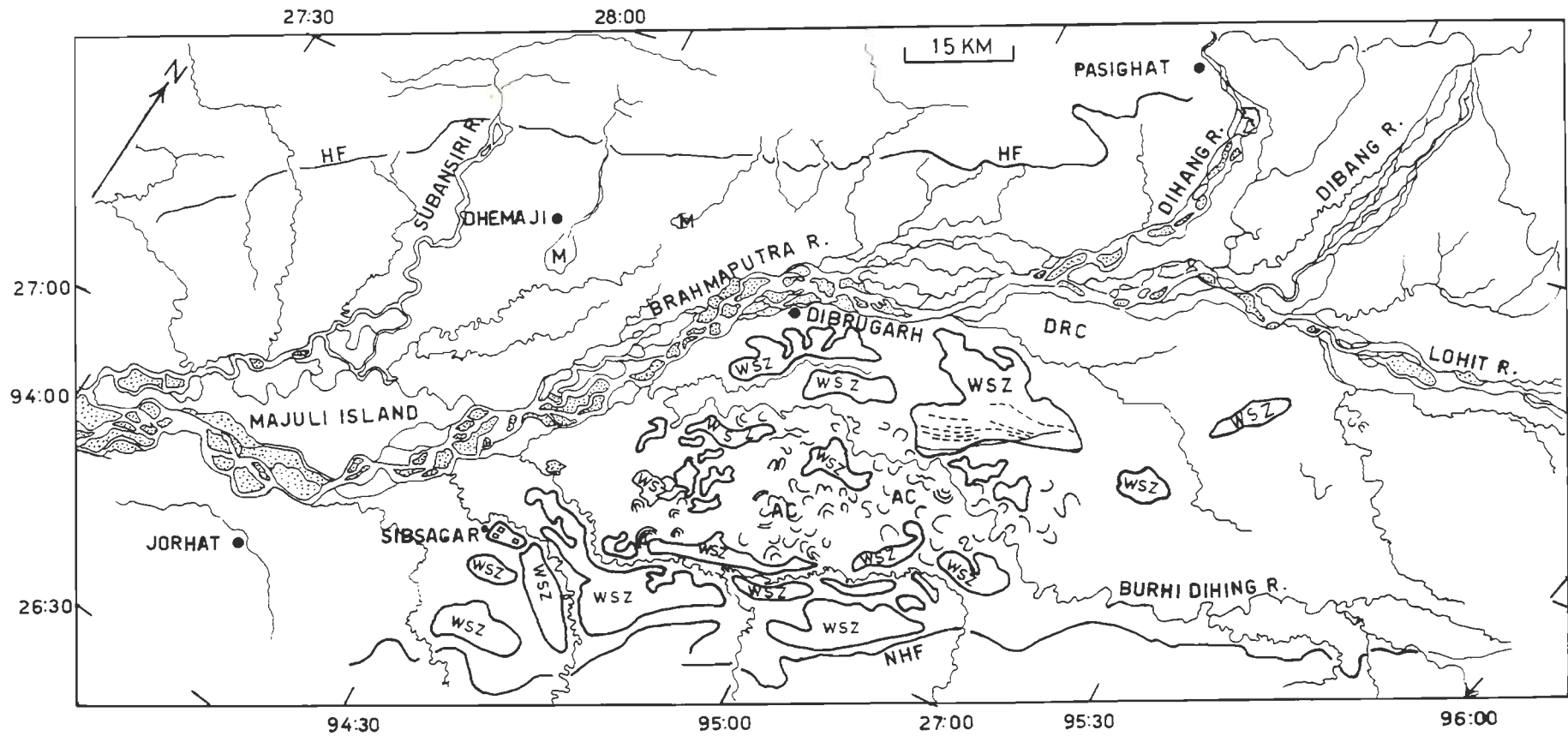


Figure 3.29. Brahmaputra River morphology in Pasighat-Jorhat sector. WSZ-Water Saturated Zone; AC-Abandoned Channel, DRC-Dried River Channel; M-Marsh; HF-Himalayan Front; NHF-Naga Hills Front. Prepared from Satellite Image.

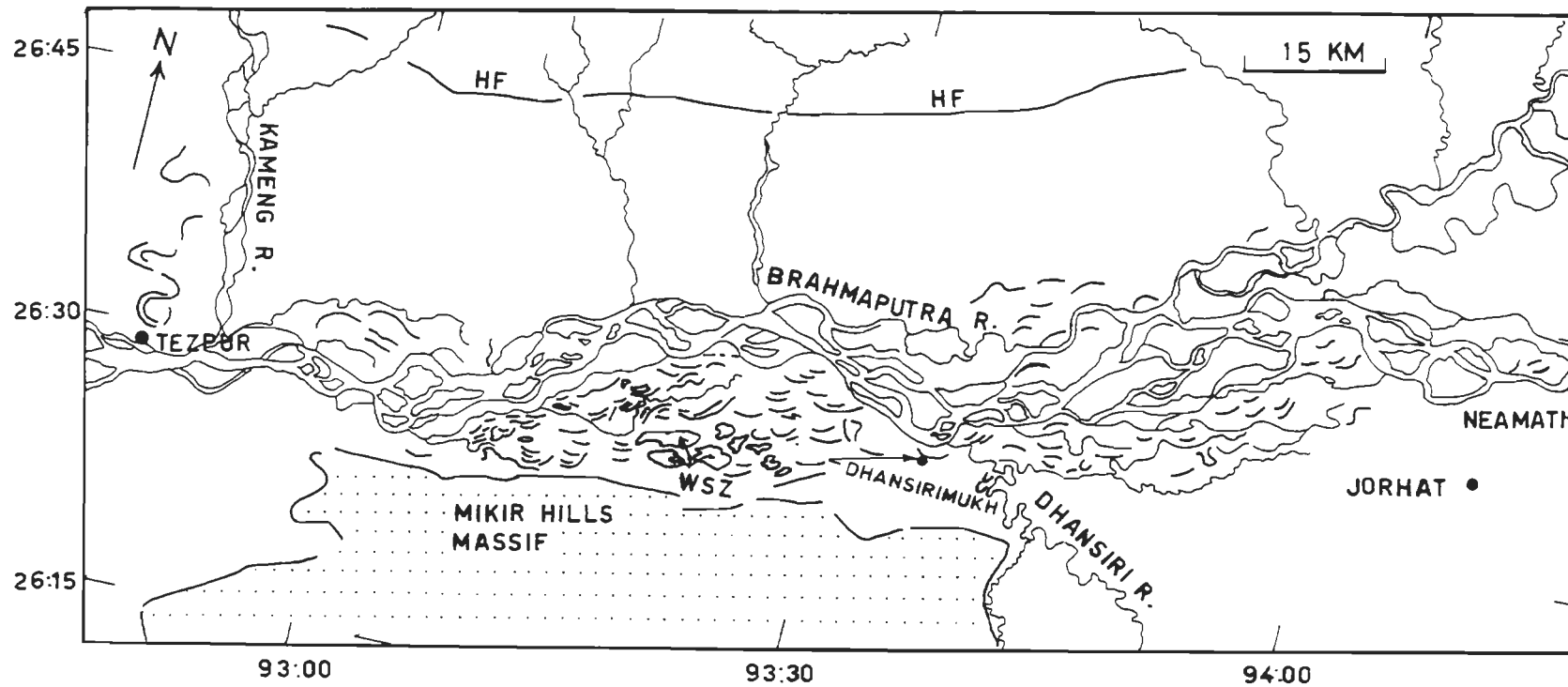


Figure 3.30 (A). Brahmaputra River morphology in Jorhat-Tezpur sector. WSZ-Water Saturated Zone; HF-Himalayan Front. Prepared from Satellite Image.

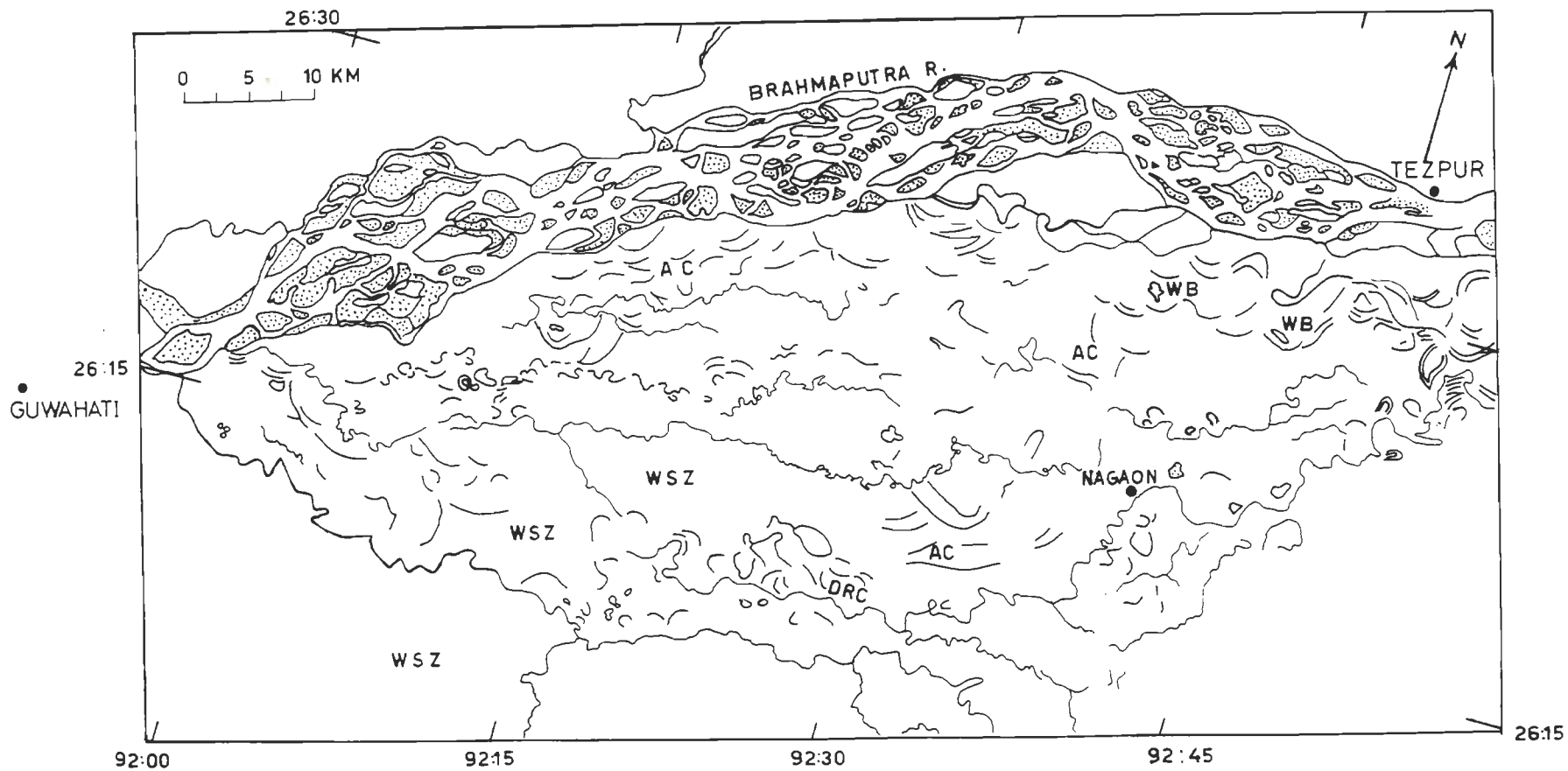


Figure 3.30 (B). Brahmaputra River morphology in Tezpur-Guwahati sector. WSZ-Water Saturated Zone; WB-Water Body; AC-Abandoned Channel; DRC-Dried River Channel. Prepared from Satellite Image.

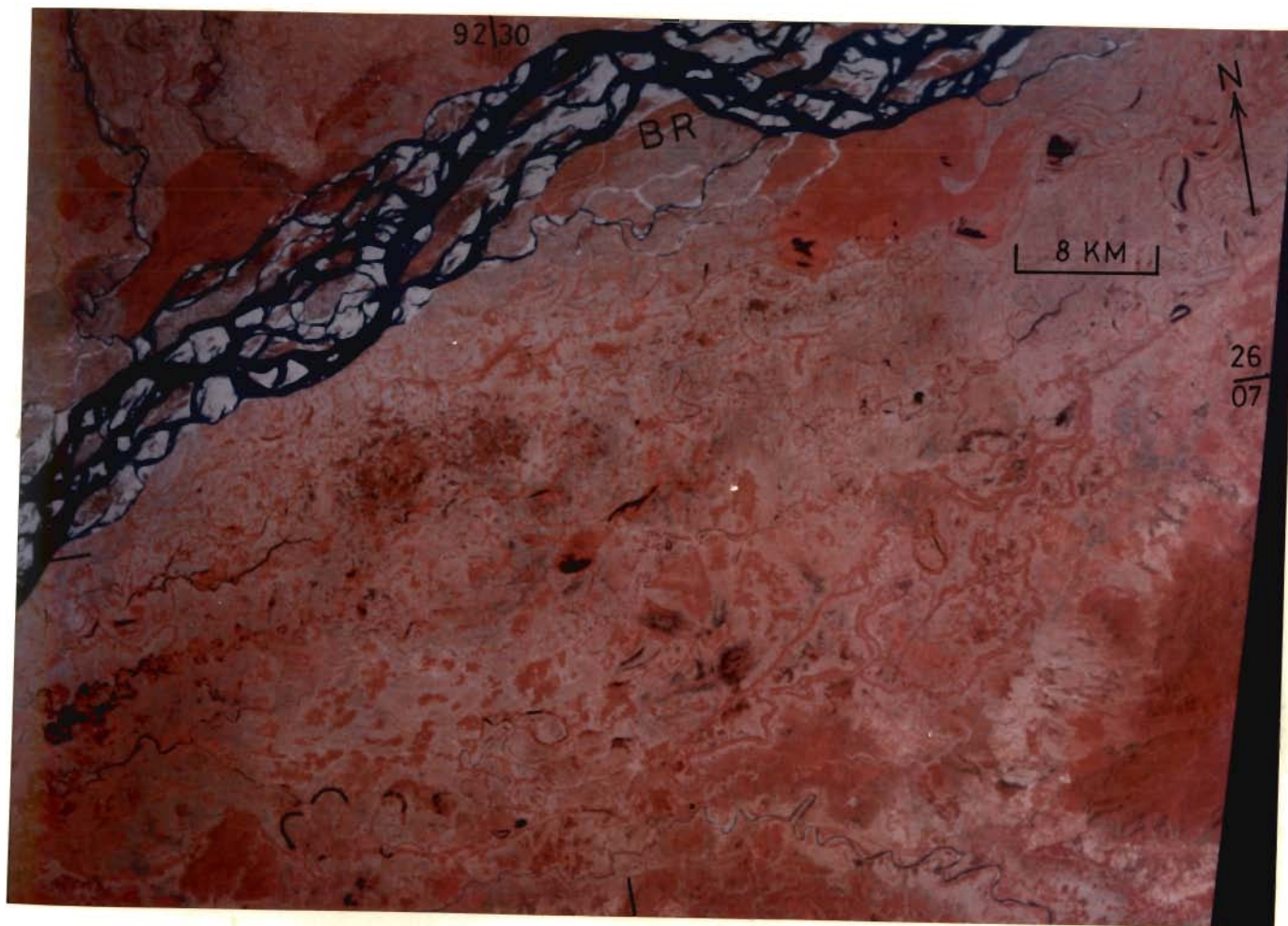


Figure 3.31. FCC (IRS LISS-II) shows northward migration of the Brahmaputra River in the area between the Shillong and Mikir Hills Massifs. Paleochannels can be seen in the lower part of image. BR-Brahmaputra River.

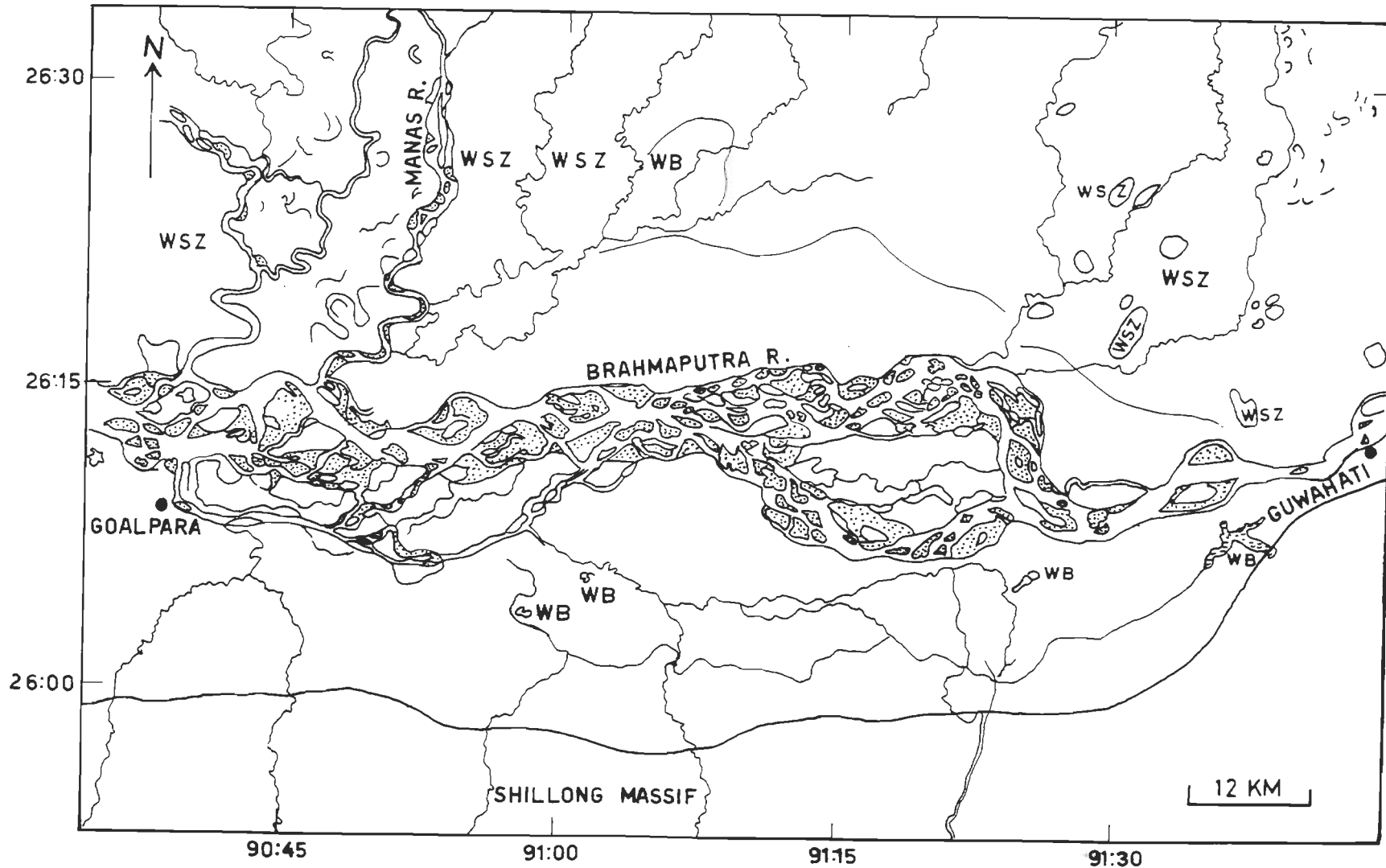


Figure 3.32. Brahmaputra River morphology in Guwahati-Goalpara sector. WSZ-Water Saturated Zone; WB-Water Body. Prepared from Satellite Image.

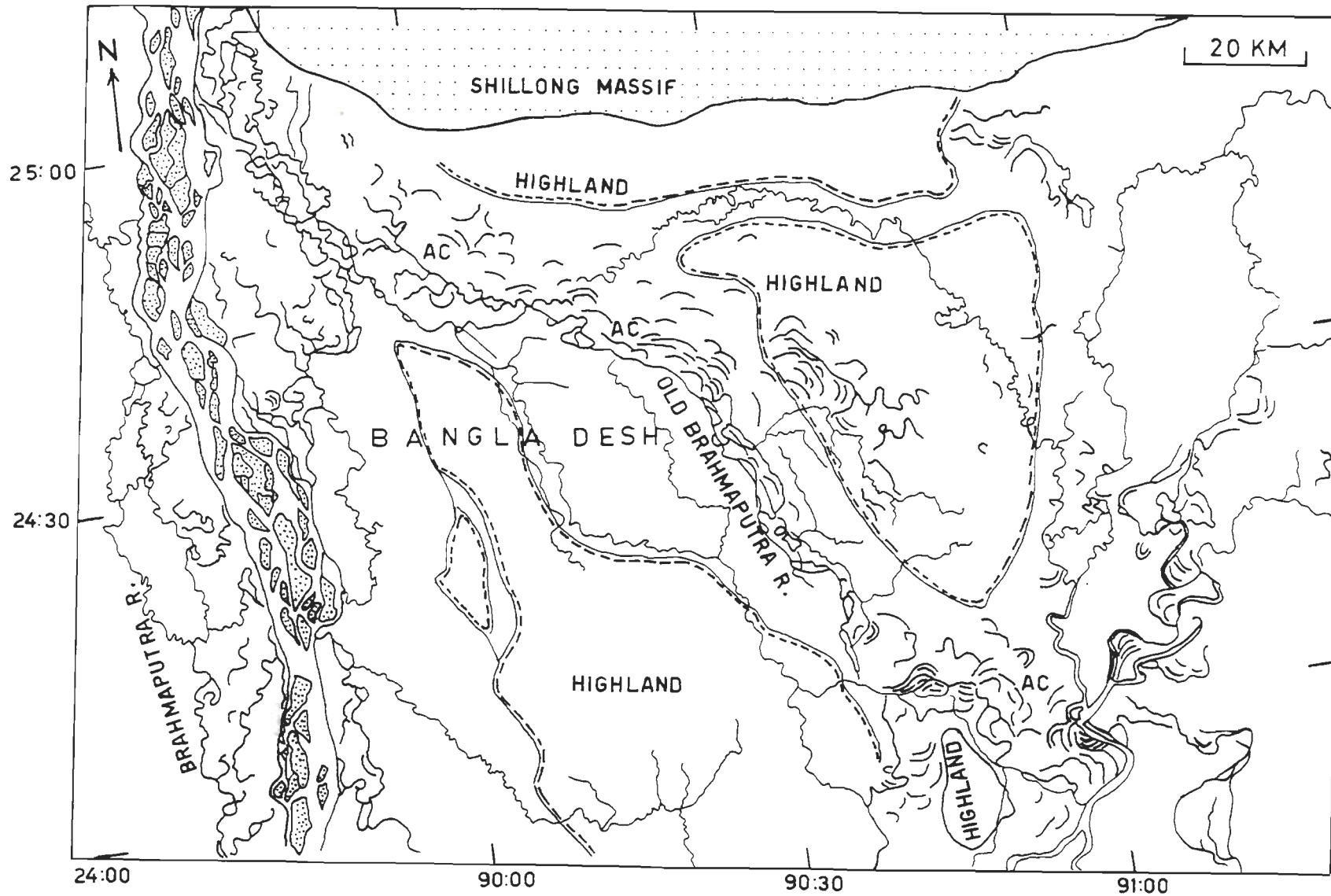


Figure 3.33. Brahmaputra River morphology in Bangladesh. AC-Abandoned Channel. Prepared from Satellite Image.

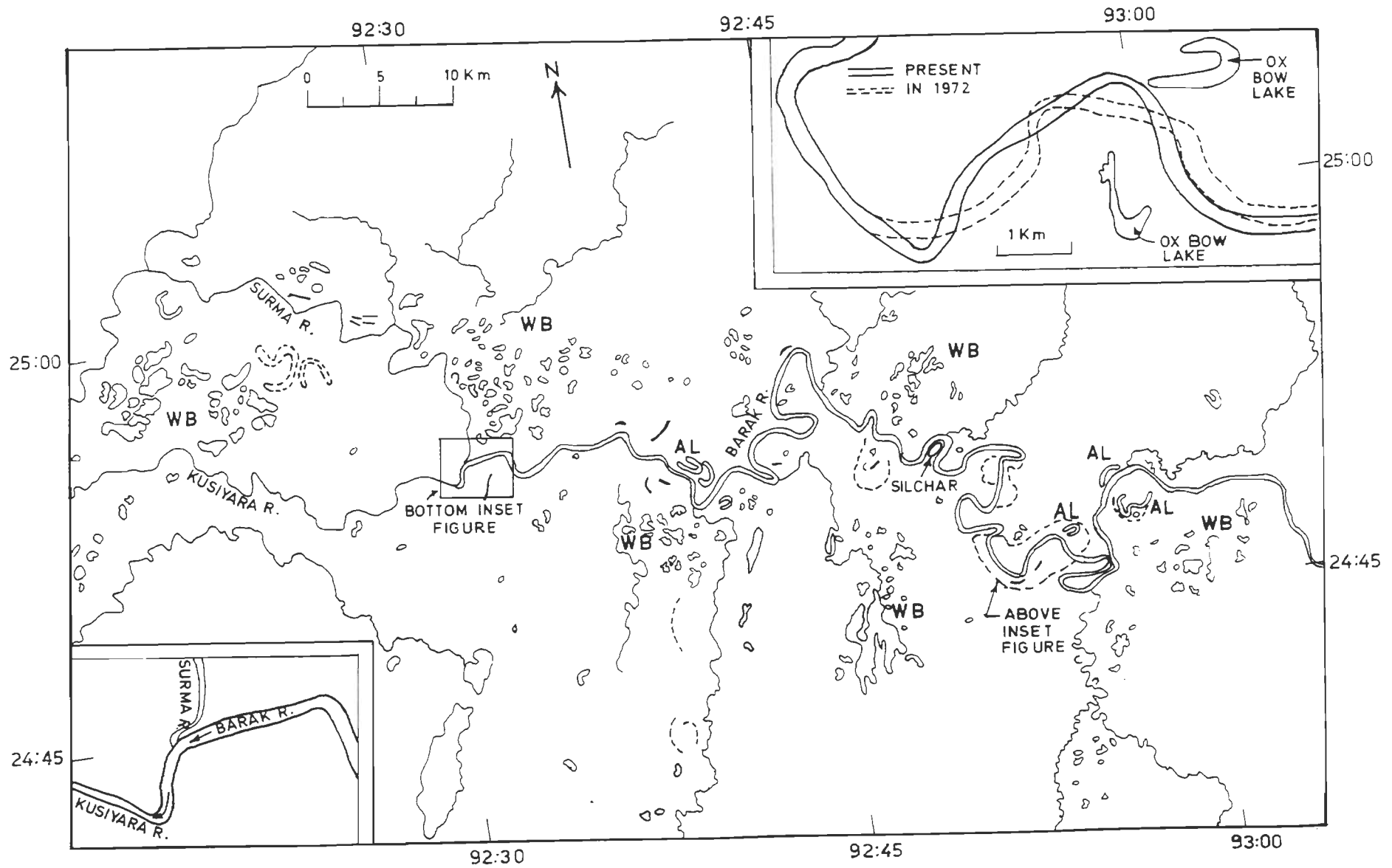


Figure 3.34. Barak River morphology. WB-Water Body; AL-Abandoned Loop. Prepared from Satellite Image.

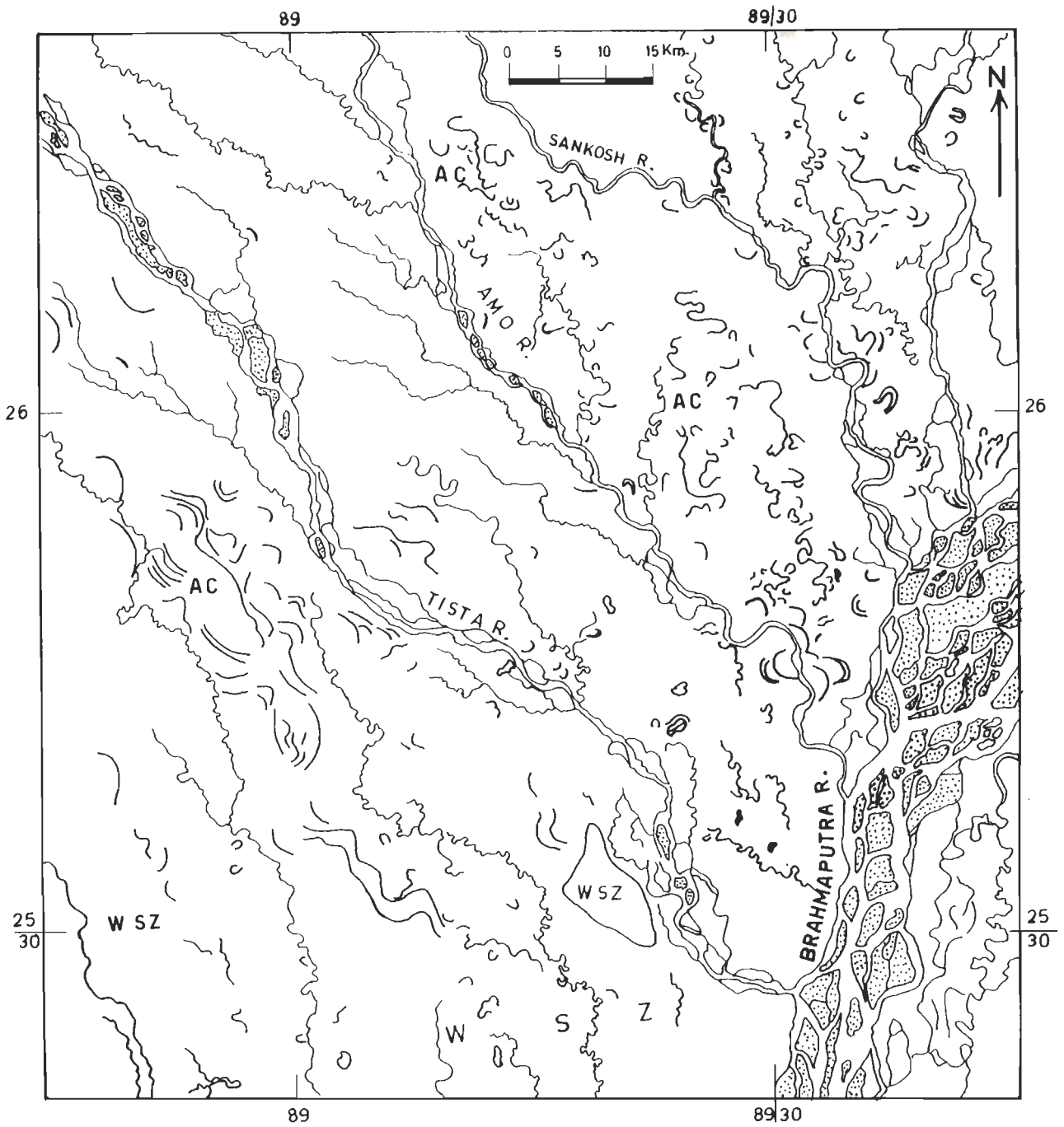


Figure 3.35. Tista River morphology. WSZ-Water Saturated Zone; AC-Abandoned Channel. Prepared from Satellite Image.

DAUKI FAULT AND BARAPANI SHEAR ZONE

4.1 INTRODUCTION

The Shillong Plateau is bounded to the south by the Dauki Fault and to the north by the Brahmaputra Basin. The E-W trending Dauki Fault is the most strikingly linear feature in the region and determines approximately the border between Meghalaya (India) and Bangladesh. The Dauki Fault Zone dissects the Mesozoic and Tertiary rocks, which were deposited along the southern fringe of the Shillong Plateau. It forms steep scarps at many places bordering Bangladesh.

The other prominent feature that could be recognized within the Shillong Plateau is the Barapani Shear Zone. This NE-SW trending shear zone is located within the Precambrian phyllite and can be clearly seen on satellite images. A large reservoir for hydroelectric purpose is located within this shear zone.

Field data on fracture patterns and geomorphological features have been collected from the Dauki Fault Zone. The southwestern part of the Barapani Shear zone was covered during the field work.

Figure 4.1 shows the location of road sections investigated during the field work.

The Dauki Fault Zone is covered by thick vegetation, and topographic maps are not available. Therefore, study of this fault zone was mainly dependent on remote sensing data.

In this chapter, analysis of the characteristics of these two important tectonic features has been presented. The associated neotectonic activities have also been recognized and discussed.

4.2 DAUKI FAULT ZONE (DFZ)

The Dauki Fault Zone (DFZ) could be traced for around 300 km on satellite images (Fig. 4.2). Towards east, this fault zone merges with the NE-trending Haflong Thrust belt, but in the west, it is covered under the alluvium from longitude 90°E. The steep escarpment would indicate vertical displacement along the Dauki Fault Zone, where the Bangladesh plains abut against this zone. This fault zone has been dissected by many N-S trending faults, as can be seen on images (Fig. 4.2).

4.2.1 Geological Background

The DFZ traverses through sedimentary geological formations along the southern edge of the Shillong Plateau. These geological formations belong to the Upper Cretaceous and Tertiary group rocks. Sedimentary rocks are exposed as huge blocks at some places along the DFZ which is conspicuous at Dauki. It can be seen that the sedimentary zone is quite wide, except at places where the Archean gneisses and Precambrian Shillong Group rocks are exposed close to the fault zone around the longitudes 91°15' and 91°45' E respectively (Fig. 4.3).

The southern edge of the basement of Shillong Plateau was broken along the Dauki Fault, which has greatly controlled the Tertiary depositional basins. The sedimentary rocks of this basin had been subjected to intense vertical tectonics as the Dauki Fault was very active during the Early Tertiary. Limited geological information is so far available (cf. Evans, 1964).

According to Evans (1964), the Dauki Fault is represented by the monoclinical structures. The stratigraphical sequence, observed around longitude 90°15' E, shows

different settings in the area north and south of the fault. To the north, the Early Miocene rocks (Lower Bhuban) and Oligocene rocks (Barail) are missing, whereas, thick deposit of these rocks are found to the south of the Dauki Fault. Further, the Early Miocene rocks (Upper Bhuban) directly overlies the Eocene Kopili beds in the north. Moreover, in this region the Dauki Fault dips northward. Towards west, the rock beds are gently flexured north of the fault and nearly horizontal to the south. Farther east, between Dauki and Haflong, the beds north of the fault are mostly horizontal or dip gently to the south, whilst those to the south of the fault dip more steeply and at places, are nearly vertical. The extensive shattering of the rocks had been observed in a belt several kilometer wide along the Dauki Fault (Evans, 1964).

4.2.2 Morphotectonics

On satellite images, the Dauki Fault Zone is represented by very high landforms at places, because the Shillong Plateau is bounded by a steep scarp to the south. This zone is marked by distinct tonal differences and reveal very sharp linear features demarcating the two regions at different levels (Fig. 4.2). Strikingly linear Dauki Fault could be traced as discrete faults (Fig. 4.3). On satellite images, it can be observed that the area is marked by E-W oriented well-defined fractures along the southern edge of the Shillong Plateau which are located mostly within the highly disturbed sedimentary rocks (Figs. 4.2, 4.3).

Although, the area is marked by high hills in Meghalaya and adjacent low lands in Bangladesh, it can be seen that landforms, developed across the Dauki Fault, are not similar all along this fault zone. These varies markedly from place to place. Figure 4.4 shows different landform patterns within the DFZ and adjoining areas. Two distinct zones could be recognized. One is between the longitudes 90° and 91° E and the other is between the longitudes 91° and 92° E (Fig. 4.4). The later zone is typically marked by steep scarp. The area, lying on the Shillong Plateau, shows intense tectonic movements, as revealed by deep gorges and intense fracturing. In this zone, the altitude difference within 25 km at longitude $91^{\circ}40'$ E is of the order of 1314 meters across the Dauki Fault Zone. However, elevation difference is of the order of 150 meters in the extreme western part of the fault zone within the same distance.

4.2.3 Drainage Pattern and Tectonics

The drainage pattern changes are quite useful indicator of neotectonic activities. All rivers, except the ones in the extreme western parts, form deep gorges along the southern edge of the plateau before entering into Bangladesh. Jadukata River forms deep gorge and flows southeastward for 25 km before entering into the Bangladesh Plains with a change in its course (Fig. 4.5). Also, there are quite a few minor streams which are structurally-controlled. In Figure 4.6 (also see Fig. 5.10), at longitude $92^{\circ}10'E$ and in Figure 4.7, also see Fig. 5.9, streams flow have been obstructed by E-W trending fold ridges. Most of the rivers flow southward, crossing the Dauki Fault Zone, making deep cuts in sedimentary rocks and some of them are antecedent in nature.

Significantly, it can be seen that some rivers after crossing DFZ form alluvial fans in Bangladesh. The area adjacent to the southern edge of Shillong Plateau, where alluvial fans have formed are shown in Figure 4.4. This feature is very clearly seen on FCC (Fig. 4.5) where Jadukata River and the other river have formed large alluvial fans which are identified by light tone of sandy material and fan-shaped features on image. Similarly, the other river also forms alluvial fan at longitude $91^{\circ}30'E$ (Fig. 4.7, also see Fig. 5.19, 5.20). Interestingly, these rivers form alluvial fan in zone of steep escarpment along the DFZ.

The rivers and streams form deep cuts into the rocks of Shillong Plateau across the DFZ. It can be seen that most of the streams get lost after forming the alluvium in the area south of the DFZ. Even, the large rivers e.g., Ronga, Jadukata and Dauki becomes very thin and form fans. On FCC, the area south of Dauki Fault have light coloured appearance and fan-shaped morphology revealing the recent alluvial deposits. This characteristics of the rivers have developed due to the formation of low land in Bangladesh adjacent to the DFZ and this process may continue as the area is actively subsiding.

4.2.4 Structural Features

On satellite image, an area between longitudes 91° and $92^{\circ}E$ shows a huge depression to the south of DFZ. This area is partly filled in with water-bodies, which

marked by dark patches on black and white TM image (Fig. 4.2). Two troughs could be recognized in the area adjacent to the DFZ. They are Sylhet and Mohanganj Troughs. In Bangladesh, the right margin of the Sylhet Trough is marked by a fault (Fig. 4.3), which has the same trend of Um Ngot Fault (see Fig. 3.13). This trough is adjacent to the Dauki Fault, where the fault forms very high and steep scarp. Elevation of this trough ranges between 5 to 20 m with numerous lakes and swamps at its surface, and is actively subsiding (Johnson and Alam, 1991). Thickness of sediments in this trough range from 13 to 17 km (Evans, 1964; Hillar and Elahi, 1984). This trough has negative gravity anomalies as low as -84 milligals. The Mohanganj Trough shows huge depression, which is marked by very large water-bodies (Fig. 4.2). The Dauki Fault forms steep scarp at this place, where Jadukata River enters into this trough.

The situation of the area, located to the west of longitude 91°E is quite different. In this region the Dauki Fault dissects the folded sedimentary sequences of Bangladesh.

From the high landmass of Shillong Massif, the rivers and streams entering into Bangladesh generally form alluvial fans (Fig. 4.2). The Old Brahmaputra River in Bangladesh shows southwestward migration, where its surrounding is marked by distinct numerous paleochannels (Fig. 4.2). Madhupur area, which is composed of Pleistocene sediments and located between the Brahmaputra and Old Brahmaputra Rivers, has been elevated recently (Khandoker, 1987) and shifted the main Brahmaputra River to the southwest (Fig. 4.4). Similarly, the Barind tract of Pleistocene sediments, west of the Brahmaputra River, forms also an elevated area (see Fig. 3.13). This indicate that the vertical subsidence was predominantly active in this area.

The most significant tectonic features observed on satellite images are the folds of Miocene and younger sedimentary rocks along the southern edge of the Shillong Plateau (Fig. 4.2). In area around longitude $90^{\circ}30'\text{E}$, sedimentary rocks show distinct E-W trending fold ridges, which extend into the Bangladesh plains (Fig. 4.2). Similarly, at longitude $91^{\circ}20'\text{E}$, the folds appears to have southward convexity as shown in Figure 4.7 (also see Fig. 5.9). During field visits of the study area it has been confirmed that

the ridges of the WNW-ESE, E-W and ENE-WSW trending folds (overlapping anticlines) of Pleistocene age possess this southward curvature. These folds might have formed due to NE-SW, N-S and NW-SE compressional forces respectively. Another set of E-W trending folds can be seen in the area just east of longitude 92°E (Fig. 4.6, also see Fig. 5.10) which are also likely to have formed during N-S compression.

4.3 FRACTURE PATTERN ALONG THE DAUKI FAULT ZONE

During the field trip, different road sections were covered along the Dauki Fault. Unfortunately, very few fresh exposures were encountered. The fracture patterns and other structural features, observed at different locations along the DFZ, are discussed below.

4.3.1 Borhir-Dauki-Muktapur Sector

In this sector, the Dauki Fault forms very steep scarps and huge block of compact sandstones are exposed. Many long E-W oriented high ridges also could be seen.

At Muktapur, conjugate set of joints have formed in sandstones (Fig. 4.8). The sandstone dips 40° due S and possesses joints which strike $N75^{\circ}$ and $N125^{\circ}$ with dips of 55°NW and 70°NE . At Dauki, clay bands within the sandstone beds show shearing evidences. The clay bands became flaky, pulverized and contain blocks of sandstones (Fig. 4.9). In Muktapur-Dauki section, a N-S trending granite surface show striations with a rake of 25° towards south (Fig. 4.10A) indicating a slip along the N-S trending surface. In Dauki-Borhir section, horizontal ridge and groove structures on NE-SW trending sandstone surface could be seen (Fig. 4.10B). The surface show recrystallization of large quartz grains.

Conjugate fractures with a slight movement in soft sandstones could be seen in this sector. In Figure 4.11 A, it may be seen that the block X has moved to the SE whereas, in Figure 4.11 B the block X has moved to west relative to the block Y. It seems that these fractures have developed due to the compressional forces.

At Dauki, the E-W trending vertical slip surface were seen at some places. On a

vertical surface, quartz grains could be seen attached to the soft sandstone (Figs. 4.12 A, B). Also, a hump (150cm x 60 cm) had formed on the surface. Vertical slip should be responsible for this type of surface.

At Borhir, huge block of sandstones (Jaintia Group) are exposed and these rocks show fractured surfaces. The E-W trending vertical surfaces, N40° trending vertical surfaces and 10°/N130° inclined surfaces have developed (Fig. 4.13). The massive sandstone show normal faulting with a southward dipping fault surface at 40° to 65° (Figs. 4.14 A, B).

On Dauki-Pynursla road (10 km towards Pynursla), an inclined slip surface has developed on soil, and strike E-W with a dip of 45° due S (Fig. 4.15). The surface also show inward directed cracks which strike E-W with a dip 50° due N. Formation of this structure is a recent phenomena.

4.3.2 Shella-Balat Sector

At Shella, a limestone exposure was encountered by the river side. The rock is intensely fractured and show slip surfaces (Fig. 4.16 A). On a surface, dipping 56° due NNW, the slickenside rake 33° towards NE and this forms a large slip surface (Fig. 4.16 B).

At Balat, exposures of shale were encountered which were intensely jointed and deformed (Figs. 4.17 A, B). The joints have developed perpendicular to the bedding plane and some are vertical. The shale shows slight deformational features as indicated by block jointing and spheroidal weathering.

4.3.3 Ratacherra Sector

This is the easternmost side of the Dauki Fault Zone covered during field work. At this place also, the fault forms very steep scarp. The rocks are mostly shales and, at places, are soft sandstones which display the deformation patterns. In Figures 4.18 A & B, it can be seen that lenses of sedimentary rocks have formed within the gently inclined shale beds. The shale lenses are 36 cm long and indicate right lateral shearing movement along the bedding plane. Another bedding plane shearing could be observed in Figures 4.19 A & B. Here, the inclined beds show lateral movement and

the intercalated shales have been deformed intensely.

The deformational movement could also be seen at other places. Figures 4.20 A & B show deformational movement of the shale rocks.

4.4 SHILLONG REGION AND BARAPANI SHEAR ZONE (BSZ)

Careful examination of morphological features in Shillong region indicate evidences of tectonic activities that were suffered by the region. Satellite image clearly depicts numerous structural features from this region (Fig. 4.21, also see Figs. 5.2, 5.3 and 5.4). A prominent fracture lineament can be seen along the Barapani reservoir (also Nandy, 1980). Effect of shearing along this zone are revealed by numerous landforms and, therefore, this shear zone has been termed as the Barapani Shear Zone (Das, 1994).

Barapani Shear Zone (BSZ) is a most striking feature in the region with a NE-SW trend. The main river in the region, Wah Umiam, flows northeasterly following the BSZ. This tectonic feature has affected the morphotectonics of the surrounding areas. Topographically, Shillong peak (1964 meters) forms highest geomorphological feature of the plateau to the SE of BSZ. The region immediately south of the Shillong peak has flat topography with gradual gentle southward slope. But, further south spectacular horst and graben structures dominate (Fig. 4.21). Fracture lineament pattern of the Shillong region shows geotectonic features (Fig. 4.22). The geomorphological features, drainage patterns related to mainly the BSZ of the region have been studied.

4.4.1 Geological Background

The Precambrian Shillong Group rocks occupy central part of the Shillong Plateau. The BSZ is located within these rocks having sub-vertical beds and NE-SW trending strikes. The Shillong group rocks are represented by a dominant arenitic facies and a subordinate pelitic facies of metasedimentaries. The commonly occurring rock types are conglomerate, gritty quartzites, arkosic quartzite, carbonaceous slates, green and pinkish slates and phyllites, phyllitic quartzites, dark grey quartzite and more metamorphosed schistose and gneissic rocks (G.S.I. Report, 1981).

The rock exposed along the BSZ are mostly phyllites and metasediments. The geological map of BSZ from Tyrsad to Barapani is shown in Figure 4.23. In northeastern part, the phyllitic quartzite shows more metamorphism southwestward. Around Tyrsad and northeastward, carbonaceous phyllite/slates are exposed. The carbonaceous band is followed by dark grey quartzite, Khasi greenstone and phyllitic quartzite. Basic intrusives, epidiorite and metadolerite known as Khasi greenstones, occur as sills and dykes in all the subfacies of the Shillong Group. Acid intrusives within the Shillong Group are represented by the porphyritic granite with associated veins of aplite and quartz.

The folds in the Shillong Group have steep dips near the crestal region and are flanked by areas with shallow dips (Mazumdar, 1976). In Tyrsad area, these are appressed intrafolial folds in the pelitic rocks, asymmetrical to isoclinal folds in arenaceous rocks and broad open to asymmetric type (Barooah, 1976). These dominantly plunge towards NE/SW with minor variations.

4.4.2 Morphological Features

Satellite image reveals that the BSZ and Shillong region is criss-crossed by numerous fractures (Fig. 4.21). The landmass has suffered protracted weathering resulting in formation of numerous eroded valleys and highlands. A perspective view of the topography of the area around Shillong is shown in Figure 4.24. The Shillong peak (highest place in the region) has NE-SW steep escarpment. Landforms of the study area is mainly fractured flat-topped hills (Fig. 4.25).

Morphologically, the region may be divided mainly into two distinct parts i.e. south and north of Shillong peak (Figs. 4.24, 4.25). To the south of Shillong peak, the landscape has gentle southward slope. Further south, the region has been subjected to block faulting and resulted into formation of horst and graben structures (Figs. 4.22, 4.24, 4.25).

The area north of Shillong peak is dominated by highland and valleys. The NE-SW trending BSZ is associated with elongated ridges. These structural features are the effect of shearing of rocks along BSZ and acts as a local watershed for that region.

4.4.3 Landforms in the BSZ

Landform developed along the BSZ reveals structural characteristics of the shear zone and nature of shearing. Along this shear zone, phyllites are highly fractured having sub-vertical dips and show polyphase deformations with effect of shearing (Barooah, 1976; Mazumdar, 1976). On satellite image significant landforms along this zone could be recognized (Fig. 4.21). Northeast of Barapani reservoir, narrow long ridges (shown as morphological traces in Fig. 4.25), display southwestward dragging effect on western block as these ridges meet the shear zone tangentially (also see Fig. 5.5). Elongated lensoid shaped ridges are seen adjacent to Barapani reservoir towards NE, NW and SW (marked as A, B and C respectively in Figs. 4.21 and 4.25, also see Figs. 5.2, 5.3 and 5.4). Shape of these and dragged linear ridges clearly indicate left lateral slip along the shear zone.

Moreover, the Barapani depression (now reservoir) might have resulted due to small-scale tilting associated with fault movements. Depressions, as a geomorphic indicators are found in the fault zone where small-scale tilting is associated with lateral fault movement (Campagna and Levandowski, 1991). Also, the river Wah Umiam, which follows the shear zone, show northeast-ward shifting, upstream side, adjacent to the reservoir, where the river had to take southwesterly U-turn (Figs. 4.21, 4.26) due to a structural barrier in front, before entering into the depression (also see Figs. 5.2, 5.3 and 5.4). This indicate northeastward shift of eastern block. Therefore, it is clear that the movement along the BSZ had been responsible for major geomorphological changes in the area adjacent to the shear zone.

4.4.4 Drainage Systems

Drainage systems in this region are strongly influenced by structural grains, which are fracture-controlled. Drainage directions in the study area are strikingly adjusted to the fracture directions. Mathur and Evans (1964) noted control of fractures on drainage directions. The fractures are parallel to structural strike occupied by the Shillong Group of rocks and most of these fractures are nearly vertical (Mazumdar, 1986). Since, drainage patterns are overwhelmingly controlled by the fracture

directions, these may also, thus be used as reliable indicators of the directions of fracturing.

Different landforms played great role in directing the streams flow. Major watersheds in the area investigated are as follows (Fig. 4.26). (i) **Watershed WS-I**: This is almost E-W trending divide, separating the Um Lew River from other southerly-flowing rivers. Landform south of this divide is predominantly controlled by horst and grabens. All the streams in this region follow deep graben valleys. **Watershed WS-II**: It is an orographical barrier between the Wah Umiam and Um Lew Rivers up to $91^{\circ}55'/N$ longitude beyond which it takes a northerly turn and separates catchment area of the Wah Umiam and other easterly flowing streams. This watershed passes through the Shillong peak and up to this peak drainage of the Wah Umiam River is separated from the drainage of the Um Lew River. **Watershed WS-III**: The third major watershed, named as WS-III, acts as a divider for the Wah Umiam River and other northward flowing streams.

There are also other important minor structural barriers in the form of isolated hills (Fig. 4.25), which played an important role in determining the streams flow directions and especially controlling the catchment area. In fact, an isolated hill (marked as B in Figs. 4.21, 4.25) adjacent to the Barapani reservoir acted as a morphological barrier for the Barapani depression where reservoir could be developed for hydroelectric purposes. Otherwise, streams could have flowed directly northwestward as the general slope from Shillong region continues further towards northwest across the reservoir as can be seen in Figure 4.26.

Other structural barrier (marked as C in Figs. 4.21, 4.25) lies just southwest of earlier one. It can be seen that along longitude $91^{\circ}47'/E$ (Fig. 4.26) the topography has northward and very gentle southward slope from the high area (1826 mts at latitude $25^{\circ}36'/N$). This structural barrier forms western end of the watershed WS-III. If this structural barrier was not there, the general slope could have been only northward all along from the Wah Umiam River.

Therefore, on the basis of characteristics of these structural barriers, it can be

inferred that BSZ had been probably greatly responsible for present morphological shape of these hills and modification of topography affecting the drainage systems.

4.5 DEFORMATION AND FRACTURE PATTERN ALONG THE BSZ

During the field trip, different road sections were covered traversing the BSZ from Barapani to Tyrsad. At some places, fresh exposures could be studied as the road was being widened by cutting the sides. The fracture patterns and other structural features, observed at different locations along the BSZ, are discussed here.

4.5.1 Shillong-Barapani Sector and Barapani Area

At a location, which is 10 km away from Shillong on Shillong-Guwahati highway, highly sheared rocks could be seen (Fig. 4.27 A). Here, the subvertical phyllite beds are highly sheared and contain large quartzite lenses. These show yellow stain due to sulfur mineralization. The largest lens is 8 meter and second largest is 6 meter long (Fig. 4.27 B). The shape of sheared lenses indicate sinistral displacement along bedding planes.

The sandstone exposure at Barapani reveals interesting shearing effects (Fig. 4.28) and contain lenses upto a meter (96 cm) and reveal recrystallization. Fractures are filled in profusely with mud stone. The sense of shearing found to be sinistral in NE-SW direction.

The Precambrian phyllites display remarkable brittle deformation at a site 13 km north of Shillong on Shillong-Barapani road (Fig. 4.29). The sub-vertical beds are broken and became inclined towards NW. Similarly, at Mawphlang also, the sub-vertical phyllites show brittle deformation where in the beds had broken and became inclined towards SE (Figs. 4.30 A, B). Nature of brittle deformation at these locations indicate lateral movement in NW-SE direction.

4.5.2 Mawphlang-Tyrsad Road Section

The fresh exposures of phyllite could be studied in this sector. The phyllites are steeply dipping to vertical at most places. Intense brittle deformation and shearing of rocks could be observed.

In this sector, NE-SW trending vertical shear zone had formed within vertical to steeply dipping phyllites. The left-lateral shearing, which were observed at Shillong-Barapani sector continues farther to the southwest. At one locality, steep phyllites show vertical shear zone (Fig. 4.31). Highly fractured phyllites exposures can be seen within narrow shear zone (Figs. 4.32 A, B) which is later displaced by sub-horizontal faulting revealing compressional effect.

At other place, moderately dipping carbonaceous phyllites show drag effects, as the phyllite beds terminate against overlying fault zone with a southeastward convexity (Fig. 4.33).

In this sector, the phyllites preserve groove markings with a plunge of 60° towards $N20^{\circ}$ on a surface striking $N20^{\circ}$ - $N200^{\circ}$ and dipping 66° towards $N290^{\circ}$ (Fig. 4.34).

4.5.3 Mawangap-Sohiong Sector

A large slip surface in phyllites could be observed in this sector dipping 65° towards NW. The slickensides plunge 50° towards WNW on this surface (Fig. 4.35).

4.6 DISCUSSIONS

The Dauki Fault is extending eastward along the latitude 25° N below the Indo-Burman fold belt and separates the high and low basement rocks exposed to the north and south of this fault. In frontal fold belt, numerous N-S trending Miocene sedimentary folds (gently plunging anticlines and synclines) have migrated freely into the Bangladesh. But, no movement along the Dauki Fault occurred probably after Miocene, as is indicated by folds in sedimentary rocks crossing the fault at longitude 93° E and remained totally undisturbed (marked by arrow in Fig. 4.2). Rather, the E-W trending transverse fault with a lateral movement, observed far south of the Dauki Fault at latitude $24^{\circ}30'$ N (Figs. 3.13, 3.28). It appears that the tectonic activities have shifted to the south which is also supported by recent earthquake occurrences in the region.

It seems that the tectonics along the DFZ have evolved into different types than

in the initial stages. Now, the area shows upliftment along the DFZ, from the longitudes 90°E (from Brahmaputra River) to 91°E and between longitudes 91° to 92°E , the area reveals subsidence. Beyond this the area of thrusting reveals sediments overriding from south along a southward thrust plane.

It has been opined that N-S convergence is now shared by thrust faulting and folding both in the Himalayas and the Shillong Plateau (Oldham, 1899; Seeber and Armbruster, 1981 and Molnar, 1987). Further, Mukhopadhyay (1990) and Khattri et al. (1992) advocated that thrusting was taking place along the Dauki Fault which is extending northward below the Shillong Plateau. However, no evidence of thrusting has been observed. Rather, the rocks of DFZ show vertical normal faulting. The huge block of sedimentary rocks show vertical slip-surfaces especially in Dauki sector and the steep escarpment itself is indicative of vertical normal faults. Recently, Das et al. (1995) have suggested mainly the vertical tectonism had been active along the Dauki Fault Zone.

From the study of fracture pattern along the DFZ, it can be seen that the area had suffered multi-directional compressional forces. The E-W trending vertical slip-surfaces are well preserved in compact sandstones. This indicate that the rocks had undergone the E-W trending fracturing due to the N-S oriented extensional forces even after compaction of the rocks has taken place. Moreover, on satellite images of DFZ and adjoining regions in Bangladesh display mainly the E-W trending folds in soft sediments of Pleistocene age. These folds had formed due to the N-S trending compressional forces between the Shillong Massif and Bangladesh Plains.

The Barapani Shear Zone (BSZ) is a significant tectonic feature in Shillong Plateau. Morphotectonics of this area must had been influenced by this structure. Considerable amount of informations are available on geological aspect of Shillong Plateau in the work of Murthy (1970); Murthy et al. (1976); Barooah (1976); Mazumdar (1976, 1986) and G.S.I. (1974). Singh (1968) and Chopra (1986) have given an account of generalized geomorphological studies of the parts of Shillong Plateau mainly on the basis of lithological effects on geomorphology. Mazumdar (1978) also gave detailed

information on morphogenetic evolution of the Khasi Hills. However, surface manifestation and geomorphological features, associated with the BSZ escaped attention so far. It has been observed in this study that geomorphological features identified on satellite images and topographic maps, could lead us to determine the sense of slip and modification in hydro-geomorphological regime in the area adjacent to BSZ.

On Satellite images, left lateral translational movement could be recognized along the NE-SW trending BSZ. The BSZ probably got reactivated due to intense N-S trending compression in Miocene time when the compression between the Indian and Tibetan plate had culminated. Intense ductile shearing of rocks in BSZ had been observed at a location 10 km north of Shillong towards Barapani where the shearing is bedding plane. But farther southwest, it has been observed in the field that the intensity of ductile shearing subsided and only very narrow vertical shear zone within the inclined phyllites had been noticed. The rocks in this part mainly show intense brittle deformation. The fracture pattern reveals compressional stresses. Further, it is expected that reactivation may take place along the BSZ in future under continued northward drift of the Indian plate.

Present topographical features are positively attributed to the tectonic activities suffered by the region. Fractures in the region were weak zones along which weathering and erosional agents could find easy path for denudation giving rise to different types of topography. The plateau has numerous granitoid plutons exposed on the surface and some may be hidden below. A plateau may form by updoming of the region due to intrusion of magma into the lower crust as pointed out by McKenzie (1984). Mazumdar (1986) recognized a major thermal event and later Ghosh et al. (1991) propounded mantle upwelling during late Proterozoic-Early Paleozoic period. Probably, present topography with the highest place, the Shillong peak, in the central region is the result of mainly updoming. Probably, a magmatic pluton is hidden below the Shillong peak area which show such a high relief. Magmatic activity accompanied by vertical movements along the fractures would have uplifted the Shillong peak region as fracture controlled block movement has been recognized by Mazumdar (1978).

Drainage systems have developed depending on the topography of the area and drainage directions are strongly governed by fracture directions riddling the regions. Elongated hills along the BSZ have controlled the valley configuration and played great role in defining the hydrological system.

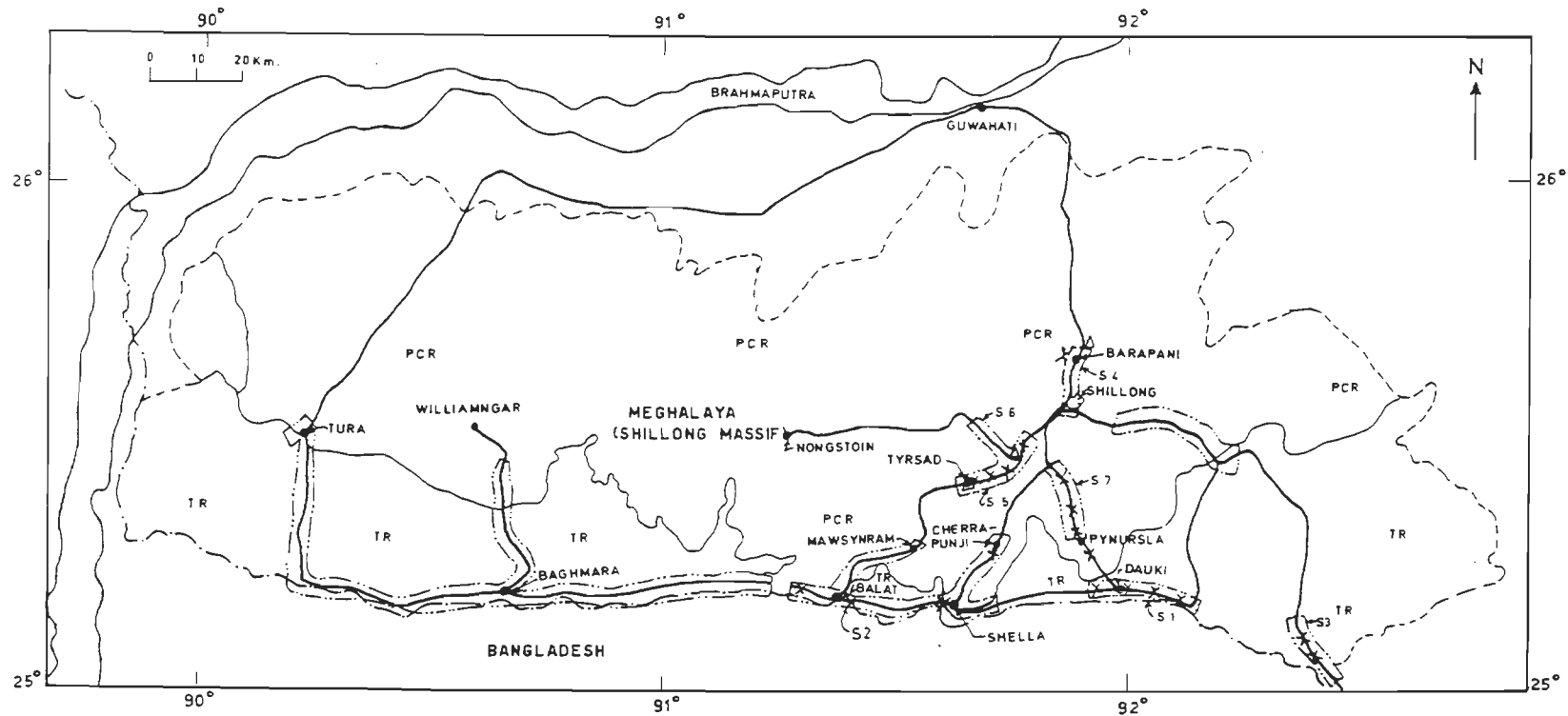



Figure 4.1. Map shows area of Shillong Plateau covered by field work, location of field photographs of rock exposures (x) and different sectors. Generalized distribution of Precambrian rocks (PCR) and Tertiary rocks (TR) of the field area is shown. Field data collected from the sectors S1-Borhir-Dauki-Muktapur; S2-Shella-Balat; S3-Ratacherra; S4-Shillong-Barapani; S5-Mawphlang-Tyrsad; S6-Mawangap-Sohiong; S7-Pynursla.  Road sections covered.

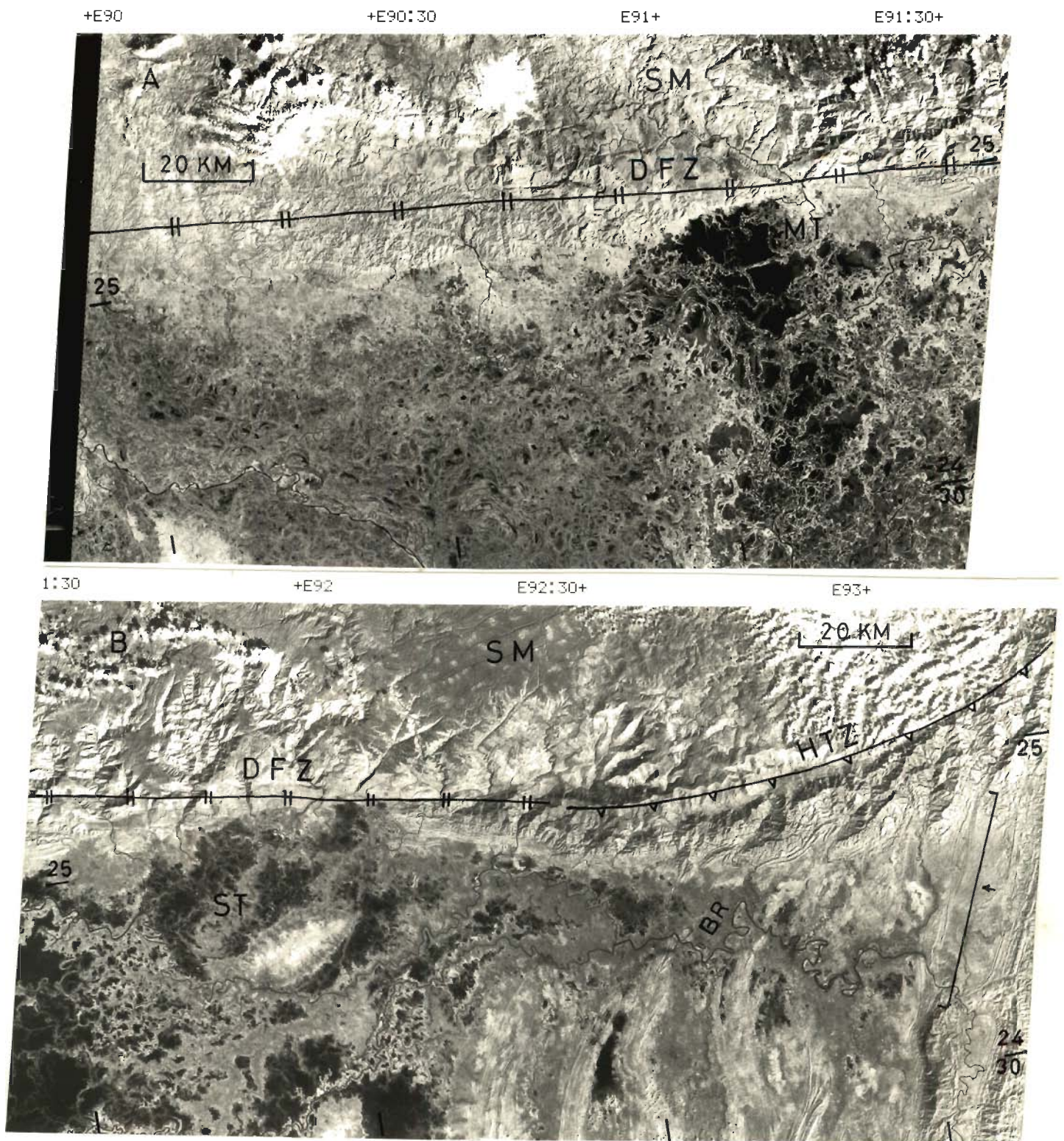


Figure 4.2 (A) & (B). Satellite images (TM Band 4) of Dauki Fault Zone and adjoining Bangladesh area. SM-Shillong Massif, DFZ-Dauki Fault Zone, HTZ-Haflong Thrust Zone, MT-Mohanganj Trough, ST-Sylhet Trough, BR-Barak river. The extreme western part of DFZ is not shown.

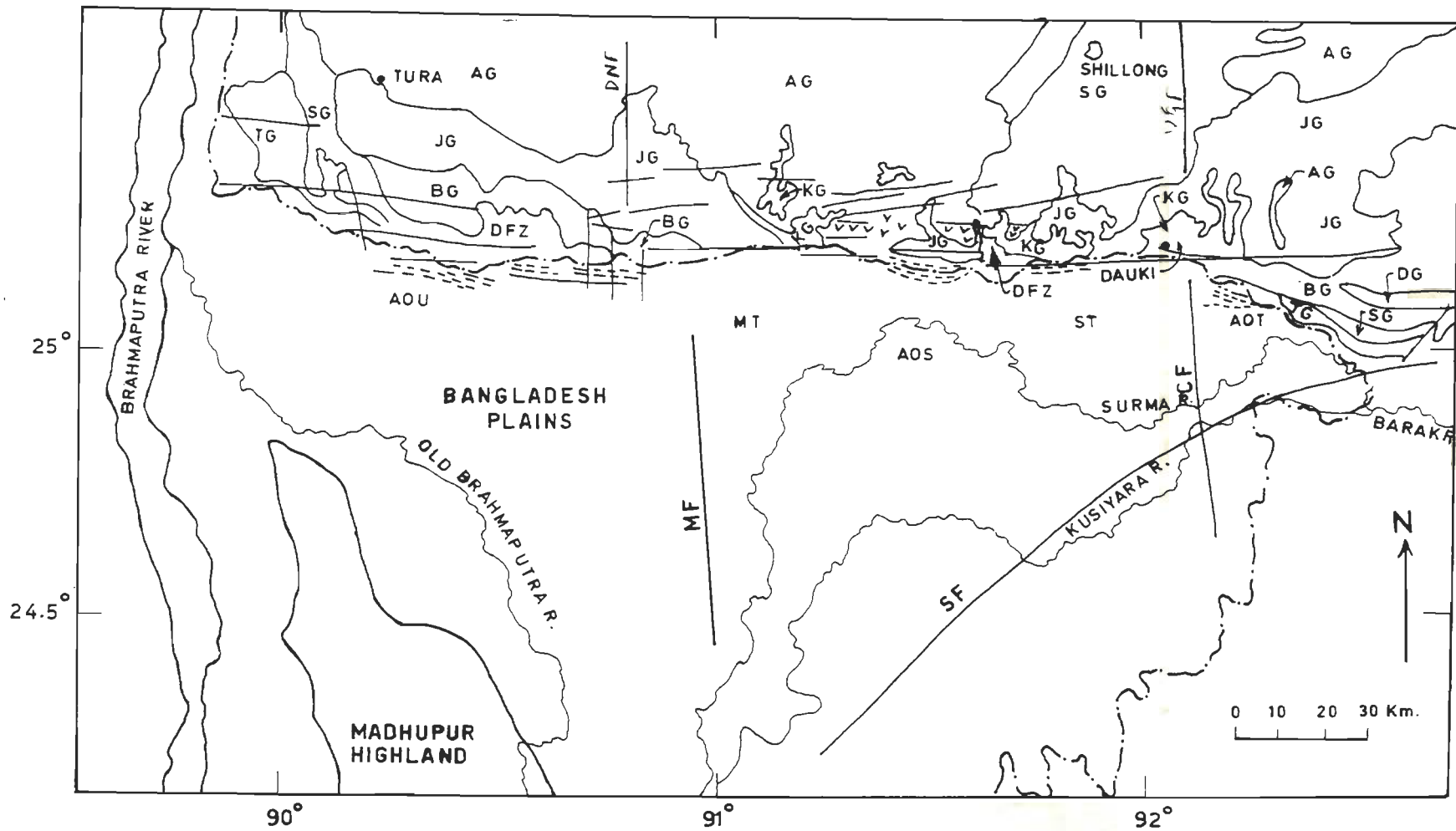


Figure 4.3. Geo-tectonic features of the Dauki Fault Zone and adjoining area in Bangladesh. TG-Tipam Group (Miocene), SG-Surma Group (Miocene), BG-Barail Group (Oligocene), JG/DG-Jaintia/Disang Group (Eocene), KG-Khasi Group (Up. Cretaceous), vvv- Sylhet Trap (Lower Cretaceous), SG-Shillong Group (Precambrian), AG-Archean Gneiss (Archean). DFZ-Dauki Fault Zone, DNF-Dudhnai Fault, UGF-Um Ngot Fault, MT-Mohanganj Trough, ST-Sylhet Trough, MF-Mohanganj Fault, CF-Chandghat Fault, SF-Sylhet Fault, AOU-Area of Uplift, AOS-Area of Subsidence, AOT-Area of Thrust. Traces of the fold ridges

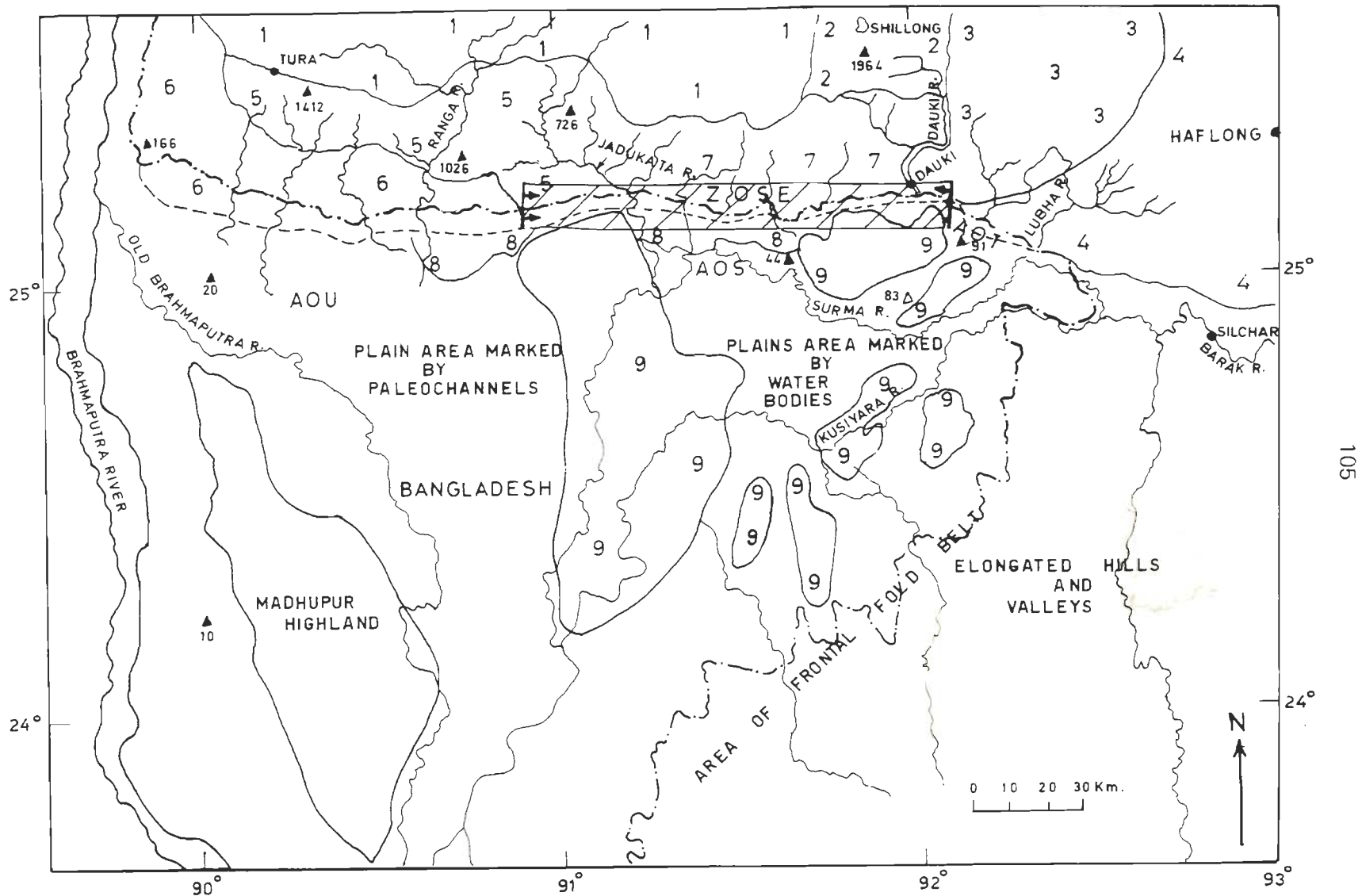


Figure 4.4. Morphological map of Dauki Fault Zone and adjoining areas in Bangladesh. LEGEND 1-Fractured high Archean table land, 2-Highly fractured land, 3-High flat land, 4-High Hills and folds in sediments, 5-High Hills, 6-Low Hills, 7-Area of horst and graben, 8-Alluvial fan, 9-Very low land area in Bangladesh, ZOSE-Zone of Steep Escarpment, AOU, AOS, AOT-as in figure 4.3.

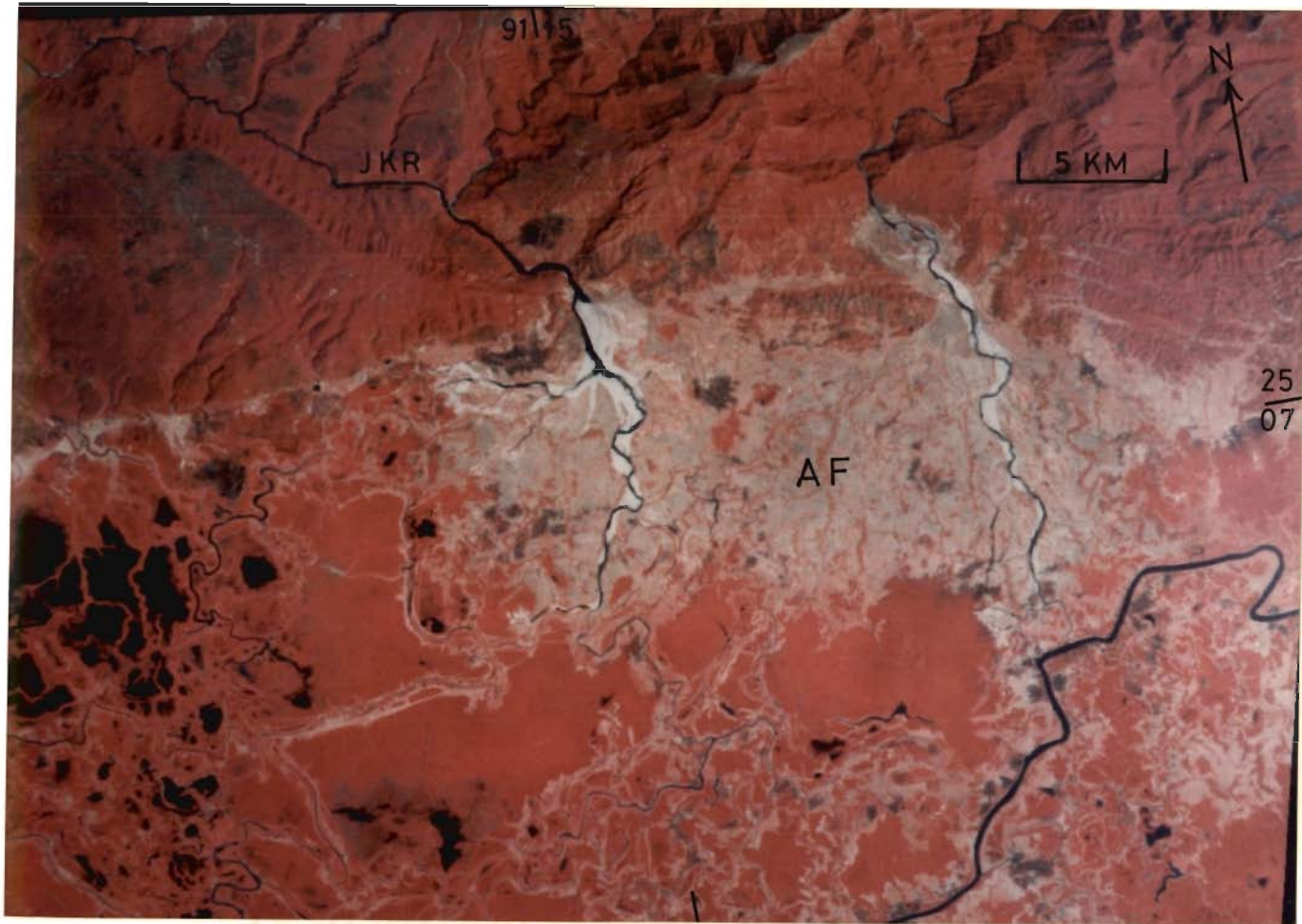


Figure 4.5. FCC (IRS LISS-II) shows Jadukata River (JKR) and morphology of the area adjacent to the Dauki Fault Zone. AF-Alluvial Fan.

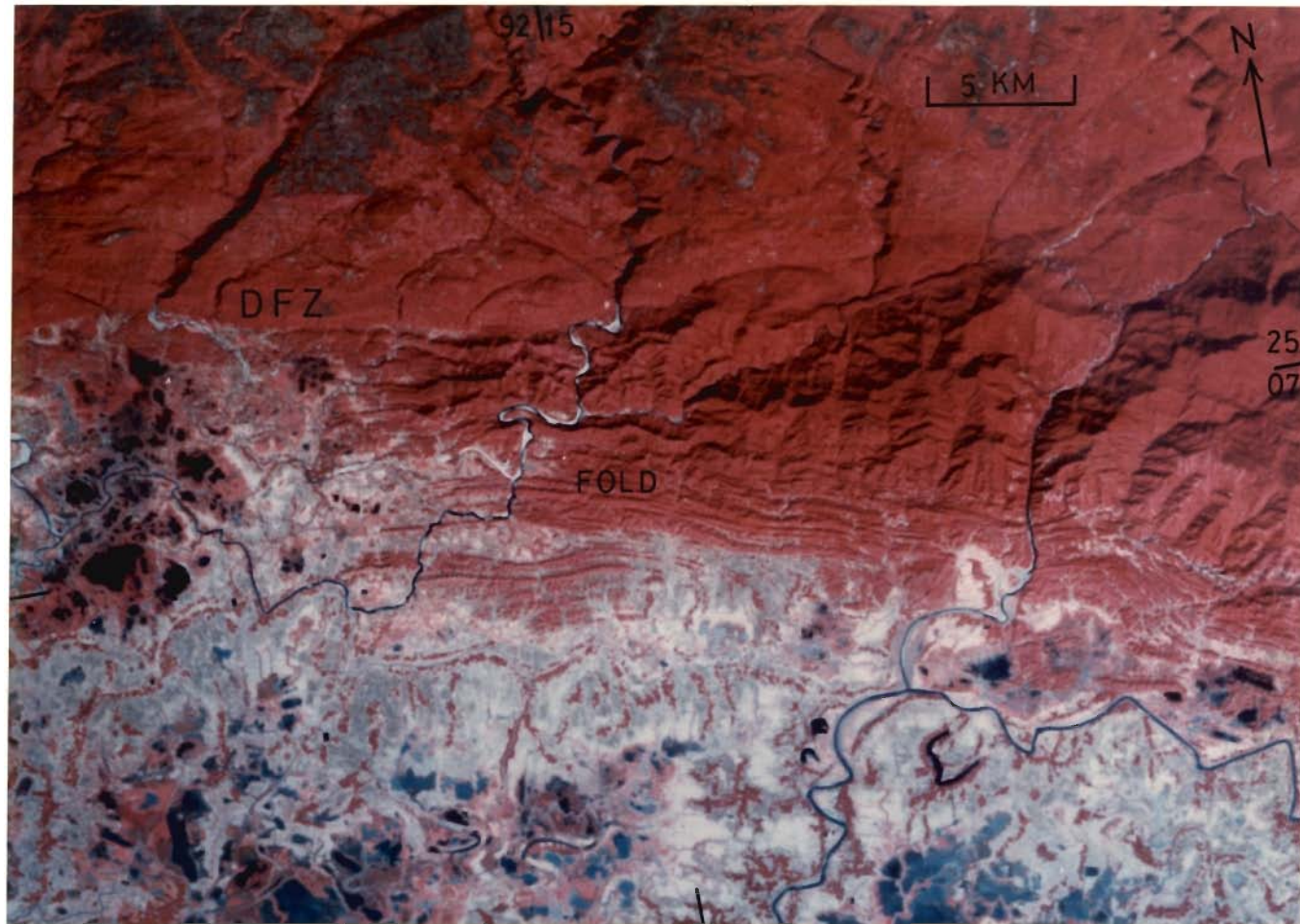


Figure 4.6. FCC (IRS LISS-II) shows E-W trending fold ridges and nature of stream just south of the Dauki Fault Zone (DFZ).



Figure 4.8. Field photograph showing conjugate fracture in sandstone. Loc.- 16 km-east of Dauki at Muktapur



Figure 4.9. Field photograph showing slightly sheared sandstone. Loc.-Dauki

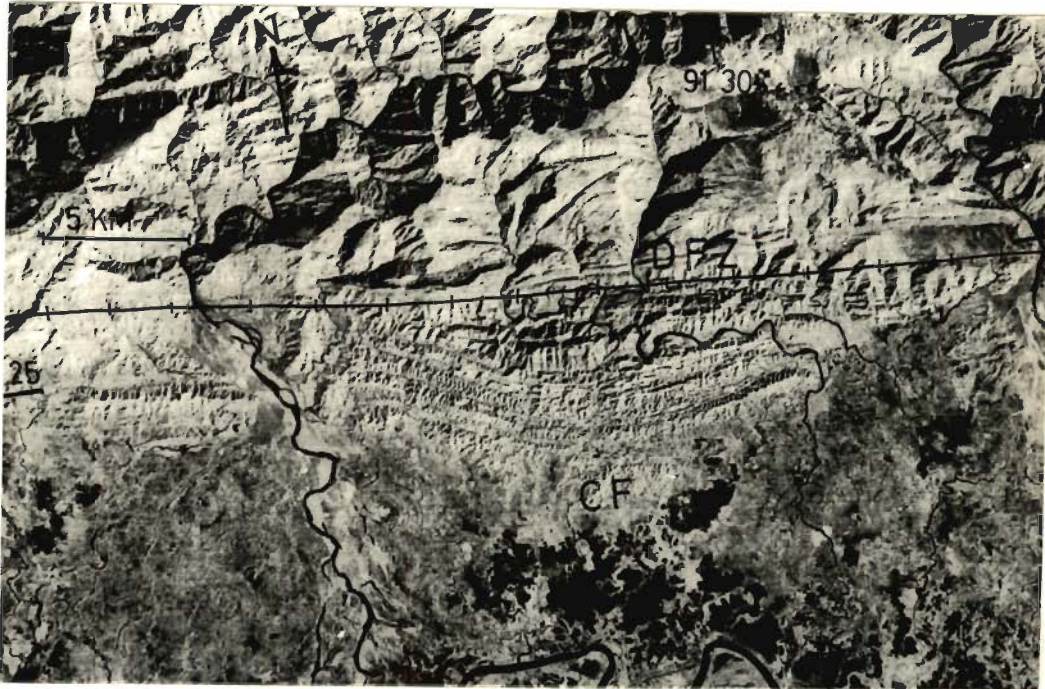


Figure 4.7. Satellite image (TM Band-4) shows southward convex folds in sedimentary rocks along the Dauki Fault Zone (DFZ). CF-Convex Fold.

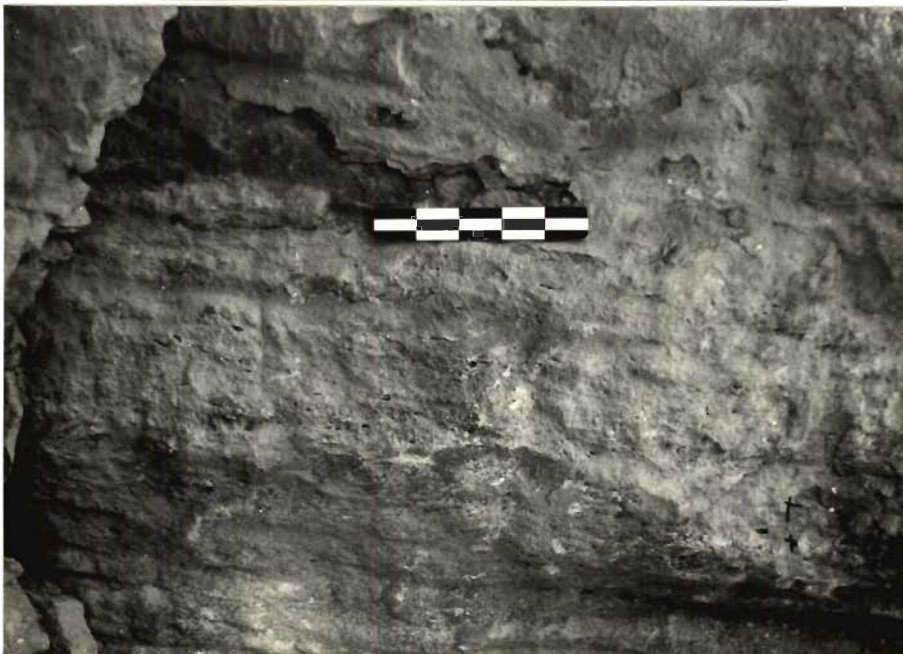


Figure 4.10 (A) & (B). Field photographs showing ridge and groove structures in granite and sandstone. Loc.- (A) 6 km east of Dauki towards Muktapur, (B) 12 km west of Dauki at Borhir.

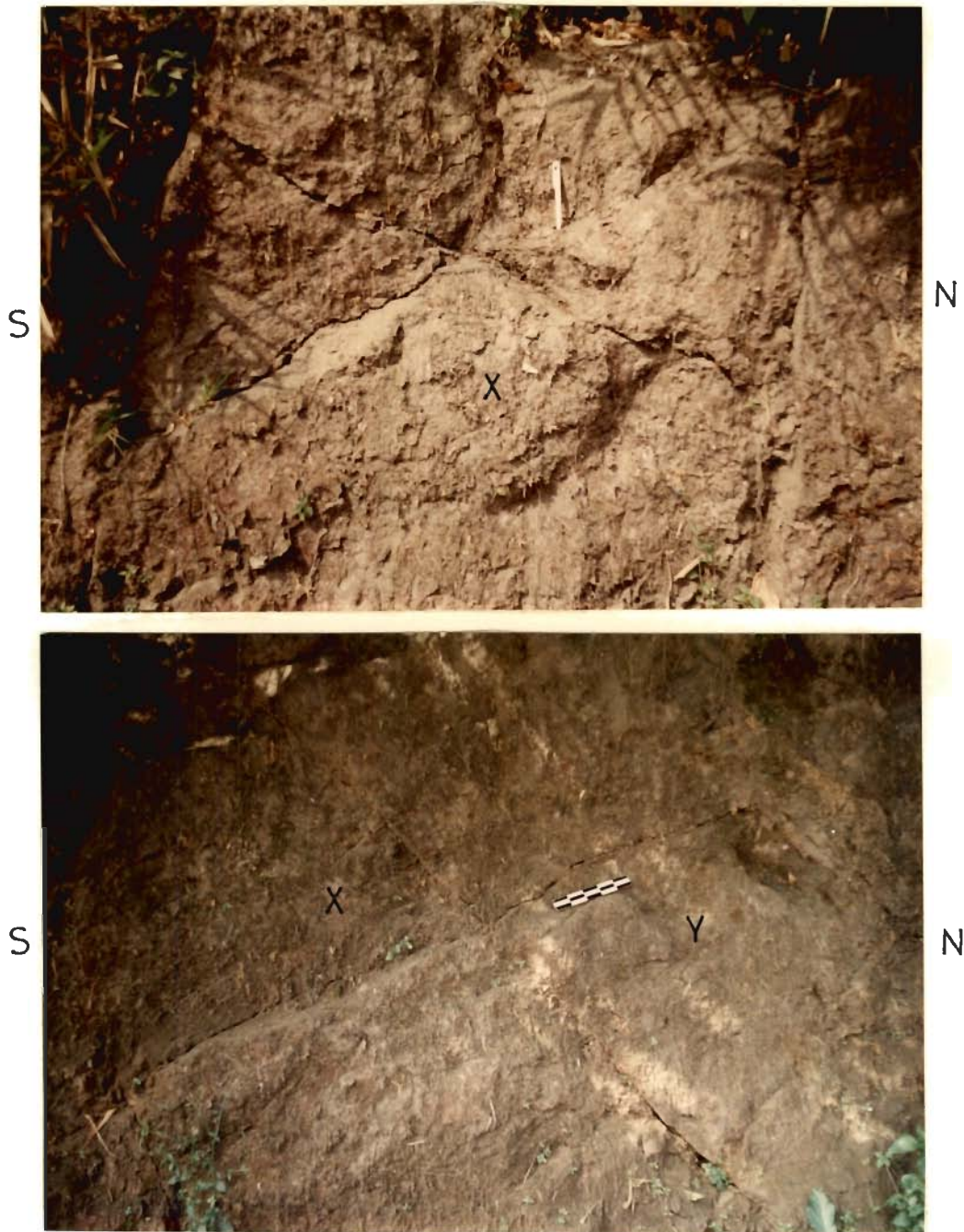


Figure 4.11 (A) & (B). Field photographs showing conjugate shear fracture in soft sandstone. (A)-Fracture trends: 25° due S and 35° due N, block X slipped to SE. (B)-Fracture trends: 30° due S and 40° due N, block X slipped to west with respect to block Y. Loc.- 9.5 km west of Dauki towards Borhir.



Figure 4.12 (A) & (B). Field photographs showing E-W trending vertical slip surface on compact sandstone along with quartz crystals on its surface (A) and a hump structure (150 cm x 60 cm) on a vertical surface (B). Loc.- Dauki



Figure 4.13. Field photograph showing E-W trending vertical surface and other fractures in compact sandstone along the Dauki Fault Zone. Loc.-10 km west of Dauki towards Borhir.



Figure 4.14 (A) & (B). Field photographs showing southward dipping normal faulting in compact sandstone at the Dauki Fault Zone. Loc.- Borhir.



Figure 4.15. Field photograph showing southward dipping (facing the viewer) fault in soil. The slip surface also show northward dipping cracks. Loc.-10 km north of Dauki towards Pynursla.



Figure 4.16 (A). Field photograph showing fracture pattern in limestone along the Dauki Fault Zone. Loc.-Shella.



Figure 4.16 (B). Field photograph showing slickensides on limestone. Loc.-Shella.



Figure 4.17 (A). Field photograph showing multiple fractures in shale. Loc.- 10 km west of Balat.



Figure 4.17 (B). Field photograph showing deformed shales along the Dauki Fault Zone. Loc.-2 km east of Balat.

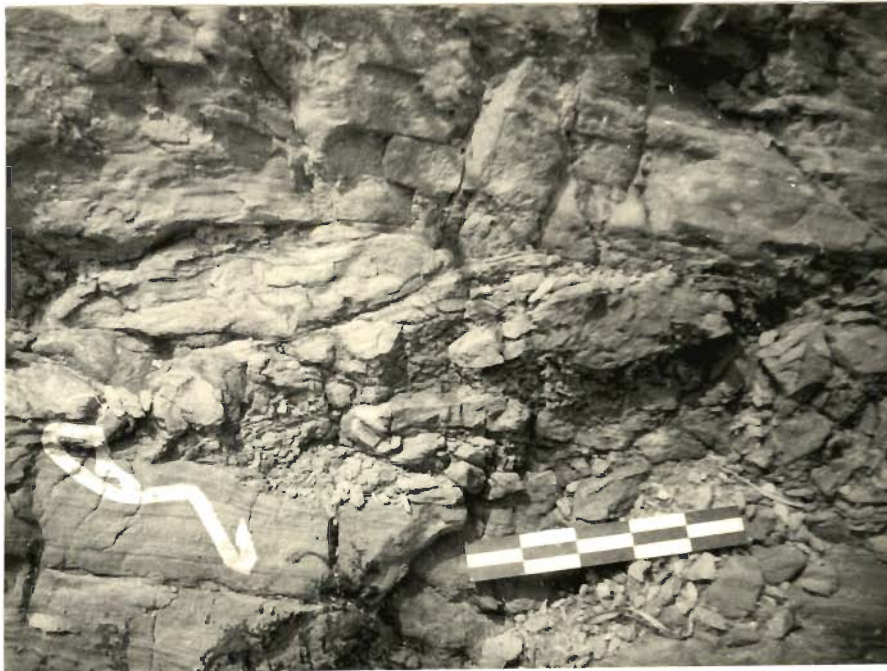


Figure 4.18 (A) & (B). Field photographs showing shearing within sedimentary layers. Photograph (B) is a close-up of (A). Loc.- Easternmost side of the Dauki Fault Zone. Site-Ratacherra from sector S3 (Fig. 4.1)



Figure 4.19 (A) & (B). Field photographs showing intense deformation of shales. Photograph (B) is a close up view of (A). Loc.-Ratacherra, Sector S3 (Fig. 4.1).



Figure 4.20 (A). Field photograph showing deformation in shale. Loc.-Ratacherra, Sector S3 (Fig. 4.1).



Figure 4.20 (B). Field photograph showing deformation in shale. Loc.-Ratacherra, Sector S3 (Fig. 4.1).



Figure 4.21. Satellite images (TM Band 4) of Shillong region showing Barapani Shear Zone and other morphotectonic features. SHL-Shillong, BR-Barapani reservoir. A, B & C are the lens shaped ridges.

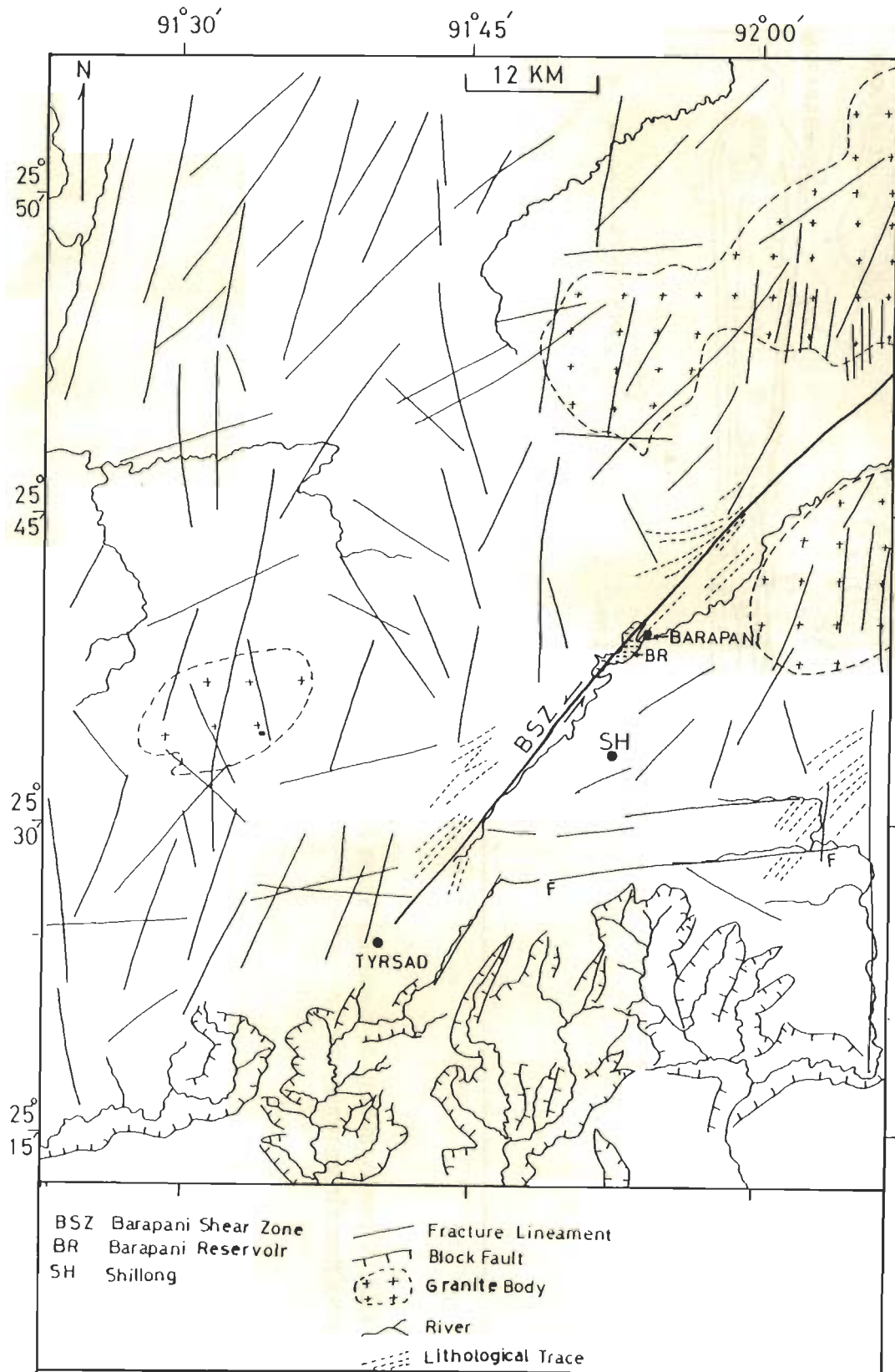


Figure 4.22. Fracture lineament map of area around Barapani Shear Zone showing the relationship between the features. BSZ-Barapani Shear Zone, BR-Barapani Reservoir, SH-Shillong. Prepared from Satellite image.

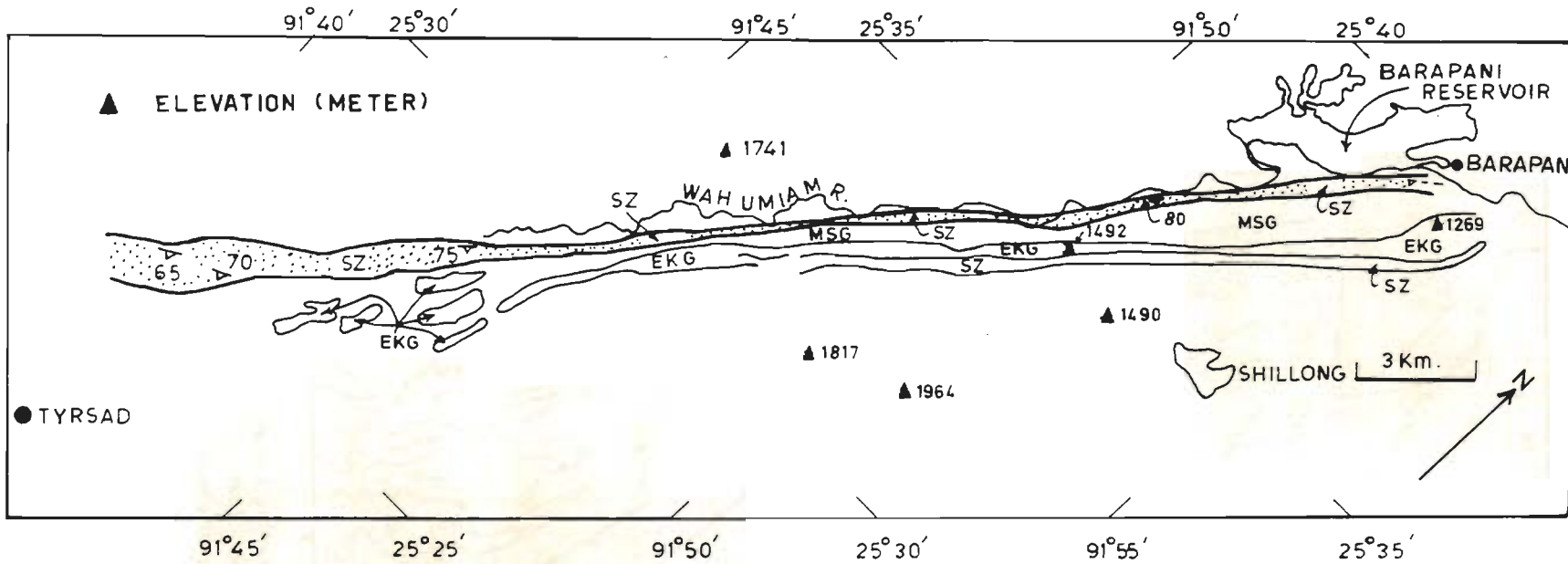


Figure 4.23. Geological map of Barapani Shear Zone. SZ-Shear Zone, MSG-Metasediments-Shillong Group, EKG-Epidiorite-Khasi Greenstone.

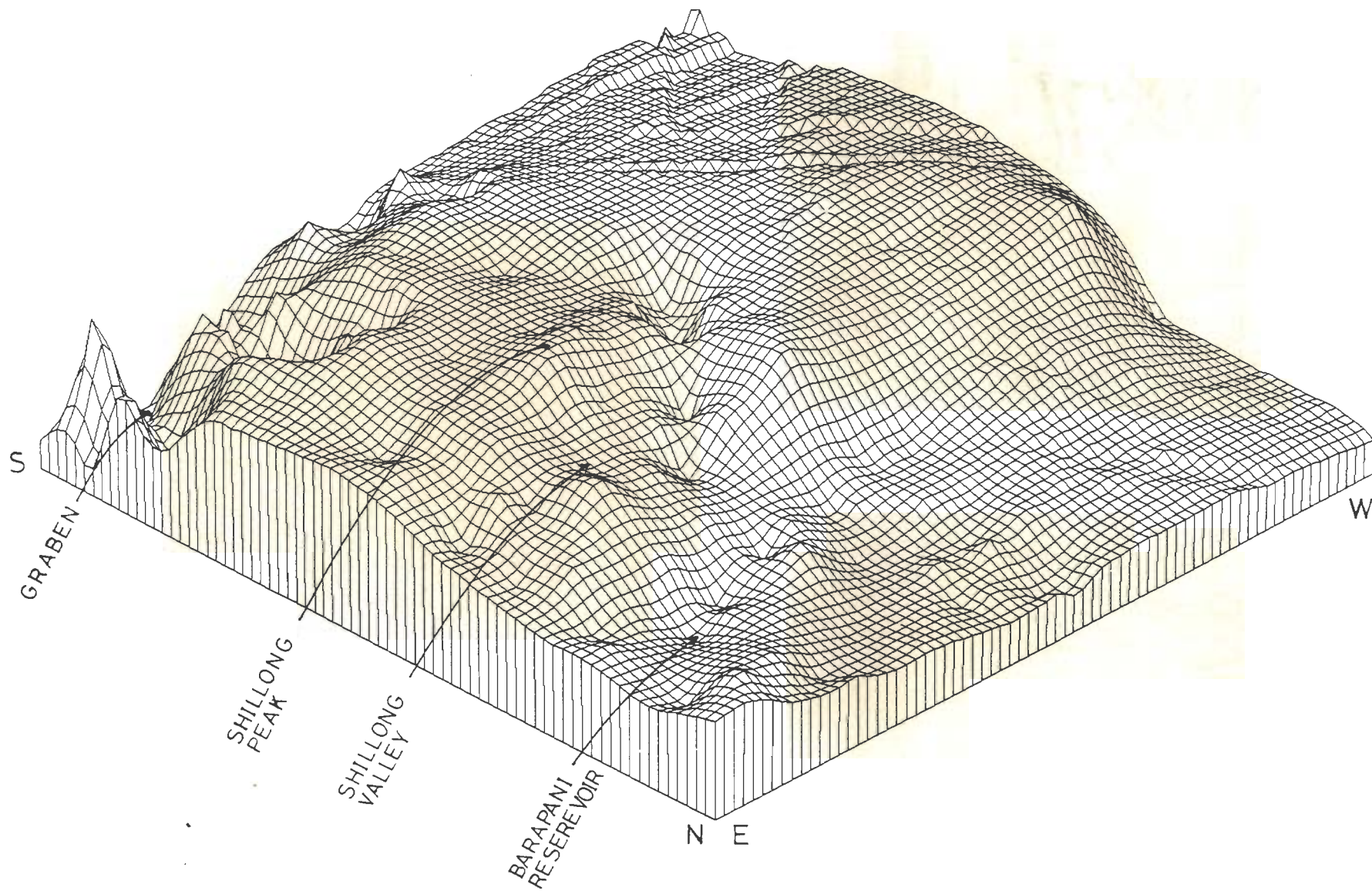


Figure 4.24. A perspective view of the topography of the area around Shillong.

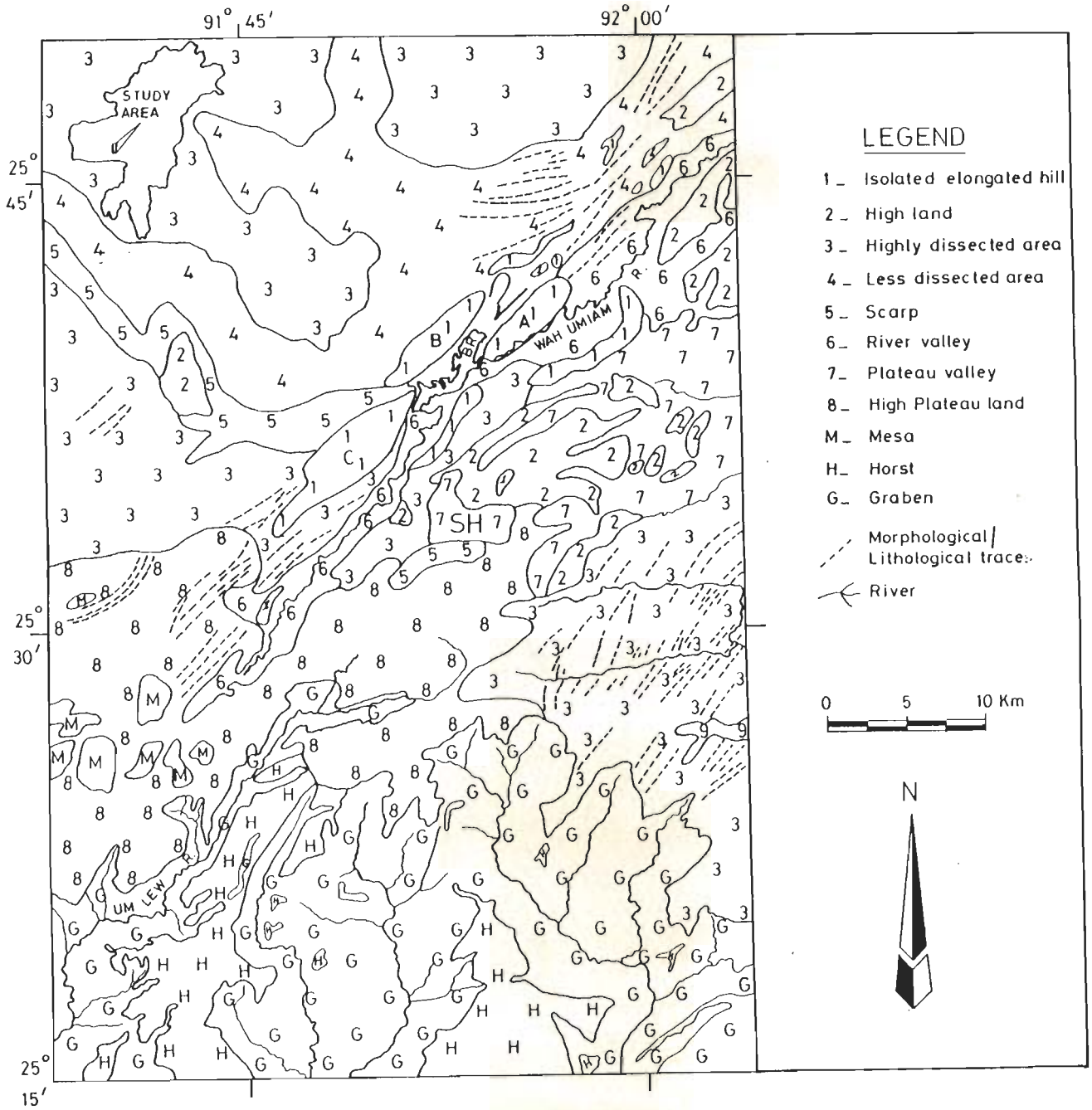


Figure 4.25. Landform map of the region around Shillong. SH-Shillong, BR-Barapani Reservoir, Elongated hills are marked as A, B and C which are described in text. Prepared from Satellite image.

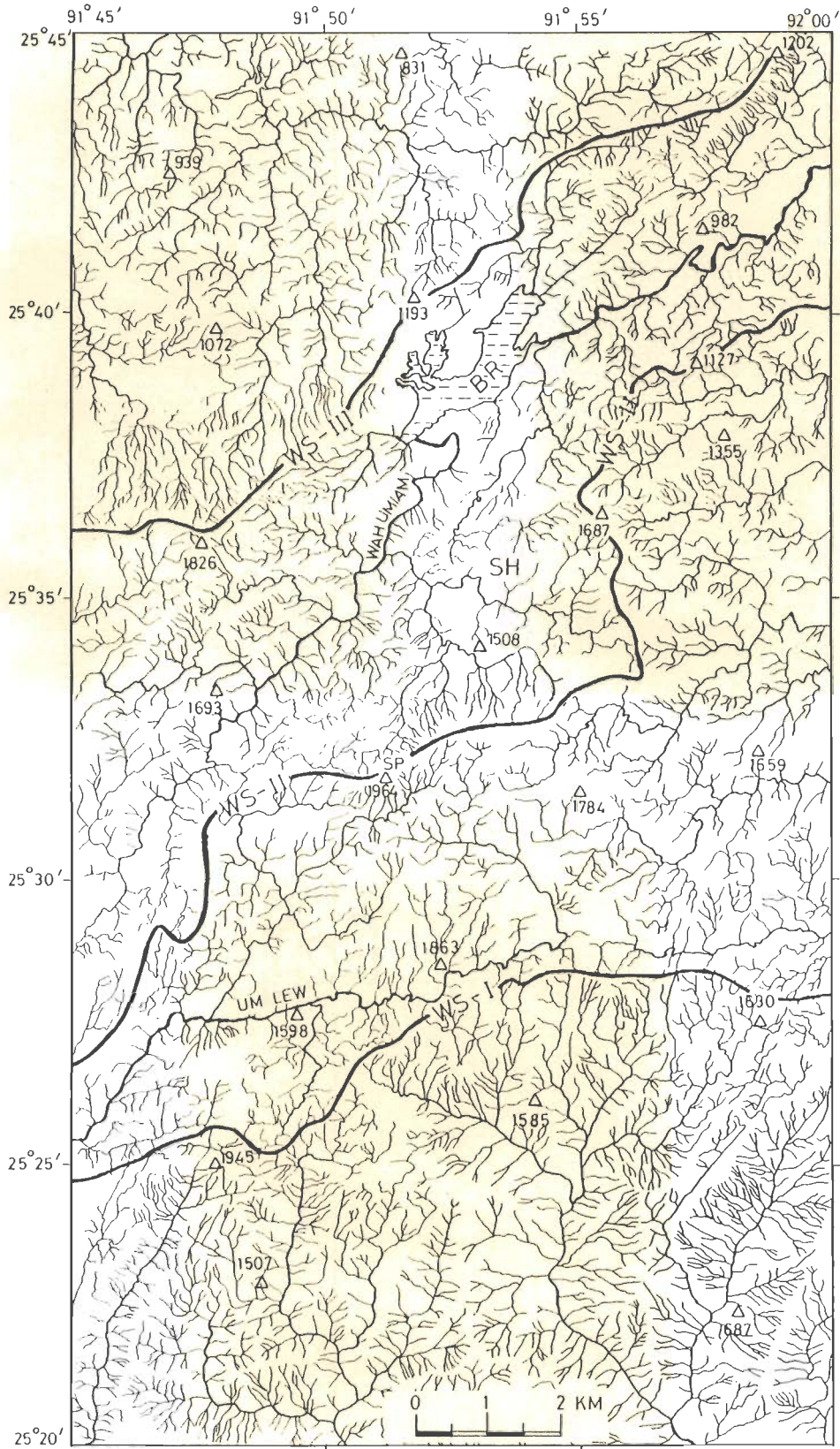


Figure 4.26. Drainage systems of the region around Shillong. Watersheds are marked as WS-I, WS-II and WS-III. SH-Shillong, SP-Shillong Peak, BR-Barapani Reservoir. Elevations are given in meters.

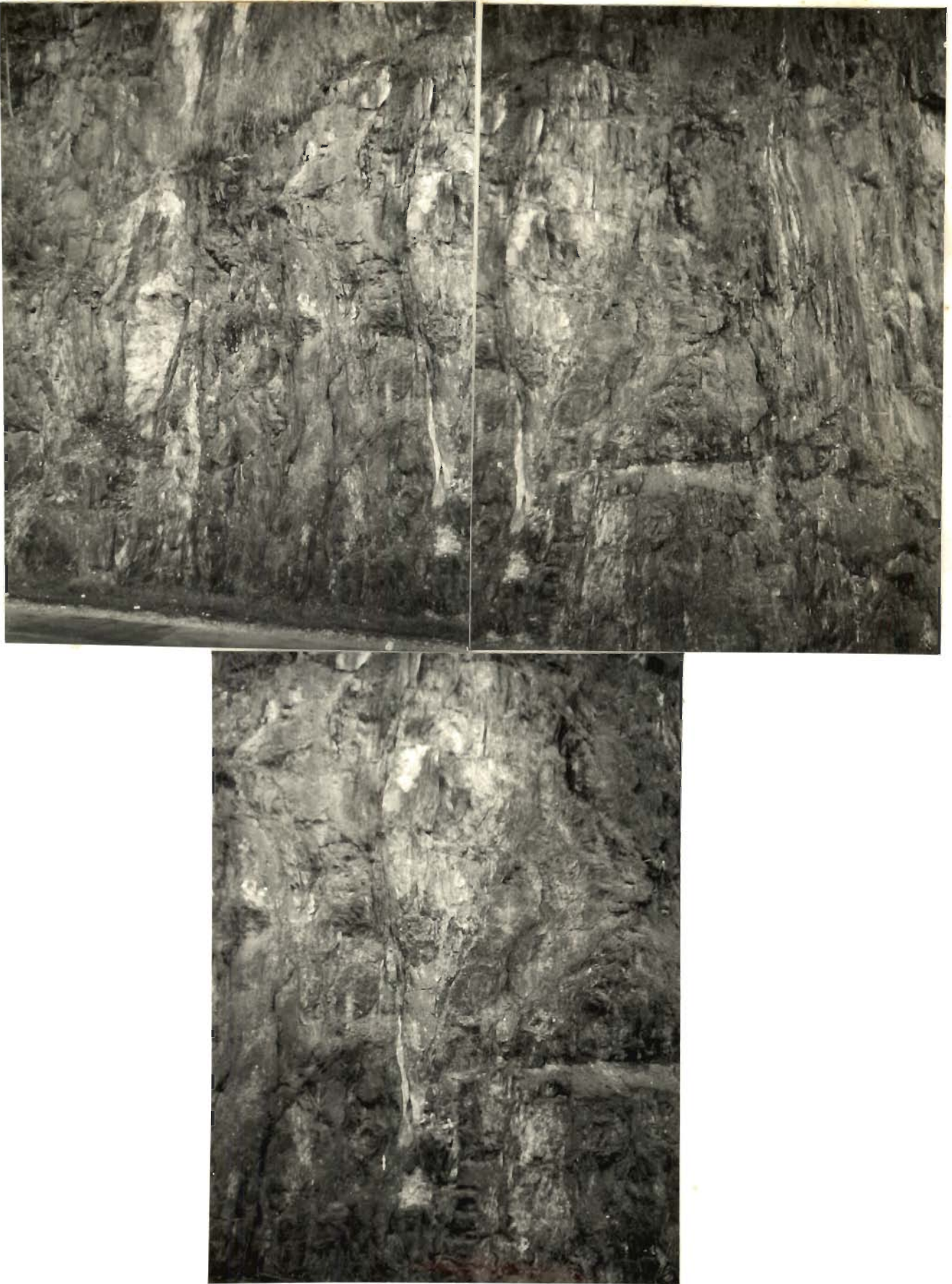


Figure 4.27 (A) & (B). Field photographs showing intensely sheared Phyllites in Barapani Shear Zone. (B)-close up view of sheared lenses. Loc.- 10 km north of Shillong towards Barapani.



Figure 4.28. Field photograph showing shearing and shattering in soft sandstone. Loc.-Barapani.

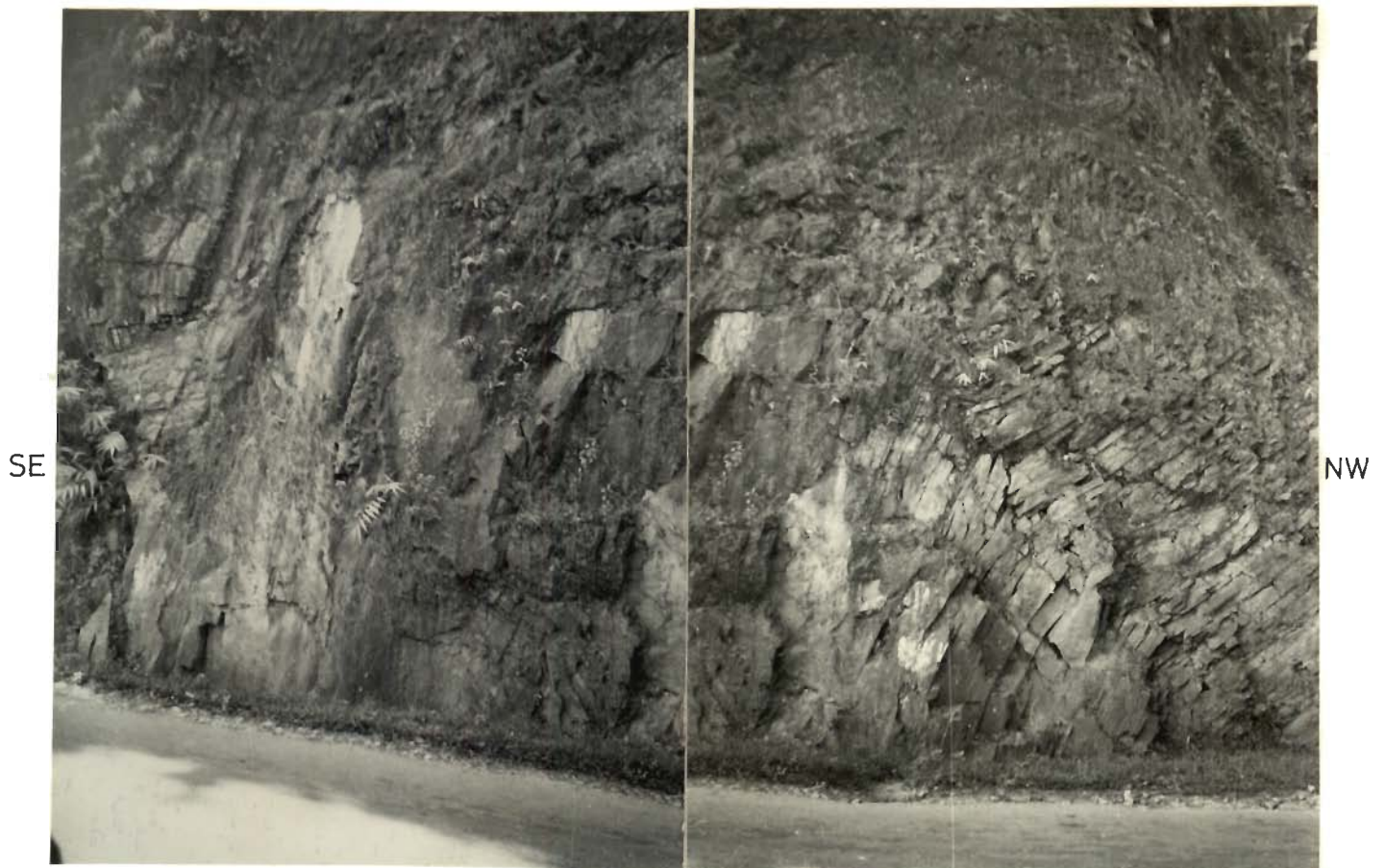


Figure 4.29. Field photograph showing brittle deformation in Precambrian sub-vertical phyllites. The beds are broken and show northwestward bending. Loc.- 13 km north of Shillong.

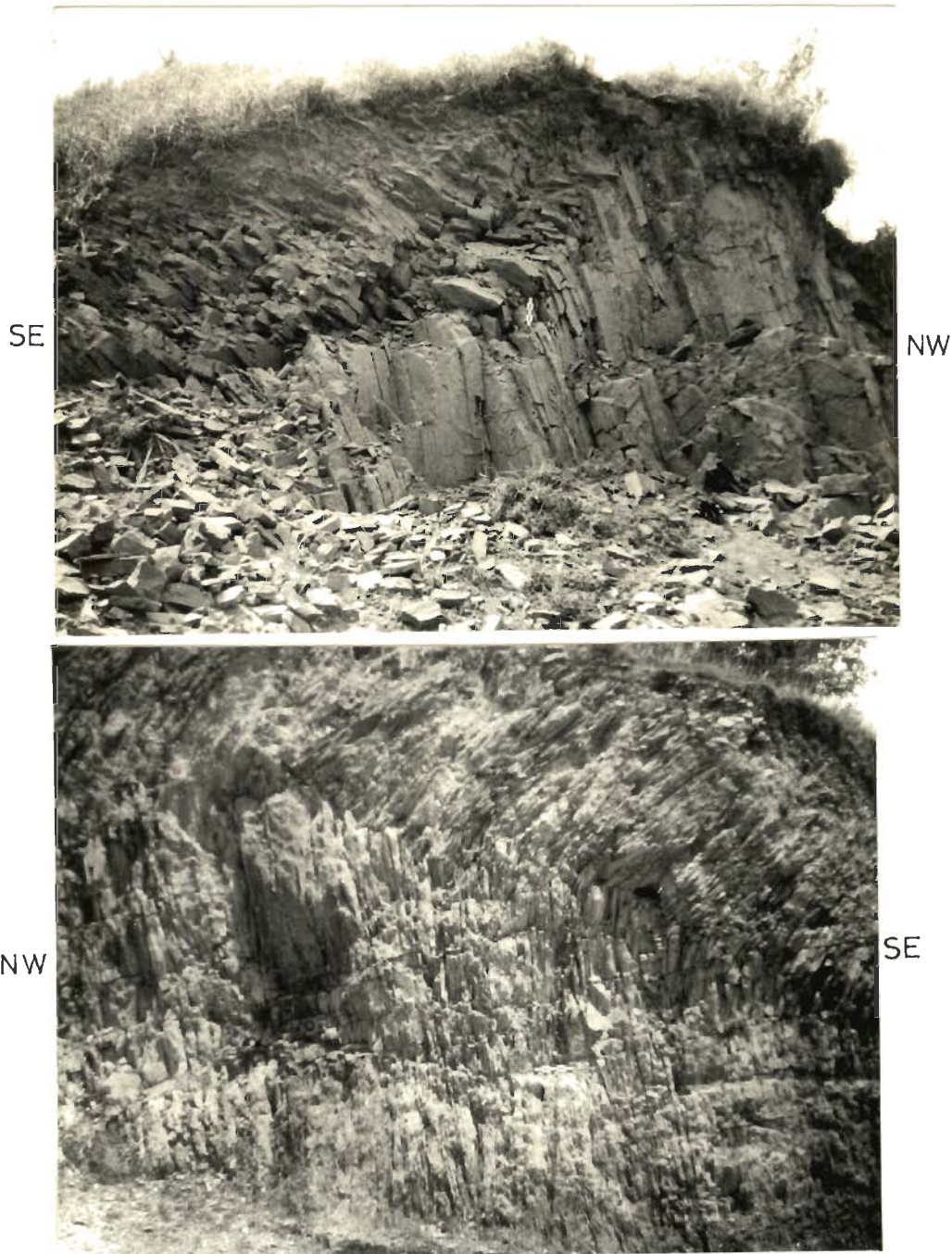


Figure 4.30 (A) & (B). Field photographs showing brittle deformation in Precambrian sub-vertical phyllite rocks. The beds are broken and show southeastward bending. Loc.- (A) 20 km SW of Shillong on Mawphlang-Tyrsad road, (B) 25 km SW of Shillong at Mawangap.



Figure 4.31. Field photograph showing vertical shearing in inclined phyllites. Loc.-Tyrсад.

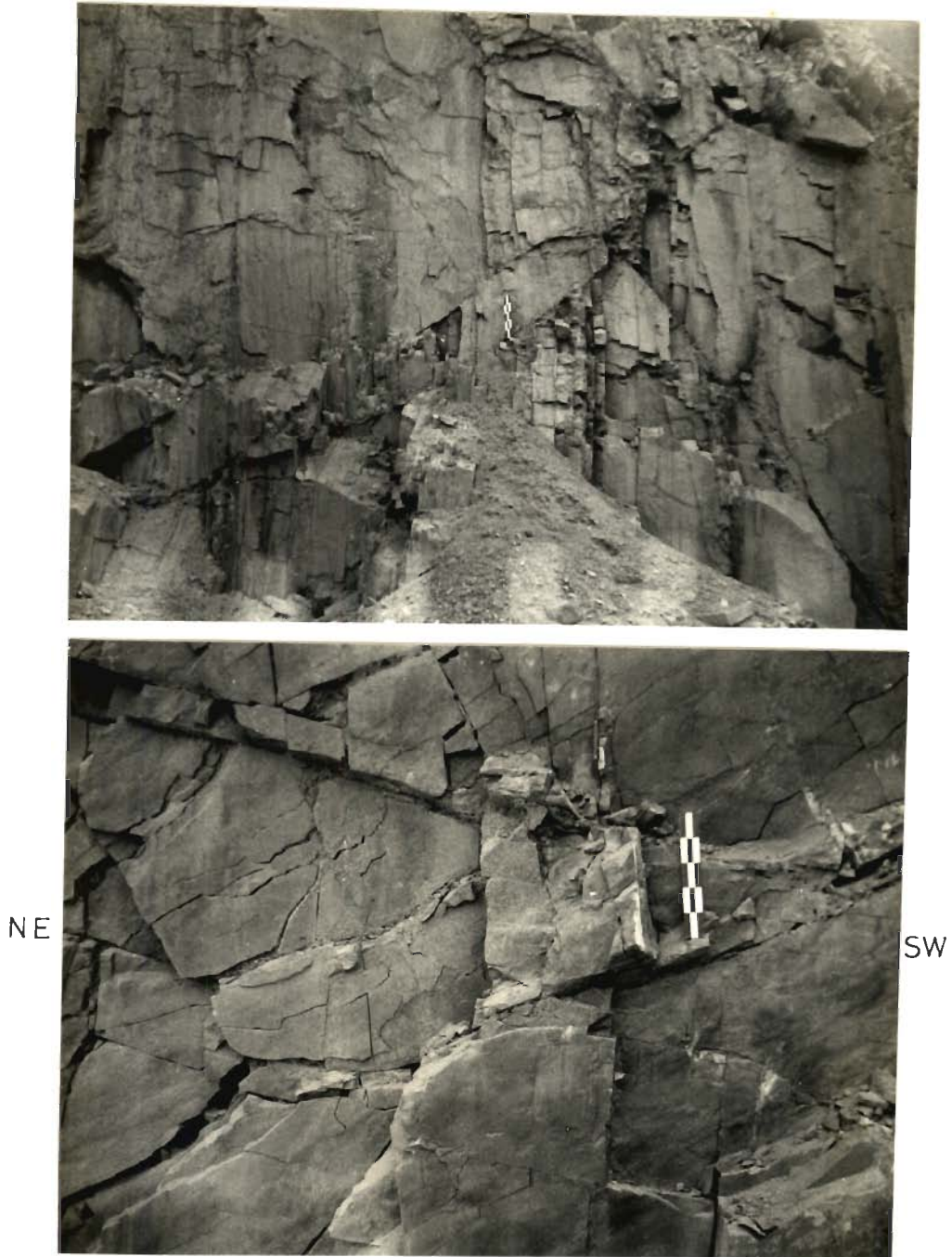


Figure 4.32 (A) & (B). Field photographs showing brittle fractures in phyllites. Loc.-7 km north of Tyrsad.



Figure 4.33. Field photograph showing deformational movement of phyllites against overlying bouldar beds. Loc.-Tyrсад.



Figure 4.34. Field photograph showing Ridge and Groove structures on phyllite. Loc.-Tyrсад.



Figure 4.35. Field photograph showing slickensides on a slipped surface of phyllite rocks. Loc.-20 km SW of Shillong.

IMAGE PROCESSING OF IMPORTANT STRUCTURES

5.1 INTRODUCTION

The satellite based remote sensing data are recorded in the form of digital numbers representing spectral reflectance value of the object on earth's surface. The electromagnetic radiation from an object is available in visible and near-infrared ranges to particular wavelength. The most commonly available wave bands for geological purpose are in the range of 0.4 to 1.2 microns. These data are produced in the form of rasters, or two dimensional arrays of pixels. Each pixel has assigned to it a digital number or DN, representing the energy associated with the range of electromagnetic radiation.

Remote sensing data are available to the users in the form of either analog i.e., paper prints or digital data stored in computer compatible medium. Already processed data in the form of paper prints have limited use, as the users are solely dependent on simple visual interpretation. On the other hand, the digital data allow the users to exploit fully the spectral characteristic of the objects at pixel level with the aid of a computer. Several techniques are available now to manipulate the digital data to serve ones purpose. The digital image processing is a powerful tool to enhance the subtle variations in spectral pattern.

It is a fact that the digital image processing has remarkable advantage over the analog data. However, for regional studies of a tectonically-active area, a considerably large area should be incorporated in order to understand the tectonic set up properly, which, otherwise, remains incomplete. For this purpose a mosaic of paper prints of satellite data (TM Band 4), as shown in Figure 3.1, has provided very useful information for understanding the geotectonics in regional perspective.

In the present study, digital image processing has been done for small areas, which incorporate very important structural features. This technique has been adopted mainly for enhancement of structural features. Image enhancement is the manipulation of remotely sensed digital data to improve the appearance of an image to have a better visual discrimination among the features of interest to the users.

The different approaches of digital image processing are as follows: 1. Contrast stretching 2. Spatial-frequency filtering 3. Principal component analysis 4. Band ratioing 5. Pattern recognition 6. Alternate colour spaces etc. The various techniques of digital image processing are described by Lillesand and Kiefer (1979), Siegal and Gillespie (1980), Hord (1982), Jensen (1986), Sabins (1987) and Drury (1987).

Since, the present study deals mainly with structural features, various digital image processing technique to improve the discernability of the particular feature have been applied.

5.2 DATA USED

5.2.1 Types of Data

In this study, the Indian Remote Sensing Satellite data has been used.

The overall specifications of IRS-1A satellite are:

Type	:Body stabilized remote sensing satellite.
Orbit	:Sun-synchronous, 904 km, orbit with equatorial crossing at 10.08 AM, descending node.

Payloads

Type	:LISS (2048 elements CCD linear array)
No. of Cameras	:Three (one of LISS-I and two of LISS-II) No. of No. of
spectral bands	:Four
Spectral Bands	:0.45 - 0.52 microns 0.52 - 0.59 microns 0.62 - 0.68 microns 0.77 - 0.86 microns
IFOV (Micro-rad)	:80.2 for LISS-I 40.1 for LISS-II
Spatial Resolution (m)	:72.5 for LISS-I
(geometrical)	36.25 for LISS-II
Swath	48.48 km for LISS-I 46.98 km for LISS-II (combined swath)
Repetivity Cycle	:307 orbits/22 days
No. of grey levels	:128 (7 bit)

5.3 IMAGE PROCESSING SYSTEM

Computer programs (algorithm), designed to read, display and statistical analysis of data in raster format, have been used for image processing. With the fast advancement of technology, a desk top computing facility is now capable of providing complete image processing in contrast to users dependency on robust computing facility dedicated to the remote sensing data processing in recent times. Software packages are also playing magic with the advancement of hardware. A number of software packages can handle remote sensing data.

In this study, software packages ILWIS (Integrated Land and Water Information System) developed by The International Institute for Aerospace Survey and Earth Sciences (ITC), The Netherlands and Aldus Photostyler belonging to Aldus Corporation,

have been utilized.

5.3.1 Integrated Land and Water Information System (ILWIS)

The ILWIS (Version 1.4) provides users with the facilities of data gathering, data input, data storage, data manipulation and analysis, and data output capabilities-integrating conventional Geographical Information Systems procedures with image processing capabilities. Image processing techniques are an essential component in the system's data analysis and data transformation capabilities.

5.3.2 Aldus Photostyler

This is the most advanced image processing and production program available for the creative users. Photostyler enables enhancement of any continuous tone gray scale or colour image.

5.4 ENHANCEMENT TECHNIQUE

The enhancement of an image implies the alteration of the appearance in such a way that the information content in the image is more readily interpreted by the viewer in terms of the particular needs. The objective is to create a new image from the original image data in order to increase the amount of information that can be visually interpreted from the data. The image enhancement is carried out by changing the gray level values of particular pixels in a particular fashion. The enhanced images can be displayed interactively on a computer monitor or these can be recorded in a hard copy format, either in black and white or in colour. There are no simple rules for producing the single best images for a particular application. Therefore, the enhancement techniques are adopted to suit users requirement. Also, the enhancement techniques for images of different areas varies as the distribution of pixel values over the particular range changes.

The knowledge of statistical data distributions in the images is the basic requirement for enhancements. The histogram describes the data distribution in a

single image and scatterogram provides an idea of relative data distribution in multiple image.

The image enhancement has been performed in the following manners.

5.4.1 Contrast Stretching

The term contrast stretching implies the stretching of gray levels in order to improve contrast between the features. The effect is to increase the visual contrast of the features in an image by changing brightness value of pixels. This helps in easy discrimination between the different features. Most commonly available computer compatible DN values are from 0 (black) to 255 (maximum intensity or saturation). Image processing software can change any DN in an image to any of these intensity levels; and also range of DN can be transformed. Since the IRS data, used in this study, consist only of 128 gray levels, the technique of contrast stretching has been very useful. The enhanced images of single band or false-colour images comprising three contrast stretched bands can be interpreted geologically with a fair measure of success (Drury, 1987).

5.4.2 Linear Stretching

The contrast of an image can be improved in a simple way by changing the range of data by spreading it equally over the 0-255 range. The minimum DN is set to 0, the maximum to 255. Each histogram bin relating to each DN originally present is moved to a new position, and the new bins are equally spaced (Fig. 5.1). The computer accomplishes this by using a look-up table (LUT). A LUT converts an input DN(x) to an output DN(y). For a linear stretch, the function is the basic equation for a straight line $y=mx+c$, which can be expressed as a graph of input DN against output DN.

An image of high quality can be produced by employing linear contrast stretch with atmospheric correction.

(i) Piece-wise linear stretching: In this method, cut-off and saturation are selected for

linear stretching of the dark and light parts of the scene to produce two separate images. Geological information of the light area is weakened in an image where dark area are stretched and this is converse, when light areas are enhanced. This type of stretching is required when a scene has areas, dominated by both light and dark surfaces, both of which contains geologically interesting informations.

5.4.3 Non-Linear Stretching

In case of linear stretching, loss of contrast takes place in the tails of the original histogram. This can be avoided by adopting more sophisticated stretches, involving LUTs and using non-linear transformations.

(i) Gaussian stretching: Here, statistical distribution follows the Gaussian laws and produces a bell-shaped histogram with its peak at a DN of 127. This results in a Gaussian stretch. In this case, the raw data is forced to resemble a normal distribution.

(ii) Histogram equalization stretching: In this case, the greatest contrast stretch is applied to the middle and most-highly populated range of DN, with extreme compression in the less densely populated low and high DN tails. The new image has an equally frequent DN values.

(iii) Logarithmic and exponential stretching: The logarithmic stretch is employed for stretching the dark part of an image as much as possible, while still retaining some contrast in the light range. On the other hand, the exponential stretching is performed by stretching the light part of an image very intensely.

5.4.4 Enhancement by Using Colour

The coloured images produce more clearer picture of the geological features. The use of colour in image processing is motivated by the following factors. The human eye can discern thousands of colour shades and intensities, compared to the dozen gray shades. The black and white images carry information in terms of only one variable i.e. tone. A colour space consists of three variables - hue, saturation and

brightness or intensity. The selection of band combination for colour display may be based on optimum index factor (OIF) technique. The technique uses the computation of total variance and correlation within and between bands, for all possible image combinations. The combination of three images with largest OIF is selected for colour display, as it provides the largest amount of information in terms of variance. The image in the RGB colour model consist of three independent image planes, one for each primary colour e.g., red (R), green (G) and blue (B).

5.5 IMAGE PROCESSING METHODOLOGY ADOPTED IN THIS STUDY

With this background of image enhancement technique of digital remote sensing data, the following methodologies have been adopted in this study.

1. The characteristic structural features have been identified by displaying the full scene of IRS: LISS-II image on a computer monitor.
2. Several small windows (all the four bands) containing the interesting and significant structural features have been extracted.
3. These small windows have been processed employing image enhancement technique.
4. The processed images have been printed using the Laser printer and colour ink jet printer.

5.6 CONCEPT OF INVERSE IMAGE

The requirements for inverting the image has arises out of the false perception of the normal image in proper orientation i.e. the north side of the scene pointing away from the viewer. When an image is seen in proper orientation, the ridge and valley appear as valley and ridge respectively (Fig. 5.2). This phenomenon occurs due to the angle of illumination of the ground, being sensed remotely.

The study area had sun illumination from southeast, when data were collected. Hence, northwestern side of the ridge falls in shadow region, whereas the northwestern wall of the valley falls in illuminated region. This illumination effect

produces dark tones in the shadow regions, as no light is reflected. In a gray scale-toned image, the brighter areas appear as floating, whereas the dark areas appear as suppressed to the viewer due to the perception effect. Therefore, in proper orientation a normal image should have brighter tone in the northwestern side of the ridge and darker tone on the northwestern wall of the valley. This tonal distribution produces real impression of ridge as ridge and valley as valley. This effect can be achieved by inverting the image (Fig. 5.3). However, the above effect can also be achieved by rotating a normal image.

Inversion of an image implies that gray scale range of 0.....255 digital values are transformed into 255.....0. Therefore, the features like dry sand body and a water body in the normal image of infrared range would appear with bright (255 DN) and dark (0 DN) tones respectively. In case of the inverse image, the appearance will be exactly opposite i.e., dry sand body would give dark tone and the water body would give bright tone. Further, the inverse image helps in interpretation of the geological features because topography appears normal i.e., ridges as ridges and valleys as valleys.

5.7 INTERPRETATION OF VARIOUS GEOLOGICAL FEATURES

5.7.1 Shillong Region

This region is dissected by the NE-SW trending Barapani Shear Zone (BSZ) with the location of a reservoir in this shear zone. This region has been studied in detail (Chapter 4). In Figure 5.2, the lens-shaped sheared ridges A, B and C, scarps, Shillong peak (SP) has become enhanced and is prominently displayed. It can be seen that boundaries of ridges have become well defined in digitally enhanced images (Figs. 5.2 and 5.3). Whereas, these features are not very prominent in Figure 4.21. Figure 5.3 is an inverse image of the Figure 5.2, which gives correct topographic perception. These structural features are more prominently seen in the colour composite (Fig. 5.4). The enhanced images, thereby, helps in confirming the sinistral-type of movement along the BSZ.

Shear-sense of the BSZ has also been discussed in Chapter 4 on the basis of curved linear ridges. These curved linear ridges (CLR) can be seen very clearly joining the BSZ tangentially revealing sinistral sense of shearing movement in enhanced image (Fig. 5.5, also see Fig. 4.21). The enhanced inverse image produces proper perception for the interpretation purpose wherein it is likely that the BSZ is a ductile shear zone of considerable importance in the Shillong Plateau.

The N-S trending Um Ngot Fault (UGF), located east of BSZ, has been identified and discussed in Chapter 3 (Fig. 3.7). This fault intersects the NE-SW trending BSZ towards north. The morphological characteristics of the UGF can be seen in digitally enhanced image (Fig. 5.6). This fault is perpendicular to the E-W trending Dauki Fault Zone (DFZ). In this case also, the curved linear ridges (CLR) are truncated by the UGF which controls the 35 km long N-S trending course of a river.

It has been identified that the intersection zone of BSZ and UGF is tectonically significant under the present compressive tectonic set up of the Shillong Plateau. Also, around the intersection zone (IZ), the granite plutons are emplaced, which are intensely fractured in the N-S direction. The nature of IZ formed by the BSZ and UGF and the fracture pattern can be seen prominently in the digitally enhanced image (Fig. 5.7, also see Fig. 4.21). The BSZ has been pushed northward by the UGF and a linear depression has formed south of IZ.

In Figures 5.8 A and B, the horst and graben structures in the area south of Shillong have been displayed beautifully. The image in B gives the proper topographic perception to the viewer, which is an inverse image of A. In the digitally enhanced image, the boundary of the grabens have become prominent.

5.7.2 Fold Structures

The image displaying folds in sediments in the area just south of the Dauki Fault Zone (DFZ) and south of the Haflong Thrust Zone (HTZ) have been discussed from tectonic point of view in Chapter 3. In order to make morphological

characteristics of these folds more prominent, interpretable and produce significant impact for visual interpretation, the images containing these structures have been enhanced.

The southward convex folds (CF) in sediments south of the DFZ at longitude $91^{\circ} 30'E$ are shown in Figures 5.9 A and B, which are digitally enhanced (also see Fig. 4.7). The features of the folds have become prominent in these figures and it is more evident in the Figure (B) which is an inverse of (A).

Towards the eastern part of the DFZ, the E-W trending folds in sediments are very prominently displayed in the images. The images of this area have been enhanced digitally and are shown in Figures 5.10 and 5.11 which are the inverse images. The area in Figure 5.10 shows the steep escarpment in the DFZ forming a narrow deep gully and the E-W trending folds (also see Fig. 4.6). The folds are very prominent in the enhanced image and formation of minor folds farther south can be seen clearly. Further, the E-W trending folds are absent in the western part of the image. These folds are truncated sharply against a N-S trending line which coincides with the N-S trending Chandghat Fault having same trend to that of Um Ngot Fault (also see Figs. 3.13, 4.6). In the area east of Figure 5.10, the E-W trending folds in sediments have been disturbed tectonically (Fig. 5.11). It can be seen that the folds are curved northward (extreme west of the Fig. 5.11, also see Fig. 3.15) and have been faulted. These structures might have resulted due to the movements during the formation of the HTZ and later.

The image, displaying the most spectacular folds south of the HTZ, has been digitally enhanced and are shown in the Figure 5.12. The image displays the NE-SW trending folds with curved limbs and tight hinges (also see Figs. 3.14A, 3.28, 4.2). The fold morphology has become very prominent in the enhanced inverse image (Fig. 5.13). The NW-SE trending compressive forces could produce this type of fold morphology. The general fold morphology is more prominent in Figures 5.14 A and B, which are the colour composite. Figure 5.14 B has been produced using three inverted image planes in gray tone.

Figure 5.15 is an inverse image and shows the effect of NE-SW trending HTZ on the N-S trending folds in sedimentary rocks in the Indo-Burman Fold Belt. The N-S trending folds are still preserved and the extreme northern part of the folds have been disturbed intensely due to thrusting effect.

The image showing folds in Arunachal Himalayan foot hills (AHFH) has been enhanced to show the pattern of foot hills deformations (Figs. 5.16 A and B). The folds and deformation in sediments can be clearly seen especially in image (B) which is an inverse image of (A).

5.7.3 Alluvium Fault

Case 1: Arunachal Pradesh

The faults in alluvium has been recognized in the area south of the Arunachal Pradesh Himalayan Foot Hills (APHFH). The image of this area has been digitally enhanced (Figs. 5.17 and 5.18). It is interesting to see that the recently-formed alluvium adjacent to the APhFH has formed higher terraces (HT). These HT have been linearly faulted, as shown by very sharp tonal differences (also see Fig. 3.25). The morphological features are very prominent in the Figure 5.18, which is an inverse image. The higher terraces show high morphology than that of the alluvium in the south. And this level differences are indicated by the streams in the HT area forming a deep cuttings in the HT especially at the scarp zone.

Case 2: Bangladesh

It has been inferred that the Bangladesh plains between the longitudes 91° and 92° E, adjacent to the DFZ show subsidence. This phenomena could be recognized depending on the development of the alluvial fans, which appears as an inland delta (also see Fig. 4.2). These geological features are shown in the digitally enhanced Figures 5.19 A and B, in which the formation of alluvial fans (AF) in the area just south of the Dauki Fault Zone has been displayed very conspicuously. In the colour composite the morphology of the AF can be seen more clearly which is represented by the light red tone (Fig. 5.20).

5.7.4 River Morphology

Case 1 : Brahmaputra River

The Brahmaputra River is represented by numerous channels. As discussed earlier, it has been inferred that the river has a tendency to migrate northward and straighten the course. Therefore, the image showing the morphological characteristics pertaining to the straightening and migrating river courses have been enhanced digitally.

In Figures 5.21 and 5.22, it can be seen that the new channels (NC) have developed on the north and south bank of the river. The present wavy course probably would become straight. In Figure 5.22, total span of the river channels can be seen, as there are no signs of vegetation close to the river channel. Figure 5.23 displays the river morphology prominently.

In the areas, north of Mikir Hills Massif and between the Shillong and Mikir Hills Massifs, the Brahmaputra River shows northward migration. The image containing these areas have been digitally enhanced to get better picture for interpretation purpose. The abandoned channels (AC) are clearly seen in the Figure 5.24, which is a band-2 image with areas of abandoned channels very prominently presenting a gray tone and indicating growing of vegetation. In the Figure 5.25, the morphology of the AC's are prominently displayed. The colour composite of this morphological feature has provided better contrast due to different colour coding (Fig. 5.26). Figure 5.27 shows the migration of the river in the area between the Shillong and Mikir Hills Massifs and is indicated by the abandoned river channels marked by AC. In fact, the river shows huge northward migration in this area, and has been discussed in detail in Chapter 3 (Figs. 3.30B, 3.31).

Case 2 : Barak River

The river morphology of the Barak River has been discussed in Chapter 3. A part of the image, displaying the characteristic river morphology, has been digitally enhanced

(Figs. 5.28 and 5.29). Some of the abandoned loops (AL) indicate that the river is becoming straight. Further, another river loop is going to be abandoned and is marked as closing loop (CL) in these figures. In these two figures, the Barak River course and the adjacent areas have sufficiently been enhanced for better interpretation. The flood plain of the river is more prominent in Figure 5.28. Figure 5.29 shows the river morphology and nature of river bank erosion more prominently. The morphological features can be seen with high contrast in the colour composite image (Fig. 5.30).

5.8 OBSERVATIONS

In this work, the study of the tectonics of the Shillong Plateau and adjoining regions has been carried out initially by identifying the various geological features, which are seen directly on the already processed paper prints. Then, the image containing the classified characteristic morphological features have been digitally enhanced. It has been observed that the following morphological features have shown remarkable improvement and enhancement for better understanding and interpretation.

1. The associated morphological features of the BSZ: lens shaped ridges, curved linear ridges and scarps.
2. The morphological features of the UGF: fracture pattern in the intersection zone of the BSZ and UGF; horst and graben structures.
3. Folds in sedimentary rocks in the area south of DFZ and HTZ.
4. The nature of deformation of sediments in Arunachal Himalayan foot hills (AHFH); alluvium fault adjacent to the AHFH.
5. Alluvial fan morphology south of the DFZ.
6. Morphological features of the Brahmaputra and Barak Rivers.

Central coordinates of the figures showing the digitally processed images containing important structural features are given below. This would help in identifying the geographical location of the particular figure with respect to the satellite image mosaic (Fig. 3.1).

Figure	Description	Lat.(⁰ N)	Long.(⁰ E)
		Deg Min	Deg Min
5.2	Barapani Shear Zone and sheared ridges	25 35	91 50
5.3	-do-	25 35	91 50
5.4	-do-	25 35	91 50
5.5	Curved linear ridges in the Barapani Shear Zone	25 45	92 00
5.6	Um Ngot Fault	25 20	92 15
5.7	Intersection zone of the Barapani Shear Zone and Um Ngot Fault	25 50	92 10
5.8	Horst and graben structure	25 20	91 50
5.9	Convex fold structure	25 00	91 30
5.10	Folds south of Dauki Fault Zone	25 00	92 10
5.11	Folds south of Dauki Fault Zone	24 50	92 30
5.12	Folds south of Haflong thrust Zone.	24 50	92 50
5.13	-do-	24 50	92 50
5.14	-do-	24 50	92 50
5.15	-do-	25 00	93 15
5.16	Foot hills fold in Arunachal Himalaya	26 45	92 40
5.17	Alluvium fault-Arunachal Himalaya	26 45	92 15

Figure	Description	Lat.(⁰ N)	Long.(⁰ E)
		Deg Min	Deg Min
5.18	Alluvium fault-Arunachal Himalaya	26 45	92 15
5.19	Alluvial fan south of Dauki Fault Zone	25 10	91 40
5.20	Alluvial fan south of Dauki Fault Zone	25 10	91 40
5.21	Brahmaputra River morphology	26 15	92 00
5.22	-do-	26 15	92 00
5.23	-do-	26 15	92 00
5.24	Brahmaputra River morphology (North of Mikir hills)	26 30	93 20
5.25	-do-	26 30	93 20
5.26	-do-	26 30	93 20
5.27	Brahmaputra River morphology (Between Shillong and Mikir Hills Massifs)	26 20	92 30
5.28	Barak River morphology	24 40	95 50
5.29	-do-	24 40	95 50
5.30	-do-	24 40	95 50

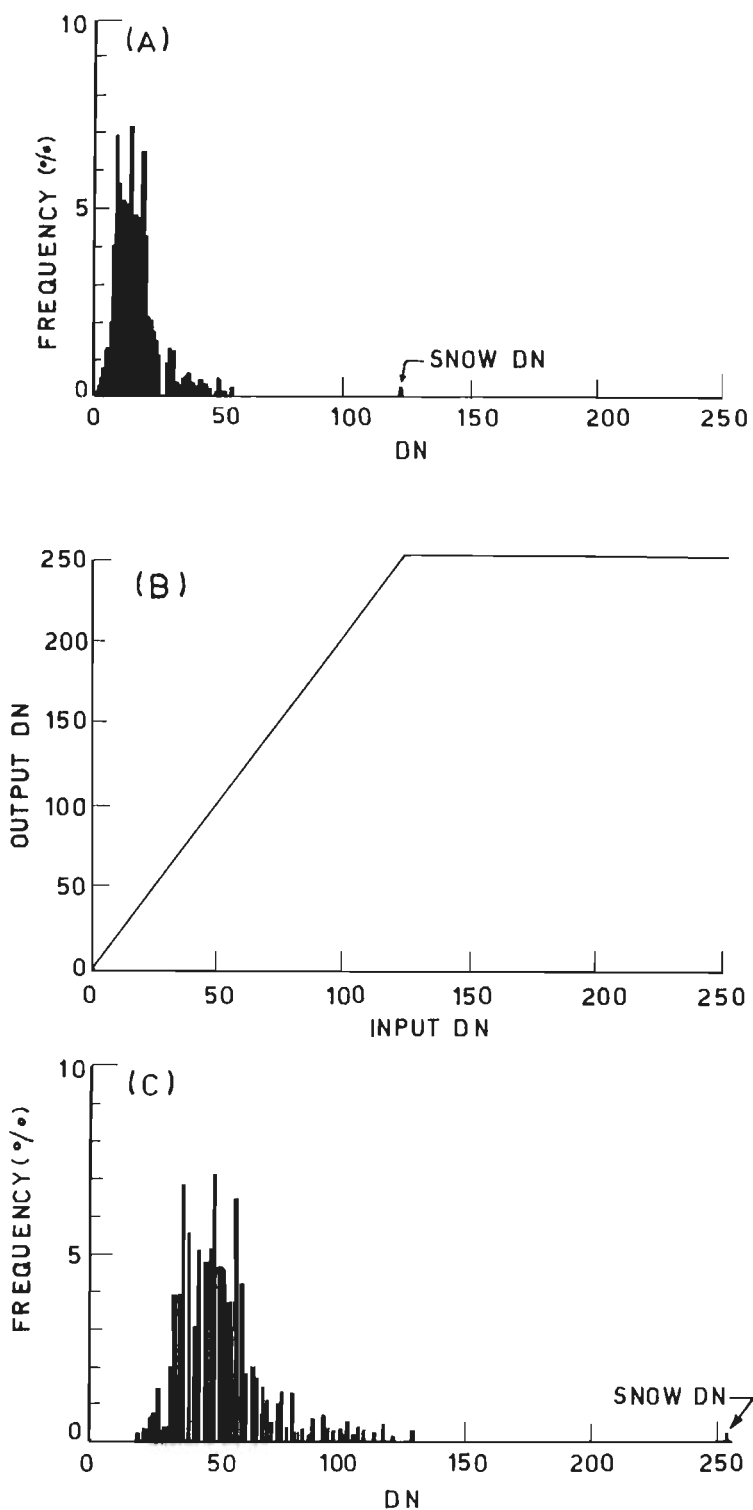


Figure 5.1 An example of raw Landsat MSS band 4 data which are compressed towards low DN (A), display of which produces a dark, low-contrast image. A linear contrast stretch is achieved by a simple straight line LUT (B), which sets the minimum DN (in this case (0) to 0 and the maximum (125) to 255). This spreads out the histogram (C) and introduces discernible contrast in the resulting image. (After Drury, 1987).

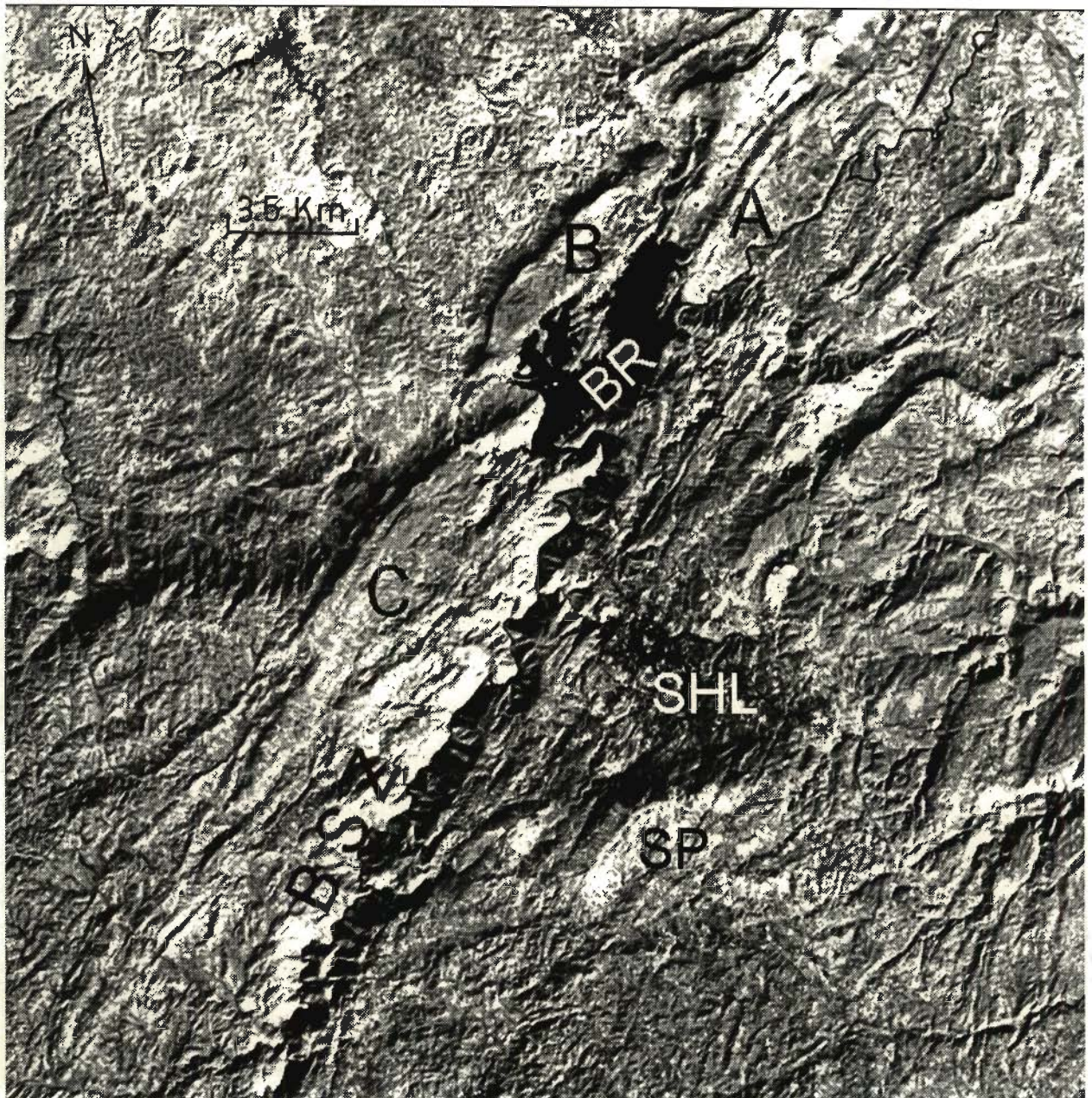


Fig.5.2 Digitally enhanced image (IRS: LISS-II, Band-4) showing the Barapani shear zone (BSZ) and lens shaped sheared ridges A,B & C. BR-Barapani reservoir. SHL-Shillong. SP-Shillong Peak.

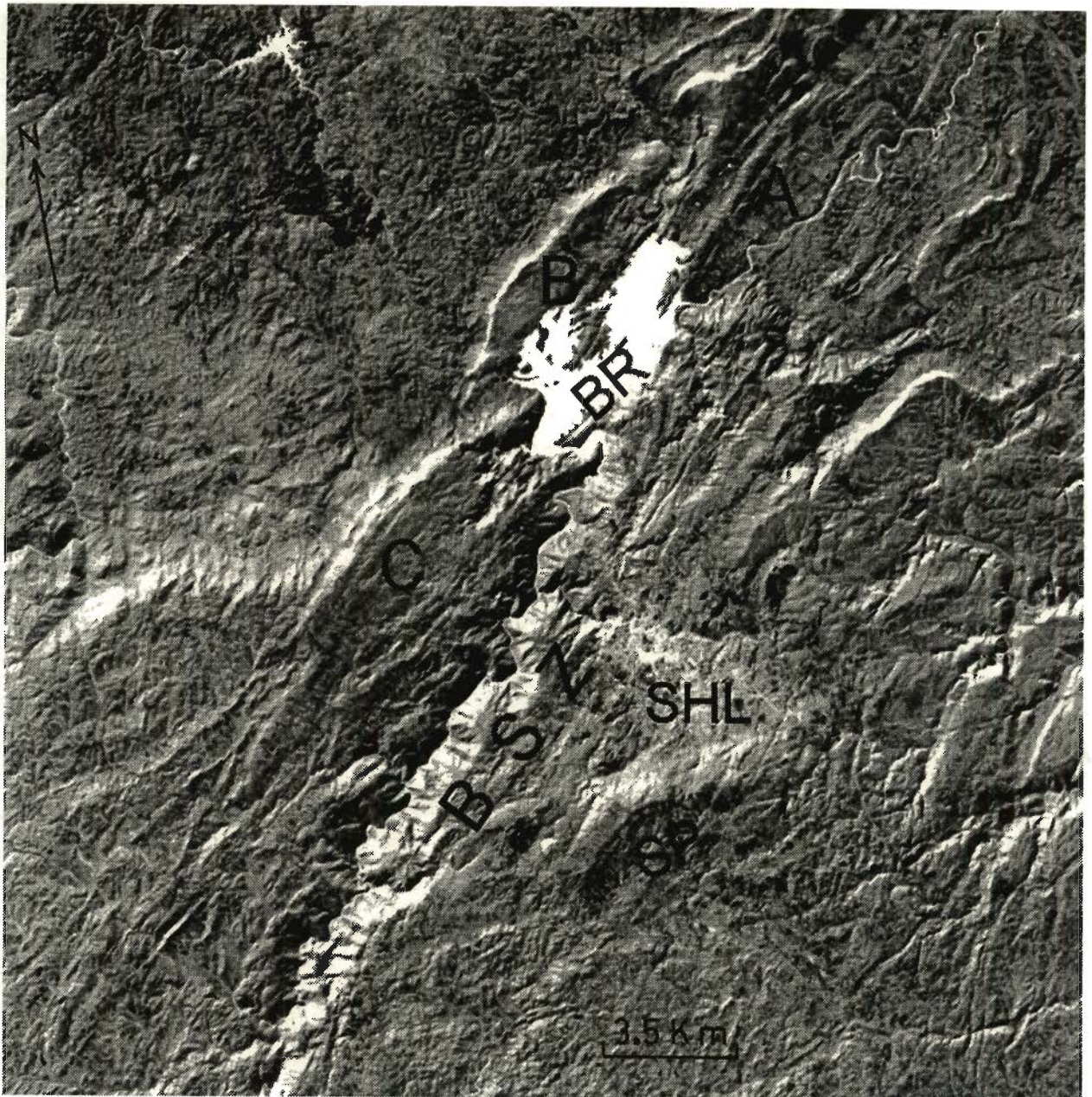


Fig.5.3 Digitally enhanced image (IRS: LISS-II, BAND-4) showing the Barapani shear zone (BSZ) and lens shaped sheared ridges A, B & C. BR-Barapani Reservoir. SHL-Shillong. SP-Shillong Peak. This is an inverse image of figure

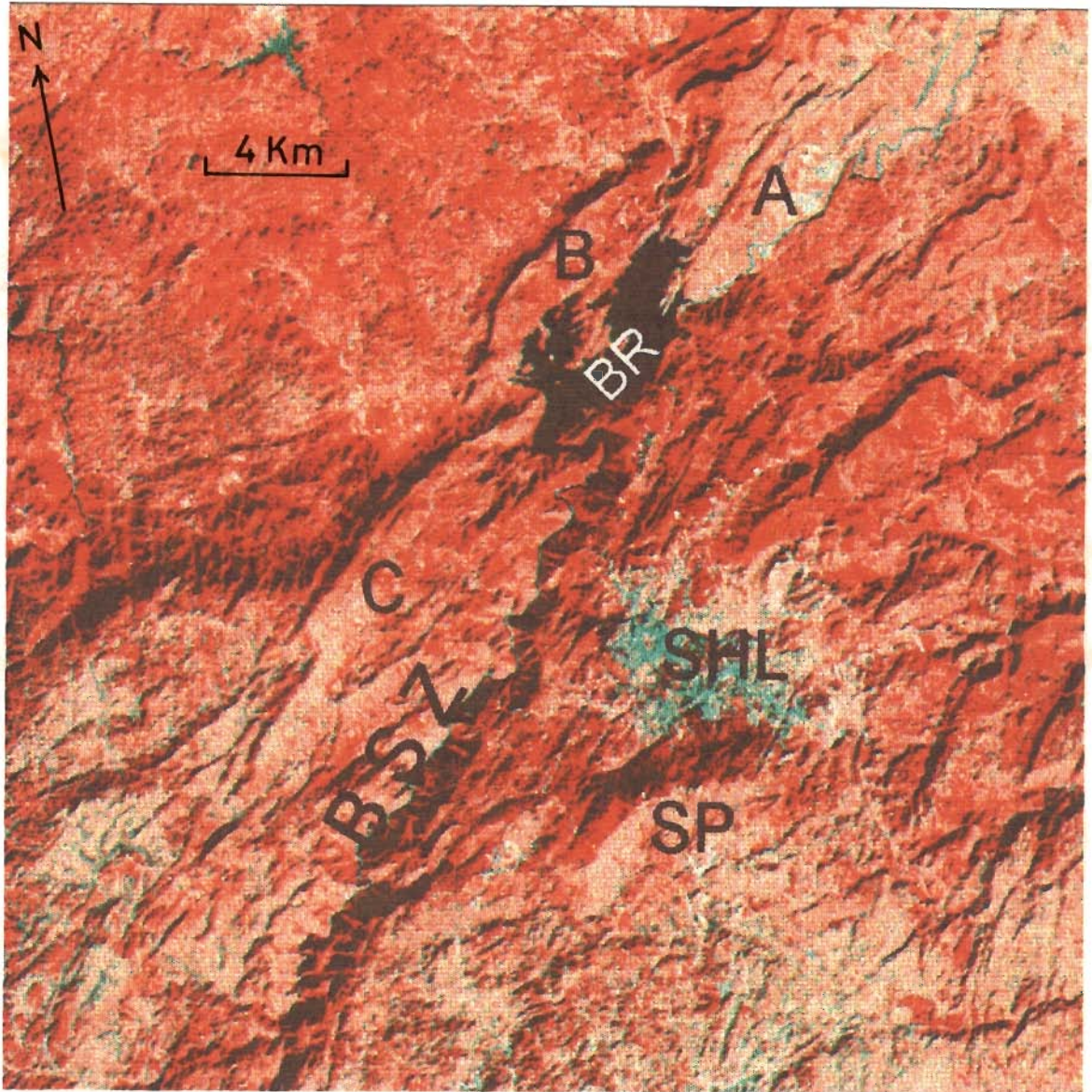


Fig. 5.4 Enhanced colour composite (IRS: LISS-II) image showing the Barapani shear zone (BSZ) and lens shaped ridges A, B and C. BR-Barapani Reservoir. SHL-Shillong. SP-Shillong Peak.

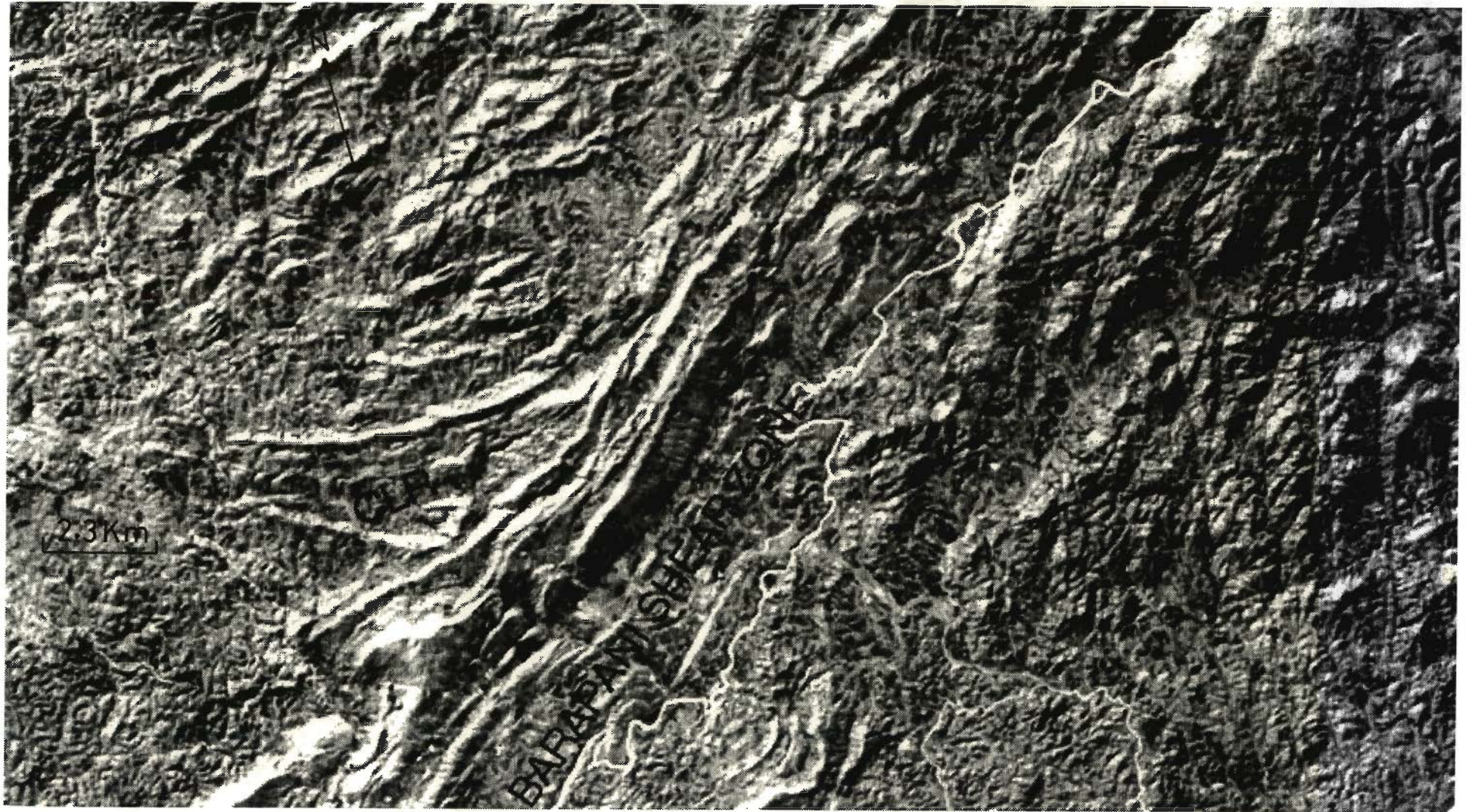


Fig.5.5 Digitally enhanced image (IRS: LISS-II, Band-4) showing the curved linear ridges (CLR) joining the Barapani shear zone tangentially. This is an inverse image.

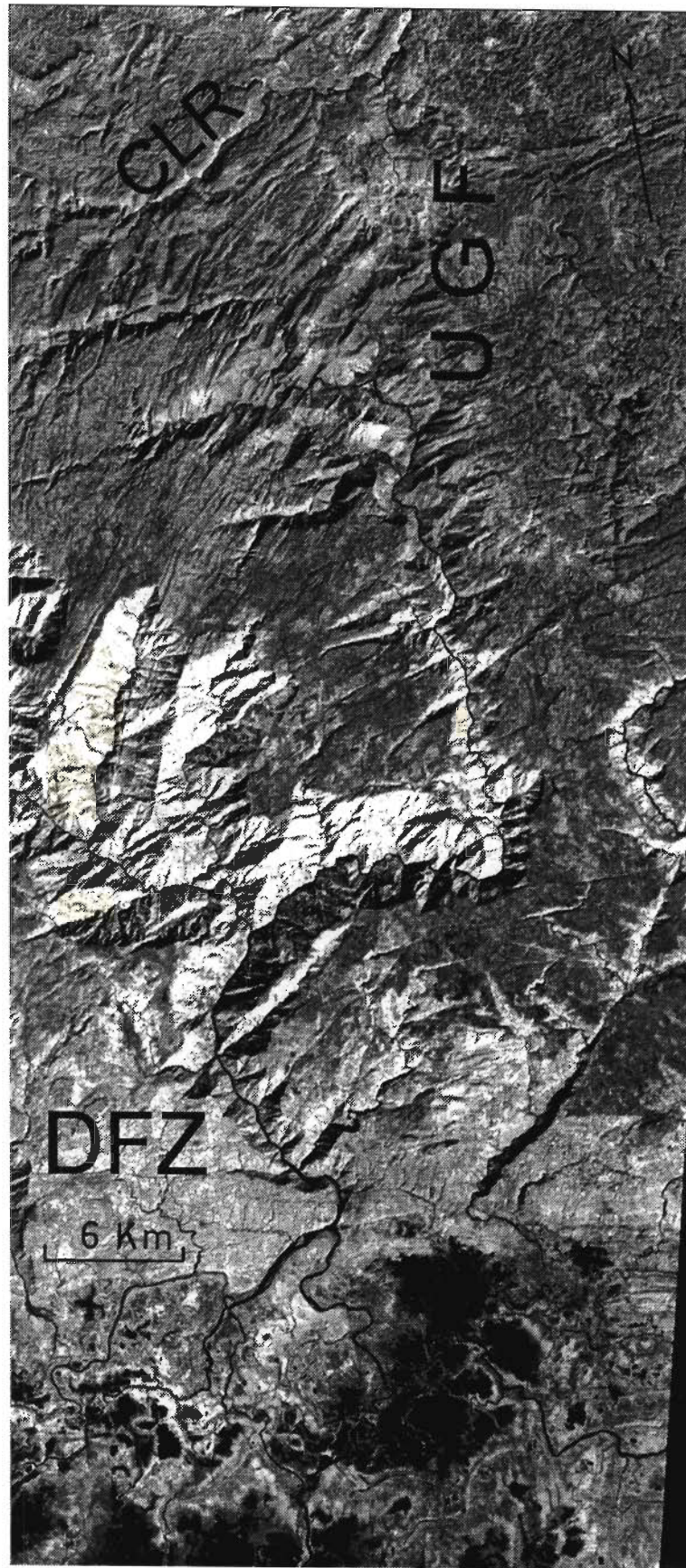


Fig. 5.6 Digitally enhanced image (IRS: LISS-II, Band-4) showing the N-S trending Um Ngot fault (UGF). CLR-Curved Linear Ridges. DFZ-Dauki Fault Zone.



Fig. 5.7 Digitally enhanced image (IRS: LISS-II, Band-4) showing intersection zone (IZ) of the Barapani shear zone (BSZ) and Um Ngot fault (UGF).

6 Km

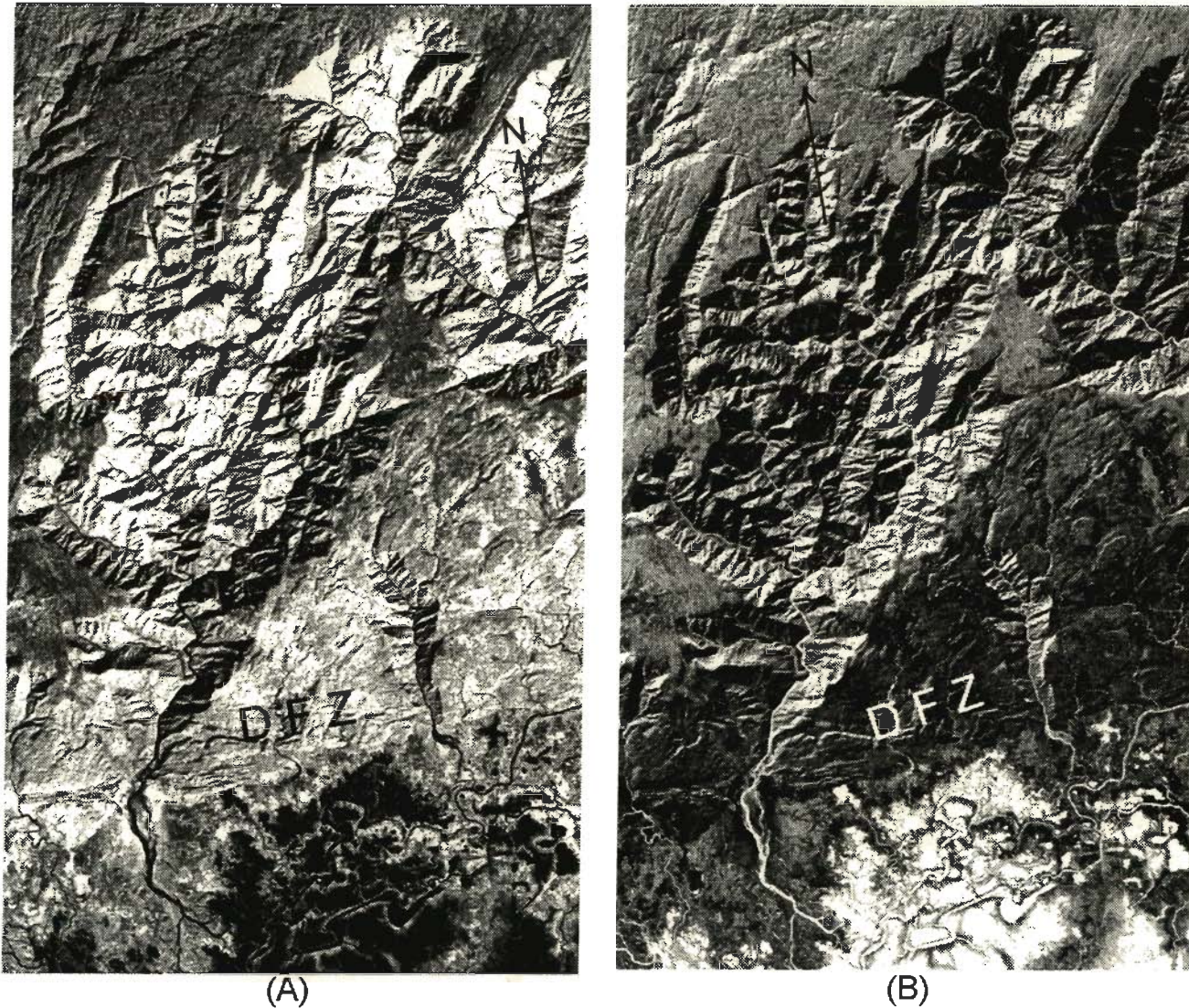
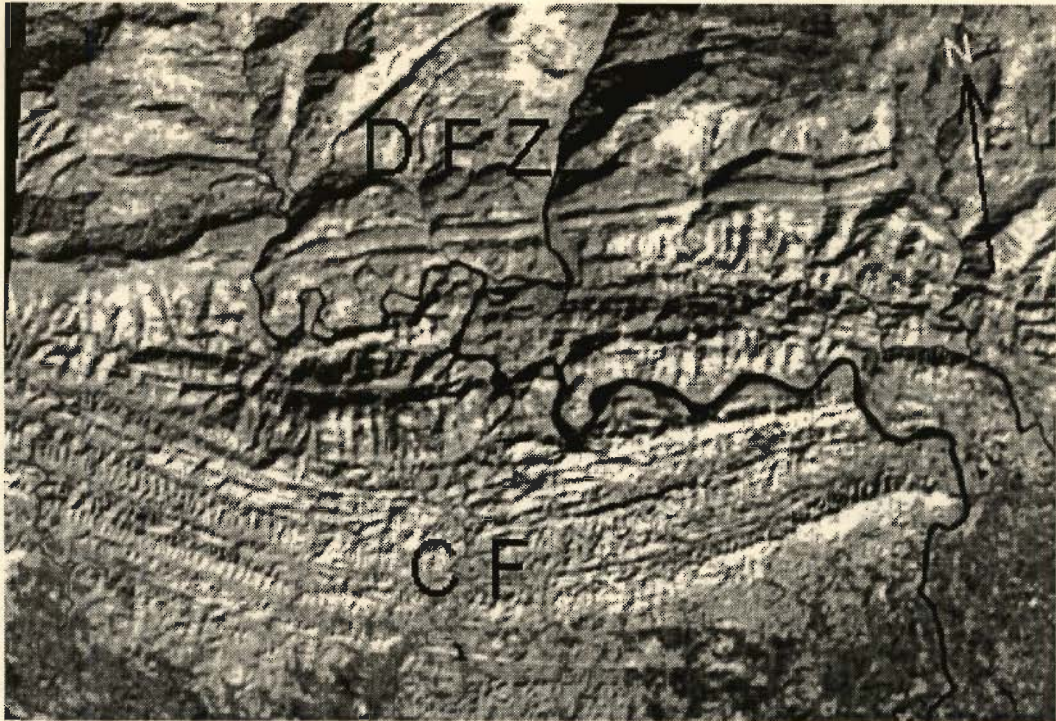
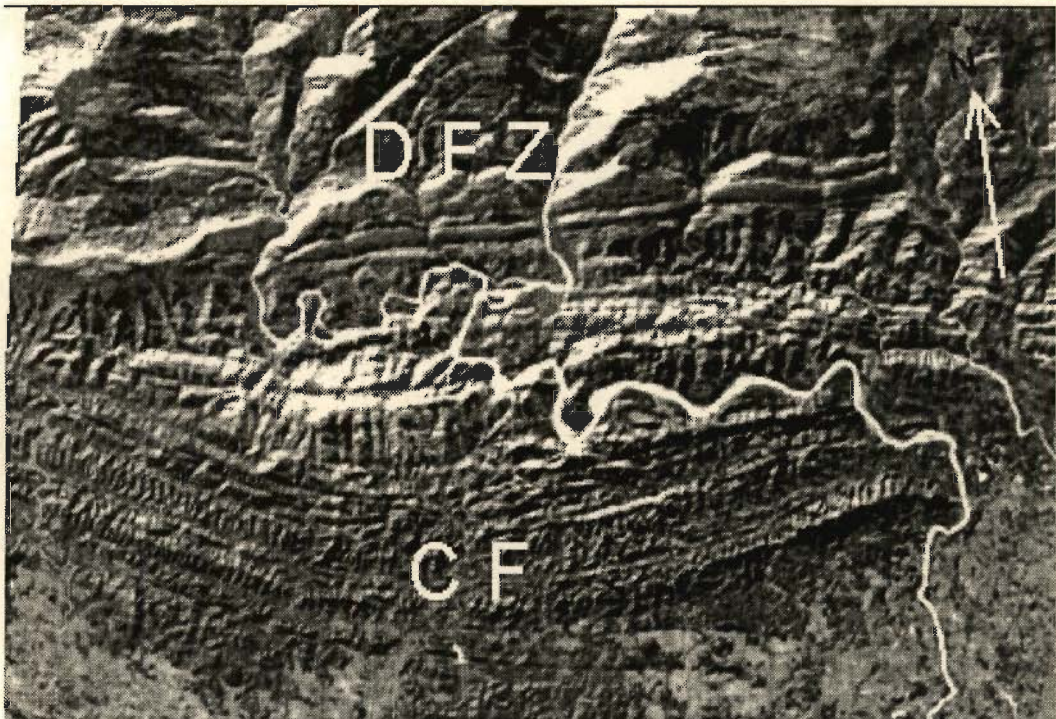


Fig. 5.8 Digitally enhanced image (IRS: LISS-II, Band-4) showing the horst and graben structures in the area south of Shillong. The image in (B) is an inverse of the image in (A).



(A)

3 Km



(B)

Fig. 5.9 Digitally enhanced image (IRS: LISS-II, Band-4) showing the southward convex folds (CF) in soft sediments adjacent to the Dauki fault zone (DFZ). The image of (B) is an inverse image of (A).



Fig. 5.10 Digitally enhanced image (IRS: LISS-II, Band-4) showing the E-W trending folds in soft sediments south of the Dauki fault zone (DFZ). This is an inverse image.



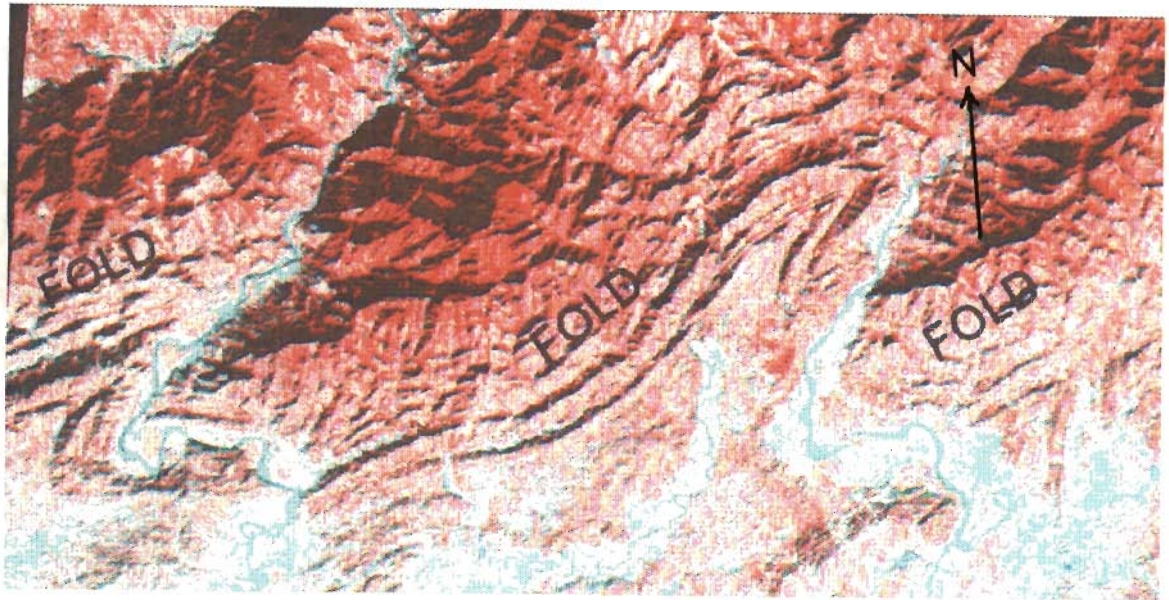
Fig. 5.11 Digitally enhanced image (IRS: LISS-II, Band-4) showing the folds and faults in soft sediments south of Haflong thrust zone (HTZ). This is an inverse image.



Fig. 5.12 Digitally enhanced image (IRS: LISS-II, Band-4) showing the NE-SW trending sedimentary folds with curved limbs and compressed noses which are displayed in the area south of the Haflong thrust zone (HTZ).

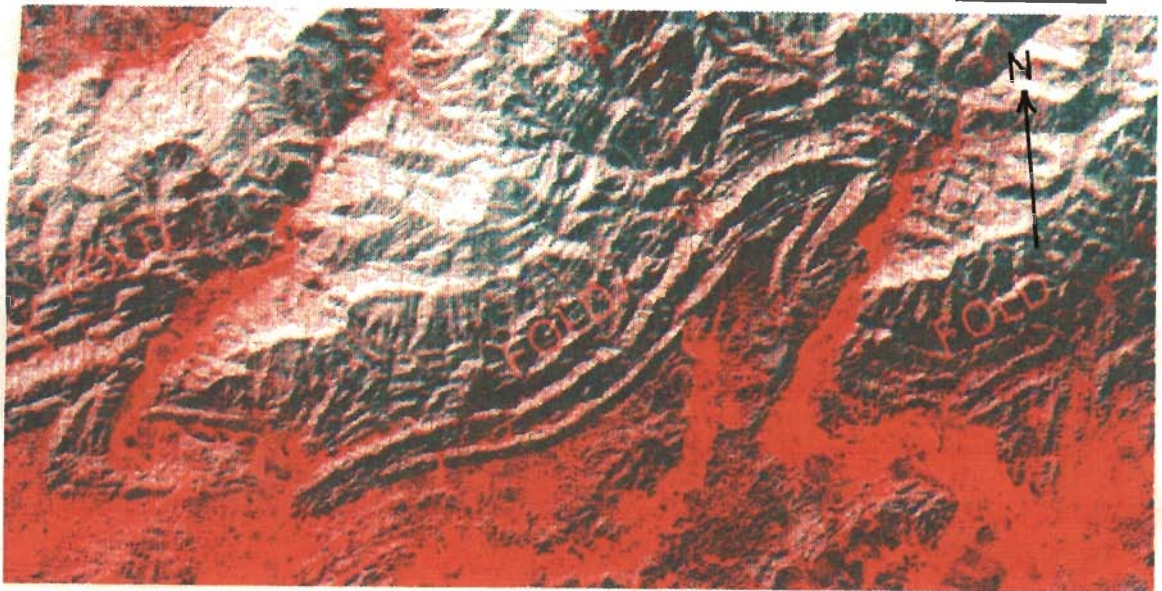


Fig. 5.13 Digitally enhanced image (IRS: LISS-II, Band-4) showing the NE-SW trending sedimentary folds with curved limbs and compressed noses which are displayed in the area south of the Haflong thrust zone (HTZ). This is the inverse image of figure 5.12 .



(A)

3 Km



(B)

Fig. 5.14 Enhanced colour composite (IRS: LISS-II) image showing the folds in sedimentary rocks in the area south of the Haflong thrust zone (HTZ). The image in (B) is an inverse of the image in (A).

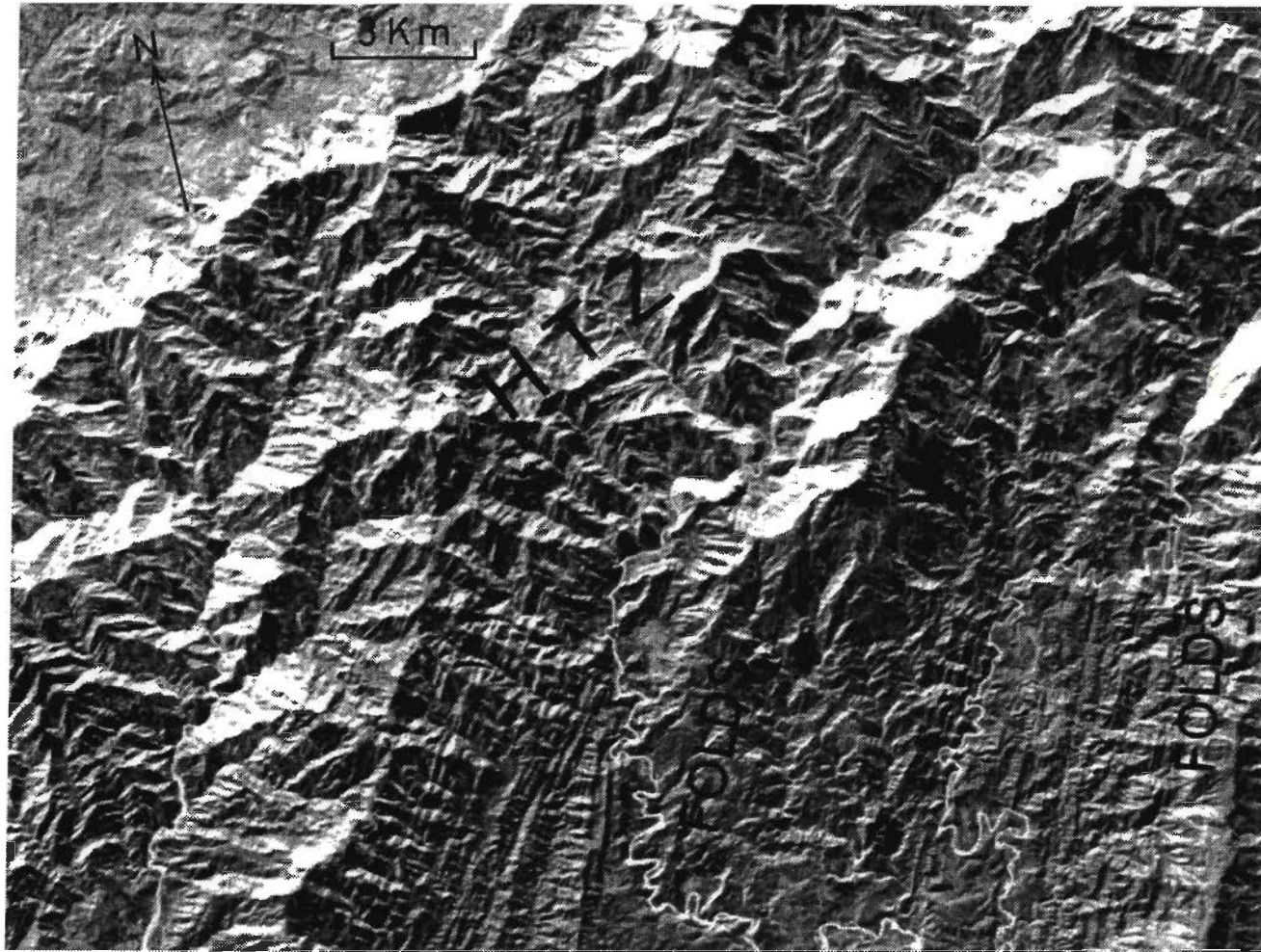
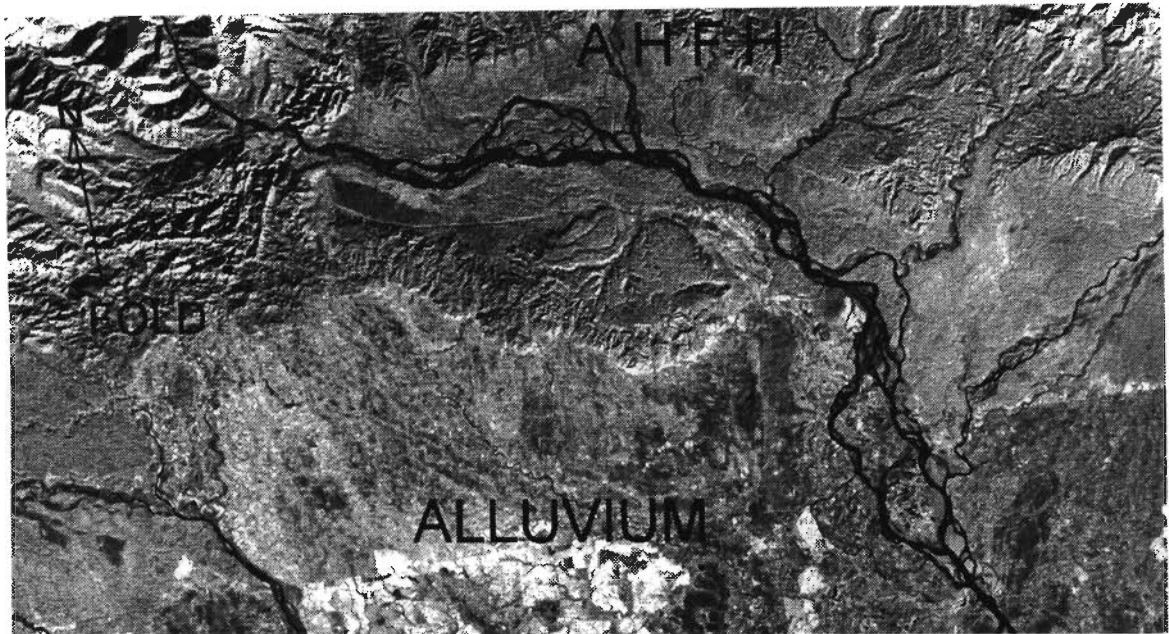
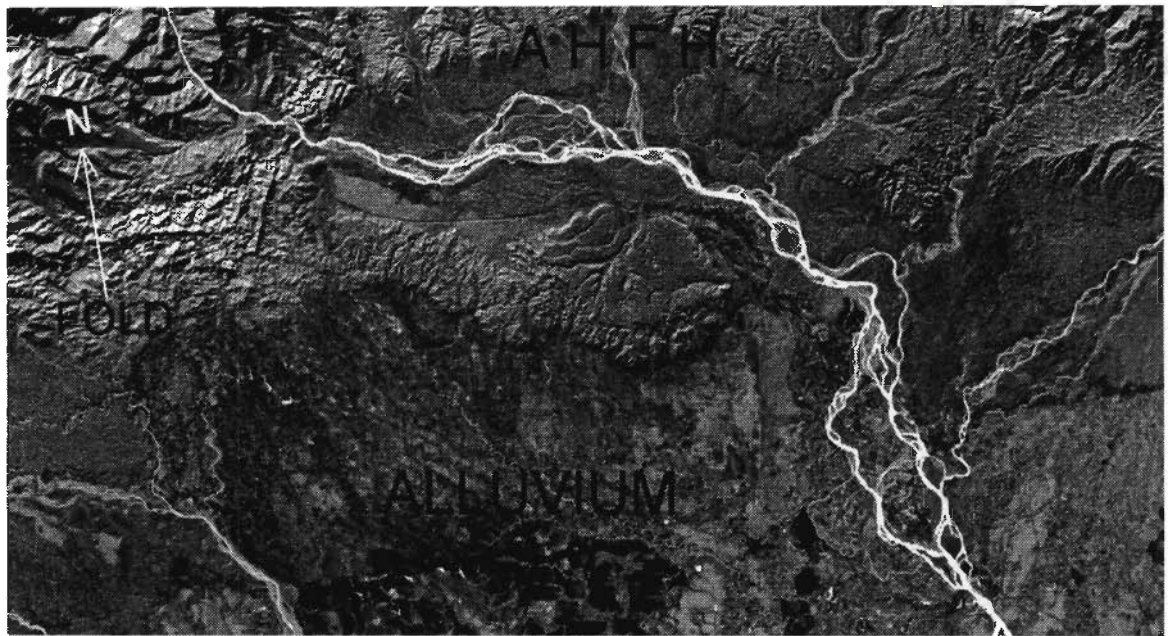


Fig. 5.15 Digitally enhanced image (IRS: LISS-II, Band-4) showing the N-S trending folds in the area SE of the Haflong thrust zone (HTZ). This is an inverse image.



(A)

6 Km



(B)

Fig. 5.16 Digitally enhanced image (IRS: LISS-II, Band-4) showing the deformation of young sediments in the Arunachal Himalayan foot hills (AHFH). The image of (B) is an inverse image of (A).

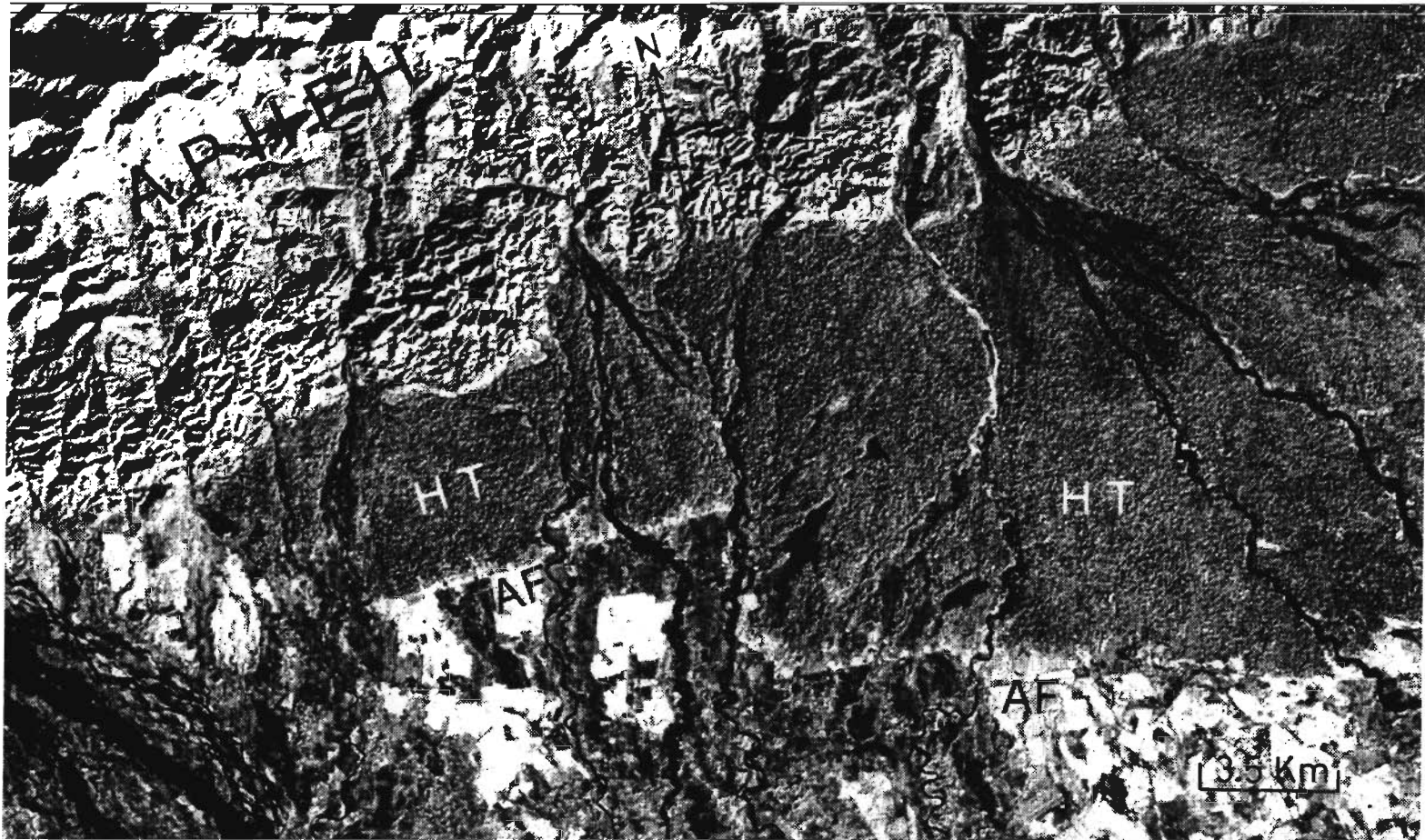


Fig. 5.17 Digitally enhanced image (IRS: LISS-II, Band-4) showing faulted alluvium APHFH-Arunachal Pradesh Himalayan Foot Hills. HT-Higher Terrace. AF-Alluvium Fault.

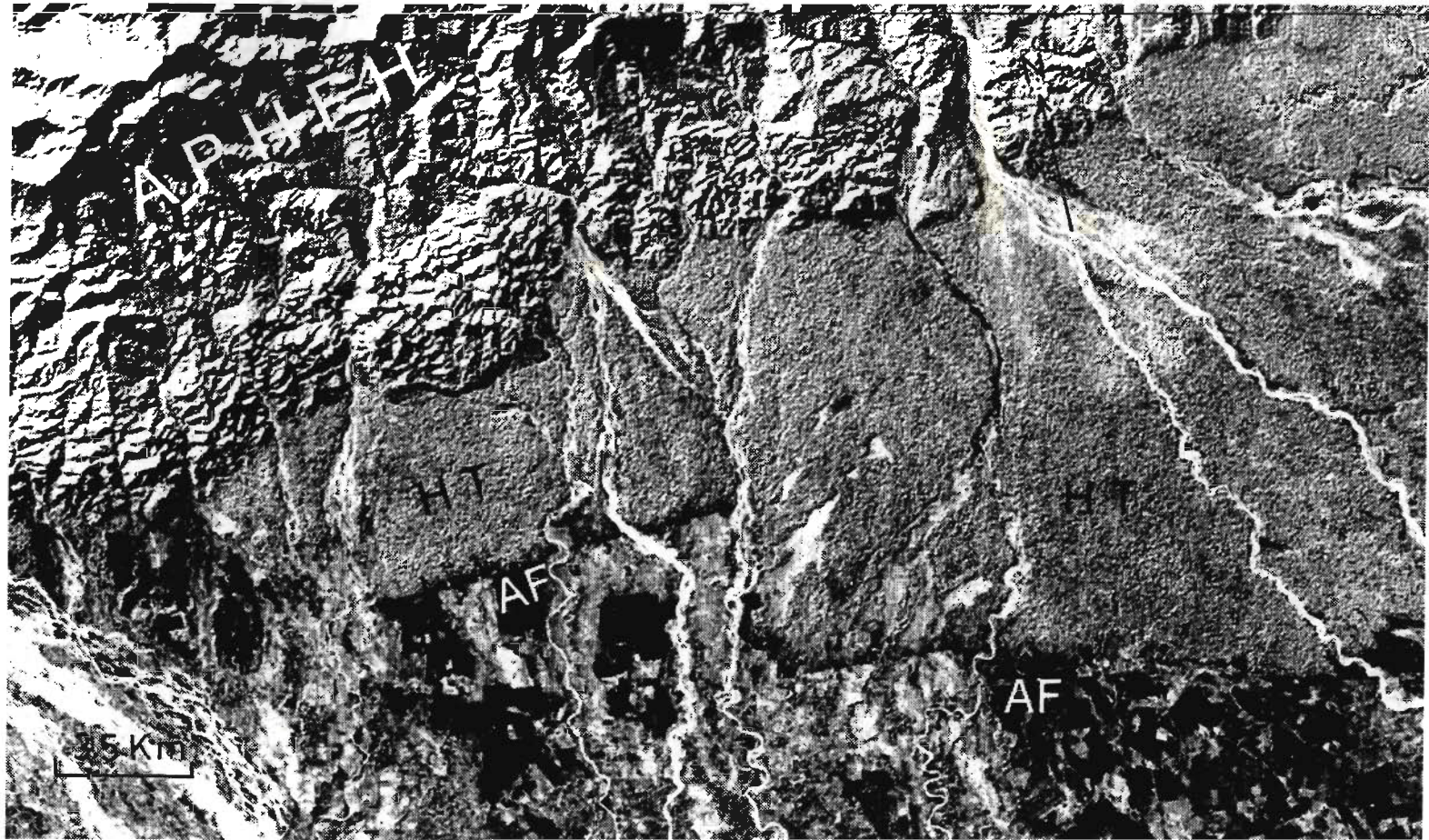
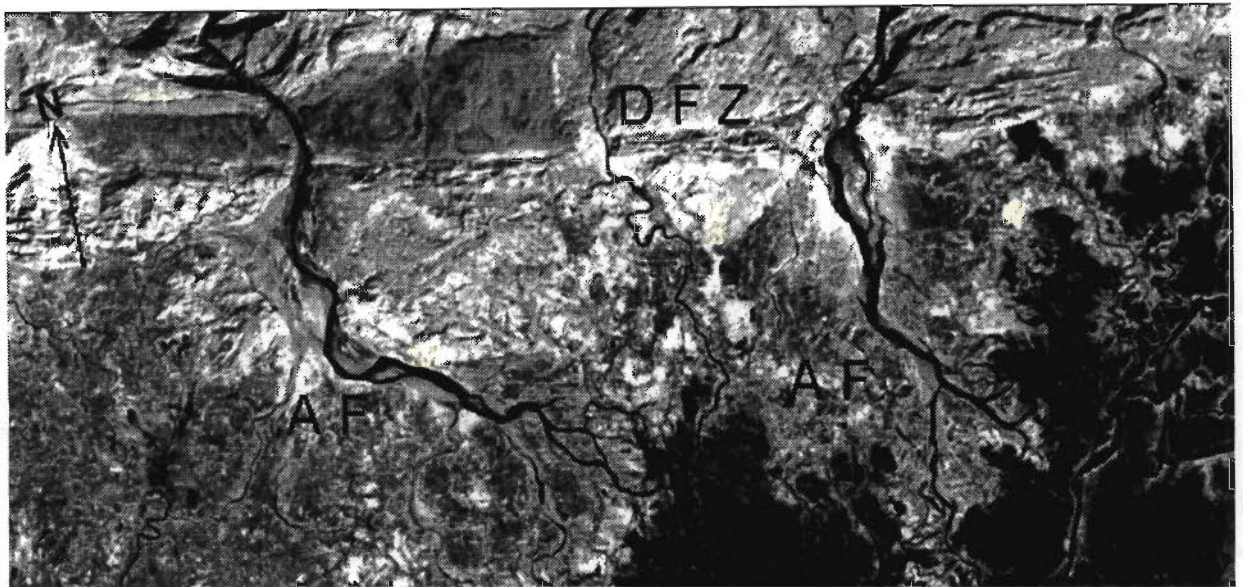
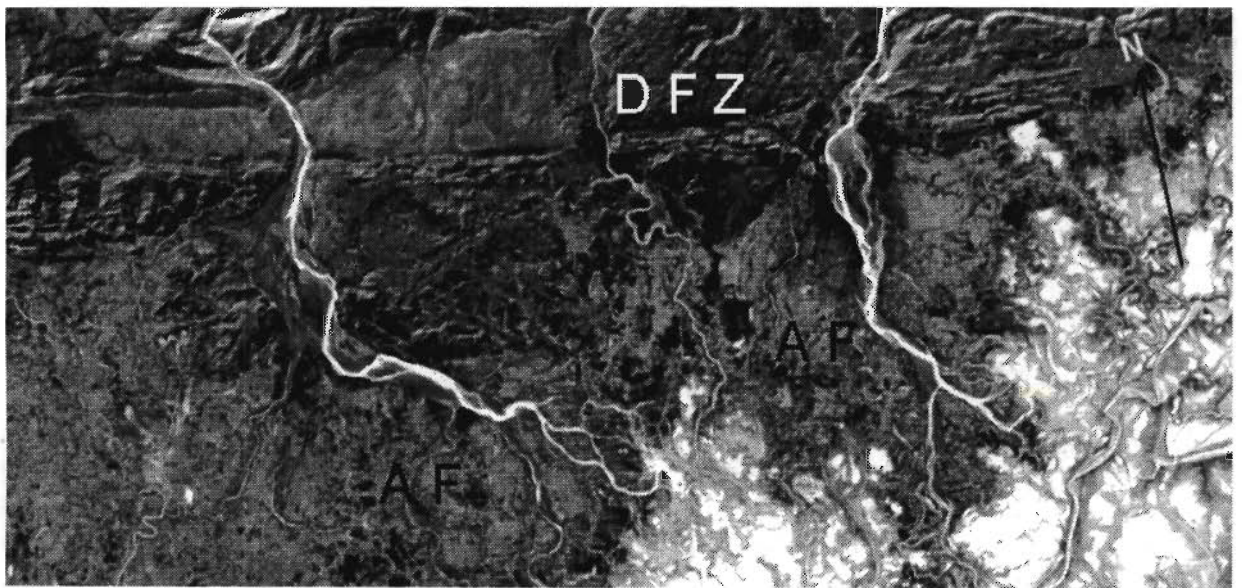


Fig. 5.18 Digitally enhanced image (IRS: LISS-II, Band-4) showing faulted alluvium. APHFH-Arunachal Pradesh Himalayan Foot Hills. HT-Higher Terrace. AF-Alluvium Fault. This is an inverse image of figure 5.17.



(A)

3 Km



(B)

Fig. 5.19 Digitally enhanced image (IRS: LISS-II, Band-4) showing development of alluvial fan (AF) in the area just south of the Dauki fault zone (DFZ). The image of (B) is an inverse image of (A).

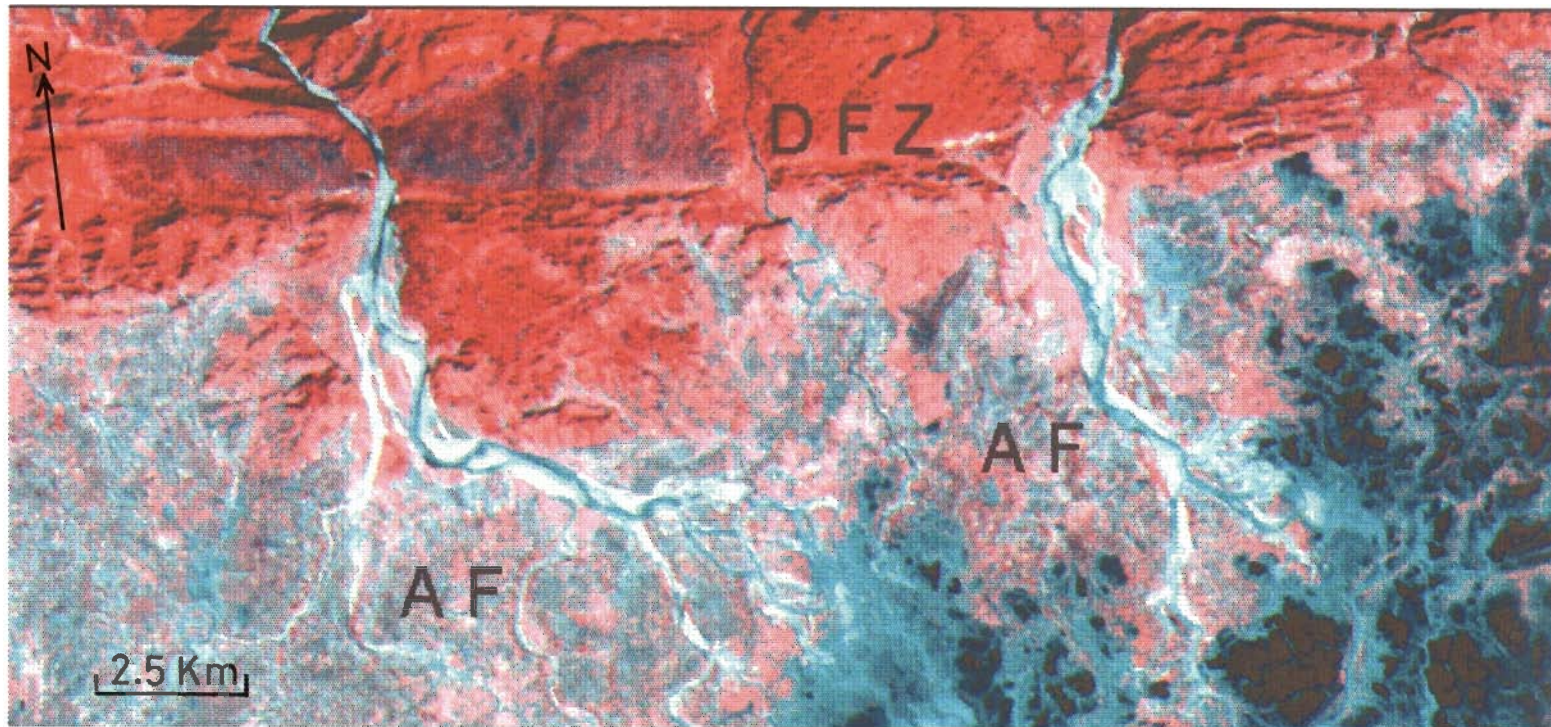


Fig. 5.20 Enhanced colour composite (IRS: LISS-II) image showing the development of alluvial fan (AF) just south of the Dauki fault zone (DFZ).



Fig. 5.21 Digitally enhanced image (IRS: LISS-II, Band-4) showing development of new channels on the north and south bank of the river. NC-New Channel.



Fig. 5.22 Digitally enhanced image (IRS: LISS-II, Band-2) showing development of new channels on the north and south bank of the river. NC-New Channel.



Fig. 5.23 Enhanced colour composite (IRS: LISS-II) image showing development of new channels on the north and south bank of the river. NC - New Channel.

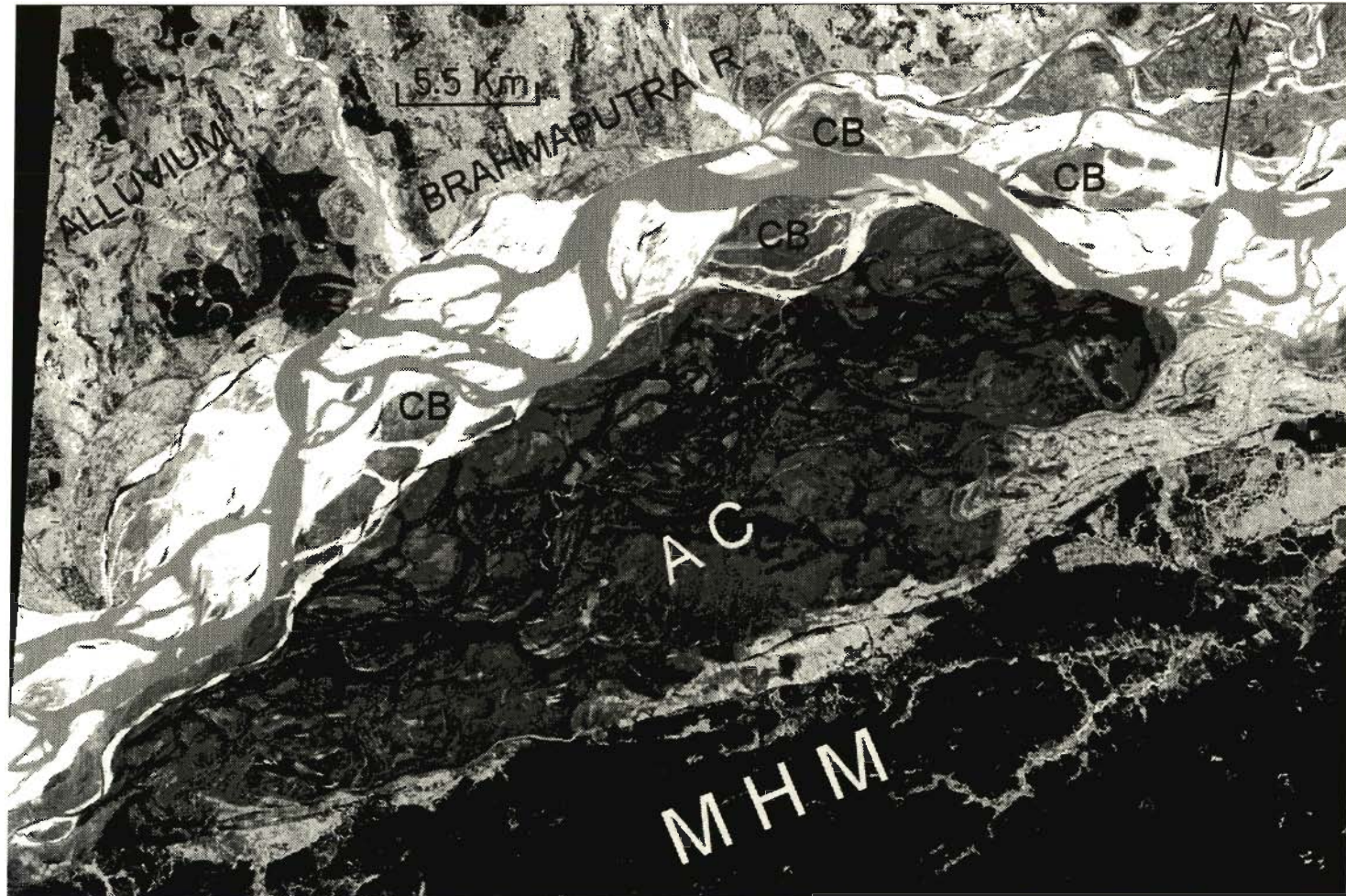


Fig. 5.24 Digitally enhanced image (IRS: LISS-II, Band-2) showing abandoned channels (AC) in the area north of Mikir Hills Massif (MHM). CB-Channel Bar.



Fig. 5.25 Digitally enhanced image (IRS: LISS-II, Band-4) showing abandoned channels (AC) in the area north of Mikir Hills Massif (MHM). CB - Channel Bar.

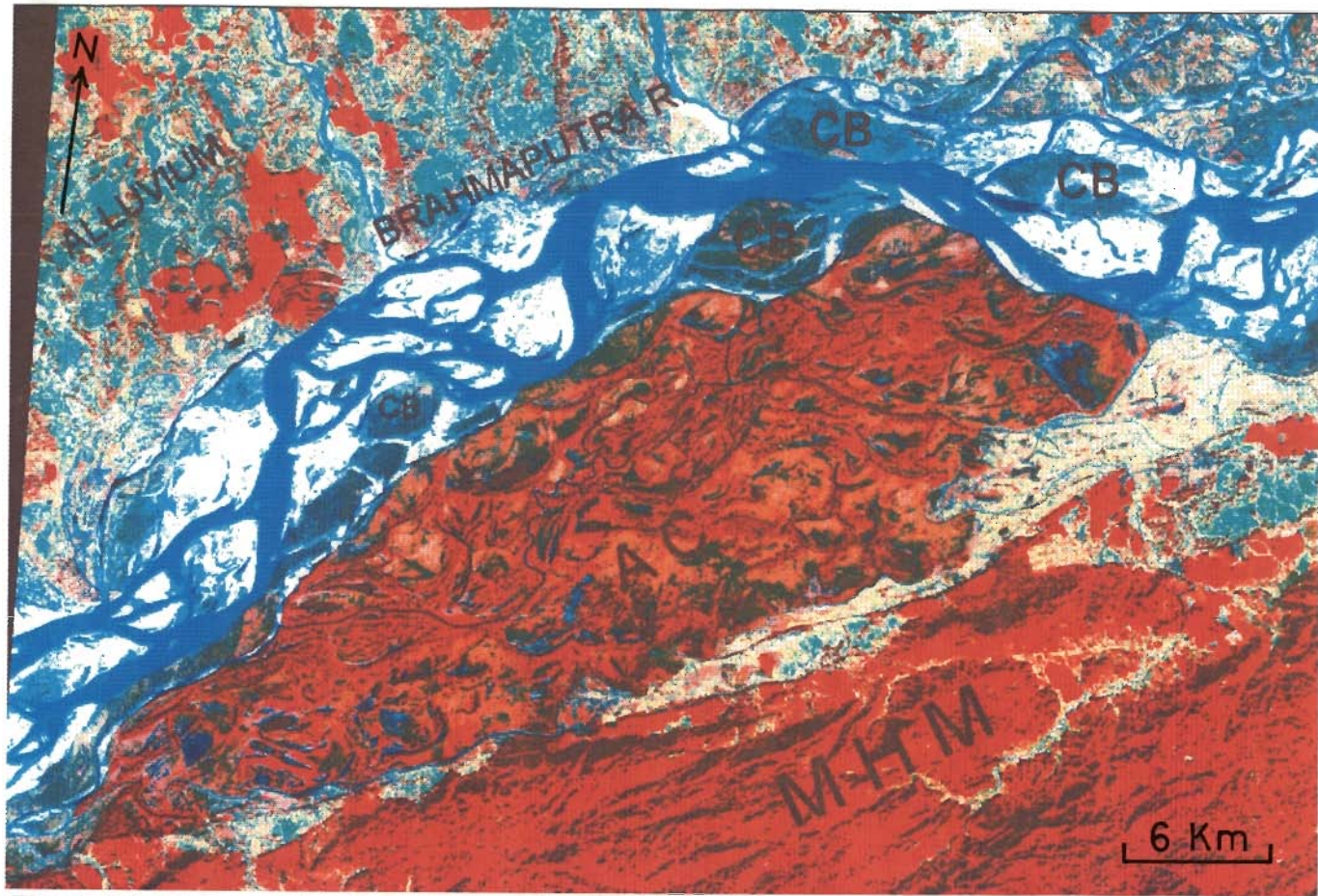


Fig. 5.26 Enhanced colour composite (IRS: LISS-II) image showing abandoned channels (AC) in the area north of Mikir hills massif (MHM). CB-Channel Bar.



Fig. 5.27 Digitally enhanced image (IRS: LISS-II, Band-4) showing northward migration of the Brahmaputra river in the area between the Shillong and Mikir hills massif. AC- Abandoned Channel.

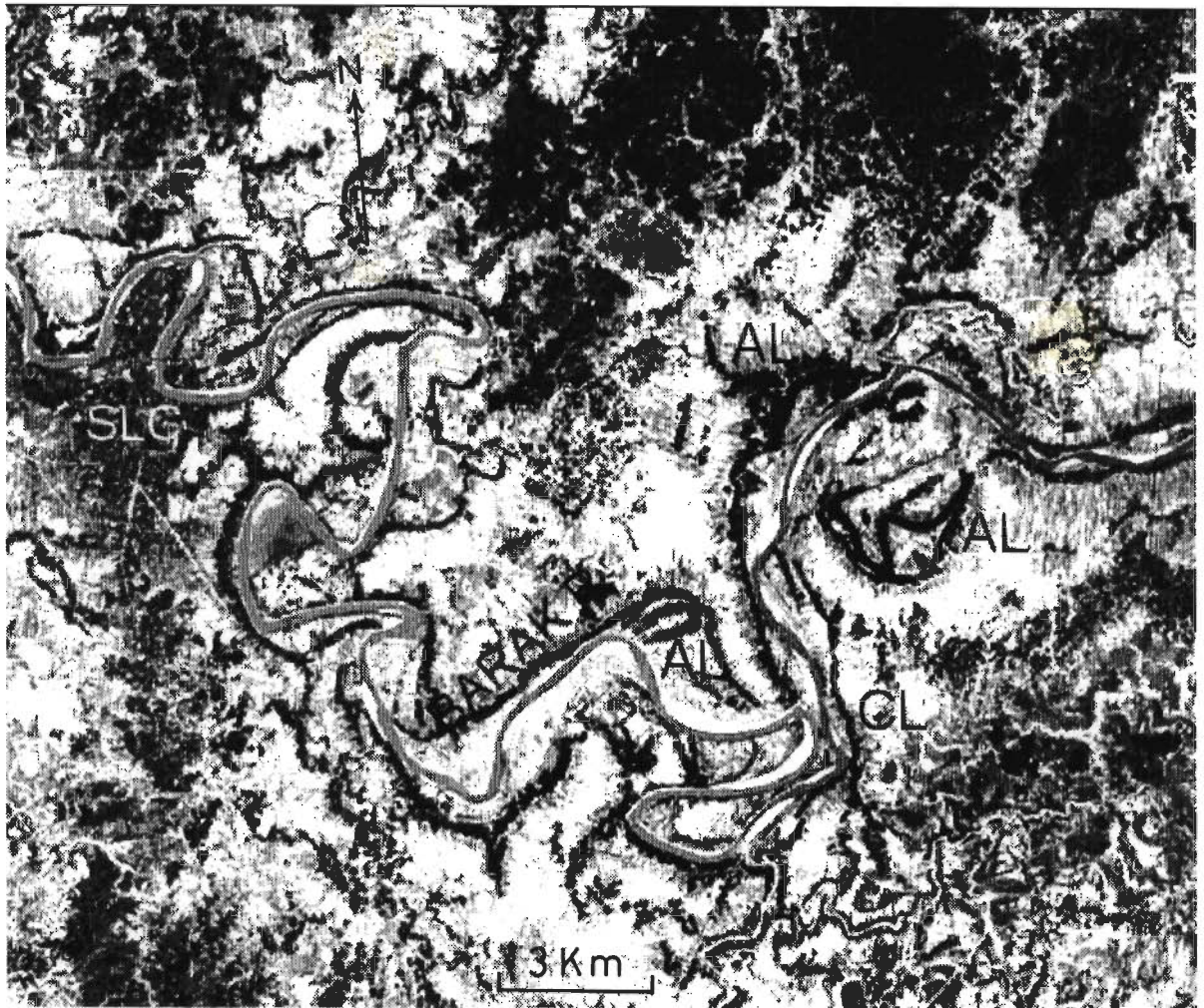


Fig. 5.28 Digitally enhanced image (IRS: LISS-II, Band-2) showing the Barak river morphology. AL-Abandoned Loop. CL-Closing Loop. SLC-Silchar.



Fig. 5.29 Digitally enhanced image (IRS: LISS-II, Band-4) showing the Barak river morphology. AL-Abandoned Loop. CL-Closing Loop. SLC-Silchar.

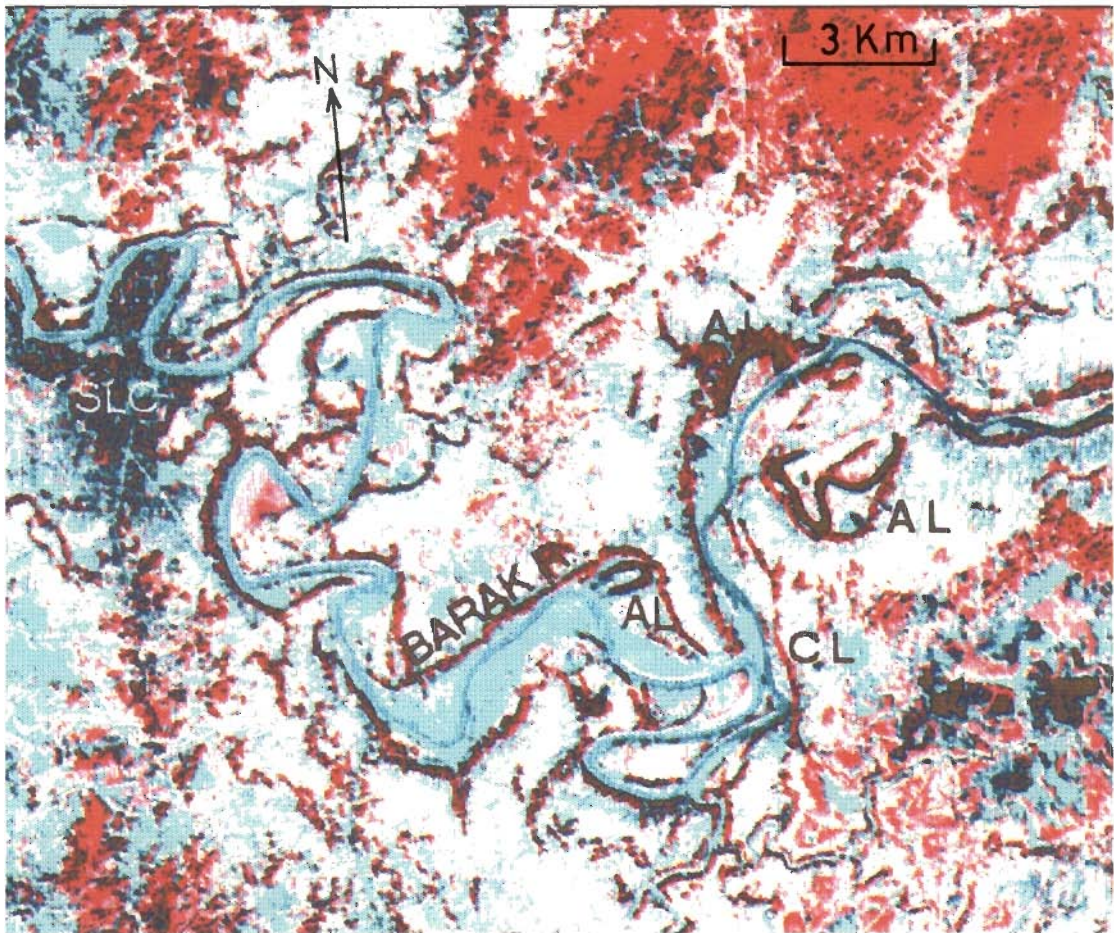


Fig. 5.30 Enhanced colour composite (IRS: LISS-II) image showing the Barak river morphology. AL - Abandoned Loop. CL - Closing Loop. SLC- Silchar.

SUMMARY AND CONCLUSIONS

6.1 INTRODUCTION

The Shillong Plateau represents the oldest tectonic unit in Northeast India and is surrounded by younger orogenic belts e.g., the Himalaya and Indo-Burman Fold Belt. This part of India had been subjected to the collision tectonics from the north and east since the subduction of the Indian Plate under the Tibetan and Burmese Plates respectively. This type of tectonics has greatly affected the Northeast India and adjoining regions, and resulted in the formation of numerous geological structures. In this region, the Shillong Plateau had witnessed prolonged tectonic activity. The present-day tectonics is manifested in high seismicity and active faulting.

Satellite images of this region provide an overview of numerous geological structures in different tectonic settings and are exceedingly useful in regional and detailed tectonic interpretations. Remotely-sensed data have been integrated with geological, geomorphological, structural and seismological data for a better understanding of various tectonic structures of the Northeast India, mainly the Shillong Plateau.

6.2 FRACTURE LINEAMENTS, JOINTS AND FAULTS

The Northeast India, especially the Shillong Plateau, can be seen as a landmass traversed by numerous fracture lineaments and faults. The mighty Brahmaputra River is also controlled by the mega-fracture lineaments. The most prominent fault along the

southern margin of the Shillong Plateau is the linear E-W trending Dauki Fault, which has major share in building-up its tectonic set up.

Some of the prominent faults in Shillong Plateau e.g., N-S trending Jamuna, Dudhnai and Um Ngot Faults are strikingly linear and deep-seated. These features might have formed under extensional tectonics. The Mohanganj and Chandghat Faults in Bangladesh appear as an extension of the Dudhnai and Um Ngot Faults respectively.

In the southern part of Shillong Plateau, numerous horst and graben structures have formed mostly in the Precambrian rocks. These structures are developed due to the vertical faulting, mainly along N-S and NE-SW trending fractures.

In the eastern part of the Shillong Massif, N-S trending fractures could be recognized, which show translational movements. The Mikir Hills Massif has shifted northward along these fractures.

The compressional tectonic features in this area are the prominent Haflong Thrust and Dapsi Reverse Fault. The Haflong Thrust was formed due to the N-S and NW-SE compression and the Dapsi Fault due to the NNE-SSW compression.

On satellite images, the Shillong Plateau can be seen criss-crossed by innumerable fractures with predominant trends in N-S and NE-SW. Frequency plotting of lineaments indicate that NW-SE trending lineaments become scarce gradually from west to east of the plateau. Further, joint data from the Precambrian rocks also show dominant trend in N-S and NE-SW directions.

Some of the tectonic blocks also reveal pattern of tectonic stresses. The detached Dafla Hills block in the Eastern Himalaya show southward migration due to N-S compressions. In the Naga Foothills, an interlocking structure has been produced by the translational movement along a regional lineament.

Moreover, folds in sedimentary rocks south of the Haflong Thrust Zone reveal NW-SE compression, whereas folds south of Dauki Fault Zone indicate variation in tectonic stresses from NE to NW.

The Himalayan Foothills show intense deformation of the Siwalik sediments.

Recent alluvium near the Himalayan Foothills have been faulted predominantly along E-W trend and are overridden by the Siwaliks along the Main Frontal Thrust (MFT).

6.2.1 River Channel Migration

It can be seen that the present day course of the Brahmaputra River has a tendency to follow a particular structural feature or a migrated path. On satellite images, prominent changes in channel patterns and their migration at some places could be noticed.

The Brahmaputra River displays northward migration in the area extreme northeast and in between Shillong and Mikir Hills Massifs. In latter sector, the river makes a huge northward curvature for about 110 km. The Brahmaputra River has a tendency to migrate towards the Himalayan Foothills. This fact indicate that the area south of the river has undergone uplift, probably due to southward thrusting of the Brahmaputra Basin against the Shillong Plateau.

6.3 DAUKI FAULT ZONE AND MORPHOTECTONICS

On satellite images, the Dauki Fault could be traced for about 300 km. The eastern part of this fault forms steep scarps. Different type of tectonics could be recognized along the Dauki Fault. The adjacent Bangladesh Plains show subsidence in the central part of the Dauki Fault Zone, whereas the western and eastern parts reveal upliftment due to thrusting. This tectonic set up is revealed by the structural features along the Dauki Fault Zone and adjoining Bangladesh area. The soft sediments in the area south of the DFZ show folding.

In the adjacent area south of DFZ, the Sylhet and Mohanganj troughs could be recognized on satellite images as dark patches and appear to be bounded by the faults.

6.4 BARAPANI SHEAR ZONE AND MORPHOTECTONICS

From the NE-SW trending Barapani Shear Zone (BSZ), some structural features could be identified on satellite images. This shear zone is located within the Precambrian phyllites belonging to the Shillong Group. On satellite image, the lensoid

shaped ridges can be seen around the Barapani reservoir. These elongated and narrow long ridges display southwestward dragging effect on the western block indicating left-lateral movement. Further, brittle deformation pattern of the rocks along the BSZ also reveals affects of tectonic stresses.

Drainage pattern of the Shillong region is strongly controlled by fracture patterns. Different landforms played great role in directing the stream flow. Along the BSZ, the northeastward flow of the Wah Umiam River has been obstructed by a ridge and the river takes a U-turn.

Therefore, it is evident that the Shillong Massif has suffered intense tectonic activities which have been manifested through different structural features. Various tectonic features of the Shillong Massif as identified in this study and the orientation of tectonic stresses are shown in Figure 6.1. Figure 6.2 shows different zones of the Shillong Plateau and adjoining regions, which had suffered different types of tectonism as suggested by this study.

6.5 SEISMICITY AND ACTIVE TECTONICS

Seismicity of the Shillong Plateau is quite scattered and spread over the whole area. Therefore, it appears that the entire area of Shillong Plateau is seismically very active. At micro level, seismicity of the plateau is very high. Moreover, as the plateau is traversed by innumerable fractures and faults, it becomes difficult to associate an earthquake event to a particular tectonic feature.

Nevertheless, earthquake activity reveals some significant informations regarding the tectonics. One of the largest earthquake of the world (Magnitude >8) occurred near Shillong and very close to the BSZ. Oldham (1899) reported numerous fissures, slumping of river-banks, landslides, surface rupture, and observed maximum destruction in the neighbourhood of Shillong.

Recently, the Shillong Plateau and adjoining regions have been affected by many earthquakes of high intensities (Fig. 6.3). Most of the moderate earthquakes have occurred at considerable depth indicating that the accumulation of stresses is more

confined to a depth range of 40 to 60 km. Chen and Molnar (1990) studied a few moderate earthquakes (30 to 50 km depth) from and around Shillong Plateau including the recent 1988 earthquake (Fig. 3.13). They opined that source mechanism of these earthquakes indicate a component of reverse faulting and compression in N-S direction, normal to the trend of Dauki Fault, while deformation has occurred deep in the crust or in the upper most part of the mantle.

On the basis of micro-earthquake studies, Mukhopadhyay (1990) suggested alternating high and low velocity zones below the Shillong Plateau at depths between 14 to 25 km, along which sediments of Bangladesh may be underthrusting beneath it. Recently recorded micro-earthquakes from the Shillong Massif are distributed in the depth range of 1 to 40 km with a cluster at 10 km (Mukhopadhyay, 1990). However, moderate earthquakes in this region are more or less sporadically distributed and also occurred at greater depth (Fig. 6.3). It is also noteworthy that some of the very deep earthquakes (more than 100 km) have occurred in the Sylhet Trough area, Kopili Gap and Brahmaputra Basin north of Guwahati (Fig. 3.13). It is, therefore, likely that stress release has occurred at various crustal depths by rupturing within the region of the Shillong Plateau.

Nevertheless, under such a active tectonic regime any fault may get reactivated, hence some of the shallow earthquakes may originate along numerous faults traversing the region. From the study of 180 micro-earthquake events (depth range of 10 to 35 km), recorded locally from the Shillong Plateau, Kayal (1987) observed ENE-WSW and NW-SE compressional stress in the Tura and Shillong regions respectively. Similarly, Mukhopadhyay (1990) has reported N-S compression, being experienced by the Shillong Plateau.

6.6 QUALITATIVE ASSESSMENT ON EARTHQUAKE-PRONE FAULT ZONES

As the Shillong Plateau is seismically active, numerous faults traversing the plateau and adjoining regions may get reactivated in near future under existing tectonic set up. An attempt has been made to identify such seismically-potential faults bounding the tectonic blocks from the Shillong Plateau and Arunachal Himalaya.

6.6.1 Shillong Block

This block is bounded by the Barapani Shear Zone and Um Ngot Fault. This block seems to have moved northward due to displacements along these faults. Moreover, the Um Ngot Fault has pushed the Barapani Shear Zone northwards dextrally. This tectonic block may be a potential zone of future intraplate earthquakes, as the movement along a fault may be inhibited by the other fault resulting into accumulation of stress. Under present style of compressive tectonism, built-up of more stresses in this block is anticipated.

6.6.2 Dafla Hills Block

This tectonic block is located in Arunachal Himalaya and demarcate a triangular area, bounded by well-defined fractures. These fractures intersect at a location 50 km NW of Itanagar. The rocks at the intersection have been intensely shattered. This tectonic block shows movements towards the Brahmaputra basin in front of Mikir Hills Massif, resulting into the narrowing of the valley. The fracture pattern would indicate that N-S-oriented stress may probably be responsible for formation of such a detached block. Therefore, under continued compression the faults of this tectonic block may get reactivated producing earthquakes.

6.6.3 Tura Block

This block is bounded by the Dudhnai Fault to the east and Jamuna Fault to the west. As discussed in Chapter 3, this block is thrust southward against a steeply-dipping Dapsi Reverse Fault. This type of thrusting took place by rupturing along a plane lying at particular depth. Since the block has a maximum northward extension of exposed massif rocks towards the Himalayan belt, the rupture plane beneath the block may get reactivated under continued resistance to northward movement of the Indian Plate. Moreover, quite a few moderate earthquakes are located in this block north of Tura and probably caused by the ruptures at depth (Fig. 3.13).

6.6.4 Other Structures

Beside these tectonic blocks, merging of two different fault structures and intersecting fracture lineaments may also be locales of future stress release.

Merging effects of two different fault structures can be seen towards east of the Dauki Fault. Here, the E-W trending Dauki Fault merges with the NE-SW trending Haflong Thrust. Further, a composite geological structure can be seen in the area (Das et al., in press). Under continued compressional stresses, the area is likely to suffer more faulting, as two weak zones are present in the form of the Dauki Fault and southward dipping Haflong Thrust. However, seismic activity of the thrust zone is quite low probably due to creep movement through which stress energy is getting dissipated.

6.7 TECTONIC MODEL

The Shillong Plateau is bordered by many faults and itself has been dissected by numerous fractures, faults and shear zone. The Shillong Plateau is a horst and has been uplifted due to the vertical movements along various faults.

At the close of Mesozoic, fractures deep into the upper mantle caused volcanic eruptions of the Sylhet and Rajmahal Traps. The Rajmahal and Kopili gaps should have formed during the late Mesozoic only, as the Shillong Plateau was a single monolithic Precambrian landmass in this part of the Indian Plate in early Mesozoic. Therefore, it seems likely that the northeastern parts of the Indian continent had suffered widespread volcanism at the close of Mesozoic. The N-S trending extensional tectonism and vertical uplift of the Shillong Massif was responsible for the formation of the E-W trending Dauki Fault. This fault shows huge vertical subsidence of about 13 km of the basement rocks in the south.

There are other E-W trending parallel faults identified along the northern margin of Shillong Massif (e.g., Brahmaputra Fault). Innumerable tensile fractures were responsible for the formation of numerous horst and graben structures on the Shillong Massif itself. As the extensional tectonism prevailed over the massif, the fractures gradually opened up and formed grabens. This situation probably continued even during the Tertiary, as some of the grabens affected the Tertiary rocks too.

During the Tertiary, major tectonic changes took place due to collision of the Indian Plate with the Tibetan Plate in the north. Similarly, the collision between the Indian Plate and the Burmese Plate in the east was at its maximum during the Miocene. Present tectonic set up indicates that the Indian Plate was undergoing northward and eastward subduction below the Tibetan and Burmese Plates respectively. The eastward subduction is still active, as is indicated by the deep earthquakes (Mukhopadhyay and Dasgupta, 1988).

During the Mid-Tertiary, the whole Northeastern India had undergone intense compressional tectonics from essentially orthogonal directions. This resulted in the formation of many thrusts e.g., Haflong Thrust, Dapsi Reverse Fault and folds in sedimentary rocks along the margin of the Shillong Massif. The NE-SW trending Barapani Shear Zone got reactivated during the Miocene due to N-S compression.

Figure 6.4 shows proposed tectonic model of the Shillong Plateau with respect to the Himalaya and the Bangladesh Plains. It is believed that in the Himalaya, convergence has migrated southward along various thrusts. The MFT is the southernmost Himalayan thrust. Structural studies reveal that the convergence may even be affecting the Brahmaputra Basin and the Shillong Massif as well. Thrust planes are probably developed beneath the Brahmaputra Basin and the Shillong Massif and result in the upliftment of the southern part of the Brahmaputra Basin, differential uplift of the southern margin of the Shillong Plateau and seismic pattern underneath this plateau.

6.8 CONCLUSIONS

1. Tectonics along the Dauki Fault Zone (DFZ) have evolved at various stages. In the initial stage, there was large-scale vertical slip along the fault under extensional tectonic regime. Later on, the vertical tectonism has ceased under the changed scenario of compressional tectonism. Along the DFZ from the longitudes 90° E to 91° E, the area shows upliftment; between longitudes 91° to 92° E, the area is of subsidence; and beyond it, is the area of thrusting where sediments override from south. Therefore, southern margin of the Shillong Plateau has undergone

differential tectonic movements, which have resulted into subsidence of the adjacent Bangladesh Plains in the central parts and upliftment on the shoulders.

2. Since Miocene, no movement occurred along the eastern part of the Dauki Fault, as is indicated by undisturbed folds in sedimentary rocks crossing the fault at longitude 93° E. Rather, the E-W transverse faults with right-lateral movements, which were observed further to the south of the Dauki Fault at latitude $24^{\circ} 30' N$ indicate a southward shifting of pattern of faulting.
3. Southeastern margin of the Shillong Massif has suffered NW-SE oriented compressional stresses, as indicated by the Haflong Thrust Zone and the spectacular folds in the sediments south of this thrust zone.
4. The Precambrians of the Shillong Plateau had suffered both ductile and brittle deformations. The Barapani Shear Zone (BSZ) has initially suffered ductile deformation probably in the Precambrian and brittle deformation later in the Miocene. This shear zone probably got reactivated in the Miocene when the N-S compression was at its culmination.
5. The N-S trending Um Ngot Fault was active only before the Eocene. However, N-S trending Dudhnai Fault remained active, as it displaces the Dauki Fault. The Kopili Mega-fractures in the area between the Shillong and Mikir Hills Massifs show translational movement and the Mikir Hills Massif has been shifted further north along these fractures.
6. The Brahmaputra River shows intense northward migration due to upliftment of the Brahmaputra Basin along its southern margin with the Shillong Plateau. It is likely that this basin is thrust over the Shillong Plateau along this margin.
7. The whole Shillong Plateau is highly prone to earthquakes. Some of the locales are identified as more potential seismic zones. These are the intersection zone of the Barapani Shear Zone and Um Ngot Fault, the Dauki and Dudhnai Faults and the Haflong Thrust Zone. The Dafla Hills tectonic block in Arunachal Himalaya and the Tura Hills block are also potential zones for the occurrence of earthquakes. Fault

plane mechanism of different earthquakes and microseismic events associated with the Shillong Plateau reveal an overall thrust type rupture zone underneath this rigid block.

8. Integrated geological, seismological and remote-sensing studies in parts of the Shillong Plateau and adjoining regions have clearly demonstrated existence of thrust faults both along the northern and southern margins of this Precambrian massif. These thrusts occur much south of the Main Frontal Thrust (MFT) in an overall compressional tectonic regime due to northward movement of the Indian Plate.

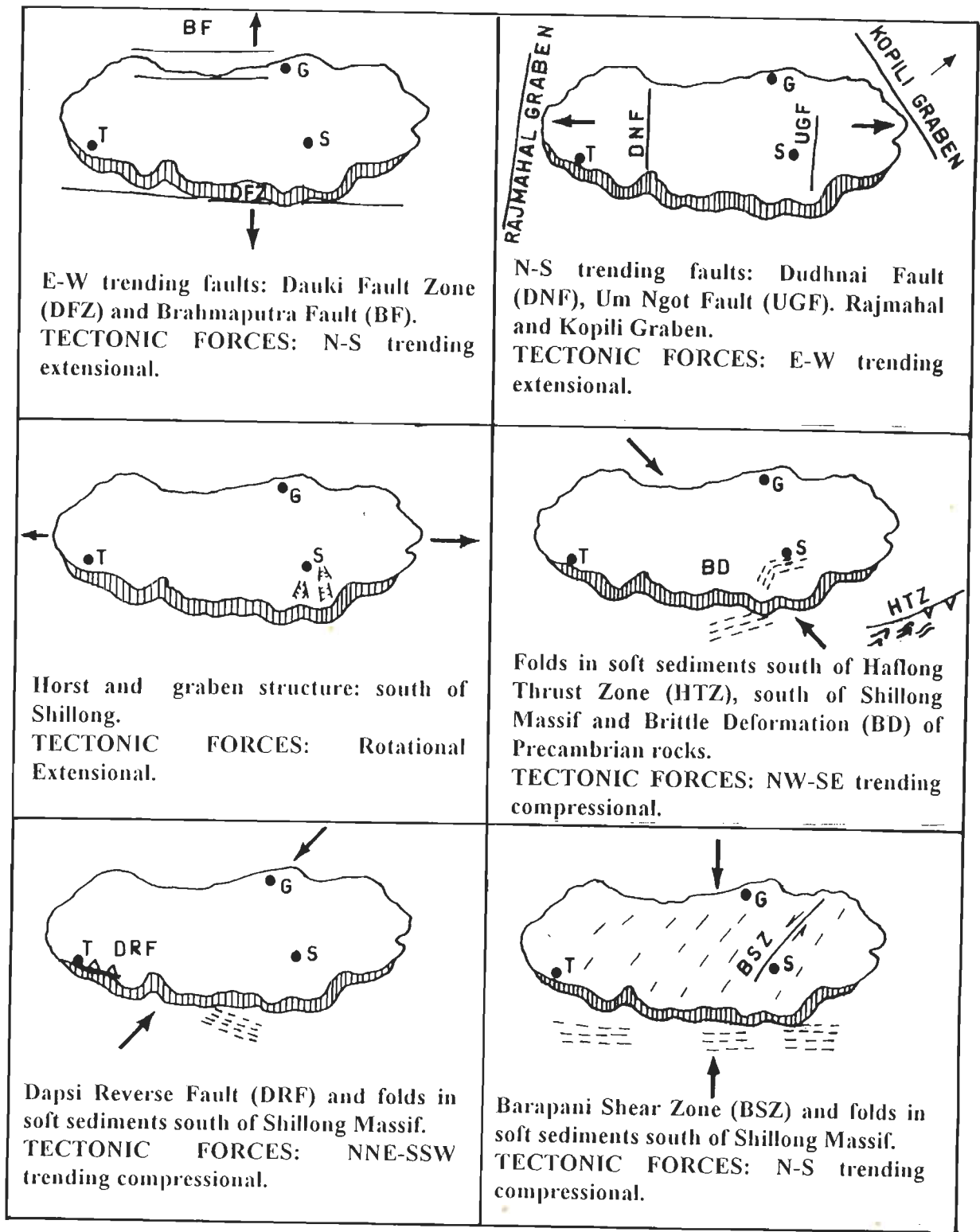
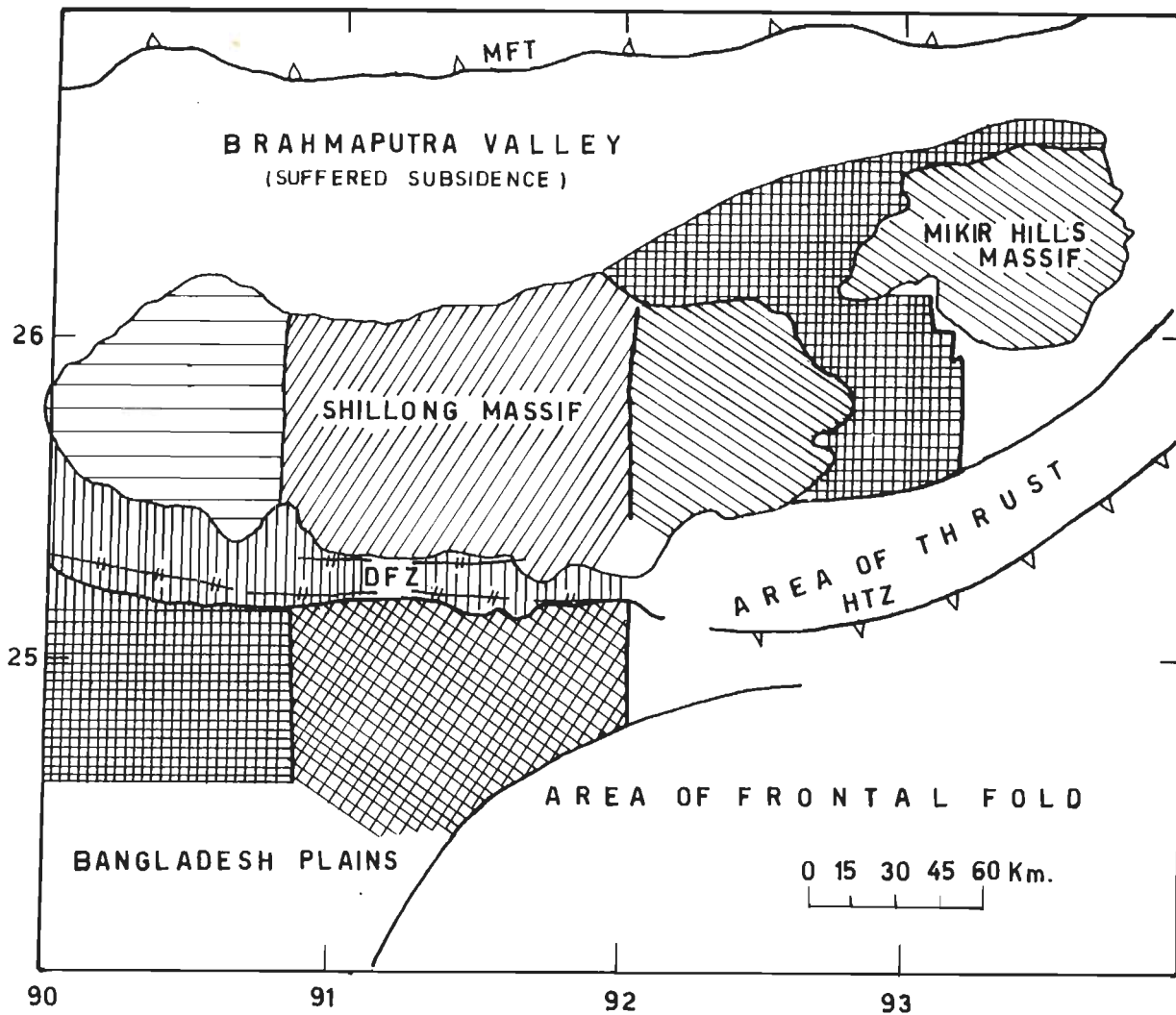


Figure 6.1. Shillong Massif and adjoining regions showing various tectonically significant structures and the orientations of tectonic stresses.




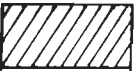

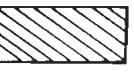


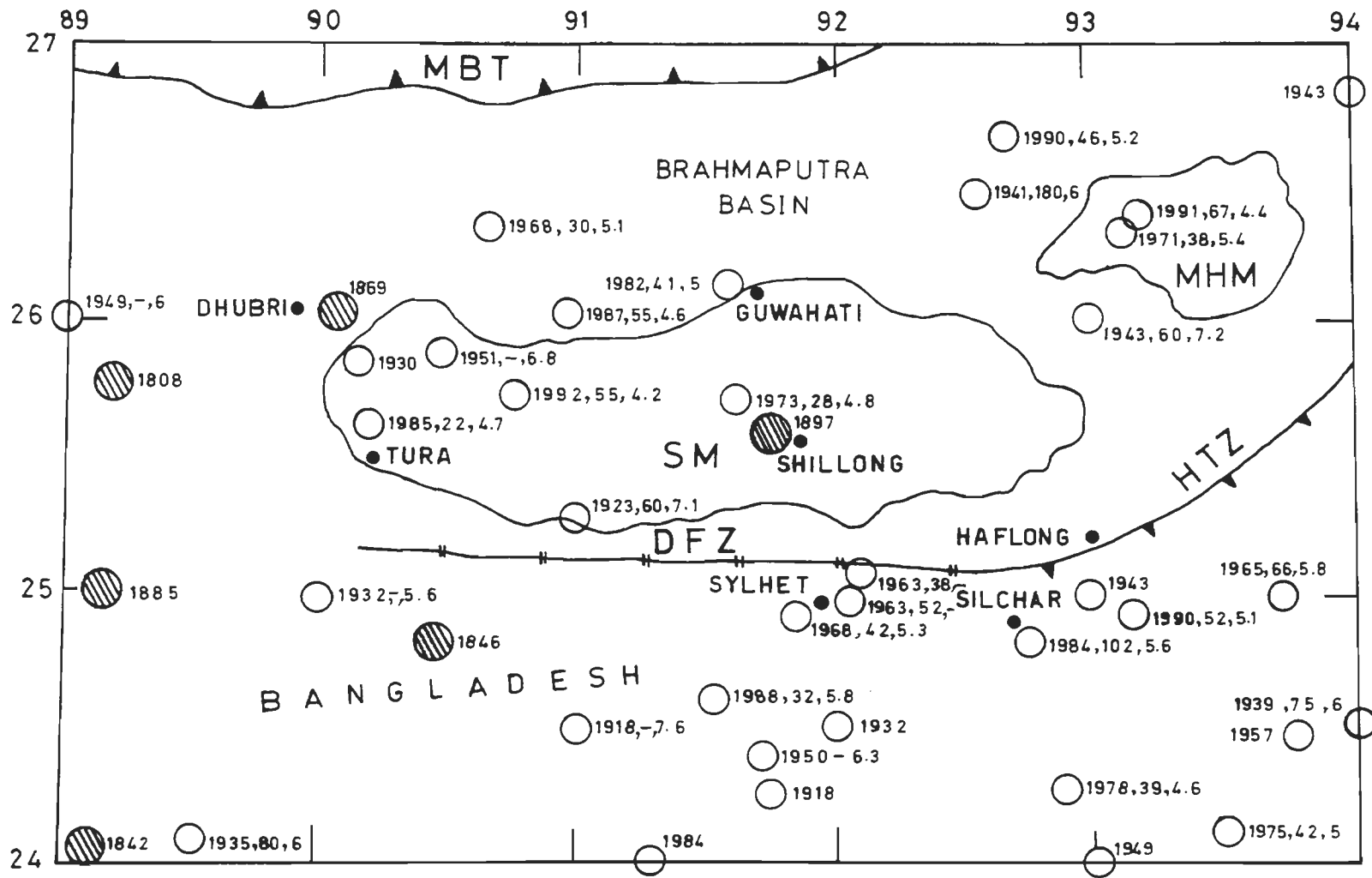
-  Area suffered maximum compression.
-  Area suffered maximum vertical movement.
-  Shattered sedimentary rocks along the Dauki Fault Zone (DFZ) which suffered extensive vertical tectonism.
-  Area of normal vertical uplift.
-  Area suffered upliftment.
-  Area south of DFZ suffered subsidence.

Figure 6.2. Shillong Plateau and adjoining regions show various tectonic units which suffered different degree of tectonic stresses.



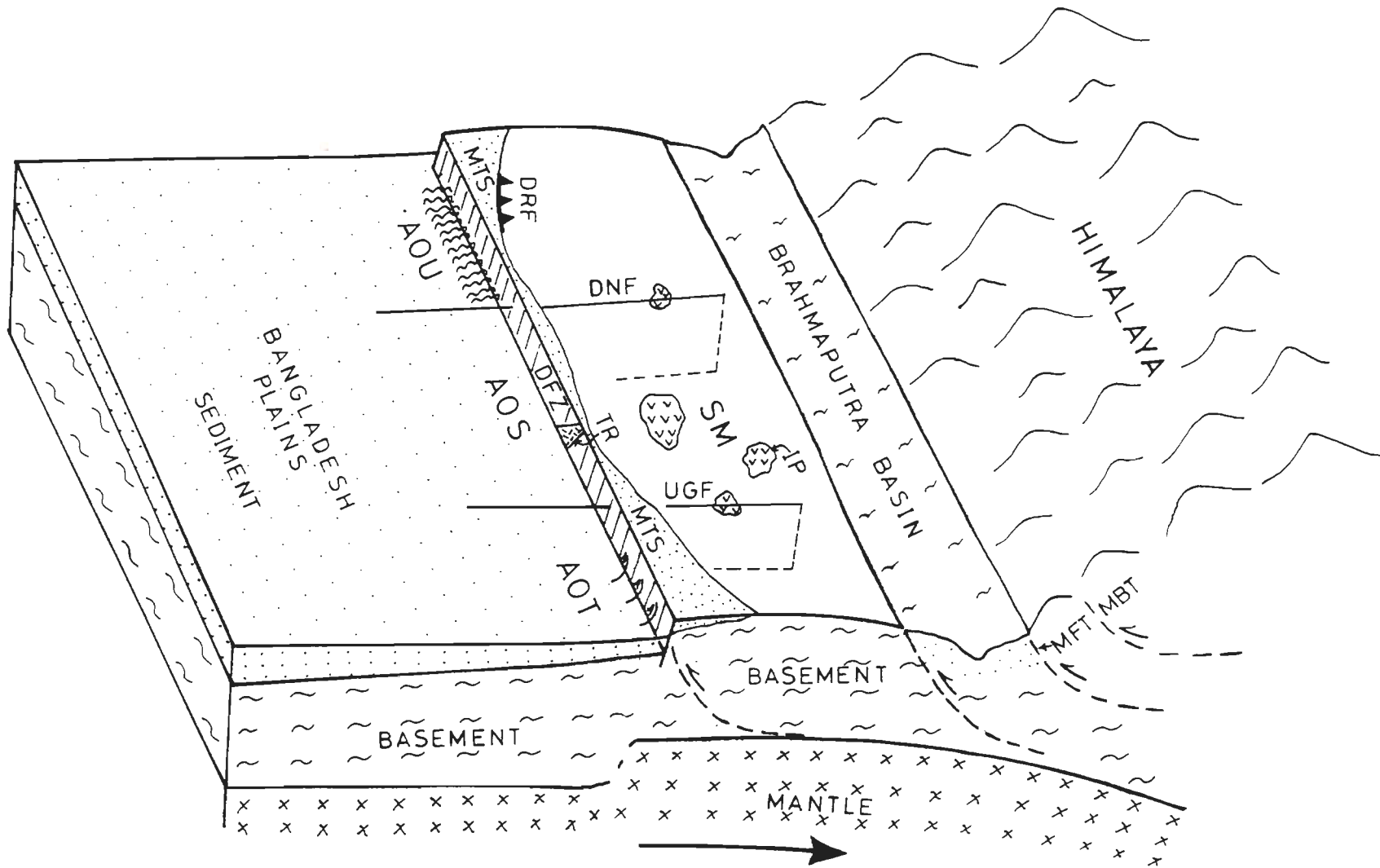


Figure 6.4. A proposed simplified longitudinal tectonic model of the Shillong Massif with respect to the Himalaya and Bangladesh Plains. SM-Shillong Massif, DFZ-Dauki Fault Zone, DNF-Dudhnai Fault, UGF-Um Ngot Fault, DRF-Dapsi Reverse Fault, IP-Igneous Pluton, TR-Trap Rock, MTS-Mesozoic-Tertiary Sediments, AOU-Area of Uplift, AOS-Area of Subsidence, AOT-Area of Thrust, MBT-Main Boundary Thrust, MFT-Main Frontal Thrust.

REFERENCES

1. Acharyya, S. K., Mitra, N. D. and Nandy, D. R. (1986). Regional geology and tectonic setting of Northeast India and adjoining regions. *Mem. Geol. Surv. India*, 119, 6-12.
2. Anderson, E.M. (1951). The dynamics of faulting and dyke formation in Great Britain. *Edinburg, Oliver and Boyd*, 206 pp.
3. Auden, J. B. (1972). Review of the tectonic map of India published by O.N.G.C. *J. Geol. Soc. India*, 13, 101-107.
4. Barooah, B. C. (1976). Tectonic pattern of the Precambrian rocks around Tyrssad, Meghalaya. *Geol. Surv. India, Misc. Publ.*, 23, 485-495.
5. Biswas, S. and Dasgupta, A. (1986). Some observations on the mechanism of earthquakes in the Himalaya and the Burmese arc. *Tectonophysics*, 122, 325-343.
6. Brune, J. N. and Singh, D. D. (1986). Continent like crustal thickness beneath the Bay of Bengal sediments. *Bull. Seism. Soc. Am.*, 76, 191-203.
7. Brune, J. N., Curray, J. R., Dorman, L. M. and Raitt, R. W. (1990). Super-thick sedimentary basin, Bay of Bengal. (*abs*) :*Eos (Transactions, American Geophysical Union)*, 71, p1444.
8. Brunnschweiler, R. O. (1966). On the geology of the Indoburman ranges. *J. Geol. Soc. Aust.*, 13, 137-194.
9. Burke, K. and Dewey, J. F. (1973). Plume-generated tripple junctions: Key indicators in applying plate tectonics to old rocks. *J. Geol.*, 81, 406-433.
10. Campagna, D. J. and Levandowski, D. W. (1991). The recognition of strike-slip fault systems using imegery, gravity and topographic data sets. *Photogrammetric Engg. and Remote Sensing*, 57, 1195-1201.
11. Chandra, U. (1975). Seismicity, earthquake mechanisms and tectonics of Burma, 20⁰N-28⁰ N. *Geophys. J.R. Astron. Soc.*, 40, 367-381.

12. Chandra, U. (1978). Seismicity, earthquake mechanisms and tectonics along the Himalayan mountain range and vicinity. *Phys. Earth Planet. Inter.*, 16, 109-131.
13. Chattopadhyay, N. and Hashimi, S. (1984). The Sung valley alkaline ultramafic carbonatite complex, East Khasi and Jaintia Hills District, Meghalaya. *Geol. Surv. India, Misc. Publ.*, No. 113, 24-33.
14. Chen, W. P. and Molnar, P. (1990). Source parameters of earthquakes and intraplate deformation beneath the Shillong plateau and the northern Indoburman ranges. *J. Geophys. Res.*, 95, 12527-12552.
15. Chopra, S. (1986). Photogeomorphological mapping of southern parts of Jadukata-Umngi river valleys, Meghalaya. *J. Ind. Soc. Remote Sensing*, 14, 37-42.
16. Coleman, J. M. (1969). Brahmaputra River-channel processes and sedimentation. *Sedimentary Geology*, 3, 129-239.
17. Curray, J. R., Emmel, F. J., Moore, D. G. and Raitt, R. W. (1982). Structure, tectonics, and geological history of the northeastern Indian ocean. In: *The ocean basins and margins*, Edited by Alan E.M. Nairn and Francis G. Stehli. Plenum Publishing Corporation, 6, 399-450.
18. *Das, J. D. (1992). The Assam basin: Tectonic relation to the surrounding structural features and Shillong plateau. *J. Geol. Soc. India*, 39, 303-311.
19. *Das, J. D. (1994). Tectonic geomorphology of Shillong region. *Indian J. Earth Sc.*, 21, 47-53.
20. *Das, J. D., Saraf, A. K. and Jain, A. K. (1995). Fault tectonics of the Shillong plateau and adjoining regions, Northeast India using remote sensing data. *Int. J. Remote Sensing*, 16, 1633-1646.
21. *Das, J. D., Saraf, A. K. and Jain, A. K. (1995). A satellite picture reveals seismically potential tectonic structures in Northeast India. *Int. J. Remote Sensing, U.K.* (in press).

NOTE: Scientific papers marked by stars (*) have been produced from the present research work. In the papers, the name of the author Josodhir Das has been abbreviated as J. D. Das.

22. Dasgupta, S. and Nandy, D. R. (1982). Seismicity and tectonics of Meghalaya plateau, Northeastern India. *VII Symp. Earthquake Engg., University of Roorkee, India*, 19-24.
23. Desikachar, S. V. (1974). A review of the tectonic and geological history of eastern India in terms of plate tectonic theory. *J. Geol. Soc. India*, 15, 137-149.
24. Drury, S. A. (1987). Image interpretation in Geology. *Allen and Unwin Ltd., London*, 243 pp.
25. Evans, P. (1964). The tectonic framework of Assam. *J. Geol. Soc. India*, 5, 80-96.
26. Fitch, T. J. (1970). Earthquake mechanisms in the Himalayan, Burmese, and Andaman regions and continental tectonics in central Asia. *J. Geophys. Res.*, 75, 2699-2709.
27. Fitch, T. J. (1972). Plate convergence, transcurrent faults, and internal deformation adjacent to southeast Asia and the Western Pacific. *J. Geophys. Res.*, 77, 4432-4460.
28. Ganju, J. L., Khar, B. M. and Chaturvedi, J. G. (1986). Geology and hydrocarbon prospects of Naga hills south of 27^o latitude. *Bull. Oil Nat. Gas Commission*, 23, 129-145.
29. Gansser, A. (1983). Geology of the Bhutan Himalaya. *Birkhauser Verlag Basel, Switzerland*, 181 pp.
30. Garg, G. R. (1953). Earthquake of August 15 and its effect on the topography, the regimes of the rivers in north-east Assam, and damage to roads. *In: A compilation of papers on the Assam earthquake of August 15, 1950. The Central Board of Geophysics, Publ. No. 1*, 65-71.
31. Gee, E. P. (1953). The Assam earthquake of 1950. *In: A compilation of papers on the Assam earthquake of August 15, 1950. The Central Board of Geophysics, Publ. No. 1*, 101-107.
32. G. S. I. (1974). Geology and mineral resources of the states of India, Part IV, Arunachal Pradesh, Assam, Manipur, Meghalaya, Mizoram, Nagaland and Tripura. *Geol. Surv. India, Misc. Publ.*, 30, 124 pp.

33. G. S. I. (1981). Final report on the assessment of potentiality for basement mineralization in Tyrsad-Barapani shear zone, Khasi Hills District, Meghalaya. (*Unpublished*).
34. Ghosh, S., Chakraborty, S., Bhalla, J. K., Paul, D. K., Sarkar, A., Bishui, P. K. and Gupta, S. N. (1991). Geochronology and geochemistry of granite plutons from east Khasi hills, Meghalaya. *J. Geol. Soc. India*, 37, 331-342.
35. Golani, P. R. (1991). Nongchram Fault: A major dislocation zone from western Meghalaya. *J. Geol. Soc. India*, 37, 31-38.
36. Goswami, A. B. (1986). Neotectonic effects on landform and drainage in Upper Assam, India. *Proc. Int. Symp. Neotectonics South Asia, Dehra Dun*, 268-281.
37. Gupta, R. P. and Sen, A. K. (1988). Imprints of the ninety-east ridge in the Shillong plateau, Indian shield. *Tectonophysics*, 154, 335-341.
38. Hillar, K. and Elahi, M. (1984). Structural development and hydrocarbon entrapment in the Surma basin, Bangladesh (northwest Indo-Burman fold belt). *Proc. Fifth Offshore Southeast Conf., Singapore*, 6.5-6.63.
39. Hord, R. M. (1982). Digital image processing of remotely sensed data. *Academic press, New York*, 256 pp.
40. Ichikawa, M., Srivastava, H. N. and Drakopoulos, J. (1972). Focal mechanism of earthquakes occurring in and around the Himalayan and Burmese mountain belt. *Pap. Meteorol. Geophys.*, 23, 149-162.
41. Jensen, J. R. (1986). Introductory digital image processing: A remote sensing perspective. *Prentice Hall, Englewood Cliffs, New Jersey*, 379 pp.
42. Johnson, S. Y. and Alam, A. M. N. (1991). Sedimentation and tectonics of the Sylhet trough, Bangladesh. *Bull. Geol. Soc. Am.*, 103, 1513-1527.
43. Kayal, J. R. (1987). Microseismicity and source mechanism study, Shilong Plateau, Northeast India. *Bull. Seism. Soc. Am.*, 77, 184-194.
44. Khandoker, R. A. (1987). Origin of elevated Barind-Madhupur areas, Bengal basin: Result of neotectonic activities. *Bangladesh Journal of Geology*, 6, 1-9.

45. Khattri, K. N. and Wyss, M. (1978). Precursory variation of seismicity rate in the Assam area, India. *Geology*, 6, 685-688.
46. Khattri, K. N., Wyss, M., Gaur, V. K., Saha, S. N. and Bansal, V. K. (1983). Local seismic activity in the region of the Assam gap, Northeast India. *Bull. Seism. Soc. Am.*, 73, 459-469.
47. Khattri, K. N., Rogers, A. M., Perkins, D. M., Algerminon, S. T. (1984). A seismic hazard map of India and adjacent areas. *Tectonophysics*, 108, 93-134.
48. Khattri, K. N., Chander, R., Mukhopadhyay, S., Sriram, V. and Khanal, K. N. (1992). A model of active tectonics in the Shillong massif region. In: *Himalayan orogen and global tectonics*, edited by A.K. Sinha, Oxford and IBH Publishing Co. Pvt. Ltd., New Delhi, 205-222.
49. Krishnamurthy, P. (1985). Petrology of the carbonatites and associated rocks of Sung valley, Jaintia hills District, Meghalaya, India. *J. Geol. Soc. India*, 26, 361-379.
50. Krishnan, M. S. (1956). Geology of India and Burma. *Higginbothams Ltd. Madras*, 604 pp.
51. Kumar, S. (1990). Petrochemistry and geochemistry of pink granite from Songsak, East Garo Hills, Meghalaya. *J. Geol. Soc. India.*, 35, 39-45.
52. Le Dain, A. Y., Tapponnier, P., Molnar, P. (1984). Active faulting and tectonics of Burma and surrounding regions. *J. Geophys. Res.*, 89, 453-472.
53. LeFort, P. (1975). Himalayas: The collided range. Present knowledge of the continental arc. *Am. J. Sci.*, 275, 1-44.
54. Lillesand, T. M. and Kiefer, R. W. (1979). Remote sensing and image interpretation. *John Wiley and Sons, New York*, 721 pp.
55. Mathur, L. P. and Evans, P. (1964). Oil in India. *Sp. brochure, 22nd Int. Geol. Congr., New Delhi*, 85 pp.
56. Mattauer, M. (1975). Sur le mecanisme de formation de la schistosite dans l'Himalaya. *Earth Planet. Sc. Lett.*, 28, 144-154.

57. Mazumdar, S. K. (1976). A summary of the Precambrian geology of the Khasi hills, Meghalaya. *Geol. Surv. India, Misc. Publ.*, No. 23(2), 311-334.
58. Mazumdar, S. K. (1978). Morphotectonic evolution of the Khasi hills, Meghalaya, India. *Geol. Surv. India, Misc. Publ.*, No. 34, 208-213.
59. Mazumdar, S. K. (1986). The Precambrian framework of part of the Khasi hills, Meghalaya. *Rec. Geol. Surv. India*, 117, 59 pp.
60. McKenzie, D. (1984). A possible mechanism for epeirogenic uplift. *Nature*, 307, 616-618.
61. Mitchell, A. H. G. (1981). Phanerozoic plate boundaries in mainland SE Asia, the Himalayas and Tibet. *J. Geol. Soc. London*, 138, 109-122.
62. Molnar, P., Fitch, T. J. and Wu, F. T. (1973). Fault plane solutions of shallow earthquakes and contemporary tectonics in Asia. *Earth Planet. Sc. Lett.*, 19, 101-112.
63. Molnar, P. (1987). The distribution of intensity associated with the great 1897 Assam earthquake and bounds on the extent of the rupture zone. *J. Geol. Soc. Ind.*, 30, 13-27.
64. Mukhopadhyay, M. (1984). Seismotectonics of transverse lineaments in the eastern Himalaya and its foredeep. *Tectonophysics*, 109, 227-240.
65. Mukhopadhyay, M. and Dasgupta, S. (1974). Role of geologic correction in defining crustal structure as evidenced from Northeastern India and its neighbouring areas. *Bull. Geophys. Res.*, 12, 49-61.
66. Mukhopadhyay, M. and Dasgupta, S. (1988). Deep structure and tectonics of the Burmese arc: constraints from earthquake and gravity data. *Tectonophysics*, 149, 299-322.
67. Mukhopadhyay, S. (1990). Seismic velocity structure and seismotectonics of the Shillong massif, North Eastern India. Ph. D. Thesis, University of Roorkee, India, 247 pp, (*Unpublished*).

68. Murthy, M. V. N. (1970). Tectonic and mafic igneous activity in Northeast India in relation to upper mantle. *Proc. Symp. Upper Mantle Project, Hyderabad*, 287-303.
69. Murthy, M. V. N., Mazumdar, S. K. and Bhaumik, N. (1976). Significance of tectonic trends in the geological evolution of the Meghalaya uplands since the Precambrian. *Geol. Surv. India, Misc. Publ.*, 23, 471-484.
70. Murthy, K. V. S. and Sastri, V. V. (1981). Tectonic influence on the course of Brahmaputra river. *Geol. Surv. India, Misc. Publ.*, 46, 129-132.
71. Nandy, D. R. (1976). Geological set up of the Eastern Himalaya and the Patkoi-Naga-Arakan-Yoma (Indo-Burman) Hill Ranges in relation to the Indian Plate movement. *Geol. Surv. India, Misc. Publ.*, 41, 205-213.
72. Nandy, D. R. (1980). Tectonic patterns in north eastern India. *Indian. J. Earth Sci.*, 7, 103-107.
73. Nandy, D. R. (1982). Geological set up of the Eastern Himalaya and the Patkoi-Naga-Arakan-Yoma (Indio-Burman) Hill Ranges in relation to the Indian Plate movement. *Proc. Himalayan Geology Seminar, New Delhi, 1976, Misc. Publ.*, 41(2A), 205-213.
74. Oldham, R. D. (1899). Report on the great earthquake of 12th June, 1897. *Mem. Geol. Surv. India*, 29, 1-379.
75. O'Leary, D. W., Friedman, J. D. and Pohn, H. A. (1976). Lineament, linear, lineation: Some proposed new standards for old terms. *Bull. Geol. Soc. Am.*, 87, 1463-1469.
76. Powell, C. McA., Roots, S. R. and Veevers, J. J. (1988). Pre-break up continental extension in east Gondwanaland and the early opening of the eastern Indian ocean. *Tectonophysics*, 155, 261-283.
77. Ramesh, N. R. and Gadagkar, N. S. (1990). Effect of 1950 earthquake on geomorphology and ecology in a part of Brahmaputra valley near Teju, Arunachal Pradesh. *J. Geol. Soc. Ind.*, 35, 87-90.
78. Ramsay, J.G. and Huber, M.I. (1987). The technique of modern structural geology. Vol. 2: Folds and Fracture. *Academic Press, London*, 700 pp.

79. Rastogi, B. K., Singh, J., Verma, R. K. (1973). Earthquake mechanisms and tectonics in the Assam-Burma region. *Tectonophysics*, 18, 355-366.
80. Richter, C. F. (1958). Elementary Seismology. *W.H. Freeman, San Francisco, California*, 768 pp.
81. Sabins, F. F. (1987). Remote Sensing-Principles and Interpretation. *W.H. Freeman and Company, New York*, 449 pp.
82. Santo, T. (1969). On the characteristic seismicity in south Asia from Hindukush to Burma. *Bull. Inter. Inst. Seism. Earthquake Engg.*, 6, 81-93.
83. Sarkar, A., Datta, A.K., Poddar, B.C., Kollapuri, V.K., Bhattacharyya, B.K. and Sanwal, R. (1992). Geochronological studies on early Cretaceous effusive and intrusive rocks from Northeast India. (Abstract). *Symp. on Mesozoic Magmatism of the Eastern Margin of India, Patna University*, 28-29.
84. Sarkar, K. and Nandy, D. R. (1976). Structures and tectonics of Tripura- Mizoram area, India. *Geol. Surv. Ind., Misc. Publ.*, No. 34, 141-148.
85. Seeber, L. and Armbruster, J. G. (1981). Great detachment earthquakes along the Himalayan arc and long term forecasting. *In: Earthquake Prediction (edited by D.W. Simpson and P.G. Richards), Am. Geophys. Un.*, 259-277.
86. Siegal, B. S. and Gillespie, A. R., eds. (1980). Remote sensing in geology. *John Wiley and Sons, New York*, 702 pp.
87. Singh, D. D. (1991). Source mechanism of the Cachar earthquake of December 30, 1984, NE India from the synthesis of body waves. *J. Geol. Soc. India*, 37, 365-373.
88. Singh, R. P. (1968). Geomorphology of the Shillong plateau, Assam. *Int. Geol. Cong., Pre. Cong. Proc., Gauhati University*.
89. Sinha Roy, S. (1976). Tectonic elements in the eastern Himalaya and geodynamic model of evolution of the Himalaya. *Geol. Surv. India, Misc. Publ.*, 34, 57-74.

90. Talukdar, S. N. (1982). Geology and hydrocarbon prospects of east coast basins of India and their relationship to evolution of the Bay of Bengal. *Offshore SE Asia Conf.*, 82, Singapore, 1-8.
91. Tandon, A. N. and Srivastava, H. N. (1975). Focal mechanism of some recent Himalayan earthquakes and regional plate tectonics. *Bull. Seism. Soc. Am.*, 65, 963-969.
92. Talwani, P. (1989). Characteristic features of intraplate earthquakes and the models proposed to explain them. In: *Earthquakes at North-Atlantic Passive Margins: Neotectonics and Postglacial Rebound*, edited by S. Gregersen and P.W. Basham, Kluwer Academic Publishers, Dordrecht, The Netherlands, 563-579.
93. Verma, R. K. (1991). Seismicity of the Himalaya and the Northeast India and nature of continent-continent collision. In: *Geology and Geodynamic Evolution of the Himalayan Collision Zone*. Edited by K.K. Sharma. Pergamon Press PLC, Oxford, 345-370.
94. Verma, R. K. and Gupta, R. P. (1973). Relationship of gravity anomalies and tectonics in Assam, India. *Tectonophysics*, 18, 19-31.
95. Verma, R. K. and Krishna Kumar, G. V. R. (1987). Seismicity and the nature of plate movement along the Himalayan arc, Northeast India and Arakan-Yoma : a review. *Tectonophysics*, 134, 153-175.
96. Verma, R. K. and Mukhopadhyay, M. (1977). An analysis of the gravity field in Northeastern India. *Tectonophysics*, 42, 283-317.
97. Verma, R. K., Mukhopadhyay, M., Ahluwalia, M. S. (1976). Seismicity, gravity and tectonics of Northeast India and Northern Burma. *Bull. Seismol. Soc. Am.*, 66, 1683-1694.
98. Verma, R. K., Mukhopadhyay, M. and Nag, A. K. (1980). Seismicity and tectonics in S. China and Burma. *Tectonophysics*, 64, 85-96.
99. Wadia, D. N. (1957). Geology of India. *McMillan and Co. Ltd., London*, 536 pp.

APPENDIX-I

LANDSAT THEMATIC MAPPER (TM) DATA OF NORTHEAST INDIA

<u>Path</u>	<u>Row</u>	<u>Sensor Particulars</u>
133	39, 40, 41, 42, 43, 44, 45	Spectral band : 4
134	39, 40, 41, 42, 43, 44, 45	Spectral Resoponse : 0.76-0.90
135	39, 40, 41, 42, 43, 44, 45	Spatial Resolution :30 (IFOV) in meters
136	39, 40, 41, 42, 43, 44, 45	Pixel size :30 X 30 (in meters)
137	39, 40, 41, 42, 43, 44, 45	Gray level : 256
138	39, 40, 41, 42, 43, 44, 45	
139	39, 40, 41, 42	

FALSE COLOUR COMPOSITE IRS LISS-II FCC OF SHILLONG PLATEAU AND ADJOINING AREAS

<u>Path</u>	<u>Row</u>	<u>Subscene</u>
14	50	A1
15	49	A2,B2
15	50	A1, B1, A2, B2
16	49	A2, B2
16	50	A1, B1, A2
17	49	A2, B2
17	50	A1, B1

DIGITAL REMOTE SENSING DATA
IRS LISS-II CCT OF SHILLONG PLATEAU AND ADJOINING
AREAS

<u>Path</u>	<u>Row</u>	<u>Subscene</u>	<u>Date of Pass</u>	<u>Sensor particulars</u>
15	49	A1	7-Dec-91	Spectral bands :1, 2, 3, 4 Spectral response Bands (in micro meters) Band 1 : 0.45 - 0.52 Band 2 : 0.52 - 0.59 Band 3 : 0.62 - 0.68 Band 4 : 0.77 - 0.86
		B1	7-Dec-91	
		A2	7-Dec-91	
		B2	7-Dec-91	
15	50	A1	7-Dec-91	Spatial Resolution : 40 IFOV (in meters) Pixel size : 36.25 (in meters)
		B1	7-Dec-91	
		A2	7-Dec-91	
		B2	7-Dec-91	
16	49	A1	19-Dec-91	Gray levels : 128
		B1	19-Dec-91	
		A2	16-Mar-92	
		B2	16-Mar-92	
16	50	A1	16-Mar-92	
		B1	9-Nov-89	

NOTE: IRS : INDIAN REMOTE SENSING SATELLITE
LISS - II : LINEAR IMAGING SELF SCANNING SENSORS

